Ingenieurfakultät Bau Geo Umwelt

Fachgebiet für Risikoanalyse und Zuverlässigkeit

Quantifying the Reliability and Component Importance of Infrastructure Networks Subject to Natural Hazards

Anke Franziska Scherb

Vollständiger Abdruck der von der Ingenieurfakultät Bau Geo Umwelt der Technischen Universität München zur Erlangung des akademischen Grades einer

Doktor-Ingenieurin (Dr.-Ing.)

genehmigten Dissertation.

Vorsitzender:
Prof. Dr.-Ing. Constantinos Antoniou

Prüfer der Dissertation:
1. Prof. Dr. sc. techn. Daniel Straub
2. Prof. Dr. Enrico Zio

Die Dissertation wurde am 23.04.2019 bei der Technischen Universität München eingereicht und durch die Ingenieurfakultät Bau Geo Umwelt am 04.09.2019 angenommen.

Declaration

With this statement, I declare that I have independently completed this thesis. The thoughts taken directly or indirectly from external sources are properly marked as such. This thesis was not previously submitted to another academic institution and has not yet been published.

Munich, April 20, 2020

Anke Scherb

Abstract

The services, productivity, and security of our societies depend on a continuous and reliable power supply. Nevertheless, regional blackouts in power grids around the world do occur, including in Europe and in North America. In many cases, natural hazards such as earthquakes, windstorms, floods, or heat waves are the initial triggering events. In order to reinforce infrastructures against natural hazard impacts, a strategic resource assignment is needed. In this context, a network reliability assessment can support the understanding of network performance under threats, including the identification of subsystems and components that play a crucial role for the overall network reliability.

This thesis addresses reliability quantification of power transmission grids subject to extreme windstorms. Windstorms are characterized by large-scale spatial dependencies and can act as a common cause for network component failures. The windstorms can be interpreted as spatial random fields. Different modelling approaches are used in this thesis: a parametric hurricane model for fast evaluation of network reliability, an abstract random field model to investigate the effect of varying spatial dependence, and a more realistic stochastic wind load model learned from European windstorm data. Component failure probabilities in function of wind speed are described by means of calibrated fragility curves. Selected models are applied for the description of the network performance, including models for potential cascading failure processes due to overloading of parts of the network because of load redistribution triggered by the initial outage of one or multiple components. Network reliability metrics are selected in function of the performance model; they can be formulated in terms of the number of lost lines, the decrease in network efficiency, or the loss of power supply.

Besides evaluating the overall network performance, selected importance measures are defined and implemented to rank single components according to their influence on the global system reliability. This helps to identify the components that have the strongest effect on system performance. In addition to classical importance measures (IMs), which are based on dichotomous component and system states, modified IMs are proposed for continuous network performance measures. It is suggested to distinguish IMs related to initial failures from IMs related to cascading failures in order to differentiate between components important for the initiation of a cascading event and components causing the failure propagation within the cascading event.

The investigated electrical networks in the case studies of this thesis are selected synthetic IEEE benchmark systems as well as the transnational European Nordic power transmission grid of Denmark, Norway, Sweden, and Finland. Results indicate that the spatial correlation has a discernible influence on the network reliability and component importance measures, while the component rankings are only mildly affected by the spatial correlation. The findings show additionally that the differentiation of the proposed importance measures according to

initial versus cascading failures enables a more efficient decision support for the planning of network improvements against natural hazards.

Zusammenfassung

Heutige Gesellschaften, Dienstleistungen, Produktivität und Sicherheit bauen auf eine kontinuierliche und zuverlässige Stromversorgung. Deshalb stellen regionale bis überregionale Stromausfälle, welche auch in Europa und Nordamerika nach wie vor häufig auftreten, immer wieder eine Herausforderung dar. Naturkatastrophen, wie Erdbeben, Stürme, Fluten, Vereisungen oder Hitzewellen, sind vielfach die Ursachen für Stromausfälle. Für die Verstärkung der Infrastruktur gegen äußere Einwirkungen müssen Investitionen strategisch eingesetzt werden. Hier kann eine Netzwerk-Zuverlässigkeitsanalyse einen Beitrag leisten, indem die Netzwerkperformance unter äußeren Einwirkungen besser verstanden werden kann, und sich zudem Systemkomponenten identifizieren lassen, die einen kritischen Einfluss auf die Netzwerk-Zuverlässigkeit haben.

Ein Hauptthema dieser Arbeit ist die Quantifizierung der Zuverlässigkeit von Stromübertragungsnetzen, welche extremen Windgeschwindigkeiten ausgesetzt sind. Windstürme zeichnen sich durch räumliche Abhängigkeiten in ihren Windgeschwindigkeitsverteilungen aus und können daher eine gemeinsame Ursache für lokal gehäufte Komponentenausfälle sein. Windstärkeverteilungen werden als räumlich-zeitliche Zufallsfelder dargestellt, wobei folgende Modellierungsansätze in dieser Arbeit zur Anwendung kommen: ein parametrisches Hurrikane-Modell für die effiziente Evaluierung von Netzwerkzuverlässigkeit, ein abstraktes Zufallsfeld für die Untersuchung der Effekte einer variierenden räumlichen Korrelation, und ein stochastisches Windlastmodell basierend auf Europäischen Sturmstatistiken. Die Wahrscheinlichkeiten für Komponentenausfälle als Funktion der Windgeschwindigkeit werden durch approximativ kalibrierte Fragilitätskurven beschrieben. Die Modellierung der Netzwerkperformance wird unter Berücksichtigung von möglichen kaskadierenden Komponentenausfällen vorgenommen. Kaskadierende Ausfälle können durch die Lastumverteilung nach initialen Ausfällen entstehen. Ausgewählte Maße für die Netzwerkperformance sind z.B. die Anzahl der Komponentenausfälle, die Abnahme der Netzwerk-Effizienz oder der Gesamtverlust an der Stromversorgung.

Ausgewählte „Importance Measures (IM)“ werden definiert und angewendet, um Netzwerkkomponenten gemäß der Stärke ihres Einflusses auf die globale Systemzuverlässigkeit zu priorisieren. Neben klassischen IM, basierend auf dichotomen Komponenten- und Systemzuständen, werden auch modifizierte IM entwickelt und vorgeschlagen, die auf kontinuierliche Performance-Maße ausgerichtet sind. Außerdem wird eine Differenzierung zwischen den IM abhängig von ihrer Aussagekraft im Hinblick auf 1) die initialen Ausfälle und 2) die kaskadierenden Ausfälle eingeführt und detailliert untersucht. Dies ermöglicht es, diejenigen Komponenten, die eher zum Initiieren eines Schadens beitragen, von denjenigen, die eher für das Propagieren eines Schadens zuständig sind, zu unterscheiden, und im Hinblick auf ihre Relevanz für Systembeeinträchtigungen einzuordnen.

Die untersuchten Netzwerke sind ausgewählte IEEE Benchmark Systeme und das transnationale Hochspannungsnetz der Länder Dänemark, Norwegen, Schweden und Finnland. Die gewonnenen Resultate zeigen, dass die räumliche Korrelation in der Windlast einen erkennbaren Einfluss sowohl auf die Netzwerkzuverlässigkeit als auch auf die Bewertungen der Komponenten durch die IM hat. Dagegen ist der Einfluss der räumlichen Korrelation auf die Rankings der Komponenten gering. Weiterhin zeigt sich, dass die eingeführte Unterscheidung der IM einen effizienteren Entscheidungsprozess für die Planung von Netzwerk-Verbesserungsmaßnahmen gegen Naturkatastrophen ermöglicht.

Acknowledgements

This work would not have been possible without the support of several persons to whom I would like to dedicate my gratefulness in the following.

Foremost, I would like to express my gratitude to my supervisor and mentor Univ.-Prof. Dr. Daniel Straub who gave me the chance to work in his group. Already during my study program and Master thesis project, I appreciated learning about risk and reliability concepts. During my dissertation period, Prof. Straub trusted me and at the same time, he was always reachable and present. I highly profited from his expertise and goal oriented, scientific guidance, motivation and critical view.

Many thanks to Prof. Dr. Enrico Zio for joining the evaluation committee and for giving me helpful and valuable comments on my final thesis. Prof. Zio agreed upon my visit and research stay in his team at Politecnico di Milano and let me learn about power flow optimization and optimized generator distribution in power grids.

I would like to express my gratitude to Dr. Luca Garrè, at the time senior researcher at DNV GL, Norway, for being my second mentor. Luca Garrè gave me great perspectives, critical views and advises in modeling questions. He helped to organize my research stay at DNV GL in Oslo, so I could collect experiences and meet numerous colleges from different fields.

My colleges in the Engineering Risk Analysis group always created a pleasant atmosphere by being helpful and loyal colleagues! Thanks to Patty for listening, caring and sharing her experiences with me.

My family and friends have played a big role in recent years; thank you for all the support and encouragement that came in many different ways. Above all, I am more than grateful for the support of my parents, Geni and Hagen. I am aware that not everyone can count themselves that lucky in this regard.

Anke Scherb, April 20, 2020

Contents

Part I – Initiation

1 Introduction

1.1 Motivation and scope

Today, reliability is a central concept in technology. The reliability concept is developed and employed to qualitatively or quantitatively describe characteristic properties of complex systems, e.g., the effectiveness, operative readiness, availability, serviceability of items in fields such diverse as the human consumption and behavior, systems safety, nuclear safety, structural engineering, hardware, software, medicine, and many more. This circumstance lets one sometimes forget that reliability is a comparably recent term and a young research field in technology, which was established only during World War II, mainly by the United States military who assessed the reliability of weapons and war strategies (Cruse, 1997, Rausand and Høyland, 2004, Saleh and Marais, 2006).

In general, reliability analysis is concerned with computing the probability of the failure of a system or a structure. The failure is an event in a system or a state of a structure entailing the inability to fulfill an "acceptable level of performance". In this context, probability theory plays a crucial role since it provides the means for describing uncertainties in the system in a quantitative manner (Stewart and Melchers, 1998). The assessment of the reliability of a system or structure and the quantification of the reliability typically faces a multitude of challenges, some of which are listed below based on Papaioannou (2012):

- Many failure possibilities or a complex failure domain
- Limited predictability of loading and resilience of system components
- Uncertainties about component or material properties
- Statistical dependencies between sub-systems or the systems' components

- Sequential or cascading failures (e.g. by load redistribution caused by damage)
- Low probabilities of failures (rare failure events)
- Lack of performance data and lack of failure data

Reliability analysis can be regarded as an element of risk analysis. Risk interpreted as the expected loss is a function of the occurrence probability of the damage or failure and the failure consequence, i.e. the costs that might be caused for the asset of interest. Engineering risk analysis has the objective to calculate the expected adverse consequences from loadings or hazardous scenarios on infrastructure items (Bedford and Cooke, 2001). Thus, reliability analysis is a precondition for the estimation of risk, as it provides the probability that a structure or a system does not perform satisfactorily. Risk and reliability analysis represent an important basis for informed decision-making where the objective is to determine the optimal decision according to the fundamental paradigm of utility theory (Raiffa and Schlaifer, 1961, Bedford and Cooke, 2001): if the occurrence probability and the costs associated with potential adverse scenarios are known they can be compared quantitatively. In case decisions are to be made about e.g. investments in rebuilding, reinforcement, mitigation strategies, and alike, the risk analysis for all decision options will reveal for which decision the utility is maximized, i.e. the risk and the expected costs are minimized (Bedford and Cooke, 2001).

The built environment may be exposed to external loading impacts from extreme weather that can reach destructive magnitudes. In the context of natural hazards, risk is a function of hazard occurrence and intensity, asset exposure, and asset vulnerability (Whitehouse, 2013). Exposure refers to the items at risk, e.g. buildings, streets, and bridges. Vulnerability is the susceptibility of an item to suffer damage from the hazardous impact (Renaud, 2006). Examples of factors that influence vulnerability or fragility, include asset characteristics such as material strength, construction quality, age, restoration time and cost after damages (Whitehouse, 2013).

During the 1970s, within the field of probabilistic risk assessment (PRA), the component-centric view was shifted towards a holistic view on general system level analysis: system reliability, availability, and safety. This paradigm change was mainly initiated by the necessity of reactor safety studies to assess the reliability of nuclear power plants. This was attempted for the first time in a report led by Professor Norman Rasmussen (WASH-1400, NUREG-75/014) (Keller and Modarres, 2005). Nowadays, these concepts are applied to study all kinds of infrastructure systems: transmission systems for utility services such as in communication, transportation, power transmission and distribution, and in gas, oil, or water supply and sewage systems, e.g. Rausand and Høyland (2004), Birolini (2007), and Straub (2017). One main motivation behind the analysis of the system reliability is that it can serve planners as a tool to identify weaknesses in systems, to understand under which conditions the system might fail, which components need to be prioritized, and, to quantify whether a system meets reliability acceptance criteria.

Network reliability can be regarded as a subordinated field in system reliability (Straub,

2017). The analysis of networks is especially demanding because networks often consist of a large number of components of potentially different types that interact with each other in a complex way following non-linear laws (Zio, 2009). Physical networks are exposed to aging and various external and internal loads and demands. Usually, the number of failure scenarios of components and failure states of the system are very large (Vaiman et al., 2012): In case of N components where x components can fail, and the sequence of component failures matters, the number of contingencies increases to $\frac{N!}{(N-x)!}$ which is computationally infeasible even for moderate numbers of components. For 70 components that all can fail one faces 70! contingencies, a number in the range of 1 googol (10^{100}). Therefore, finding the right level of detail or abstraction for models that are aimed at depicting the reality is crucial as this means setting up an efficient simulation framework for conducting system performance analyses.

Dependence among components is a crucial aspect in network performance and reliability assessment, not least since dependent failure events are an important source of failures in technical systems (Rausand and Høyland, 2004). Dependencies have to be taken into account when conducting a risk assessment of networks to ensure appropriate performance estimation, i.e. to avoid unrealistically short recovery times and too low monetary losses (Ouyang and Dueñas-Osorio, 2014). Dependencies stem e.g. from common factors or properties influencing multiple system components simultaneously; they exist to some degree in all systems. The term Common Cause Failures (CCF) is used to describe multiple failures of components in a system from shared root causes (Wierman et al., 2007). In particular, spatially distributed networks are prone to different kinds of CCF because various potential root causes are associated with external impacts on the system. One instance of such root causes are large-scale natural hazards (e.g. earthquake, wind storm, flood, icing, landslides). These hazards are characterized by a spatial distribution and variability, which should be accounted for in the analysis of the reliability of the system, a task that is one of the focal points of this thesis. Another main source of dependence in networks can be an internal domino effect, i.e. a cascading of additional component failures. This effect may be a consequence of the initially triggered failures leading to a change in the system loading profile due to the redistribution of load and the subsequent overloading and failure of affected components (Vaiman et al., 2012). This type of dependence is also investigated in this thesis. Classical models for system dependencies generally do not consider specifically spatial correlation in the CCF characterized by spatial distributions and variability, which might stem from the exposure to natural hazard impacts and loads, as will be discussed in more detail in Chapter 5.3.1. However, network vulnerability and reliability with regard to natural hazards has been assessed and modelled synoptically in a number of studies (e.g., Dongwei et al., 1996, Dueñas-Osorio, 2005, Adachi, 2007, Neumayer et al., 2008, Javanbarg et al., 2009, Dueñas-Osorio and Vemuru, 2009, Winkler et al., 2010, Agarwal et al., 2010, Neumayer and Modiano, 2010, Lim and Song, 2012, Ouyang and Dueñas-Osorio, 2012, Bernstein et al., 2014, Ouyang and Dueñas-Osorio, 2014, Javanbakht and Mohagheghi, 2014, Panteli et al., 2017). These studies focus on scenario-based reliability

analyses of specific infrastructures subjected to hazards, but do not systematically investigate and quantify the effects of varying correlation structures in the hazard on system reliability. Andreasson et al. (2011a) analyze a model for the Nordic power grid to investigate the effects of correlated failures of power lines on the total system load shed in a non-spatial context. They conclude that with an increased dependence among line failures, the expected value and the variance of the system load shed increases significantly. Rahnamay-Naeini et al. (2011) model correlated failures as spatial point processes and their effects on network reliability for communication networks in the US. They find that the network performance in terms of network efficiency decreases with increasing degree of correlation among component failures. Both Andreasson et al. (2011a) and Rahnamay-Naeini et al. (2011) do not consider the effects of cascading failure events following initial failure-triggering events in the network due to load redistribution and thus potential overloading of topologically, structurally, and/or spatially neighboring components.

In system reliability assessments, component importance measures (IM) are employed to rank system components, i.e., to arrange the components in the order of increasing or decreasing importance based on their influence on the overall system reliability, e.g., Vesely et al. (1983), Gandini (1990), Meng (1996), and Cheok et al. (1998). The resulting rankings can serve the network designer and maintainer for the identification of components to be inspected, repaired, strengthened, replaced, or alleviated from external or internal load impacts. Importance measures can further support the improvement of operating methods and network expansion planning. Besides looking at the effect of CCF on the overall system reliability, it is interesting to assess the effect of CCF on component importance. The effect of CCF on the importance of components for system reliability has been explicitly studied for general networks by Bérenguer et al. (2006) and Tanguy (2011). The latter assessed the effect of generic CCF models on the system reliability and various IMs in a small network with 9 nodes and 14 lines. Tanguy (2011) concludes that adding CCF effects to the model of a small sized network does not profoundly change the ranking of the system components. None of these studies investigate systematically how spatial dependence (spatial correlation) influences the behavior of component importance measures in spatially distributed networks.

1.2 Research questions and contributions

This thesis establishes a stochastic network reliability framework in the presence of uncertainty. Structural component failures are related to system reliability expressed in terms of selected network performance metrics. The general network reliability problem is embedded into the context of natural hazard impacts, here represented by extreme wind loads on network components, which lead to potentially correlated initial and cascading component failures.

Methods and models are developed and employed within the scope of this thesis that enable the computationally efficient analysis of large and complex infrastructure networks. Therefore, a suitable level of abstraction is needed. In the following, the elaborated research questions are sorted according to research subjects:

Dependencies in systems

One main focal point of this thesis is the determination of the criticality of spatially correlated component failures with respect to the overall network reliability. Therefore, spatial dependence structures among hazardous load impacts and consequent component failure probabilities are examined in order to investigate the effect on the corresponding network reliability. In this thesis, the goal is to study both in combination: the spatially dependent initial component failures as well as the subsequent failures in a cascading process; the aim is to investigate the reliability in spatially distributed infrastructures, accounting for the spatial dependency between the exogenous hazard and the resulting cascading failure processes.

- *How to effectively introduce common cause failures induced by spatially correlated hazard intensities into models for the reliability analysis of networks? How does a varying correlation length of spatially distributed hazard intensities affect network reliability?* – Different approaches of modelling spatial dependencies in the system are examined:
    - Three-parametric hurricane wind field model based on hurricane data
    - Spatial random field (SRF) based on historical European storms
    - Generic SRF model for hazard representation with a continuous variation of the correlation length
- *How to assess network performance considering cascading failures? How do different network performance models and indicators compare? Moreover, what are suitable methods and measures for analyzing specifically power infrastructure systems?* - The most suitable metrics for network performance assessment are determined from different approaches available in the literature. It is possible to model networks from a graph theory perspective (static structure of networks) or based on physical network models (dynamic processes in networks) that aggregate information about network performance.
- *How does the interplay between external CCF and cascading failures affect the system reliability?* – The network performance after initial disturbances is assessed based on cascading failure models. In this context it is studied how important the process of cascading failures is, compared to the initial component failures against the backdrop of spatial dependencies.

Component fragility

- *How to derive a valid model for the component fragility?* - Modelling the response of individual components to hazardous loads like wind speed and wind pressure is a challenging task, mainly due to a lack of detailed empirical failure data at the component level. In this thesis, the component lognormal fragility curves are calibrated based on several assumptions with the goal to meet good approximate parameter estimations. One consideration is that equipment deployed in the field shall meet design requirements based on characteristic wind speeds of established wind zones in the study area. The calibration is derived from historical line (segment) failure statistics in the European Nordic countries.

Component importance and network improvement strategies

- *How do component importance rankings differ based on different importance measures (IMs)?* - A combination of component-level reliability assessment and overall system reliability is applied for a better understanding of the impact of critical components using component importance measures. Different measures are applied and compared with respect to the resulting component rankings.
- *How to formulate IMs based on continuous network performance measures?* – In order to not only rely on a binary system failure definition, IMs are suggested that are based on determining the effect of component failure on the continuous network performance measure applied.
- *How does a varying correlation length of spatially distributed hazard intensities affect component importance rankings?* - The effect of CCFs on the reliability importance rankings of network components based on selected IMs is assessed. The aim is to investigate the reliability and component importance in spatially distributed infrastructures, accounting for the spatial dependence of the exogenous hazard and resulting cascading failure processes. The IMs are thereby formulated once with respect to failures caused directly by the hazard event, and once with respect to cascading failures. These two IM formulations are compared, and it is suggested that the distinction made by the two formulations is key to identifying efficient network improvement strategies.
- *What type of network improvement strategies can be derived based on component rankings, and how effective are they regarding the improved network reliability?* - Component importance measures are the basis for targeted strengthening actions on individual components to improve or optimize the overall system performance and reliability. Selected improvement scenarios for the studied network systems subject to natural hazards are suggested. Results of the assessments shall support future infrastructure planning and operation, maintenance action planning, and the planning of

potential hazard mitigation strategies.

1.3 Thesis outline

This thesis is composed of four main parts:

Part I contains the overall broad introduction into the field of power transmission infrastructures. The importance of reliable power infrastructure and typical causes of power outages are discussed. Finally, an outline of the corresponding literature on (infrastructure) reliability analysis in the context of natural hazards is given.

In Part II, firstly, the proposed general flexible assessment framework of this thesis is presented - this framework is adjusted for several case studies later in the thesis. Further, the theoretical background underlying the network reliability analysis in this thesis is explained, and the methods of the pertinent research fields for network reliability are introduced such as complex graph theory, reliability assessment methods with an emphasis on system dependencies, and non-simulation-based versus simulation-based assessment methods. In Chapter 6, the concept of fragility is discussed and a novel approach of deriving and calibrating a component fragility model is introduced. In Chapter 7, a selection of component importance measures is compiled. The main contribution at this point is the investigation and characterization of separate sensitivity (importance) measures for initial and cascading correlated component failure events. On this basis, potential network reliability improvement strategies are detailed and suggested.

In Part III, example case studies are investigated more closely. The methods and the models developed and suggested earlier in this thesis are applied to a selection of synthetic (academic) transmission power systems as well as to a model of the real world trans-national power grid in the European Nordic countries Denmark, Norway, Sweden, and Finland. For each case study an own appropriate hazard representation is developed, not at least depending on the data foundation. A central theme of this thesis is the effect of the variability of the SRF correlation length on pertinent grid performance measures, which is assessed in the final case studies of Chapter 10 based on a generic environmental hazard representation in terms of spatial random fields.

Finally, Part IV contains the discussion and the conclusions.

2 Electrical power transmission

In this thesis, the suggested reliability assessment frameworks are applied to power transmission systems. These systems expand over larger regional areas, often connecting several countries enabling cross border power load exchange. In such indispensable infrastructures, outages of serviceability can create tremendous damages as will be exemplified below. Furthermore, in most parts of the world, such important infrastructures are exposed to environmental impacts from weather and natural hazards and are thus, good examples of systems, which are exposed to spatially correlated loads and consequently spatially correlated component failures. In the following, the importance of a reliable power supply is shortly discussed as well as typical reasons for power outages, and the general characteristics and elements of electrical power transmission infrastructure and selected benchmark systems.

2.1 The importance of reliable power supply

Societal requirements on continuous and reliable power supply are increasing. Requirements are especially high in the light of increasingly many and increasingly dense conurbations overall in the world. At the same time societies rely more and more on infrastructures dependent on continuous electrical power. The data on the world's electrical energy production shown in Figure 1 highlights these observations. Yet, regional blackouts have occurred frequently in the last two to three decades, also in Europe and North America where power grids are ranked among the more reliable ones in the world (Bruch et al., 2011, Böttcher, 2016).

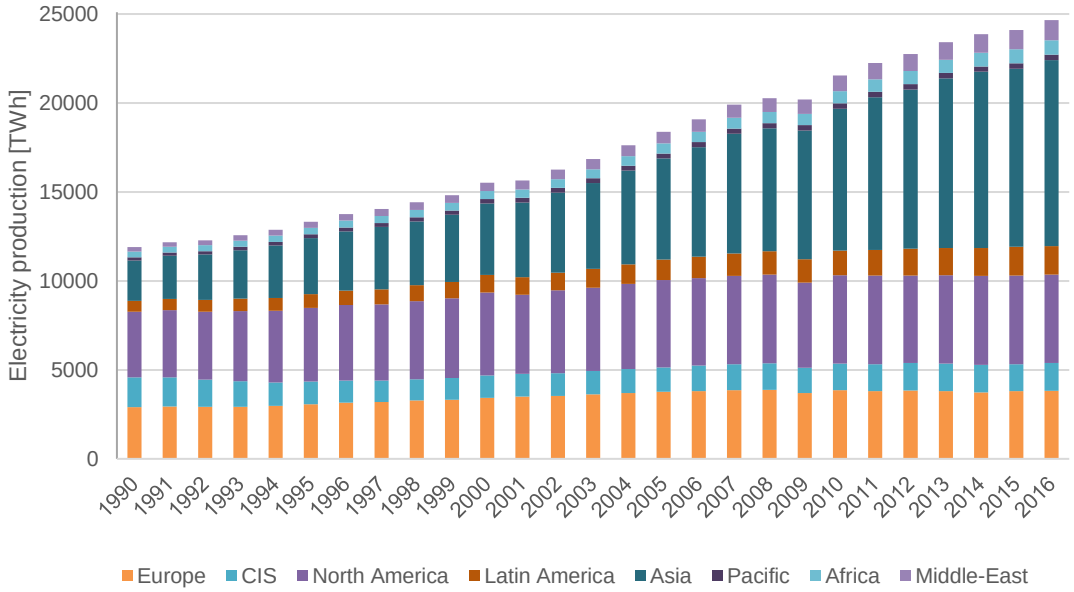

Figure 1: The worlds electricity production broken down to different regions of the world, based on data from Enerdata (2017).

Short time blackouts alone lead to an estimated annual economic loss of between 104 billion and 164 billion US Dollar in the USA (Hodge, 2012). Some example estimates of how high the costs from a blackout can rise for different industry sectors are shown in Table 1. Generally, the damages depend on the duration of the blackout, the onset time of the day, the onset day type (weekday versus weekend), the season (summer versus winter), as well as on the extent of advance notice of the upcoming interruption and thus, eventual operational counter measures. The values in Table 1 represent highly aggregated data that was averaged over regional insurance data in blackout events all over the world, e.g. Brazil, USA, Canada, Italy, India, Korea, New Zealand, and Indonesia. Since there is in general only limited insurance coverage, the numbers in Table 1 can only indicate the order of magnitude of the costs and potentially are rather conservative, i.e. too low estimates. The data would need to be differentiated in further detail for a specific cost analysis for a region or a country, as it has been attempted for the USA by Sullivan et al. (2009) or Whitehouse (2013). It has been estimated that in the United States alone, power outages due to hurricane events lead to yearly nationwide costs ranging between 18 and 33 billion US Dollar (Whitehouse, 2013).

Table 1: Cost analysis of historic blackout scenarios based on data from the Copper Development Association; Source: Hodge (2012). Data is given per hour or per event.

Industry branch	Typical financial loss
Financial trading	6,000,000 € per hour
Telecommunications	1,800,000 € per hour
Semiconductor production	3,800,000 € per event
Computer center	750,000 € per event
Steel works	350,000 € per event
Glass industry	250,000 € per event

2.2 Causes of power outages

Causes of power outages besides weather and natural hazards include operational failures, equipment (hard- and software) malfunctions, circuit overloads, vehicle accidents, fuel supply deficiencies, and load shedding, which occurs when the grid is intentionally shut down to contain the spread of an ongoing power outage (US Department of Energy, 2017). An overview of some main potential causes is given in Figure 2 based on Bruch et al. (2011); note that often combinations of initial causes lead to major blackouts. Power transmission grids run through any type of terrain and they are exposed to a wide variety of weather impacts: bush fires, extreme heat, sandstorms, typhoons, tornadoes, hurricanes, extratropical weather systems, lightning, sprays of sea salt, freezing rain, rime ice, snow storms and wet snow/icing, floods, and extreme rain (Fikke, 2017).

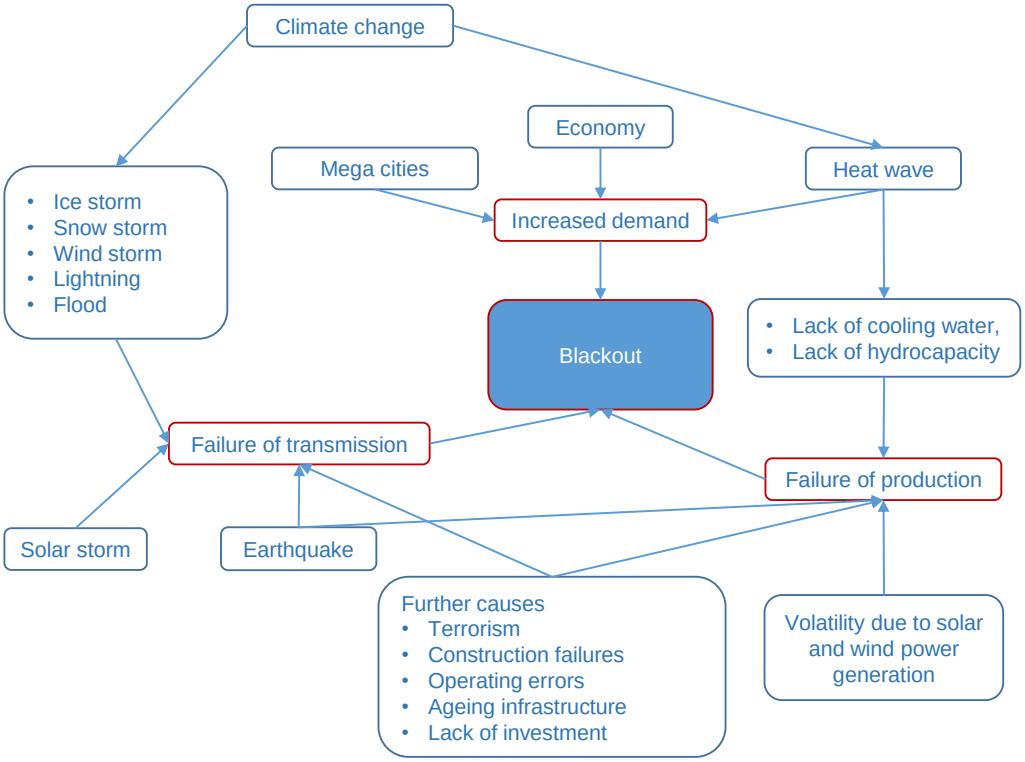

Figure 2: Potential causes of power blackouts, adapted from Bruch et al. (2011).

In principle, the causes due to natural hazards have to be distinguished from typical system inherent causes. These differences have been characterized and summarized by Wang et al. (2016) in a general review on power system resilience in the face of natural hazard impacts, shown here in Table 2.

Table 2: Differences between general outages and outages due to natural hazards, adapted from Wang et al. (2016).

General outage	Outage due to natural hazards
• Often single initial fault at a time in one component • No spatiotemporal correlation in the fault events; fault occurs randomly • More likely that power generation units stay connected and undamaged • More likely that short time to repair and restore	• Often multiple faults in several components within the time span during or after the hazard event • Spatiotemporal correlation of the faults due to natural hazards • Power generation units might be affected dependent on the hazard type • Often difficult to repair and restore, e.g. due to lasting events and implications, e.g. debris flow after hurricanes

In fact, natural hazards are a major cause of outages and related costs in the US, measured by the number of outages and the number of customers affected. The US Energy Information Administration provides some meta-data about power outages since 2002, where initial triggering events and the customers affected are listed per event (US Department of

Energy, 2017)[1]. Based on an analysis of this data, some conclusions can be drawn, see Figure 3. From 2002 to 2012 almost 60% of the outages observed were due to extreme weather events and earthquakes. This rate lowered after 2010; however, the overall average rate over 2002 to July 2017 is 53%. Outages that are caused by natural disasters leave higher numbers of customers affected. This pattern is confirmed by the corresponding values of power demand losses in Megawatt [MW] in the data source (not depicted here); however, a high number of missing data is adding uncertainty to the statistics. The values of the outages caused by natural disasters and extreme weather range between 200 MW and 1200 MW average power loss between 2002 and 2017.

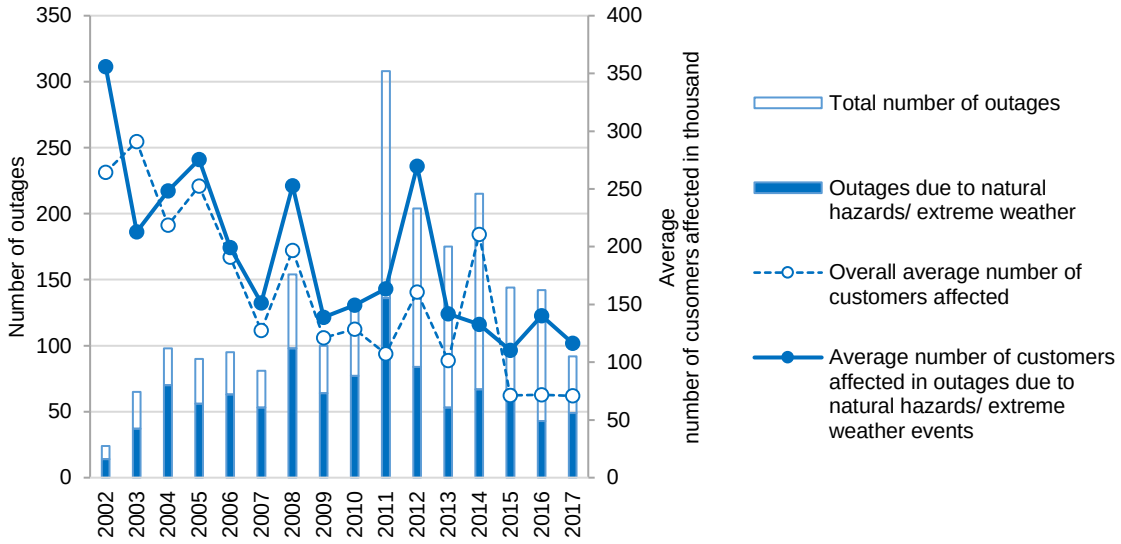

Figure 3: Statistics based on data from the United States Department of Energy (US Department of Energy, 2017). Overall number of outages per year and fraction of outages triggered by natural hazards (extreme weather events like heat, icing, snowstorm, extreme winds and earthquakes etc.). Line plots show the overall average number of customers affected by all events (dashed line) versus the average number of customers affected in an outage triggered by a natural hazard or an extreme weather event.

One impressive example of a regional power outage happened on 28 September 2003 in Europe. Almost all of Italy - except of the islands Sardinia and Elba - was involved as well as parts of Switzerland around Geneva for up to 16 hours in the worst cases. In total, 56 million people were affected. This event was initiated by the tripping of only one important single transmission line between Switzerland and Italy that was damaged by a wind storm and falling trees. The failure of this line lead to a sudden increase in power demand (load) on the two HV lines between France and Italy, and a subsequent cascading failure process throughout the system (UCTE, 2004), see Figure 4.

[1] Data available at: https://www.oe.netl.doe.gov/OE417_annual_summary.aspx [access date 2017/09/04].

Figure 4: Illustration of the extension of the large-scale blackout event in Italy in 2003. Map created based on UCTE (2004).

2.3 Elements of transmission infrastructures

Power grids are multi-layered systems with different types of sub-systems interconnected with each other. For example, the European power transmission grid is composed of mainly national grids that are maintained and operated by the Transmission System Operators (TSOs) of the corresponding country. In general, a power grid contains three functional systems: the generation, the transmission, and the distribution of power. Thus, power is transferred through transmission lines from generation buses to distribution buses for supplying commercial, industrial, or residential consumers. Between generation and consumption, the voltage level needs to be adapted several times. For transferring power over wide distances, the extra high-voltage (EHV) system is used with a voltage dependent on the country or region (range of 345 to 765 kV). A high-voltage (HV) transmission grid, i.e. with a voltage of 110 to 230 kV, is connected to the EHV grid via transmission substations and supplies the medium voltage (MV) distribution grid and industrial customers

with more than 5 MV (Sivanagaraju and Sreenivasan, 2009, Gönen, 2015).

As discussed in Chapter 5.4, different models for the network performance are implemented in this thesis, among which one model is based on the DC power flow equations that can capture potential cascading failure processes in outage events. In this model the main information used is the type of the buses (generation, transmission substation, distribution substation, voltage transformers), the power load of the buses (power generation versus power demand), and the load capacity of the transmission lines.

2.3.1 IEEE benchmark systems

There exist various benchmark systems that serve in literature as test cases e.g. for model development or reliability studies. The Institute of Electrical and Electronics Engineers (IEEE) defined the applied standards for the exchange of solved load flow data structures (IEEE, 1973). The great advantage of the IEEE benchmark systems is that they build a common ground and, therefore, make studies comparable to each other.

The benchmarks represent power transmission and partly power distribution networks. They have different sizes and differ in their setup. Most of them have been compiled in the 50s or 60s of the last century for US standards and thus, do not reflect current power network conditions with a higher amount of distributed renewable power generators. Furthermore, they are expected to only partly reflect the European power system infrastructure, which differs in its layout, voltage levels, and standards. The IEEE benchmark cases are made available online in the Power Systems Test Case Archive by the University of Washington (Christie, 2000) and they are included as example cases in the Matlab tool Matpower[2].

Power transmission test cases used in this thesis are shown in Figure 5 to Figure 8. The smallest artificial transmission benchmark system IEEE 14 (Figure 5) is oriented at a portion of the American electric power system. The network system consists of 14 buses that are connected by 20 lines. The system operates at two different voltage levels: 132 kV in the lower half, and 230 kV in the upper half with separating buses/transformers 4, 5, and 7. Buses 1 and 2 are generating units, buses 13 and 14 are so called load buses, where consumers are connected. Zio and Piccinelli (2010) applied a randomized flow model and a centrality betweenness measure to rank the components of the IEEE 14.

The IEEE one area RTS-96 benchmark power transmission network composed of 24 nodes and 38 lines is oriented at a portion of the American electric power system (Grigg et al.,

[2] Matpower is a power system simulation package built upon Matlab and available at: http://www.pserc.cornell.edu/matpower/ [access date 2018/11/11].

1999), Figure 6. It has been used in a number of studies e.g., Dobson et al. (2001), Xingbin and Chanan (2004), Delgadillo et al. (2010), Daemi et al. (2012).

The IEEE 39 benchmark is composed of 39 buses and 46 transmission lines and transformers (Figure 7). It contains 10 generator buses which are all modelled as leaf nodes. The buses with an arrow sign are load buses. The IEEE 39 bus benchmark system for transmission power grids has been designed to be representative of the New England transmission power network (Christie, 2000), and it was the subject of a large number of studies (e.g., North American Rockwell et al., 1970, Athay et al., 1979, Dwivedi et al., 2009, Panigrahi, 2013). Dwivedi et al. (2009) found that the IEEE 39 is a rather stable and reliable system. They conclude that the system is robust with respect to random attacks; there is hardly any effect on the efficiency if single lines are randomly selected and removed.

The IEEE 118, Figure 8, is composed of 118 buses (54 generators, 9 power transformers and 91 load buses) and 179 lines, thus it is a considerably larger network than the IEEE 39. It has been used by e.g., Dwivedi et al. (2009), Chen et al. (2010), Panigrahi (2013), Javanbakht and Mohagheghi (2014), Koç et al. (2014), Scherb et al. (2017).

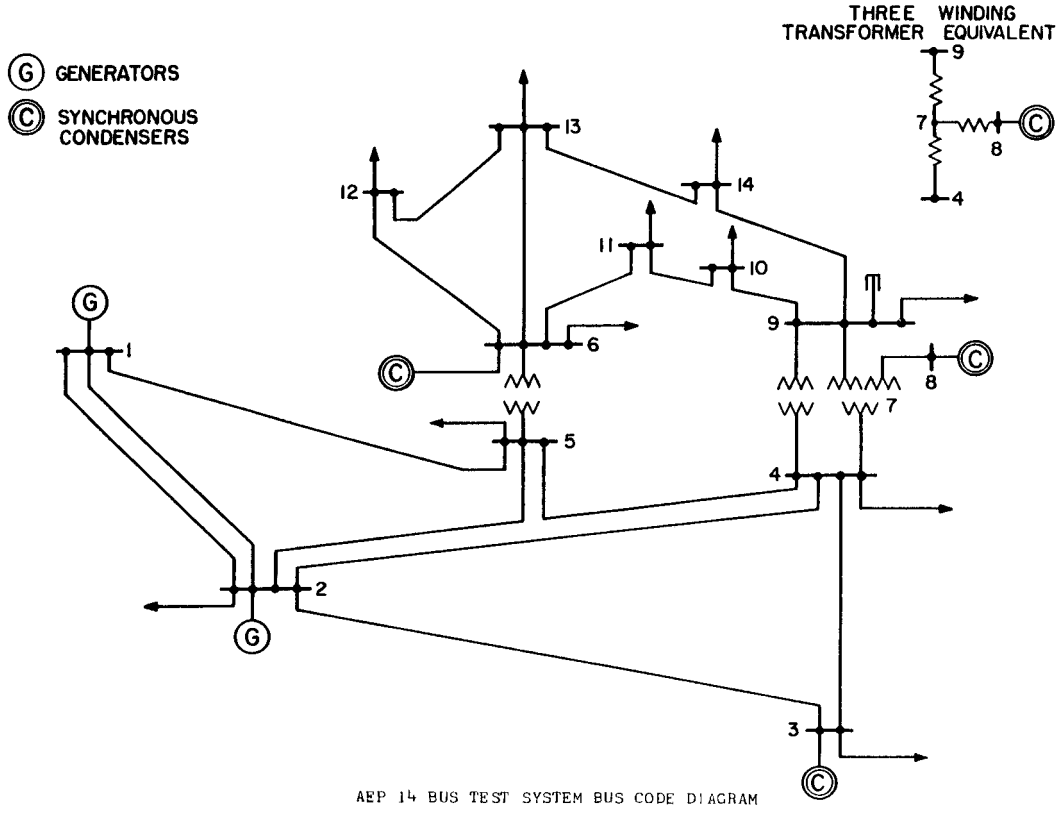

Figure 5. Circuit diagram of the IEEE 14 bus benchmark system taken from Christie (2000).

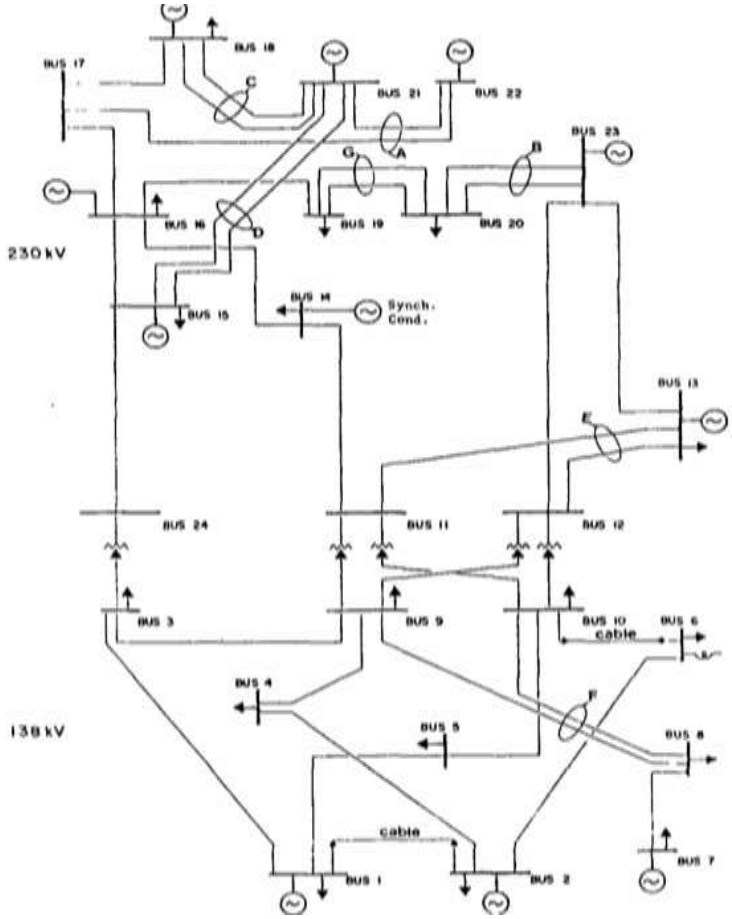

Figure 6. Circuit diagram of the IEEE 24 (RTS 96) bus benchmark system taken from Christie (2000).

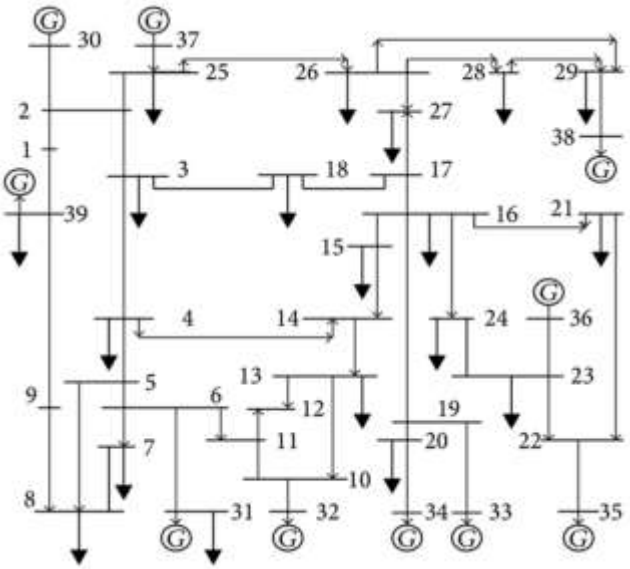

Figure 7. Circuit diagram of the IEEE 39 bus benchmark system taken from Athay et al. (1979) .

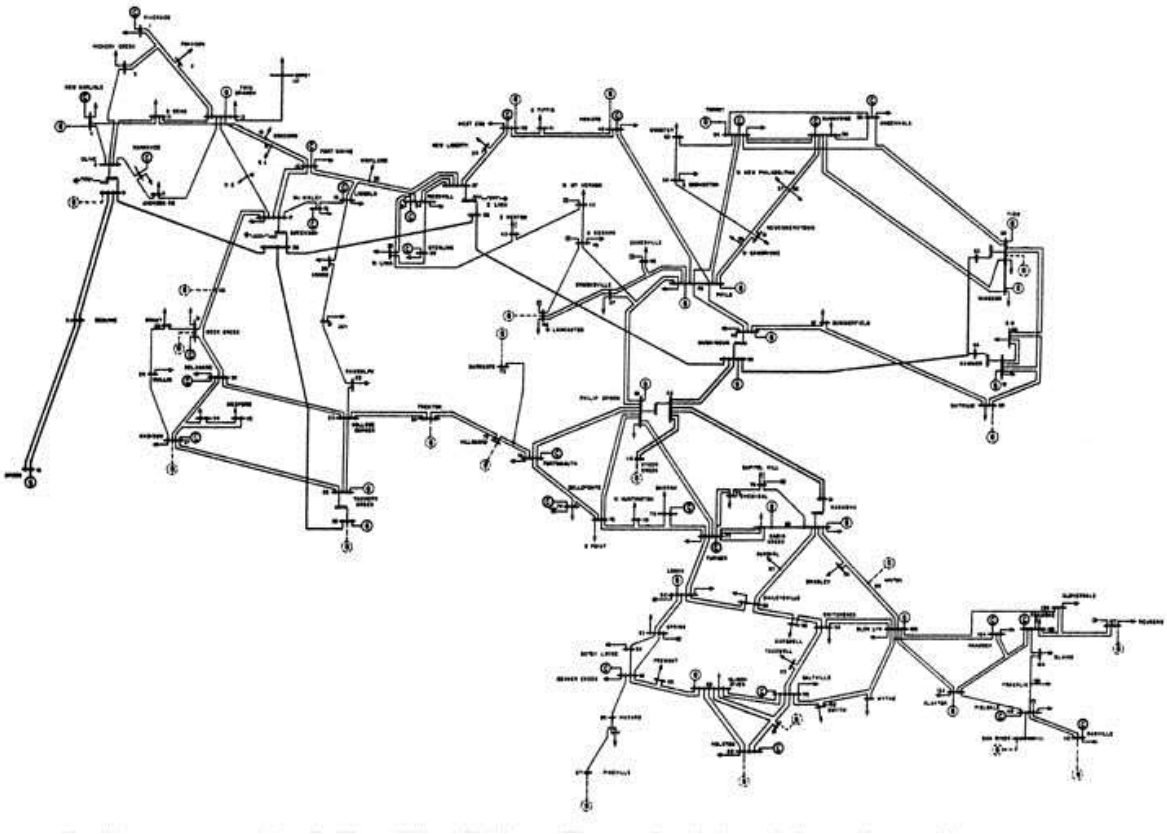

Figure 8. Circuit diagram of the IEEE 118 bus benchmark system taken from Christie (2000).

2.3.2 The Nordic power grid

While IEEE standard power systems offer great transparency and can function as benchmark systems for grid topology research, failure risk assessment, and system improvement strategies, they most often do not represent the most recent power grid conditions. For Europe, some specific benchmarks are available, like the UCTE or CIGRE networks. Andreasson et al. (2011a) alternatively considered a model of the real Nordic power system based on publicly available data of grid characteristics for Denmark, Finland, Norway, and Sweden to demonstrate appropriate sampling techniques and concepts of system failure analysis.

The Nordic power grid connects the transmission systems of Norway, Sweden, Finland, and Denmark, Figure 9. The system is subject to ongoing developments and reconfigurations, because of renewable energy integration and different network expansion strategies at regional and over-regional levels and because power exchange and investments in the cross sections between Continental Europe and the Baltic States are increasing (Stattnet et al., 2014).

The electricity sources and the distribution of the power generation are rather divergent

among the Nordic countries. In Norway 99% of the generated electrical power is from hydro power plants mostly located in the southern parts of Norway. Sweden has mainly hydro power and nuclear power generation, the latter from four nuclear power plants located near the largest metropolitan areas of Sweden. Finland, in contrast, relies more on thermal power plants and has a higher import of fossil fuels for its electricity generation. Denmark has a larger share of wind power generation (mainly offshore), but especially important in Denmark are thermal power plants located close to the metropolitan areas (Energistyrelsen, 2015, Vesely, 1977, NVE, 2017).

Data for the model of the Nordic grid has been provided by Andreasson et al. (2011a), collected mainly from publicly available data about network topology, transmission line parameters, power generation, and power demand derived from population density data. The model comprises in total 470 nodes and 636 power transmission lines (without counting parallel installed lines). The mean line length based on the model data is 83.8 km with minimum 2.5 km, maximum 1206.5 km, and median 48.8 km.

The Nordic Grid's reliability has been studied by Andreasson et al. (2011a) with focus on effects of correlated failures of power lines on the total system load shed. However, they did not assess the effect of cascading failure events after spatially correlated hazardous impacts. A further vulnerability study for the Nordic grid was conducted by Holmgren (2006) using a graph theoretic model based on topological characteristics of the network. The Nordic grid complies with the $(n-1)$-criterion, i.e. if one component is removed from the system, the elements remaining in operation are capable of accommodating the new operational situation without violating operational security limits; the $(n-1)$-rule is explained in more detail in Chapter 5.5.3. Since the Nordic grid generally fulfills this criterion, it can be assumed resilient to independent failures assuming that all components have low failure rates (Andreasson et al., 2011a). In case the component failures are dependent, and there is an underlying correlation structure, due to hazards impacts, the $(n-1)$-criterion might not be sufficient to describe the reliability of the system. Moreover, to the knowledge of the author, there is also no study about hazard impacts on the Nordic grid taking into account subsequent cascading failure effects.

The study on the Nordic grid is presented in Chapter 9.

Figure 9: Illustration of the transmission system network operated by members of the European Network of Transmission System Operators (TSOs). Network elements are located only at their approximate geographic location. Important transmission sections, generators and substations in the so called Nordel area and neighboring areas are shown; use permitted by Entsoe (2018)[3].

[3] Source: https://docstore.entsoe.eu/Documents/Publications/maps/2018/2018_Map_Northern-Europe-3.000.000.pdf; [access date 2018/11/30].

2.4 Summary

Chapter 2 contains an introduction to power transmission infrastructures and important reasons for power outages are outlined. Power infrastructure networks are often subject to natural hazards and high costs are estimated from severe power outages. Some statistics are presented highlighting those facts. E.g. from 2002 to 2012 almost 60% of the outages observed in the United States were due to extreme weather events and earthquakes. It has been estimated that in the United States alone, power outages due to hurricane events lead to yearly nationwide costs ranging between 18 to 33 billion US Dollar.

Publicly available model representations of transmission systems commonly used in literature, so called IEEE benchmark systems, are presented. They cover different sizes and formations of power transmission networks oriented at power grids of the 20^{th} century in the USA. In the course of this thesis, studies are made for selected IEEE benchmark systems as well as for the Nordic Grid of the European Nordic countries.

3 Modelling approaches

In the following, selected studies in the field of risk and reliability of civil infrastructure systems subject to natural hazards are discussed. An increasing number of contributions and publications during the last 10 to 15 years can be observed. Most studies of the vulnerability of power networks and the occurrence of outages in hurricane prone regions have been conducted for the USA. Overall, the reviewed and presented studies are predominantly interested in two hazard types: earthquakes and tropical cyclones. Earlier studies developed regression models to estimate and predict the spatial distribution of power outages based on outage data from past hurricanes along with physical data and environmental conditions of the system component sites, Section 3.1. More recent studies rather examine the system behavior and evaluate the performance, e.g. under consideration of cascading failure events with the aim to estimate the potential damages after hazardous events, Section 3.2.

3.1 Statistical modelling approach

There are a number of statistical models based on spatial outage databases from different historical hazards, which are mainly regression models. Some earlier studies developed regression and correlation models to predict the spatial distribution of power outages based on outage data from past hurricanes along with physical data and environmental conditions of the system component sites (e.g., Liu et al., 2005, Han et al., 2009a, Han et al., 2009b, Staid et al., 2014, Liu et al., 2008). Some of these studies are introduced shortly in the following.

Liu et al. (2005) developed negative binomial regression models for electric power outage events during hurricanes. The study is based on three hurricane events (Hurricane Floyd 1999, Hurricane Bonnie 1998, Hurricane Fran 1996) and outage data in North and South Carolina. It is found that the best explanatory variables for the expected number of outages are the number of transformers in the area, maximum gust wind speed, utility company affected, and hurricane event. A main output of the study is the spatial density of outages in a region dependent on theses variables. However, due to data limitation, this model is only representative for the study area and would need to be adjusted for other regions. Liu et al. (2008) used a similar approach as Liu et al. (2005). A spatially generalized linear mixed model (GLMM) is developed for a Hurricane prone region stratified by 3x3 km^2 grid cells based on data from six hurricanes and eight ice storms. In this case, the variables in the regression model with the best predictive power were: number of protective devices, maximum gust wind speeds, hurricane indicator, and utility company indicators. Zhu et al. (2007) conduct storm and lightning modelling for the prediction of power system outages. The correlation between flash density and outages caused by lightning is studied and found to follow almost a linear function within a certain distance from the lines of the network.

Building on past statistical power outage estimation models, Han et al. (2009b) estimate the spatial distribution of power outages during hurricanes in the Gulf coast region of the United States using measurable hurricane parameters with generalized linear models (GLMs). Han et al. (2009a) improve the predictive accuracy of hurricane power outage forecasts using generalized additive models (GAMs) comparing to previously used GLMs. Guikema (2009) used an approach based on statistical learning theory to draw inferences from complex data sets. Generally, he defines the problem of spatially spread infrastructure system failure assessment as a problem of data overabundance. He argues that there is a need for statistical learning methods rather than probabilistic risk analysis (PRA) methods, which have historically been developed for problems where only limited data is available.

Nateghi et al. (2014) present a power outage estimation model for tropical cyclones based on the method of random forests, using data from a power distribution system serving two states in the Gulf Coast region of the United States. One result is that estimates of system reliability based on wind speed alone are not sufficient for adequately capturing the reliability of system components. Guikema et al. (2014) aim for a predictive model in advance of a hurricane that is applicable not only to a specific utility company but along the full US coastline, using only publicly available data of upcoming hurricane events. The response variable is the number of customers without power supply in each grid cell of the study area. Important hurricane parameters are the maximum 3 second gust wind speed and the duration of time with wind speeds exceeding 20 m/s. Further parameters taken into consideration in the random forest model include land cover, soil moisture, and topography (elevation).

The statistical models presented above are relatively strong in predicting regional outages due to distinct hazards but tend to not have sufficient resolution at the network topology and the component fragility level. Therefore, they do not provide enough information and

understanding about actual causal relations and processes within the networks (Mensah and Duenas-Osorio, 2014).

3.2 System modelling approach

The studies presented in this section aim at a resilience, risk, or reliability assessment for civil infrastructure systems while considering their response to destructive events at the system level by simulating the system behavior. A main and mostly common goal of these studies is to be able to predict the possible network damages and to contribute to better pre-disaster mitigation and post-disaster recovery actions or to identify the importance that each network component has in maintaining network connectivity or optimal flow. One crucial task in this context is to find or develop performance metrics for quantifying (generic) network functionality. In Table 3, an overview on selected studies is listed. As introduced in Chapter 1.1, dependencies in systems have been studied from different perspectives. The review here is limited to studies that account for the problem of dependent component failures (CCF) due to hazardous events.

The first three studies listed in Table 3 and the study by Cavalieri et al. (2014) have in common a focus on infrastructure exposed to seismic hazards. Dueñas-Osorio (2005) approached the problem with an emphasis on the network topology for potentially interdependent network types, e.g. the interplay between water distribution and power grids. He used a probabilistic response characterization of networked systems when subjected to internal or external disturbances from seismic hazards. The probability of component failure given seismic ground motion is computed using the fragility curves implemented in Hazus-MH, a methodology and natural hazard analysis tool developed by the Federal Emergency Management Agency (FEMA). An overall network performance measure that is often used is the connectivity loss, which is computed as the ratio of the number of lost paths between supply and demand facilities to the number of the paths within the infrastructure system prior to damage. Dueñas-Osorio (2005) and Adachi (2007) examine interdependent water distribution and power transmission systems employing a probabilistic seismic hazard analysis. A model of spatial intensity correlations of earthquake ground motion for the vulnerability assessment of distributed infrastructure facilities is implemented additionally in Adachi (2007) as compared to Dueñas-Osorio (2005). The functional interactions among facilities are modelled by fault trees, and the impact of cascading failures on serviceability of a networked system is computed by a procedure based on the concept of shortest paths. One further study in this direction by Dueñas-Osorio and Vemuru (2009) models the seismic risk to power infrastructures. They account for cascading failures and state that the additional loss of performance due to cascading failures can be orders of magnitudes larger than the initial loss of performance regardless of the hazard type. The assessment framework is applied to the IEEE 118 node and the IEEE 300 node

power transmission test systems exposed to seismic and lightning hazards as well as random hazards and targeted attacks. It is stated that improvement of the network component tolerance alone does not ensure system robustness or protection against disproportionate cascading failures. The authors state that managing the risk of network unavailability requires a combination of redundant topology, increased flow carrying capacity, layout homogenization, and deliberate inclusion of weak links for network islanding. Cavalieri et al. (2014) assess power networks subjected to seismic hazards with varying intensity. Different modelling approaches concerning the network performance are compared based on Monte Carlo Simulation. Two models use connectivity-based measures and further three models use power flow analysis. The IEEE 118 test case is used for illustration purposes assuming that the test case is in central USA. A main result is that models reflecting accurate power flow are needed if the actual performance of the systems is of interest.

Several contributions are interested in hurricane hazards causing damage to infrastructure systems. Winkler et al. (2010) conduct a performance assessment of topologically diverse power transmission and distribution systems subjected to hurricane events at the US Gulf coast based on component fragility models predicting failure probability for individual transmission and distribution power network elements. They combine hurricane damage predictions and topological assessments to characterize the impact of hurricanes on power system reliability. Simulated hurricane events are applied to measure the hurricane reliability of three topologically distinct transmission networks. Performance is measured in terms of the largest connected component (LCC) after a damage event. Reliability is found to correlate directly with topological features, such as network meshedness, centrality, and clustering: the compact irregular ring mesh topology is identified as particularly favorable.

Ouyang and Dueñas-Osorio (2012) develop a time dependent resilience metric for urban infrastructure systems using the IEEE RTS 96 test case and the power transmission grid in Harris County, Texas, USA as examples. The modelling of the system evolvement and improvement mechanism is supposed to reflect possible inter-hazard interactions such as the occurrences and the effects of future hazards, which are affected by previous hazards and cannot be addressed by static resilience analysis. The study wants to contribute to a better assessment of long-term effectiveness of resilience-inspired intervention strategies to support decision making. Strategies like the enhancement of situational awareness, management of consumer demand, and integration of distributed generators are simulated. Finally, the authors found that there might be counter-productive effects of short term versus long term resilience improvement measures.

Another study by Ouyang et al. (2012) focuses on the development of an expected annual resilience metric for single hazards and multiple hazards. The study is also applied to the power transmission grid in Harris County, Texas, USA as well as to modified networks to compare their resilience while accounting for power redistribution processes. Resilience is measured by the number of normally operating components within the system, and cost is quantified in terms of impact area size. It is concluded that the expected annual resilience is mainly compromised by random hazards due to their higher frequency of occurrence

relative to hurricane hazards. Measures like deploying redundancy, hardening critical components, and ensuring rapid recovery all entail effective responses. The authors claim that further refinements can be made towards other, e.g., social, organizational, and economic responses.

Similar to the studies above, Javanbakht and Mohagheghi (2014) conduct a $(n-k)$-contingency analysis using an AC power flow model to assess the response to hurricane events. The IEEE 118 test case system is used and georeferenced while assuming to be located in Texas, USA. In contrast to the previous studies, the hurricane parameters are modelled with historical data on past hurricane events in the United States and are then used to simulate hurricane events. The outage probability of transmission lines affected by the wind field is calculated. The specific focus of this study is on the operational action of power generation dispatch before an imminent hazard event, which is supposed to be an effective mitigation measure for grid operators.

Ouyang and Dueñas-Osorio (2014) follow a probabilistic modelling approach in order to quantify the hurricane resilience of contemporary electric power transmission and distribution systems similar to the studies above. They implement a hurricane model, component fragility models, a power system performance model based on DC-flow equations, and a system restoration model. They suggest several improvement strategies in relation to the restoration time, resource mobilization, and enhancement of the rate of underground lines. One aspect of the study is the model calibration using the outage and restoration data after Hurricane Ike (2008). As in most of the studies in the domain, a consequent validation with real data is vague or missing, supposedly due to lack of data, Table 3.

Compared to the studies above, the contribution by Panteli et al. (2017) stands out with respect to the fragility modelling approach. Several of the studies mentioned used assumptions and parameters prescribed in the HAZUS application of FEMA (Vickery et al., 2006) in order to model their fragility of system components. The development of fragility curves is one focus point in Panteli et al. (2017) and is conducted based on structural analysis for transmission towers and based on statistical analysis for transmission lines specifically for the power grid of Great Britain. Furthermore, in Panteli et al. (2017) a focus is laid on component rankings based on the Risk Achievement Worth (RAW), a convenient component reliability measure. The results show the resilience of power systems to severe weather and demonstrate that the criticality of network sections depends on the hazard intensity.

Table 3: Example studies in the field of infrastructure resilience and reliability against the backdrop of natural hazard impacts.

Study	Hazard type considered	Hazard model	Infrastructure type	Component fragility model	Network model/ performance measure	Cascading failure	Component importance	Network improvement strategies	Simulation method	Calibration/ Validation / Sensitivity analysis
Dueñas-Osorio (2005)	Earthquake	Hazus-MH	Interconnected networks: power and water supply	Generic fragility curves (Hazus-MH)	Graph efficiency, connectivity, service flow reduction	-	yes	Improvement in interdependent networks	Monte Carlo	-
Adachi (2007)	Earthquake	Hazus-MH, upper and lower bounds of spatial correlations	Interconnected networks: power and water supply	Generic fragility curves (Hazus-MH)	Based on shortest paths	yes	-	-	Monte Carlo	Sensitivity analysis
Dueñas-Osorio and Vemuru (2009)	Earthquake, lightning, targeted attacks	Hazus-MH	Power transmission (IEEE 118, IEEE 300)	Generic fragility curves (Hazus-MH)	Graph efficiency, connectivity loss	yes	-	Topological mitigation actions: reducing the vertex degree of the four most connected nodes	Monte Carlo	-
Winkler et al. (2010)	Hurricane	Empirical model calibrated with Hurricane Ike 2008	Power distribution and transmission with main focus on transmission	Fragility curve parameters based on Hazus-MH, ASCE standards and literature	Largest connected component (LCC)	-	-	-	Monte Carlo	Validation against ZIP code data of affected customers in historical events
Ouyang et al. (2012)	Hurricane and random hazards	Hazus-MH	Power systems	Based on Winkler et al. 2010	Response considering time for restoration, number of components in function	yes	yes	Improvement of fragility curve mean values; assumption of shorter recovery response times and better recovery sequences	Monte Carlo	-
Ouyang and Dueñas-Osorio (2014)	Hurricane	Hazus-MH	Power distribution and transmission	Generic fragility curves (Hazus-MH)	Loss of load based on DC power flow model	-	-	Improvement of restoration time and resource mobilization, increase of the rate of underground lines	Monte Carlo	Calibration based on outage and restoration data after Hurricane Ike in 2008
Javanbakht and Mohagheghi (2014)	Hurricane	Wind field model based on analysis of Hurricane Katrina	Power transmission (IEEE 118)	Line failure probability based on assumptions; dependent on wind speed	Loss of load based on AC power flow model in Matpower	-	-	-	Monte Carlo	Parameter variation
Cavalieri et al. (2014)	Earthquake	Shake-field models based on SYNER-G project (2011)	Power transmission (IEEE118)	Fragility curves with parameters: median peak ground acceleration (PGA) and standard deviation of natural logarithm of PGA	Comparison of five models: efficiency, connectivity, flow-based models	-	-	-	Monte Carlo	-
Panteli et al. (2017)	Wind storms	Historical data	The reduced 29-bus Great Britain power transmission network	Fragility curve calibration based on individual case studies	Loss of load frequency per year, energy not supplied per year	-	yes	Improvement of resilience indices based on RAW rankings	Sequential Monte Carlo	-

3.3 Summary

Against the backdrop of the research questions described in Chapter 1.2 and the importance of power outage damage estimation discussed in Chapter 2, the concerned literature of the last decades is reviewed. The focus in the considered publications is on the modelling of the vulnerability, resilience, and reliability of infrastructure networks in the context of natural hazard impacts.

Part II – Methodology

4 General analysis framework

The general framework, which is proposed and employed in this thesis, is summarized in Figure 10. This general framework is later adapted in selected aspects for the individual case studies, as explained further in the corresponding Chapters 8-10. The principle elements of the reliability assessment used in this thesis are introduced in detail in the following Chapters 5 to 7. Chapter 5 is about network reliability analysis methodologies in general. Chapter 6 is an introduction to the concept of component fragility, based on structural reliability concepts. Chapter 7 introduces and discusses different deterministic versus reliability-based component importance measures.

Hazard representation and component dependencies

In this thesis, hazard modelling approaches are based on spatial random fields (SRF). In general, SRF models of either the hazard intensity (wind speeds) or the component failure probability are developed. This produces, within a Monte Carlo simulation process, SRF realizations of the wind field or directly of the component failure probabilities. The models are either based on historical hazard data (Chapter 8.2 and 9.2) or based on assumptions on the level of component failure rates for a generic hazard representation (Chapter 10.3). In the latter case study, a model with a varying correlation length parameter is examined in order to assess the effect of a varying SRF dependence structure on the system reliability and component importance.

An overview of the dependence types and how they can be treated is given in Chapter 5.3.

Component fragility

In the case studies that represent wind speeds via SRF simulations (Chapter 8.2 and 9.2), the explicit modelling of the component fragility is necessary. The fragility describes the probability of component failure given a hazard intensity/load (e.g. wind speed in m/s). Fragility is a probability defined conditional on loads to which the system might be exposed. Based on this probability, Monte Carlo Simulation is used to generate data sets of (binary) component failure sets, so called contingencies where m components out of total n components are in a failure state. These failure sets are then linked to the associated network performance and potential initial as well as cascading damages. In Chapter 6.2, the concept of component fragility is introduced.

The use of fragility in risk and reliability analysis is elaborated in Chapter 6.3. Generally, the fragility concept can be used in a risk assessment in the following way:

$$Risk = E_{h,d}[cost] = \int_H p(h) \left[\int_D p(d|h)\, cost(d,h) dd \right] dh \quad (1)$$

The risk as defined in Equation (1) is the expected value of the costs of a hazard equal to the integration over the hazard and damage outcome space: $p(d|h)$ is the probability distribution of damage d conditional on a hazard intensity h; it describes the fragility. $cost(d,h)$ is the cost as a function of damage and hazard intensity, it describes the exposure; $p(h)$ is the probability distribution of the hazard intensity.

Network performance and reliability

In order to estimate the potential damages caused by initial triggering component failures one needs 1) a network representation and 2) a network performance model.

Based on the performance definition, the network reliability, $1 - \Pr(failure)$, is quantified accordingly. Performance indices can be the system failure probability itself, the loss of graph efficiency, the loss of power load, the number of lines out of service or the loss of source-target (s-t)-connectivity. In case of the modelling based on power flow equations or the graph efficiency concept, it is a goal to also model and represent cascading failure processes in the network that are caused by load propagation after initial triggering events.

The reliability concept that is used in this thesis is defined in Chapter 5.2.1, followed by some principle performance measures in Chapter 5.2.2 and 5.2.3. Different network performance models are applied as explained in Chapter 5.4.

Component importance and network improvement strategies

In Chapter 7, the concept of component importance is introduced, starting with deterministic measures to indicate network components with outstanding (topological) characteristics (e.g. in terms of betweenness). In Chapter 7.2 and Chapter 7.3 reliability importance measures (IM) are discussed for a) binary state systems and b) for systems with continuous performance and reliability measures. A differentiation of IM in cascading failure events is defined in Chapter 7.4. The goal is to find the components with the highest impact on the overall network reliability and to differentiate the components important for the initiation of network damages versus the components important for the further damage propagation. The component rankings are used to establish reliability enhancement strategies as explained in Chapter 7.5. A line (segment) strengthening relates to the initial component failure probability and a line capacity increase relates to the network performance model and vulnerability to power overload propagation. In the case studies in Chapter 9 and 10, component importance rankings are calculated in the modelling process and several component improvement strategies are tested and compared based on selected rankings.

Reliability evaluation

The results of this thesis are produced based on Monte Carlo simulations, see Chapter 5.5. The Monte Carlo approach is a scenario-based model, with a large number of numerically generated scenarios. As illustrated in Figure 10, each Monte Carlo sample is a scenario comprising:

1) A hazard representation, i.e. a maximum wind speed value at each location, with an explicit consideration of the spatial correlation in the hazard (the wind field),
2) A sample for each component from a Bernoulli distribution with parameter equal to the probability of failure resulting from the fragility curve whose argument is the sampled wind speed at the location,
3) A resulting vector of initial and final failure states of the network components
4) A resulting value for the network performance

This allows to compute the component importance measures considering the spatial correlation of the hazard and to reevaluate component measures and component rankings after network modifications.

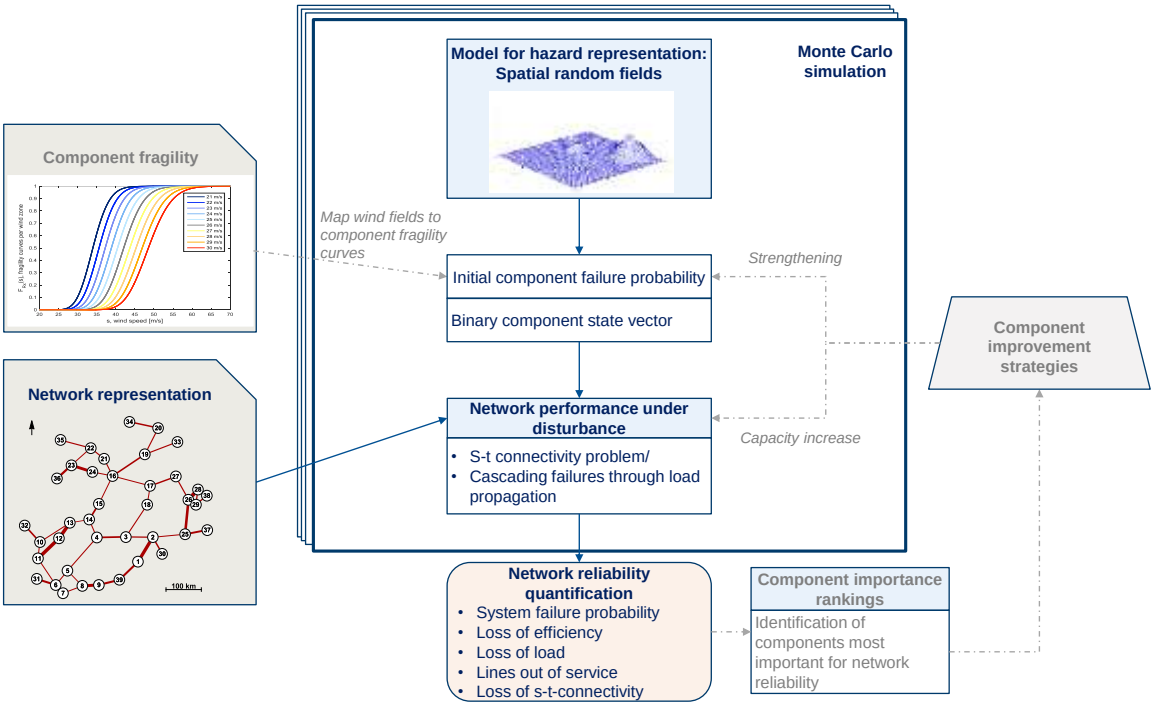

Figure 10: General network reliability analysis framework applied in this thesis. Dashed lines indicate steps that are not considered in every case study of this thesis.

5 Network reliability analysis

This chapter presents selected concepts for reliability analysis of network systems. In Chapter 5.1, the term graph/network is introduced based on graph theory. Next, in Chapter 5.2 the term reliability is defined in general, and approaches to model network performance and to define network reliability are developed. Relevant sources for dependencies in networks are discussed in Chapter 5.3. One of the central problems is how to model the network performance after initial component failures in the course of potential cascading failure events (Chapter 5.4). Finally, in Chapter 5.5, some overall assessment methods are discussed and compared: analyses based on deterministic methods versus analyses based on Monte Carlo Simulation as a central concept used in this thesis.

5.1 Network formulation as complex graph

In the literature, the terms “critical infrastructures” or “lifelines” are used in the context of civil infrastructure modelling, (e.g., Murray and Grubesic, 2007, Guikema, 2009, Zio, 2014, Johansson and Hassel, 2014). These terms categorize systems that a society relies upon and are, therefore, rather critical for a functioning and safe daily life, which is essentially true in one way or the other for all types of civil infrastructures (European Council Directive 2008/114/EC). In this thesis, the terms network and graph modelling concepts are used for these kind of critical infrastructures.

The term “complex network” stems from graph theory, a subdomain of mathematics and a relatively young field of research, e.g., Floyd (1962), Sedlacek (1968), Aigner (1984), and Strogatz (2001). From a graph theory perspective, a network can be defined as graph with vertexes and edges that own certain attributes, for instance name, nature, state, function. Often the terms network and graph are used interchangeably in this context. The attribute “complex” is assigned to networks that have a non-trivial topology, as opposed to regular graphs, e.g. lattices or random graphs (Albert and Barabási, 2002). Many real-

world infrastructure systems exhibit a non-trivial topology, often those networks were developed over time in a non-regular way. In graph theory, static and dynamic properties of networks are studied, where the static properties relate to the topology of the system and the dynamic properties relate to the function and behavior of the components and of the whole system.

From a system reliability perspective, a system is complex when the reliability block diagram (RBD) either cannot be reduced to a series-parallel structure with independent elements or does not exist at all. The latter is the case for instance if more than two states or more than one failure mode of an element have to be considered (Birolini, 2007). Often, the components are physically and functionally heterogeneous, and might be organized in a hierarchy of subsystems. Complexity can be of both structural and dynamic type: structural complexity manifests through the heterogeneity of components, through a large number of components that might be highly interconnected and (inter-) dependent. Dynamic complexity manifests through the (often unexpected) system behavior in response to changes in the environmental and operational conditions of its components and compartments.

5.1.1 Undirected and weighted graphs

Applying a complex graph representation, the infrastructure network is described by a graph object G consisting of a set of nodes (vertices) $N = \{n_1, \dots, n_n\}$ and a set of lines (edges or links) $L = \{l_1, \dots, l_l\}$:

$$G = (N, L) \tag{2}$$

The $n \times n$ adjacency matrix $\boldsymbol{A} = \{a_{ij}\}$ of the graph G describes its topology. If there is a direct line between i and j, the entry a_{ij} in $\boldsymbol{A}$ is the weight assigned to the line. The entry a_{ij} takes value zero if no direct line between nodes i and j exists. In case all non-zero entries a_{ij} of the adjacency matrix are set to one or a constant for the entire network, i.e. all connecting lines have the same weight, the graph/network describes an unweighted graph.

G is an undirected graph if it holds that $a_{ij} = a_{ji}\ for\ all\ i, j$, i.e. if the adjacency matrix of the graph is symmetric. A directed graph has an asymmetric adjacency matrix, i.e. the connections between two nodes can be assigned differing values in both directions.

An example network model together with its adjacency matrix can be seen in Figure 11; it is an example of an undirected, unweighted graph with 8 nodes and 9 lines, where node 8 is disconnected from the remaining network, i.e. no lines link the node 8 to the other nodes. Node 1 is a so-called leaf node, i.e. only one line connects node 1 to the connected rest of

the network. In Figure 12, the example is modified for the case of weighted lines. The weights in the graph may represent quantities as diverse as, e.g., line length, line reactance, power flow through the line, line failure probability, and line importance according to certain criteria. In general, also the nodes can be assigned appropriate attributes, e.g. flow production/generation, demand, capacity, resistance.

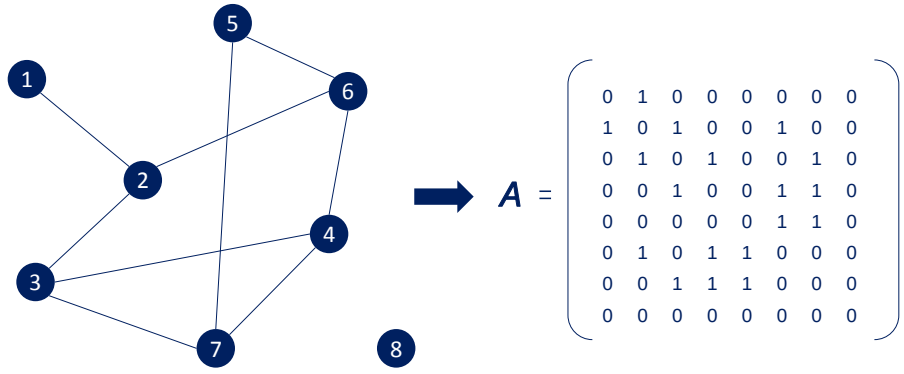

Figure 11: Example network and its corresponding adjacency matrix, $\boldsymbol{A}$. Node 8 is disconnected from the remaining network, i.e. row 8 and column 8 of $\boldsymbol{A}$ consist of only zero elements. Node 1 is a leaf node, i.e. only one line connects node 1 to the rest of the network.

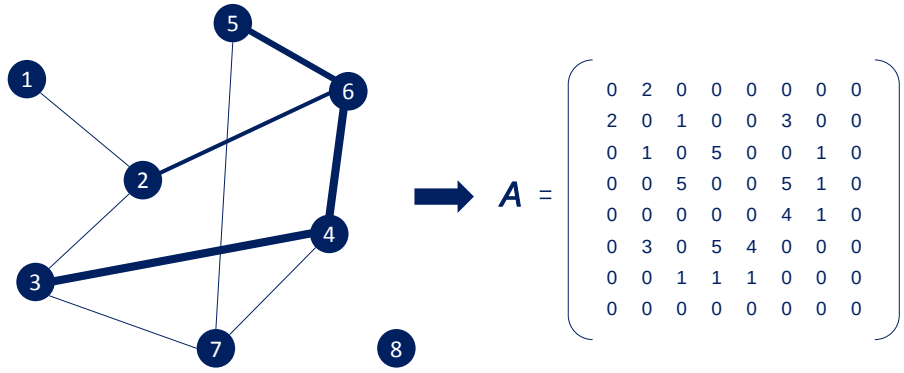

Figure 12: Example network from Figure 11 with line weights and corresponding adjacency matrix, $\boldsymbol{A}_{\boldsymbol{weighted}}$. The line weights are indicated by their assigned line thicknesses.

The graph representations can be the base for a network model. Generally, network models can be classified as 1) topological models, which are exclusively described by the network's graphical layout, 2) flow models, which additionally consider the capacity of each line and node and 3) physical models that consider at least some selected physical processes of flows in the network. This is discussed in more detail in the context of reliability analysis methods in the following sections.

5.1.2 Graph characteristics

There are numerous indices to describe the graph's characteristics. Only some metrics are introduced here, for a further review see e.g., Newman (2003) and Newman (2008). Several pertinent indices, like the vertex degree distribution, the $characteristic/\ average\ path\ length$, or the network average $clustering\ coefficient$ are explained in the following.

In an undirected graph $G(N, L)$ with N-set of vertices and L-set of edges/ lines, the $node\ degree$ is the number of connections the node has to other nodes. The node/vertex degree distribution is the statistic over all $node\ degrees$ of all nodes in the network. For some network types, e.g. the so-called scale-free networks, the degree distribution follows a power law, Equation (3).

$$P(k) \sim k_{n_i}^{-\gamma} \tag{3}$$

with γ typically being $2 < \gamma < 3$. This means that the fraction of nodes $P(k_{n_i})$ that have number of k_{n_i} connections follows the power law for large values of k. Scale-free networks have drawn attention in research (e.g. Motter et al., 2002), as they have specific interesting characteristics: They have a few nodes with a $node\ degree$ that highly exceeds the average $node\ degree$; so-called hubs. Hubs are mainly neighbored by nodes with smaller degree, which are again neighbored by nodes with even smaller degree. This circumstance makes the networks relatively fault tolerant to random failures since the probability that a hub, and thus a very important node is hit, is relatively small or sometimes even negligible.

The $average\ path\ length$ of a graph is the average number of steps along the shortest paths for all node pairs in the network.

$$L_G = \frac{1}{n(n-1)} \sum_{i \neq j} \delta_{ij} \tag{4}$$

δ_{ij} is the shortest distance between node i and node j. The $graph\ diameter$ should not be confused with the shortest distance across the graph. The diameter of a graph is the maximum of all shortest paths between any node pair in the network: $\delta_G = \max(\delta_{ij})$.

The $averge\ clustering\ coefficient$ as suggested by Watts and Strogatz (1998) can be defined as follows:

$$C_G = \frac{1}{n}\sum_{i=1}^{n} c_i \tag{5}$$

A node n_i has k_{n_i} neighbors including n_i itself; at most $\frac{k_{n_i}(k_{n_i}-1)}{2}$ lines can exist between the node and its neighbors; c_i is the fraction of these maximum lines that actually exist; C_G is the average over all c_i in the network.

There are some special cases of network topologies, see Figure 13. A regular graph, e.g., a lattice network, has typically both a rather high $average\ path\ length$ and a rather high $averge\ clustering\ coefficient$: $L_{G_{regular}} \sim \frac{N}{2K}\ (high),\ C_{G_{regular}} = \frac{3}{4}\frac{k-2}{k-1}\ (high)$ (Ball and Coxeter, 2010). In turn, in a random graph, both characteristic measures obtain rather small values: $L_{G_{random}} \sim \frac{\ln N}{\ln(k-1)}\ (small),\ C_{G_{random}} \sim \frac{k}{N}\ (small)$.

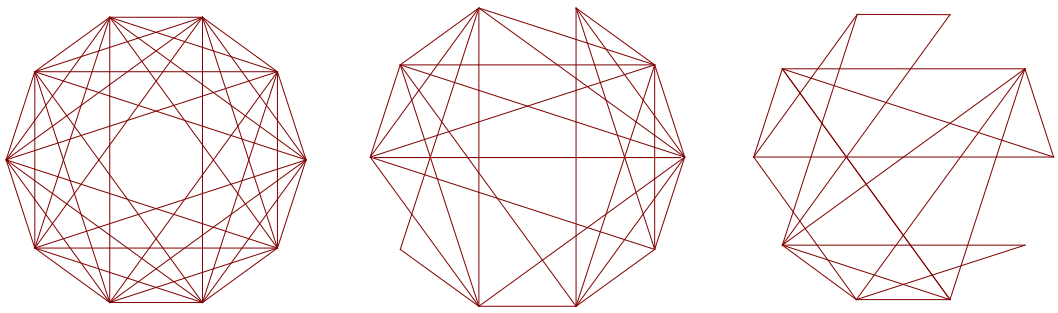

Figure 13: Three examples of (undirected) graph types. Left: regular lattice graph, where each node has the same number of neighbors. Middle: example of a small-world network which is highly clustered, yet with a small characteristic path length. Right: random graph with complete randomly connected nodes.

In some cases, power grids have been identified as so-called small world networks (Watts and Strogatz, 1998): small world networks are highly clustered like regular lattices and have at the same time a small characteristic path length like random graphs. Studies in the field of graph theory are made, e.g., for different graph types: random graphs, small-world graphs, and scale-free graphs with and without high local clustering: E.g., Holme et al. (2002) showed that random graphs and small-world graphs are equally vulnerable to random or targeted attacks, whereas scale-free graphs are resilient to random disturbances, but also highly vulnerable to targeted attacks.

Making inference from graph characteristics about its vulnerability, performance, or reliability is a challenging task and matter of intense research (Watts and Strogatz, 1998, Latora and Marchiori, 2001, Girvan and Newman, 2002, Motter et al., 2002, Crucitti et al., 2003).

As described in detail by Albert and Barabási (2002), mathematical networks or graphs are widely used in the natural and social sciences to model the behavior of systems with many components. At a first glance, one might think that the more connections a network has, the stronger it is against external impacts. One illustration given in Verma (2012) shows the uncertainty of this assumption: e.g. in a social network, more connections mean stronger relations between persons and perhaps better exchange of information. At the same time, more connections would also mean a more efficient spreading of a virus among connected persons. This can be transferred to the case of power grids, where many connections would mean a good connectivity, but also the potential for consequent cascading failures.

5.1.3 Alienability of graph representations to power networks

With the goal to reduce complexity in the analysis of power grids, i.e. to enhance computational efficiency, power grids are often represented as complex weighted graphs in literature (e.g., Motter and Lai, 2002, Crucitti et al., 2004b, Crucitti et al., 2005, Holmgren, 2006, Rosas-Casals et al., 2007, Arianos et al., 2009, Rosas-Casals and Corominas, 2009, Wang et al., 2010, Panigrahi, 2013, Zuev et al., 2015). Thus, power grids are modelled as a graph consisting of lines and nodes. Nodes represent components that can be assumed to be localized at one point coordinate. Lines stand for the distribution/ transmission elements connecting those point coordinates. In a graph representation of a power transmission grid, nodes typify generation buses, transmission poles, and distribution buses, or substations and load points. Lines model the transmission cables and transformers (Adachi, 2007). Further, it would seem reasonable to use a weighted, undirected graph, e.g. the reactance values of the transmission lines as line weights. The reactance of a transmission line is an indicator of the amount of power flowing through a line under the assumption of lossless conditions (Saccomanno, 2003, Dwivedi et al., 2009). The lower the reactance of a path between two nodes, the more power may flow through the path in principle.

For the IEEE 39 benchmark system introduced in Chapter 2.3.1, an example is illustrated in Figure 14: On the left side, the classical illustration as a circuit diagram of the power grid is shown, on the right side, the power grid is illustrated as a georeferenced graph object with weighted lines (reactance values).

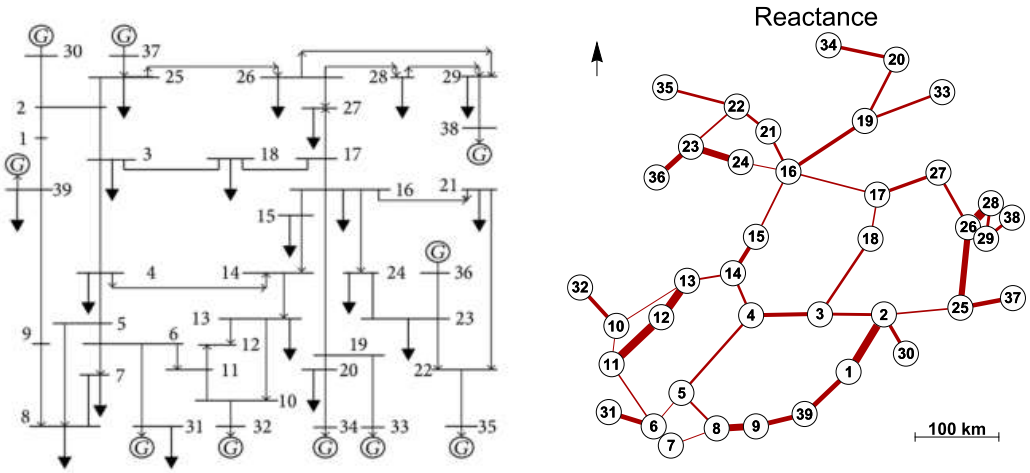

Figure 14: Left: The IEEE 39 bus system. Right: The IEEE 39 as a complex graph with geo referenced nodes and weighted lines, here line thicknesses indicate the reactance values of the lines.

5.2 Concepts of network performance and reliability

In the following, selected concepts are summarized from reliability engineering and specifically from system reliability as introduced in Chapter 1. These selected concepts are specifically formulated and prepare and represent the framework and the terminology to be employed in the subsequent chapters.

5.2.1 Reliability definition

The reliability of a component or system $R(t)$ is defined as the probability of functioning under given environmental and operational conditions and for a stated period of time t, ISO 8402, (Rausand and Høyland, 2004, Lê, 2014). The reliability $R(t)$ is a function of time, which is not made explicit in the following definitions. In systems where failures are not repaired and where no maintenance is conducted, the term availability can be used interchangeably with reliability: $A(t) = R(t)$ (Straub, 2017). For a more detailed introduction to the principles, the reader is referred to e.g., Rausand and Høyland (2004). Network reliability analysis can serve system architects as a tool to identify weaknesses in systems and to quantify weather a system meets reliability acceptance criteria.

In reliability and risk analysis models, many factors of interest are treated as random variables (RV). This allows the qualification and the probabilistic estimation of selected parameters and inherent uncertainties in the system. A key challenge is to capture all possible failure modes of the system depending on the random variables such as input stimuli, network settings, and, dynamics in the system topology. Therefore, to quantify and estimate the reliability and risk of a system, it is necessary to know the probabilities of relevant combinations of conditions leading to system failure under uncertainty. Since reliability is the complement of the probability of failure, the commonly used reliability measure p_S can be formulated as:

$$p_S = Pr(X_S = 1) = 1 - p_F = 1 - Pr(X_S = 0) \tag{6}$$

With the index s indicating system reliability, $X_S = 1$ being the event of system functioning, and, $X_S = 0$ the event of system failure.

In the course of the following definitions and statements, it is assumed that the network nodes have a failure probability of zero, i.e. they are perfectly reliable. In Colbourn (1987) it was shown that a network problem, where node failures are considered, can be reduced in polynomial-time into an equivalent problem with line failures only. In case a node failure occurs, it can be translated into the corresponding line failures of the lines that connect the specific node to the network.

5.2.2 Binary networks based on the connectivity problem

The complexity of the analysis is reduced to some extent if the system can be defined as a binary system. This is a system, in which all individual components and the system itself can only be in either an UP (functioning) or a DOWN (failure) state. This means that the components are modeled by binary random variables X_{l_i}. The component states are collected in the so-called component state vector $\boldsymbol{x_l} = \left[x_{l_1}, x_{l_2}, \dots, x_{l_l}\right]^T$, i.e. an l-tuple; l components (e.g. network lines) whose states are described by binary outcomes $x_{l_i} \in \{0,1\},\ i = 1, 2, \dots, l$:

$$x_{l_i} = \begin{cases} 0 & \text{if component } l_i \text{ is in a failure state (DOWN)} \\ 1 & \text{if component } l_i \text{ is in a non} - \text{failure state (UP)} \end{cases} \tag{7}$$

Each component is characterized by its reliability (i.e. probability of functioning) $p_{l_i} = \Pr\left(X_{l_i} = 1\right)$.

In case that the system state is unambiguously determined by the state vector, i.e. no additional uncertainty would influence the system state (i.e. static networks), the relation between component and system states can be described by a so-called structure function $\phi(\boldsymbol{x}) = \phi(x_{l_1}, x_{l_2}, \dots, x_{l_l})$. The binary structure function $\phi: \{0,1\}^l \rightarrow \{0,1\}$ returns the value of the system state dependent on the combination of component states x_{l_i} for all possible $\boldsymbol{x_l}$:

$$\phi(\boldsymbol{x_l}) = \begin{cases} 0 & \text{if the system is in a failure state} \\ 1 & \text{if the system is in a non} - \text{failure state} \end{cases} \quad (8)$$

Since the component states of vector $\boldsymbol{x_l}$ are random variables, the system state $\phi(\boldsymbol{x_l})$ is also a random variable. For a risk and reliability assessment of a system, the goal is to estimate the probability of the structure function becoming zero:

$$p_F = \Pr[\, \phi(\boldsymbol{x_l}) = 0] \quad (9)$$

The system reliability is written as $p_S = \Pr[\, \phi(\boldsymbol{x_l}) = 1]$.

In other words, the structure function determines the system state variable X_S:

$$X_S = \phi(\boldsymbol{x_l}) \quad (10)$$

In order to quantify the system reliability p_S, models are required that describe the system and its performance in function of the state of the system components, i.e. the structure function needs to be specified. In case of purely topological (static) network models, the structure function depends on the topology of the network and could e.g. be defined through the connectivity problem: Since infrastructure systems are designed to transfer goods or flows between sources (generation nodes) and destinations (load nodes), those nodes must remain connected (e.g. via by-pass) in order for the network to fulfill its function. Hence, the performance metric in many network reliability studies based on topological models is the (source-target) connectivity, which verifies the existence of a path from the origin to the destination node(s), e.g. Motter and Lai (2002), Newman (2003). The connectivity can also be expressed as the probability that all target nodes are connected to defined source nodes of the system. Performance measures of the static network that are used extensively in graph theory are e.g. based on Ball and Colbourn (1992):

- **Source-target (s-t)-connectivity:** the probability that there exists a path between two specified nodes.
- **Overall connectivity (or all-target connectivity)**: the probability that the network is overall connected, i.e. no component is isolated.

- **K-terminal measure**: the probability that a subset of nodes, K, is connected to the network.

Testing for connectivity for small networks is unproblematic. In order to test a larger network for connectivity a number of efficient path search algorithms are available in the literature. The Dijkstra-algorithm (Dijkstra, 1959) has been broadly used. This algorithm solves the single source-target shortest path problem, if the source-target connectivity is fulfilled between a prescribed node pair. Furthermore, also the overall connectivity problem can be solved with the Dijkstra-algorithm: if there exists one shortest path between all node pairs in the network, the overall connectivity is fulfilled. An alternative algorithm in the literature, the Floyd-Warshall algorithm, finds all node pairs shortest paths at once (Floyd, 1962).

Connectivity is often defined as the minimum necessary condition for a network to function followed by further and maybe more sophisticated measures such as travel time or flow capacity (Rokneddin, 2013), as explained in the next section.

5.2.3 Non-binary networks based on continuous performance functions

Network performance can be defined through a variety of concepts. In literature, there is a wide range of different approaches: logical, topological, flow and physically based, and empirical models. In this section these are going to be discussed further in the context of performance metrics defined in the real space. Shpungin and Gertsbakh (2009) and Ball and Colbourn (1992) give a broad introduction to the field, and several examples for performance models are evaluated.

As introduced under Section 5.2.2, network components are modeled by binary random variables X_{l_i}. The component states are collected in the component state vector $\boldsymbol{x_l} = \left[x_{l_1}, x_{l_2}, \dots, x_{l_l}\right]^T$, with $x_{l_i} \in \{0,1\},\ i = 1, 2, \dots,\ l$.

In principle any meaningful input-output model can be used that quantifies the network performance based on a function τ: $\{0,1\}^l \rightarrow \mathbb{R}$, i.e. the performance is measured by a continuous variable. The function or model τ is used to quantify the degree to which the network provides a required service dependent on the component states, such as power supply.

Consequently, the system failure domain can be described e.g. by the performance falling below a prescribed critical threshold value, $t \in \mathbb{R}$. Thus, the system state variable S with $s \in [0,1]$, can be described by a binary variable in the following way:

$$x_S = \begin{cases} 0 & \text{for } \tau(\boldsymbol{x_l}) < t \\ 1 & \text{for } \tau(\boldsymbol{x_l}) > t \end{cases} \tag{11}$$

The system failure probability can then be calculated analogous to Equation (9):

$$p_F = \Pr[\, \tau(\boldsymbol{x_l}) < t] \tag{12}$$

One main task in network reliability analysis is to compute the probability of the failure domain of the network, p_F.

Example performance models or measures are:

- **Shortest path models:** The problem of finding a path between two nodes in a network such that the sum of the weights of its constituent lines is minimized. Based on all shortest paths between all node pairs, indicators can be built that describe the network performance, e.g. the graph efficiency (Motter and Lai, 2002). The concept of graph efficiency is applied in this thesis, and it is explained in more detail in Chapter 5.4.
- **Maximum flow models:** The problem of how much flow/capacity is available between specified source and target nodes without specific modelling of the flow dynamics in a supply network (Ford and Fulkerson, 1956).
- **Physical flow models:** The question of how much supply can be performed overall in the network, taking all source and target nodes into account; the attempt to model and solve the actual (dynamic) flow problem on the network. One implementation of power flow modelling is presented in this thesis and explained in more detail in Chapter 5.4.2.

Applications of physical performance measures are used, e.g., in transportation or water supply infrastructure modelling. For power transmission networks, a measure commonly used is the load supply value, i.e., the sum of the load that can be supplied to customers in the grid. Further measures for power systems could be the largest component size, or components survived (Ouyang et al., 2014). Specific selected performance models in the context of component dependencies will be discussed in more detail in Chapter 5.4.

5.3 Component dependencies

By nature, every real-world system has several inherent (inter-) dependencies that can lead to component failures. In Straub (2017) and Rausand and Høyland (2004) the differentiation of dependence types is made mainly between common cause failures (CCF), cascading failures, and relief as shown in Table 4. The additional differentiation between extrinsic and intrinsic dependencies emphasizes the circumstance that dependencies can be due to external loading impacts or internal loading impacts.

Table 4: Categories of dependencies in network systems.

	Category of dependence
Extrinsic	• Common cause failures (CCF): One or more immediate or perpetual common causes or factors lead or contribute to failures in multiple components
Intrinsic	• Cascading failures: Failure of components can lead to a change of the system, e.g., a redistribution of loads, which can cause additional components to fail. • Relief: In some systems, failure of one or more components can lead to a reduced failure rate of other components

The system reliability analysis under consideration of dependent components is generally computationally more expensive than if the components are assumed to be independent. A reason for this is that the joint probability density functions (PDFs) of n component reliabilities that contain the full information on dependence among components in a binary system have size 2^n. It might be possible to explicitly specify this joint distribution for up to about 20 components but not much more. Additionally, the marginal PDFs and the dependence structure are typically changing with time t, so that the joint PDF has to be defined as a function of t. Finally, yet importantly, there is often a substantial lack of data on the actual dependence structure among component and system failures.

In order to circumvent these challenges mentioned above, often the assumption of component independence is used. Nevertheless, it is worth to study at least the sensitivity of the system performance towards an introduction of component dependences, also if no quantitative estimates of this dependence exist: Independence is in most cases a non-conservative and thus, potentially dangerous assumption (Rausand and Høyland, 2004, Straub, 2017). Fleming (1975) proved for redundant safety systems a significant increase in the probability of failure when common failure modes are considered.

Since the aim of this thesis is to account for dependencies in the network reliability analysis, the three main categories of dependencies are further reviewed.

5.3.1 Common cause failures

The term common cause failures (CCF) can be used if there are one or more immediate or perpetual common factors that lead to, or at least contribute to, correlated damage or failure events of multiple components. Probabilistic models and procedures for the treatment of CCF in system reliability analysis are described in the literature e.g., Vesely (1977), Mosleh et al. (1988), Mosleh (1991), Cheok et al. (1998), and Vaurio (1998). Bedford and Cooke (2001) as well as Rausand and Høyland (2004) give an introduction into the models of dependences in system analysis such as the beta binomial, the α-factor, or the beta-factor

models. These models have in common that they reflect the mechanisms leading to the dependence but they do not require establishing the joint PDF explicitly.

Fleming (1975) introduced the β-factor model that is commonly used to model CCF since it is rather easy to implement: It has only one additional parameter β, which can be interpreted as the conditional probability that the failure of an item is a CCF, given that the item has failed. The model assumes that all system failures are either single independent failures or common cause failures where the components of the system fail simultaneously. Therefore, a limitation of the β-factor model is that it does not allow that only a certain fraction of the components fails; this becomes an important constraint if more complex models are required to be analyzed and the role of single components is sought to be understood (Rausand and Høyland, 2004). Bedford and Cooke (2001), Rausand and Høyland (2004), and Straub (2017) suggest approaches to generalize the β-factor model in order to extend the applicability.

The context of this thesis are spatially distributed natural hazards that lead to potential CCF. As mentioned already in Chapter 3, in several previous studies this question is approached based on modelling the natural hazard intensity as a spatial random field (SRF) or based on a parametric or empirical spatial hazard model. Using the spatial characteristics of the hazard intensity, the component fragility and thus, the component failure probability can be defined. The whole assessment is often embedded into a Monte Carlo simulation in a number of studies (e.g., Dueñas-Osorio, 2005, Adachi, 2007, Winkler et al., 2010, Rokneddin, 2013, Ouyang and Dueñas-Osorio, 2014, Javanbakht and Mohagheghi, 2014, Cavalieri et al., 2014, Lim et al., 2015, Panteli et al., 2017).

In this thesis (Chapters 8-10), several approaches to account for the component dependence in the models are applied. One approach is the SRF model of wind speeds and component failure probabilities in extreme wind events based on a varying correlation length value of the random field. An illustration of three of such SRF realizations is given in Figure 15, where an increasing underlying correlation length in the fields entails decreased heterogeneity in the wind speeds and component failure probabilities.

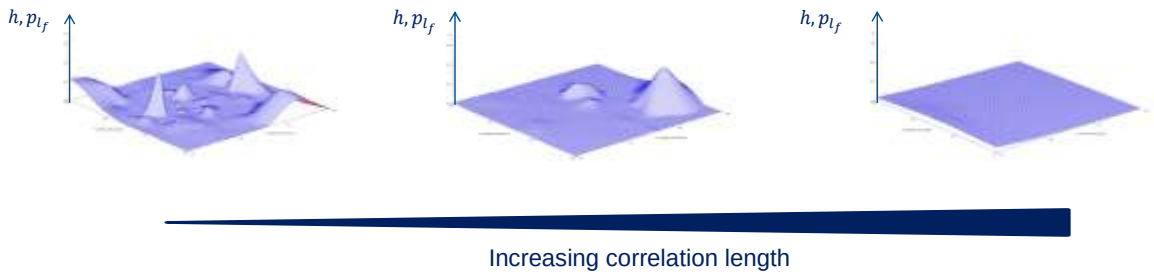

Figure 15: Spatial random field realizations of a modelled hazard intensity h of the component failure probability p_{l_f}. The underlying correlation length is increasing from the left to the right side of the three realizations, i.e. the homogeneity is increasing or the heterogeneity is decreasing from left to right.

5.3.2 Cascading failures

A cascading failure event is a sequence of failures following one or multiple initial disturbances in a network. In principle, one reason for cascading failures can be the failure propagation due to functional overloading (Daqing et al., 2014). According to their connectedness and their dependence on each other, network components might be affected, e.g., by overload when one component or a set of components fails initially. If the additional load is exceeding the affected components' tolerance levels, those components are likely to fail, and the cascading failure may subsequently spread into the network by overloading further components (Zio and Sansavini, 2011). In the context of the cascading outage, uncertainties stem from three primary sources: 1) the initiating events, 2) the sequence of dependent events that could unfold as a result of the initiating events, and 3) the ultimate costs of a blackout of a known size (Vaiman et al., 2012). Together with a prevalent lack of real failure data this makes the study of propagation behavior of cascading overload failures challenging, and thus, the investigation of cascading failures is an active field of research (Daqing et al., 2014). The cascading failure models employed in the case studies later in the thesis are explained in Chapter 5.4.

5.3.3 Relief

In some system configurations, the failure of one or more components can lead to reduced failure rates of other components (Rausand and Høyland, 2004). This "relief-effect" is a specific type of dependence between components conditioned by the dynamical loading distribution in a power transmission system.

In case of a disturbance in a part of the power grid, it might be necessary that the system operators initiate a so-called "load shedding". This is the action of intentionally curtailing service to consumers in some areas to protect the integrity of other parts of the grid. Another instance of relief is when, within a cascading failure process, the failure of some components leads to a relief of other remaining components, e.g. if load nodes are disconnected from the grid. In this thesis, these relief effects are not modelled explicitly, although they may well occur in a complex cascading sequence.

5.4 Selected network performance models

As introduced in Chapter 5.2.3 there are various options to describe the network performance, expressed in the performance function τ: $\{0,1\}^l \rightarrow \mathbb{R}$. The models applied in this thesis are presented in the following subchapters.

5.4.1 Graph efficiency-based model

Several studies apply topological measures and properties of networks from a graph theoretical perspective. Example models in the field of graph theory are Motter and Lai (2002), Holme et al. (2002), and Crucitti et al. (2004a). In these studies, after either random or targeted removal of a component, the status of the network in terms of several functionality parameters is monitored. For the topological models, the model performance is assessed by measuring e.g., the networks largest connected subgraph, the $average\ path\ length$ between nodes, or the network diameter. Furthermore, pertinent topological properties of electrical and other infrastructures include $network\ centralization$, $node\ degree$, or edge (link) distributions between network elements to identify critical components and cascading susceptibility (Winkler et al., 2010). A topological network model has been used by Winkler et al. (2010) to study cascading failures in forthcoming hurricane events. This allowed to link reliability to topological features, such as meshedness, centrality, and clustering. Winkler et al. (2010) found that the more compact and irregular a network is built, the more reliable it is.

Motter and Lai (2002) estimate the load at a node by the total number of shortest paths passing through the node (betweenness), which is altered, as soon as a node of the network fails. The model is a main base for the following model.

The efficiency of a single line e_{ij} is defined as the inverse of its reactance (line weight), π_{ij} (with $\pi_{ij} > 0$):

$$e_{ij} = \frac{1}{\pi_{ij}} \left[\frac{1}{\Omega}\right] \tag{13}$$

The efficiency of a path between two nodes is the sum of the efficiencies of the lines that constitute the path. In defining the efficiency of the network, it is assumed that the connection between any pair of nodes i and j is governed by its most efficient path.

ϵ_{ij} denotes the maximum efficiency of all paths between i and j; its inverse is $d_{ij} = \frac{1}{\epsilon_{ij}}$, the shortest electrical distance between i and j (Dwivedi et al., 2009). If there is no connection between two nodes, i.e. if they are disconnected, ϵ_{ij} is set to zero. The shortest paths for all node pairs in a weighted graph can be obtained efficiently through the Floyd-Warshall algorithm (Floyd, 1962).

The overall efficiency of the whole network is defined following Latora and Marchiori (2001) proportional to the sum over all ϵ_{ij}:

$$E(G) = \frac{1}{N(N-1)} \sum_{i \neq j \in G} \epsilon_{ij} \tag{14}$$

Based on Motter and Lai (2002), the cascading failure model describes the evolution of failures in the network, considering the redistribution of loads in the network following initial line failures. In a first step, the loads on the network lines are determined from the analysis of the intact network, i.e. at time 0. The initial load $L_{ij}(0)$ on a line l_{ij} is defined as the total number of most efficient paths between any node pair passing through that line (Motter and Lai, 2002, Crucitti et al., 2004a).

Each line l_{ij} is characterized by a capacity C_{ij}, which is proportional to its initial load:

$$C_{ij} = \alpha_{ij}\, L_{ij}(0) \tag{15}$$

where $\alpha \geq 1$ is the tolerance parameter of the network that quantifies the ratio of the line capacity to the initial line load. It corresponds to a safety factor of the network and is set constant here. In a real network, α_{ij} might vary among different lines. This option will be utilized in network strengthening strategies in Section 7.5.

Cascading failures are triggered by initial line failures. The interest here is in initial failures caused by a natural hazard event, independent of the load and capacity of the lines. These initial failures are reflected in an updated adjacency matrix $\boldsymbol{A}$, in which the entries for all failed lines are set to zero. The network is then re-analyzed with the updated adjacency matrix. In particular, the most efficient paths among all node combinations are evaluated, and the new loads $L_{ij}(1)$ in all lines $1, \ldots, l$ are computed. It is assumed that overloaded lines fail, i.e. all lines for which $L_{ij}(1) > C_{ij}$ fail. The entries in the adjacency matrix corresponding to these lines are set to zero, and the process is repeated until it converges, i.e. until in one step no new line overloads occur.

Finally, the efficiency of the resulting (damaged) network is computed through Equation (14). To obtain a normalized measure of network damage, the efficiency of the damaged network is divided by the efficiency of the intact network:

$$E_{norm} = \frac{E(G_{damaged})}{E(G)} \tag{16}$$

In the following, one illustration of the cascading failure model is presented for the IEEE 14 system. Note, the loading concept employed in the example is the reactance weighted graph with the line load defined as the total of the most efficient (shortest) paths passing through any line. The tolerance level is set to $\alpha = 2$. In Figure 16 and Table 5, the resulting cascading event is depicted as it would follow from an initial simultaneous failure of the lines between nodes 3 and 4 as well as nodes 7 and 9, which are marked red in the upper most graph on the left side in Figure 16. In the subsequent four time steps, the consequent overloading propagates through the network. The overloaded lines are marked thick and red in the plots. In each step one to two lines get overloaded until in step 5, the cascade

comes to a halt.

In Table 5 the initial network conditions of the IEEE 14 network are depicted, i.e. the line reactance, initial line load, and line capacity values. The loading on the lines is listed for each cascading step after the initial failure event. In the lower part of the table, the decrease of the overall network efficiency level is recorded: the efficiency decreases in each step until it reaches 17.5% of the initial efficiency by the end of the cascading process.

Depending on the application or question, topological models might not have sufficient accuracy in depicting the actual grid properties and processes in the grid, since purely topological measures can provide some indication of general vulnerability trends but can be misleading when used in isolation as compared to performance estimates from a physical load flow model (e.g., Hines et al., 2010, LaRocca et al., 2015).

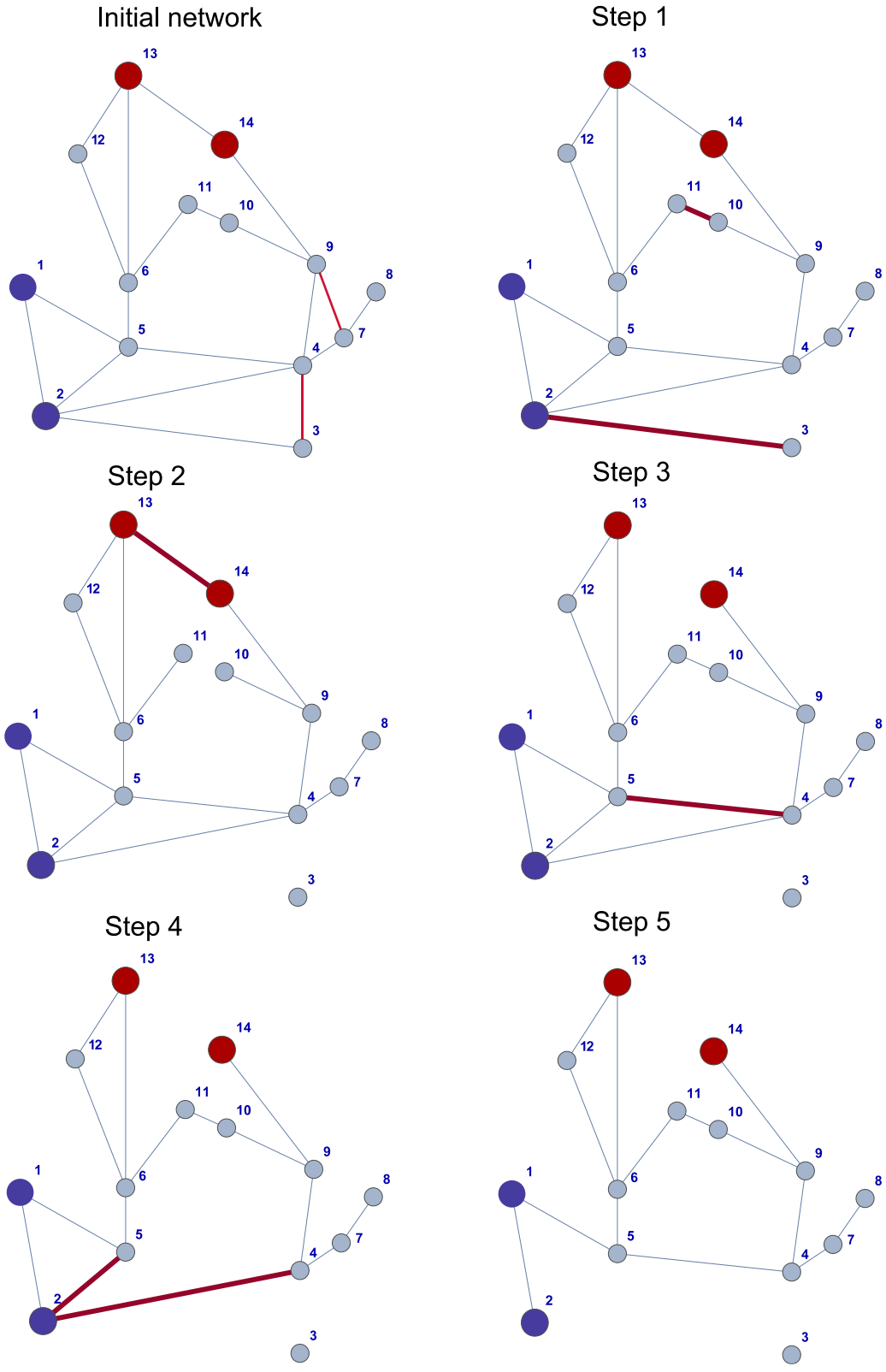

Figure 16: The IEEE 14 benchmark system displayed as complex graph. Blue nodes: source, red nodes: target/sink. An example cascading event is depicted that stems from the initial simultaneous failure of the two lines 3–4 and 7–9. The cascading failure model is based on the graph efficiency concept.

Table 5: Description of the initial network conditions of the IEEE 14 (line reactance, initial line load, and line capacity values). The loading on the lines is listed for each cascading step after an initial, simultaneous failure event of the lines connecting nodes 3 and 4 as well as 7 and 9. In the lower part of the table, the corresponding decrease of the overall network efficiency level is shown; $\alpha = 2.0$.

Line		Undisturbed network			Cascading failure process				
From node	To node	Reactance	Initial load	Capacity	Load step 1	Load step 2	Load step 3	Load step 4	Load step 5
1	2	1.94	8	16	3.7	2.8	3	5	6
2	3	4.70	2	4	11.0	-	-	-	-
2	4	5.81	12	24	9.7	5.8	6	28	-
3	4	6.70	11	22	-	-	-	-	-
1	5	5.40	5	10	7.3	7.2	7	5	10
2	5	5.70	5	10	10.0	5.0	5	25	-
4	5	1.34	10	20	8.0	10.8	22	-	-
5	6	1.00	21	42	21.0	18.3	28	28	12
4	7	1.00	8	16	0.0	0.0	0	0	0
7	8	1.00	5	10	1.0	1.0	1	1	1
4	9	1.00	12	24	14.7	13.7	24	24	3
7	9	1.00	4	8	-	-	-	-	-
9	10	3.18	8	16	9.0	10.0	10	10	3
6	11	9.50	6	12	11.7	10.0	10	10	6
10	11	8.21	3	6	6.7	-	-	-	-
6	12	12.29	6	12	8.0	6.0	9	9	5
6	13	6.62	8	16	9.7	10.3	9	9	5
12	13	22.09	2	4	3.0	4.0	1	1	1
9	14	12.71	6	12	10.0	11.7	10	10	3
13	14	17.09	4	8	7.7	11.3	-	-	-
		Graph Efficiency							
			19.4		6.27	5.69	5.69	4.46	3.4
		[%]	100		32.3	29.3	29.3	23.0	17.5

5.4.2 DC Power flow equations

To overcome constraints of a purely topological model, the power flow in the network can be computed with a physics-based model. This allows accounting for the dependency of network components in a more realistic way and to estimate if, and to which extent, initial component failures cascade through the network and cause partial or complete network collapse. Physical models estimate power flows across the grid according to Kirchhoff's laws.

In this thesis, a cascading failure model based on direct current (DC) power flow equations similar to implementations introduced by Dobson et al. (2001), Pepyne (2007), and Koç (2015) is employed. The power flow in the power grid is dependent on the transmission line parameters, node voltages, and phase angles at generator buses. Under the simplifying assumption that the lines are lossless, the power flow is dependent on node voltages and inversely proportional to the line reactance values (Grainger and Stevenson, 1994,

Saccomanno, 2003). DC power flow equations are linearized approximations of the alternating current (AC) power flow equations and only consider flow of active power. One main assumption of the DC model relates to small voltage angle deviations, i.e., deviations of less than 30 degrees between nodes, which would make the system able to maintain voltage levels thus avoiding voltage collapses (Wood and Wollenberg, 1996, Van Hertem et al., 2006). In literature, few studies apply AC power flow equations (Javanbakht and Mohagheghi, 2014) that are computationally more expensive but often assumed to be more accurate and close to real world conditions (Johansson and Hassel, 2014). The accuracy of DC power flow systems is e.g., discussed in Van Hertem et al. (2006) and it is concluded that the model can give in general a good approximation of active power flows in transmission networks.

Examples in the domain of physical power network models that incorporate cascading failure models are Koç et al. (2013) and Henneaux et al. (2012). The models differ in whether they approach the problem deterministically, e.g. Koç et al. (2013), or if they account for (possibly correlated) components' failure probabilities, e.g. Henneaux et al. (2012), Mensah and Duenas-Osorio (2014). For physical flow models, the pertinent performance measures are the unsupplied load, connectivity loss, survived demand, or the number of customers without power.

Applying the network formulation from 5.1, the transmission grid is described by a set of N nodes (buses) that are connected via a set of L lines. There are three types of buses:

- Slack or reference bus;
- Generator buses, representing power plants; and
- Load buses, representing electricity consumers such as industrial production sites, cities or villages.

Lines between the nodes in the network represent transmission cables and transformers. The power flow in the lines can be computed based on the direct current (DC) power flow equations, relating power injections and demand at the nodes to the power flows through the transmission lines according to Kirchhoff's laws.

The active power flow f_{ij} through a line l_{ij} is the product of the voltage phase difference between node i and node j, $\theta_i - \theta_j$, and the reciprocal of the line reactance π_{ij} or the line susceptance b_{ij} respectively:

$$f_{ij} = \frac{\theta_i - \theta_j}{\pi_{ij}} = b_{ij}(\theta_i - \theta_j) \tag{17}$$

The entire network system can be modeled by:

$$\boldsymbol{P} = \boldsymbol{B\theta} \tag{18}$$

Where **P** is the $Nx1$ vector of the net active power injections at the nodes $1, \dots, N$ (power generation minus power demand), **B** is the NxN susceptance matrix, and **θ** is the $Nx1$ vector of the voltage phase angle at each node $1, \dots, N$.

The capacity limit, i.e., the maximum load that can be transferred through a line, stems mainly from thermal limits of stability or voltage drop constraints (Papailiou, 2017). The line capacity is defined as the product of the tolerance parameter α_{ij} and the initial load $L_{ij}(0) = f_{ij}(0)$, see Dobson et al. (2001).

$$C_{ij} = \alpha_{ij}\, L_{ij}(0) \tag{19}$$

In analogy to the model in Chapter 5.4.1, the cascading failure model is set up. Here, the load on the lines is not explicitly referred to the shortest path problem in a (weighted) graph, but it is modeled as the actual power flow through the lines based on Equation (18). Initial line failures change the topology of the power grid resulting in a new configuration of power flow across the remaining components. Power flows in the damaged lines are set to zero and the whole network is reanalyzed, i.e., the nodal power injections are redistributed among all remaining components by solving the DC power flow equations in Equation (18) for the new configuration, which in turn may lead to further overloading and tripping of additional components. Line overloads are determined assessing for each i-th line in the damaged configuration the power flow relative to the capacity of the line C_{ij}. Failure of the line occurs if the power flow exceeds the line capacity. The network is iteratively evaluated and failure cascaded until no further lines are overloaded and equilibrium is reached. The resulting network damage is quantified as $\mathrm{L_{norm}}$ [%], the fraction of loss of load to the initial cumulative load supplied through the network as defined in Equation (20).

$$L_{norm} = \frac{\text{Power load loss [MW]}}{\text{Power load in undamaged grid [MW]}} \tag{20}$$

A second measure for performance is the number of deactivated lines after initial and cascading failure.

Cascading failures are likely to lead to so-called islands, i.e., sections which are disconnected from the rest of the network. An island that experiences a shortage of power generation compared to its total load demand is assumed to lose a fraction of load amounting to the concerned shortage. This is a simplified assumption, as in reality disconnected islands are likely to experience blackouts due to increased voltage instabilities (Dobson et al., 2001, Vaiman et al., 2012). In addition, the model is designed to assess line failure

events and no node failures are considered at this stage, see Section 5.2.1.

In analogy to Figure 16, the following illustration in Figure 17 shows an example for a cascading event for the IEEE 14 system based on the power flow equations. In Figure 17, the resulting cascading event is depicted as it would follow from an initial simultaneous failure of the lines 3–4 and 7–9, which are marked red in the upper most graph on the left side in Figure 17. In the following three steps, the overloading propagates through the network. The further overloaded lines are marked thick and red, in the concerned plots. In each step one to three further lines get overloaded until in step 4, the cascade comes to a halt.

Comparing the cascading process in Figure 17 to the results of Figure 16, it becomes clear that the two cascading failure models produce significantly different results in the example cases. The lines that fail subsequent of the initial two line failures diverge from each other. With the efficiency based model (Figure 16), one more line fails than in the case of the power equations based model (Figure 17). However, in the case of the power flow model, the network is finally split into 4 parts with 2 isolated nodes (leaf node 11 and leaf node 8). In case of the efficiency based cascading failure model, all nodes remain connected except node 3. The difference in the results among the two models is mainly due to the different quantification of the load on the lines: shortest paths vs. power flow. Therefore, the physical power flow equation delivers different results as the topology-based model, since the line capacities and the (topological/electrical) distances between the nodes differ significantly.

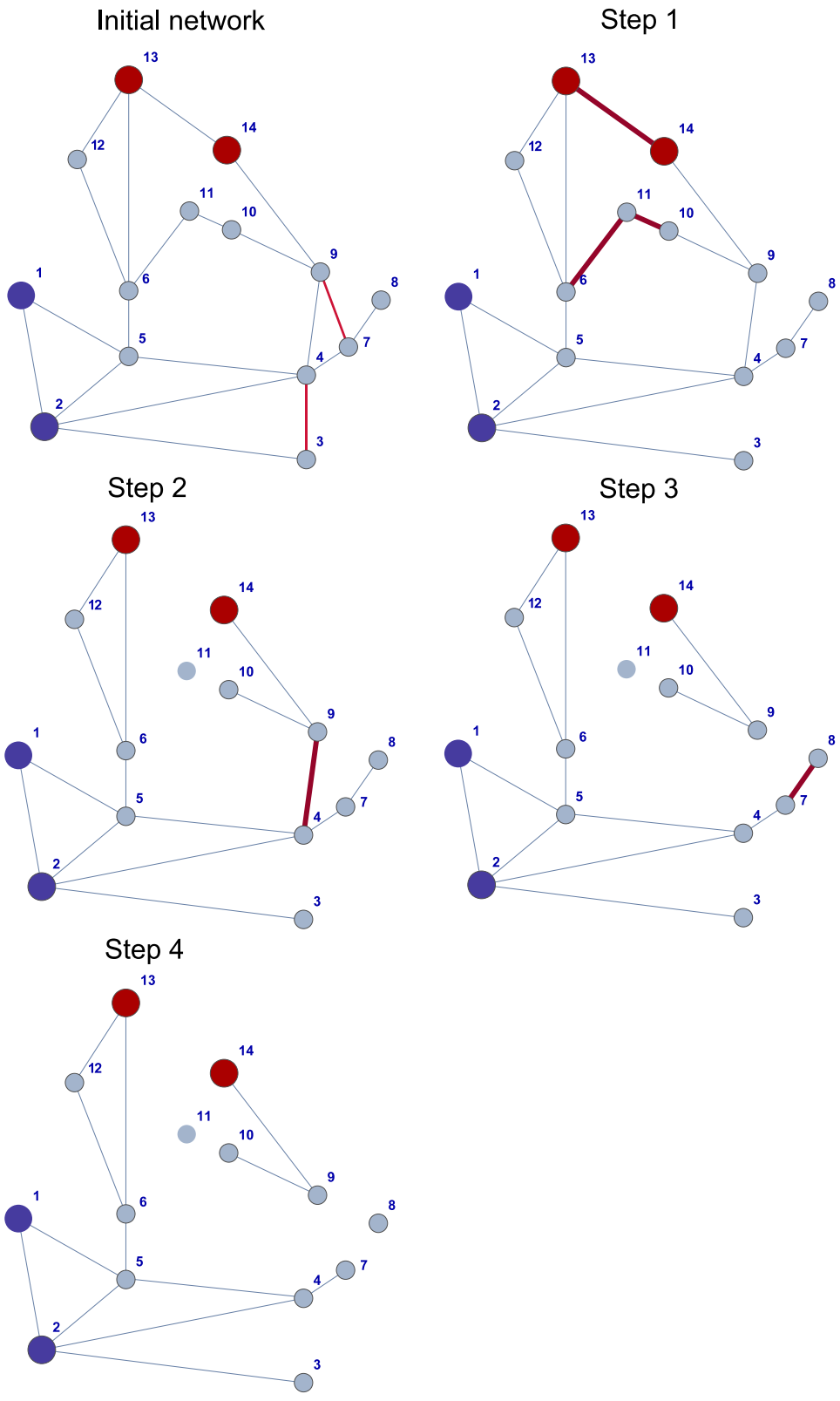

Figure 17: The IEEE 14 benchmark system depicted as complex graph. An example cascading event is shown that stems from the initial, simultaneous failure of the two lines 3–4 and 7–9. The cascading failure model is based on the power flow equations explained in this chapter.

5.5 Methods for network reliability analysis

In this chapter, simulation based versus non-simulation based methods are discussed. Corresponding subordinated methods are classified, and their advantages and limitations are discussed.

5.5.1 Non-simulation-based analysis

As introduced in Zuev et al. (2015), traditional methods for network reliability analysis emerged from graph theory. In the development of these methods, often rather small networks are investigated. In studies about the network evaluation by a topological model, and mainly with connectivity-based performance measures, a branch of non-simulation based methods has been developed. The methods in the field of complex network theory comprise the following techniques, sometimes used in combination; the categorization is partly based on Jonczy and Haenni (2007); the categories are not mutually exclusive.

- **Direct methods:** Methods based on the structure function of the graph (network) for the reliability assessment. One method is to reformulate the graph as series and parallel sub-graphs and take the parts connected in series and in parallel as basis for the overall reliability calculation. In the context of the source-target connectivity problem, a further method is to search for all minimal cut sets or alternatively for all minimal path sets in the network (enumeration), and then use these sets as basis for the system reliability calculation, see Rausand and Høyland (2004) and Straub (2017).

- **Reduction and decomposition methods:** Methods based on the division of the network into subnetworks. The overall network reliability is then calculated based on the reliabilities of the corresponding subnetworks (Li and He, 2002, Lim and Song, 2012, Kim et al., 2012, Lim et al., 2015).

- **Enumeration methods:** Methods based on the complete state enumeration of the network components and corresponding network performance (Lê, 2014). The matrix based system reliability method by Song and Kang (2009) is a related method: it builds on bounds on system reliability and linear programming (Song and Der Kiureghian, 2003) and provides a closed form solution to the network connectivity reliability problem (examination of the connectivity between source and target nodes). The matrix based method can be seen as an enumeration since it uses the complete set of mutually exclusive and collectively exhaustive events, i.e. the complete component and system state space is known and considered. The crude complete enumeration method is introduced briefly in Section 5.5.1.1. The

approach can also work with incomplete sets, leading to bounds on reliability.

- **Bounds on reliability:** Bounds on system reliability may be established to relax the computational costs e.g., compared to the direct and enumeration methods (Der Kiureghian and Song, 2008); however, the most probable events may not be identified.

5.5.1.1 Complete enumeration

For a network composed of l lines, the explicit evaluation of the network reliability means the consideration of all 2^l possible component state vectors $\boldsymbol{x}^{(k)}, k = 1, \dots, 2^l$. All possible component state combinations are therefore listed, i.e., complete enumeration.

For every state of $\boldsymbol{x}$, the corresponding system state or system performance is then evaluated:

$$s_k = \Phi(\boldsymbol{x}^{(k)}), \quad k = 1,\ 2,\ \dots, 2^l \tag{21}$$

Each component state vector has to be assigned a probability in order to determine the reliability of the system. In case the components are independent, then the probability q_k of component state vector k can be computed as:

$$q_k = \prod_{i=1}^{l} [x_{l_i}^{(k)} p_{l_i} + (1 - x_{l_i}^{(k)})(1 - p_{l_i})], \qquad k = 1, 2, \dots, 2^l \tag{22}$$

Where $x_{l_i}^{(k)}$ is the value of x_{l_i} in the binary component state vector k. In case of dependent components, adjustments in the determination of q_k have to be done as discussed in Chapter 5.3.

The system failure probability can finally be determined from the following equation with s^T being the system state vector:

$$p_F = s^T q \tag{23}$$

In Figure 18 an example is shown, a network of three components subject to failure. The corresponding component state vectors are completely enumerated together with the corresponding system state vector, based on the (s-t)-connectivity problem. Assuming a

component failure probability of 0.1 for all three components, Equation (22) and Equation (23) result in a system failure probability of 0.109.

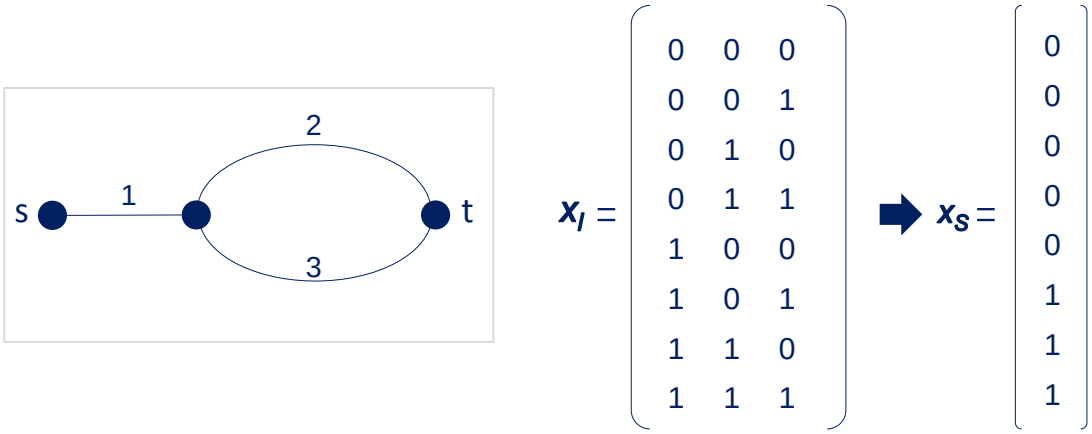

Figure 18: Example three component network (three lines that are subject to possible failure) and corresponding component state vectors $\boldsymbol{x_l}$ and system state vector $\boldsymbol{x_S}$ based on the (s-t)-connectivity problem. Assuming a component failure probability of e.g. 0.1, being equal for all three lines; from Equation (22) and Equation (23), it can be derived a system failure probability of 0.109.

5.5.1.2 Limitations of non-simulation based methods

The complete enumeration approach can be seen as a brute-force method to calculate the system reliability, as 2^l system configurations must be evaluated. Thus, this approach is limited by the number of system components; to about 30 components, corresponding to about one million to one billion system configurations.

One more limitation is that complex networks are not reducible to series and parallel subsystems. Thus, methods which use this translation of system formulation are infeasible to apply to large, highly redundant networks (Rokneddin, 2013).

Some of the non-simulation based methods mentioned before are developed for topological performance measures, in specific for the connectivity problem (e.g., Li and He, 2002, Lim and Song, 2012, Lim et al., 2015, Kim et al., 2012, Rausand and Høyland, 2004, Straub, 2017). They are not formulated for assessing the network reliability based on a continuous performance function.

5.5.2 Simulation-based analysis

As shown above, the number of event combinations increases rapidly and is thus challenging to evaluate for only mid-sized systems (Dueñas-Osorio and Vemuru, 2009). For large

systems, non-simulation-based analyses become computationally too expensive or even prohibitive in practice. Because an efficient analysis is often essential for infrastructure planning and safety, there is a need for simulation and sampling-based approaches.

5.5.2.1 Monte Carlo simulation

The Monte Carlo simulation (MCS) method is a well-established numerical integration technique for the evaluation of the failure probability of a system. Fishman (1986) explores MCS for the source target connectivity problem of networks. MCS is based on random sampling of the basic random variable space. The method could be theoretically exact, since an evaluation of an infinite number of samples would reveal the exact solution of the probability of failure. The method is straightforward to implement and widely used; however, the required number of samples can be rather high, and thus computationally expensive, especially for low probabilities to be examined: the number of samples for a postulated accuracy of estimates is inversely proportional to the probability of (system) failure (Papaioannou, 2012).

For the reliability analysis, the employed k ($k = 1, \dots, n_{MC}$) MCS samples encompass the realization of L random Bernoulli trials by drawing from the component failure probability distributions $\boldsymbol{p_f} \in [0,1]^T$. This yields the L-dimensional binary component state vector $\boldsymbol{x_l^k} \in \{0,1\}^L$. Applying a model or performance function $\tau(\boldsymbol{x_l})$ to evaluate the property of interest of the given network (load loss, number of lost lines, etc.) the MCS-estimate of the expected value of $\tau(\boldsymbol{x_l})$ is as follows:

$$E[\tau(x_l)] \approx \frac{1}{n_{MC}} \sum_{k=1}^{n_{MC}} \tau(\boldsymbol{x_l^k}) \tag{24}$$

The system failure probability (or reliability) is derived from the count of all samples in n_{MC}, for which the function value is lower (or larger) than a prescribed critical threshold t, indicated by the indicator function $I_S = \begin{cases} 1 & for\ \tau(\boldsymbol{x_l^k}) < t \\ 0 & for\ \tau(\boldsymbol{x_l^k}) > t \end{cases}$:

$$p_S = 1 - p_F \approx 1 - \frac{1}{n_{MC}} \sum_{k=1}^{n_{MC}} I_S(\boldsymbol{x_l^k}) \tag{25}$$

In case the network model is the binary structure function $\Phi(\boldsymbol{x_l})$, the MCS-estimate of the overall system reliability and complementary failure probability is obtained as:

$$p_S \approx \frac{1}{n_{MC}} \sum_{k=1}^{n_{MC}} \Phi(\boldsymbol{x}_l^k) \tag{26}$$

By computing the variance, the standard deviation, and the standard error of the performance function, i.e., the accuracy of the obtained MCS-estimates by appropriate confidence limits can be described. Also, estimating the standard deviations of the performance functions allows to compute MCS-sample sizes n_{MC} that guarantee a desired prescribed precision of the MCS-estimates.

Most studies in the field of system reliability and specifically power system reliability have used MCS since for moderate sized networks, e.g., a number of components smaller than 10,000, it is feasible to perform evaluation of failure (Dueñas-Osorio, 2005). Example studies that used MCS generally in the field of (infrastructure) network analysis are Adachi (2007), Kang (2011), Rokneddin (2013), (2014), Salman (2016).

For cases where crude Monte Carlo Simulation is too inefficient due to small probabilities of failure and/or demanding network models, alternative simulation methods have been developed such as Latin hypercube sampling, importance sampling, and subset simulation; some of which are explained briefly in the context of network reliability assessment in the following Section 5.5.2.2.

5.5.2.2 Advanced simulation methods

To overcome the inefficiency of crude MCS, several approaches have been developed that aim at a variance reduction, and thus a reduction of the computation time of the analysis for system reliability. Examples are: importance sampling (IS), (discrete) Latin hypercube sampling (LHS), control variate or antithetic variate methods, and subset simulation (SuS) (Hastings, 1970, McKay et al., 1979, Loh, 1994, Au and Beck, 2001). These methods have been applied for power systems in diverse contexts, in many cases for load loss and reliability estimations: Billinton and Jonnavithula (1997), Xingbin and Chanan (2004), Jirutitijaroen and Singh (2008), Zuev et al. (2015). For a detailed overview about the different simulation techniques see e.g. Papaioannou (2012).

Latin hypercube sampling, developed by McKay et al. (1979), is a combination of stratified and random sampling with the aim to better represent the complete sample space relative to MCS based on random samples. The outcome space of the input random variables is divided into i intervals with equal probability of occurrence. Random sampling is then performed for each interval corresponding to the probability distribution function in each interval. Generally, LHS has the potential to produce estimates more precise than MCS with the same sample size, because it ensures a more representative sample compared to an unrestricted random sample, since any subset is sampled with the same frequency.

Jirutitijaroen and Singh (2008) use LHS for the reliability index estimation of power systems. However, they report that a disadvantage of LHS can be the high storage requirement during sampling and additional computation time for equivalent distribution construction.

The principle behind importance sampling is to focus the sampling on the more important regions of the sample space. For small failure probabilities of system components causing relatively large MCS variances, this may be accomplished by modifying the probability distribution of the system components so that rare system failure (e.g. large loss of load) is more likely to occur in the sampling distributions (Papaioannou, 2012). The IS methods work well for a small to medium number of random variables (Wetzel, 2009). For larger numbers of random variables, IS is less straightforward, as explained in Katafygiotis and Zuev (2008). Xingbin and Chanan (2004) study and discuss IS for the expected power loss calculation.

Subset simulation (SuS) is a method developed by Au and Beck (2001), originally for structural reliability problems concerning rare events encountered in engineering systems. In SuS, appropriate progressively smaller intermediate failure events (levels) are constructed that converge to the targeted rare event. The actual system failure event is the intersection of the intermediate failure events, and, consequently, the actual system failure probability can be obtained as the product of the conditional failure probabilities of the converging failure event sequence. A detailed motivation of SuS as well as a presentation and derivation of the method is provided by Zuev (2014). However, SuS is not without difficulties as it might fail to identify all the relevant failure domains for complex network systems. Zuev et al. (2015) provide an application of SuS for a problem in network reliability: they assess the road networks of Beijing and Los Angeles based on their maximum flow capacity.

Control variate or antithetic variate methods exploit correlations among random variables to achieve variance reduction, e.g. Law and Kelton (1991). The principle is to add to the target random variable another appropriately determined auxiliary random variable: the antithetic or the control variable. Typically, the control variable has zero expectation and a known negative correlation with the target variable. Firstly, this has the consequence that the mean of the sum of the target and the control variables is still equal to the mean of the target variable (unbiasedness). Secondly, the negative correlation between the target and the control variables associates (by trend) larger values of the original variable with lower control values, and vice versa. This leads to the desired variance reduction of the sum of the original and the control variable. In these methods, more rapid convergence or greater efficiency is obtained by the skillful utilization of an auxiliary random variable. Billinton and Jonnavithula (1997) discuss these methods in the context of sequential MCS for power system assessment with a time-varying load distribution at each load bus. This with the aim to portraying numerous operating policies in the system.

In the course of this thesis, the Monte Carlo method is chosen since it can seamlessly integrate correlated component failures for reliability assessments of rather large networks. An advantage of the direct MCS that may be emphasized is its transparency and robustness,

especially compared to the advanced indirect methods outlined above. Often, ordinary direct MCS is used to check and calibrate more sophisticated methods, see Zuev (2014). In this thesis, the affordable network performance models in terms of computational time (e.g., application of a DC power flow model instead of an AC power flow model) made it possible to use MCS.

5.5.3 N-1 contingency versus reliability-based analysis

Many current standards and design practices for power infrastructure are of the deterministic type. Contingency analysis is applied when planning new networks or when evaluating current networks with new system conditions. The goal is to identify weak system elements, which experience overloads or under voltages subject to the conditions of contingency. The basic idea in those analyses is to deactivate a part of the network model and to investigate the stability of the network using, e.g., a power flow model. The number m of deactivated elements defines the $(n-m)$-contingency (Li, 2011).

In practice, the so called deterministic $(n-1)$-rule requires that a transmission system must be able to withstand an outage or fault disturbance of a single element in any system condition by providing enough elements with sufficient capacity to protect against overloading, under- or overvoltage, disconnection of other components, unplanned load curtailment, transient instability, and voltage instability (Li, 2011). High voltage transmission systems are frequently designed as redundant systems with generally two parallel lines that each run with 50% utilization and, thus, can take over the load of the neighboring line, in case it fails (Schwab, 2009).

The $(n-1)$-criterion has two drawbacks: 1) multiple component failure combinations are not considered, and 2) only the outcomes of single-component failure events are analysed but their probabilities of occurrence are not taken into account. This can lead to overinvestments, since a failure event, even if extremely undesirable, is of little consequence in case it is very unlikely. An underestimation of the total risk stems from rather likely events with comparably low consequences. “Major outages are usually associated with multiple component failures or cascading events in real life. This suggests that the $(n-1)$ criterion is insufficient to preserve a reasonable level of system reliability” (Li, 2011). In a recent study by Li et al. (2017) it is claimed that a $(n-3)$ analysis is sufficient to measure the importance of a network component.

The advantage of probabilistic reliability and risk assessment, e.g., using Monte Carlo Simulation methods for component state sampling, is the consideration of multiple, i.e. $(n-m)$ component failure events also called ‘multiple contingencies’. This enables the modelling of not only the severity of the events, but also of the probability of their occurrence, allowing a better description of the actual system risk. A number of additional useful metrics can be derived, comprising probable damage configurations, topological patterns of

cascading failure, and expected loss per component failure.

Generally, the treatment of loads and strengths (e.g., wind, temperature, resistance) as random variables is helpful in order to include the randomness of conditions or constraints in planning, and to recognize that absolute reliability cannot be achieved because there will always be a chance that several components' loads exceed design values. The goal of reliability-based design is, thus, to guarantee an upper limit of the probability of failure, or accordingly a lower limit of reliability (Ghannoum, 2017).

It is of increasing interest in science and industry to assess not only the risk associated with an individual contingency scenario, but rather to estimate the overall system risk as expected adverse consequences. If the probability density functions f of all contingencies are known, including the economic consequences associated with the contingencies (e.g. in MW), then the total risk can be calculated as integral over all possible contingencies:

$$Risk = \int f(\tau(x))c(x)dx \tag{27}$$

5.6 Summary

This chapter is a broad outline of the methodology of network reliability analysis. As such, it is the basis for what will be established in this thesis in the subsequent chapters.

The term complex graph is introduced, the definition of network reliability is given, based on different network representation approaches (performance measures). The problem of dependent component failures is discussed, and two selected approaches of modelling cascading failures are pointed out. Finally, non-simulation-based reliability assessment methods are compared to simulation-based methods. A short outline of advanced simulation methods completes the chapter.

6 Component fragility

Network reliability analysis requires the knowledge of component failure probabilities. The component failure probability is a measure for the susceptibility to external hazards in the context of this thesis. The network components are typically assumed to have binary states (failure versus non-failure), although, it is possible to address multiple component state systems with some adjustments, see e.g. Lisnianski et al. (2010).

This chapter compiles types of failure, spatial and temporal discretization of component load, and the following central topics: the concept of fragility as well as the calibration of specific fragility curves. The fragility concept employed here is taken from the field of structural reliability. Storm fragility is defined as the conditional probability for failure of a component conditional on (local) wind speed in a storm event.

6.1 Spatial-temporal discretization and types of failure

All lines of the power transmission network are divided into segments of 1 km length, if not stated differently in the individual application cases. The probability of failure, respectively the reliability, of these line segments is evaluated. The wind load onto each line segment is represented by the wind speed at the location point in the spatial random field representative for one point in time or for the maximum wind speed at the location in one storm event that is nearest to the line segment's midpoint. A more sophisticated interpolation method can be employed, but due to the fine discretization of the wind field model, no relevant difference in the result is expected. The failure probability is determined by

mapping the wind field at the line segment mid points to the corresponding component fragility function.

Each segment consists of a series of structures (mostly steel towers and the lines themselves), which are not modelled explicitly. Instead, the fragility model is formulated directly for the 1 km segments, which are the *components* of the transmission grid system. We do not consider failures of substations or other bus types during storm events, as these are less frequent than line failures. This means that, e.g., power generation is assumed to be unaffected by windstorms. The only case where power generation is unavailable is when a disconnection with the network occurs as the result of failures of transmission lines branching out from the generation site or due to consecutive cascading failures. Similarly, power demand is assumed unaffected. Thus, only if a consumer is disconnected from the grid due to line failures, the decrease in the power demand is considered in the model.

6.2 The concept of fragility

A fragility curve is a probability distribution indicating the probability that a structure or structural component will reach a prescribed damage state or failure state as a function of a predictive load/demand parameter (OSCE, 2016). The fragility curve is a function that describes the probability of failure conditioned on the load defined by the hazard intensity (e.g., wind speed on a transmission tower or line). Consequently, the full range of loads to which the component might be subject to is considered (Casciati and Faravelli, 1991, Shinozuka et al., 2000).

The concept of fragility has been used extensively for the seismic risk and reliability assessment, e.g., for substation equipment (Straub and Der Kiureghian, 2008), for wood constructions (Ellingwood B. et al., 2004), and highway networks (Shinozuka et al., 2000). Simm (2009) used fragility curves for flood protections with the aim to prioritize investments on improvements in the United Kingdom. Only a few studies are available in the context of wind load on power transmission or distribution infrastructures. Shafieezadeh et al. (2014) assessed specifically the age-dependent fragility of wood poles in power distribution networks against extreme winds. A recent study addressed power transmission networks subject to wind loads in Great Britain (Panteli et al., 2017).

The specific shape of the fragility curves expresses the uncertainty of the structure/component to resist a certain load: If there is no uncertainty about what critical load would cause the component to fail, the fragility curve would be a step function, illustrated in Figure 19 (right). The step function has $\Pr(F) = 0$ below the critical load and $\Pr(F) = 1$ above the critical load. A step function would be valid a well-understood system with no uncertainties. In many cases, the appropriate model is an s-shaped fragility curve as a function of the intensity of the load $F_R(s)$, see Figure 19 (left), reflecting uncertainty in the

capacity of the system to withstand a load (Ellingwood and Tekie, 2001, Ellingwood B. et al., 2004, Straub and Der Kiureghian, 2008, Simm, 2009, Schultz et al., 2010, Dunn et al., 2015).

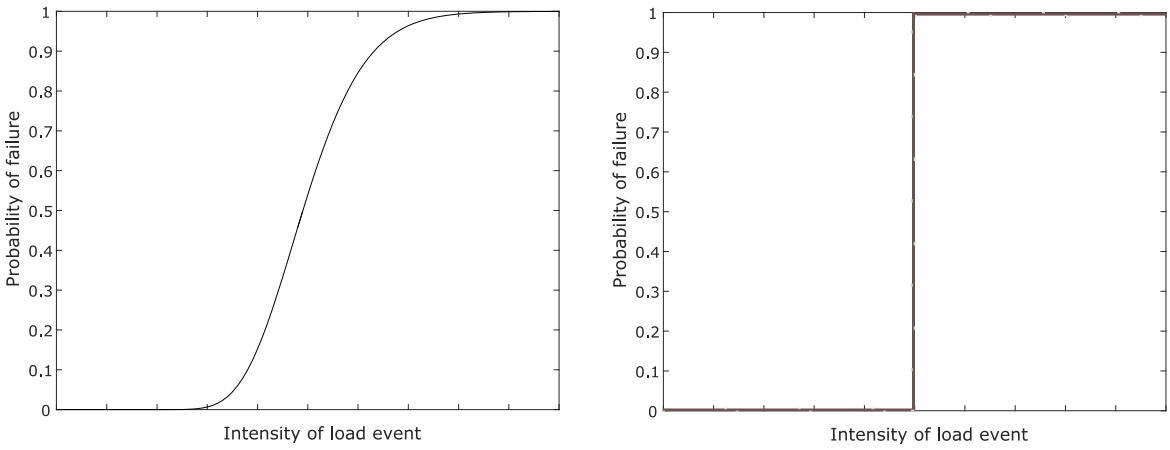

Figure 19: Conceptual fragility curves: The fragility curve is an S-shaped function for less understood or elastic systems (left), $F_R(s)$. The fragility curve is a step function for very well understood or brittle systems (right).

The term "failure" is a relative term that can generally be understood as the components inability to provide a prescribed level of service. In other terms, a failure event corresponds to the value of the performance function being smaller than the prescribed critical limit state. There is also the possibility to use multiple performance levels for one component simultaneously (Shinozuka et al., 2000): A component might suffer mutually exclusive damage states given a load event, s, such as 1) minimal damage but fully serviceable D_1, 2) moderate damage and serviceable D_2, 3) severe damage and not serviceable D_3, 4) major damage/collapse D_4. If there are four different damage stages, as in this example, a family of three fragility curves exists for this component that indicates the corresponding probability of exceeding the damage state, see Figure 20 for the following 4 exceedance probabilities:

$$Pr(D_1) = 1 - F_1(s) \tag{28}$$

$$Pr(D_2) = F_1(s) - F_2(s) \tag{29}$$

$$Pr(D_3) = F_2(s) - F_3(s) \tag{30}$$

$$Pr(D_4) = F_3(s) \tag{31}$$

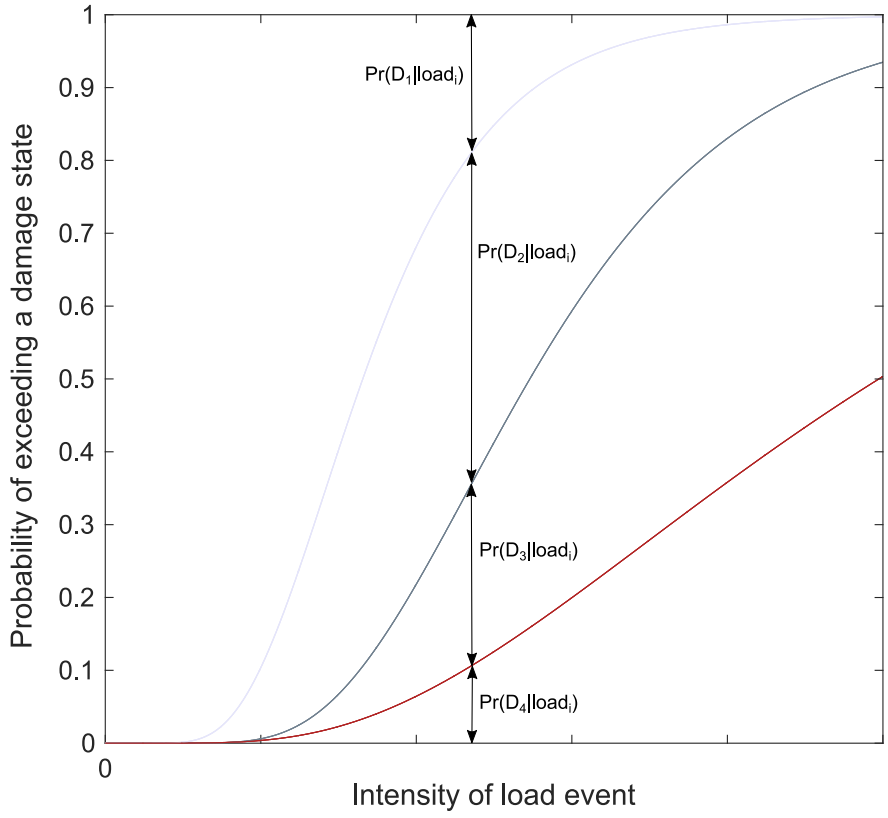

Figure 20: Example scheme of a component with four different prescribed damage states D_j: minimal, moderate, severe, and major damage. The fragility curves indicate the corresponding probability of exceeding a damage state given a hazard load $\Pr(D_j)$.

Fragility curves can be derived in essentially four different ways, see e.g. Schultz et al. (2010):

1) Based on expert judgement
2) Empirically based on statistical analysis of an ideally large data set of observed failures
3) Experimentally based on deliberately induced failure events on example or model components
4) Analytically, based on structural models
5) Based on an appropriate combination of 1) - 4)

Empirical curves can be constructed for cases where there is sufficient statistical data on graded failure events for specific components. This is applicable where it is possible to assess replicable specimens, which may be the case for distribution network infrastructures (towers and lines), for which failure records are more likely to exist due to their greater number and lower design standards (Dunn et al., 2015). In the context of earthquake hazards this has been done e.g., for substation components by Straub and Der Kiureghian (2008). As opposed to this, for structures where no sufficient data on (wind-related) failures is available, it is reasonable to derive analytical fragility curves. Generally, conducting

experiments for large-scale infrastructures is unlikely to be affordable and expert judgement would be rather uncertain since there is only little experience to learn from (Panteli et al., 2017).

6.3 Structural reliability

In structural engineering, the performance of structural systems is modeled by limit state functions g, where negative and positive values of g indicate failure and non-failure of the system, respectively (Melchers, 1999). A generic limit state function describing failure (or survival) of a network component (line segment j) subject to wind load S_j is:

$$g(R_j, S_j) = R_j - S_j \tag{32}$$

with R_j being the component capacity to wind loads. S_j is the wind speed acting on the component. The limit state function g is also known as margin of safety or performance function (Schultz et al., 2010). Owing to the definition of the system components as 1 km line segments, the parameter R_j has no direct physical interpretation. It is the capacity of the line segment against a wind event along its 1 km length, which is characterized by the maximum gust wind speed at 25 m height at one representative location. This implies that – because of the random nature of the wind field – the maximum gust wind speed experienced by the line segment is going to be very likely larger than S_j.

Due to the uncertainty in the resistance of a structure and in the actual loading, R and S are treated as random variables described by probability distributions, see Figure 21. In our case R and S are measured in wind speed $\frac{m}{s}$.

The probability of failure $\Pr(F_j)$ of a component/line segment j is the probability that g takes a value smaller than zero, which is equivalent to the probability of the resistance being smaller than the load:

$$Pr(F_j) = Pr[g(R_j, S_j) \leq 0] = Pr(R_j \leq S_j) \tag{33}$$

For a given component, the conditional probability of failure for a given wind speed s_j is:

$$Pr(F_j | S_j = s_j) = Pr(R_j \leq s_j) = F_{R_j}(s_j) \tag{34}$$

wherein F_{R_j} is the CDF of the capacity R_j. This is the fragility model of the component. The fragility model is assumed to follow the lognormal distribution, in line with common practice, see Allen et al. (2005). The unconditional failure probability can be obtained by the total probability theorem:

$$Pr(F_j) = \int_0^\infty Pr(F_j|S_j = s_j)\, f_{S_j}(s_j)ds = \int_0^\infty F_{R_j}(s_j) f_{S_j}(s_j)ds_j \quad (35)$$

wherein $f_{S_j}(s_j)$ is the PDF describing the distribution of the wind speed.

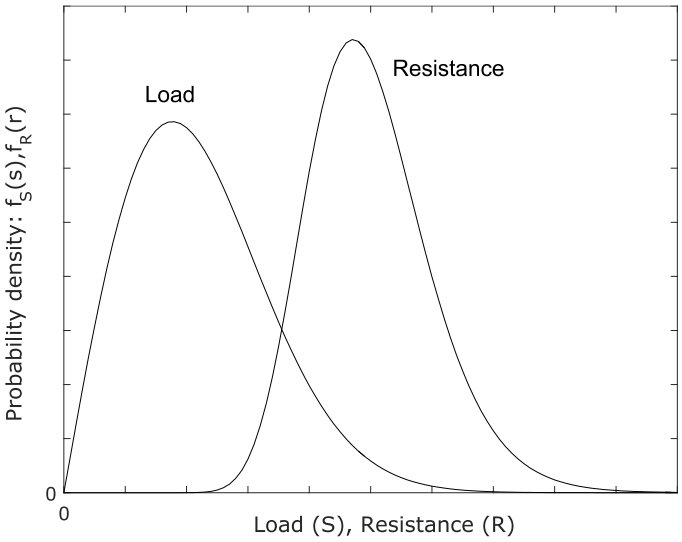

Figure 21: Probability distributions of load (S) and Resistance (R). Information about the uncertainty in load and resistance can be used to derive the probability density function of the safety margin R-S.

6.4 Component fragility model calibration

The calibration of the component fragility model in this thesis is based on the assumption that all structures (at least approximately) comply with the requirements of current standards. In particular, we assume that all support constructions have been planned and built according to the country-specific code or standard. In Europe, this would be e.g., the Eurocode 1-4 (CEN, 1991). The national annexes to Eurocode 1-4 provide the characteristic wind speed values v_b as a function of the geographical location. These values, which are the basis for the design of structures against wind loads, correspond to the 50-year return levels (yearly exceedance probability of 0.02) of the 10-minute wind speed at 10 m height.

The characteristic 50-year wind speed values following Eurocode 1-4 cannot be applied

directly to determine the fragility. However, we can exploit the knowledge that structures in areas with higher characteristic wind speeds will on average have a higher resistance to wind forces. Consider two structures that are identical except that they are designed for different wind zones. If they are designed to the limit (i.e. with a usage factor of 1), their resistances with respect to the maximum wind speed should be proportional to the characteristic wind speed of the respective wind zone. Since there is an approximate linear relation between 10 min wind speed and gust wind speed in the Eurocode, this observation applies to both wind speed definitions. We therefore model the capacity, and hence the fragility model, in function of the wind zones z.

The characteristic value for resistance used in structural design is the 5% quantile, $F_{R_z}^{-1}(0.05)$. On this basis, we argue that the ratio between the 5% quantile values of the component capacities in two wind zones y and z is equal to the ratio of the corresponding characteristic wind speed values:

$$\frac{F_{R_y}^{-1}(0.05)}{F_{R_z}^{-1}(0.05)} = \frac{v_{b,y}}{v_{b,z}} \tag{36}$$

The coefficient of variation (c.o.v.) of the capacity δ_R is taken as 10% for all wind zones z, which is consistent with values used for individual structures, e.g., Ellingwood and Tekie (1999) or Shafieezadeh et al. (2014). Note that with a constant δ_R, the mean value of the lognormal distribution is proportional to the 5% quantile value, and it follows that

$$\frac{\mu_{R_y}}{\mu_{R_z}} = \frac{v_{b,y}}{v_{b,z}} \tag{37}$$

With the relationships of Equations (36) or (37), and the fixed c.o.v., it is only necessary to define the mean value of the capacity in one wind zone, and all distributions of R_z, and hence the full fragility models follow. Therefore, the calibration requires to find a single parameter.

Further, to calibrate the fragility models, we account for the observed line failure rates over a chosen time period, i.e. an average failure rate r_F per year and line kilometer due to wind hazards for the study area. The estimate is an aggregate number, as it does not distinguish between different failure types, failure durations, or severity of the disturbance.

The calibration is then performed by computing the overall failure rate for a given value of μ_{R_z}. With the random field wind speed representation (Section 9.2.2.) it is:

$$\lambda_F = \lambda_S \frac{1}{n_{lines}} \sum_{i=1}^{n_{lines}} \int_0^{\infty} f_{S_i}(s_i) F_{R_i}(s_i)\, ds_i \tag{38}$$

wherein λ_S is the rate of storm events and F_{R_i} is the lognormal CDF associated with the wind zone in which component i is located, which is a function of μ_{F_z}. The final value of μ_{R_z} is found iteratively as the value that fulfills Equation (38).

6.5 Summary

The concept of the fragility curve is developed and detailed. It describes the component failure probability in function of the wind load. This again is a prerequisite for the overall assessment of network reliability, or it can be an element of a risk analysis. We suggest a specific calibration method that is applied in the case study of Chapter 9.3. The advantage of this method is that it bypasses the problem of missing (detailed) component failure data.

7 Component importance

One important goal of the network reliability analysis in this thesis is the identification of the most important components in a network. Importance can be defined as the level to which the functioning versus non-functioning of a component contributes to the system performance and thus to the system reliability. Classical reliability importance measures describe either how the strengthening of individual components influences the system reliability, or they measure the impact of component failures on system reliability (Vesely et al., 1983, Rausand and Høyland, 2004, Daemi and Ebrahimi, 2012). Since the system performance is not inherently binary, we include additionally importance measures based on the effect of the component reliability on graph efficiency and power loss, respectively. The goal is the investigation of component rankings based on different importance measures that are introduced in the following, as well as the subsequent utilization of those rankings.

7.1 Deterministic component indices

In many cases, deterministic indices are employed in order to quantify and compare the importance of a network component. This can be done either based on purely topological measures (Cadini et al., 2009, Koç, 2015) or based on the so-called $(n-1)$-contingency analysis introduced above in Chapter 5.5.3. In these cases, the analysis is a non-probabilistic analysis, thus, neither the probability of component failure nor the probability of system failure is considered. Instead, the importance is defined by, e.g., the position of the

component in the network, its connectivity to other components, or the effect on performance functions when the component in question is defected. This will be elaborated in more detail in the following Sections 7.1.1 and 7.1.2.

7.1.1 Betweenness centrality

In order to rank the importance of nodes in the field of graph theory, betweenness centrality is a measure, which is based on the concept of shortest paths. As introduced in Section 5.1.2, for every node pair in a fully connected graph, there exists at least one shortest paths connecting the node pair. The shortest path is thus composed of either the minimal amount of lines connecting the node pair (for an unweighted graph) or it is the path with the minimal sum of weights for each line (for weighted graphs). Then, the betweenness centrality is defined for a component (node or line) as the number of shortest paths that pass through the node or line (Freeman, 1977). Given an undirected graph $G(N, L)$, the betweenness $B(v)$ of a node v of n nodes is:

$$B_v = \frac{\sum_{s \neq v \neq t} \frac{\omega_{st}(v)}{\omega_{st}}}{\frac{(n-1)(n-2)}{2}} \tag{39}$$

Where ω_{st} is the total number of shortest paths from node s to node t and $\omega_{st}(v)$ is the number of those paths that pass through node v.

The definition can be adopted for edges in a network, as suggested by Girvan and Newman (2002). The edge betweenness index for a line component l_i of the network is:

$$B_{l_i} = \frac{\sum_{s \neq t} \frac{\omega_{st}(l_i)}{\omega_{st}}}{\frac{n(n-1)}{2}} \tag{40}$$

If there is more than one shortest path between two nodes, each path is equally weighted such that the total weight of all of the paths is unity (Girvan and Newman, 2002). A component with a high betweenness centrality index is supposed to play a rather more important role than a component with a lower index, thus a smaller number of shortest paths passing through that component. This assumption implies that the flow in the network under investigation is governed by (mainly) the shortest paths available. Betweenness centrality is widely applied in network theory. The removal of the nodes or edges with larger betweenness will make the network more prone to disconnection (Wang et al., 2010).

The betweenness centrality measure has as well been applied in power grid analysis, e.g.,

by Bompard et al. (2009), Cadini et al. (2009) and more generally for the vulnerability assessment of infrastructures by Wang et al. (2010) and Wang et al. (2012). Cadini et al. (2009) applied a number of topological centrality measures to rank the nodes of the IEEE 14 power transmission benchmark with regard to their influence on network connectivity. Zio and Piccinelli (2010) as well examined the same network with topological betweenness measures. However, Cadini et al. (2009) as well as Zio and Piccinelli (2010) extended the concept to account for actual failure probabilities of the components and for flow propagations across the network.

Zio and Sansavini (2011) suggest criticality indicators (based on the frequency of participation to a cascade, the average time before its entrance into a cascade, number of time steps after the component failure event, final size of the cascade emerging from its failure) and compare them to classical measures of topological centrality to identify the most influential components in a network with regard to the cascade process of consideration. They use a random failure process versus a targeted attack strategy of one initial component failure initiating the cascading failure process. The study shows that the suggested indicators match very well with the purely topological measure of the node degree of connectivity. It is found that the degree and betweenness centrality indices show to point out those components that contribute most to the failure propagation process (Zio and Sansavini, 2011).

Further centrality measures have been used in the literature for network reliability and partly for power grid reliability assessment, such as

- Degree centrality: the number of direct neighbors of a component
- Eigenvector centrality: the number and the quality of connections - the quality of a connection increases if the connection is to a node with a high connectivity/centrality
- Closeness centrality: the mean geodesic distance, i.e., the shortest path lengths between a node n and all the other nodes reachable from n, see Newman (2008) and Wang et al. (2010).

7.1.2 N-1 contingency criteria

We additionally apply an alternative approach to obtain a component ranking, which is based on the so-called $(n-1)$-contingency analysis of the power grid. This approach is commonly used in industry to define most important components.

The performance of the network is assessed based on the load loss after cascading failures, but without the hazard context, i.e. the load loss is recorded that results from removing each line individually from the network. The measure is a deterministic criterion, since it

does not account for (correlated) component failure probabilities, nor does it contain information about the system failure probability. Nevertheless, this measure may be useful for a rapid assessment of component importance.

The deterministic measure "load loss" LL_{n-1} indicates the final loss of load after cascading failure that results from removing only one single line l_i individually from the network:

$$LL_{n-1,l_i} = \frac{\text{Load Loss } (X_i=0)}{\text{Load in undamaged graph}} \tag{41}$$

7.2 Reliability importance measures in binary state systems

In the field of system reliability, component importance measures (IM) are employed to rank components, i.e., to arrange the components in the order of increasing or decreasing importance based on their influence on the overall system reliability.

IMs are probabilistic measures, i.e., they are reliability based. Most importance measures utilized in literature depend on the component's function in the system and on the reliability of the component in question (Kuo and Zhu, 2012), but also on the specified system function and the chosen performance measure. A concise overview of some typical IMs is given by van der Borst and Schoonakker (2001) and Kuo and Zhu (2012) in the context of risk and reliability assessment. There are manifold different IMs introduced e.g., by Vesely et al. (1983), Gandini (1990), Meng (1996), and Cheok et al. (1998). Selected examples for IMs are given in Table 6.

IMs have been used frequently for probabilistic risk assessments of nuclear power plants (Rausand and Høyland, 2004). Several studies applied IMs to network reliability analysis and more specifically to electrical power transmission systems. Espiritu et al. (2007), Hilber and Bertling (2007), Daemi and Ebrahimi (2012), and Salman and Li (2018) used classical IMs (Birnbaum's measure, RRW, RAW, FV) for their system analysis. Hilber and Bertling (2007) linked the IM to the actual monetary costs caused by damages through component failures and used these cost values to rank components. Daemi and Ebrahimi (2012) examined the IEEE 24 power transmission benchmark with the goal to compare different component rankings received from different IMs. All three studies rather focus on a contingency analysis by leaving one component out of the system to assess the effect on system performance. An earlier study by Wang et al. (2004) applied IMs in a simulation context to evaluate different component states simultaneously and thus to create a number of different scenarios to be compared. Cadini et al. (2009) and Zio and Piccinelli (2010) applied a number of topological centrality measures to rank the nodes of the IEEE 14 power transmission benchmark with regard to their influence on network connectivity and

on network flow.

In this work, we study whether the component's importance scores can be used to improve overall system reliability by changing the conditions of the selected components. Thus, in this thesis, there are set up some experiments where the network system is reevaluated after the improvement of selected components. These reevaluations will be studied in Sections 9.6, 10.4.3, and 10.5.5. This will show, whether the IM rankings have the potential to add some extra value of information to the reliability analysis of the overall system as explained in Chapter 7.5.

Table 6: Overview of selected Importance Measures, where $F_s = \{X_S = 0\}$ is the system failure event, $F_i = \{X_{l_i} = 0\}$ is the component failure event of component l_i, and M_j denotes a minimal cut set j containing the component l_i failure event.

Birnbaum measure	$BM = \frac{\delta Pr(F_S)}{\delta Pr(F_i)}$	Indicator of change of system unavailability with changes in unavailability of the $i-th$ component
Critically importance factor	$CI = \frac{Pr(F_i)}{Pr(F_S)}\, BM$	Extension of BM with inclusion of failure probability of $i-th$ component; a less reliable component is more critical
Risk achievement worth	$RAW = \frac{Pr(F_S \mid F_i)}{Pr(F_S)}$	Indicator for increase in system unavailability given component l_i fails
Risk reduction worth	$RRW = \frac{Pr(F_S)}{Pr(F_S \mid \overline{F_i})}$	Indicator for the decrease in system unavailability when component l_i never fails
Fussel – Vesely	$FV = Pr(M_j \mid F_s) = \frac{Pr(M_j \cap F_s)}{Pr(F_s)}$	Conditional probability that a minimal cut set j containing the component i has failed, given that the system has failed.

Based on van der Borst and Schoonakker (2001) and Rausand and Høyland (2004), the following are goals pursued by the use of IMs:

- Provide a coarse ranking of the components with respect to their influence on the system reliability
- Help focusing on the top contributors to system unreliability and relax requirements to the lowest contributors to system unreliability
- Focus on improvements with the greatest effect on system reliability and help making cost-efficient decisions about (re)design- and maintenance strategies
- Indicate sensitivity for model parameters

The risk achievement worth (RAW) is a measure of the usefulness of component l_i in achieving the present level of system reliability. It is an indicator for the importance of maintaining the current level of reliability for the component. RAW may be used for inspection, preventive maintenance, and to identify potentially safety-significant components for reliability maintenance. According to Rausand and Høyland (2004), the RAW is a useful measure for estimating the importance of components that are removed from the system. The risk reduction worth (RRW) is the ratio of the actual system unreliability with the (conditional) system unreliability if component i is replaced by a perfect component. It is an index measuring the potential damage caused to the system by a particular component. The RRW can be used to replace or upgrade components for reliability improvement. If RRW is close to 1, it can be concluded that improving the reliability of the component does not have a significant effect on the system reliability.

Note that in the definitions given in Table 6 and in the following sections, the time dependence of the IMs is neglected, although the system and component reliabilities are functions of time. Thus the IMs should be interpreted as idealized point measures with regard to a given point in time t.

Two selected classical importance measures, the BM and the CI, are introduced in more detail in the following, since they are central in Part III of this thesis.

7.2.1 Birnbaum's measure for a binary system

Birnbaum's measure (BM) describes the sensitivity of system reliability p_s to a change in the component reliability $p_{l_i} = \Pr(X_{l_i} = 1)$:

$$BM_i = \frac{\partial p_S}{\partial p_{l_i}} = Pr\left(X_S = 1 \middle| X_{l_i} = 1\right) - Pr\left(X_S = 1 \middle| X_{l_i} = 0\right) \tag{42}$$

This approach is commonly known from classical sensitivity analysis. Following the second equality in Equation (42), the BM can be computed as the difference between the conditional probability that the system is functioning given component i is functioning and the conditional probability that the system is functioning given component i has failed (Rausand and Høyland, 2004). This shows that BM is independent of individual component reliability, which can be seen as a weakness of this IM but at the same time it might be a desirable characteristic (van der Borst and Schoonakker, 2001). The BM can be used to differentiate between those components that influence the system reliability significantly and those that do not. It can thus serve to identify components of the network worthy of further detailed investigation. If the BM value for a component is large, it means that a small change in the component reliability leads to a rather large change in the system reliability.

In a practical network reliability study, the most time-consuming work is to find data for

the model inputs, like components failure rates, repair rates, material characteristics etc. Thus, it is one option to start with a pre-analysis based on rather rough data estimates, calculate the BM for the components and subsequently focus on finding more detailed data on the most important components found in the pre-analysis since components with a very low BM value would be expected to have a negligible effect on the system reliability (Rausand and Høyland, 2004).

7.2.2 Criticality importance for a binary system

The criticality importance (CI) measure of a component l_i is the probability that failure of component l_i is the cause of system failure, conditional on system failure having occurred. It can be defined as a function of BM:

$$CI_i = \frac{BM_i\,(1 - p_{l_i})}{1 - p_S} \tag{43}$$

While the BM is related mainly to the effect of increasing the component reliability, the CI includes the ratio of component to system unreliability (Rausand and Høyland, 2004). Based on CI rankings, a less reliable component is deemed more critical. This makes CI suitable for planning and prioritizing maintenance actions in complex networks.

7.2.3 The usage of IM for network reliability

It is rather straightforward to determine the IMs like the BM, CI, RAW, and RRW based on MCS, if the network model is computationally cheap. The system state is evaluated for each component state vector, thus, it is evaluated based on the chosen network performance model whether the system is in a failure state or in a non-failure state. This leads to two matrices or vectors: 1) the n-by-l matrix x_l where all n_{MC} MCS simulations are listed and in each row the corresponding component state vector is written, i.e., for each component $1 \ldots l$, it is 1 for non-failure or 0 for failure state, 2) the system state vector x_S. Based on x_l and x_S, it is possible to compare for each component the events 'component failure' versus 'system failure' as illustrated in the fourfold table in Figure 22. In all simulations n_{MC}, it is counted for each component the number of casas of:

- component failure and system failure $\{X_{l_i} = 0 \cap X_S = 0\}$
- component non-failure and system failure $\{X_{l_i} = 1 \cap X_S = 0\}$
- component failure and system survival $\{X_{l_i} = 0 \cap X_S = 1\}$
- component survival and system survival $\{X_{l_i} = 1 \cap X_S = 1\}$

Dividing the counts by the number of MCS simulations n_{MC}, leads to the MCS approximate of the probabilities given in Figure 22. Further, one can receive the probability values

to finally calculate the IMs of interest (compare Table 6), e.g.:

$$Pr\left(X_S = 1 \middle| X_{l_i} = 1\right) = \frac{Pr(X_S = 1 \cap X_{l_i} = 1)}{Pr(X_{l_i} = 1)} \tag{44}$$

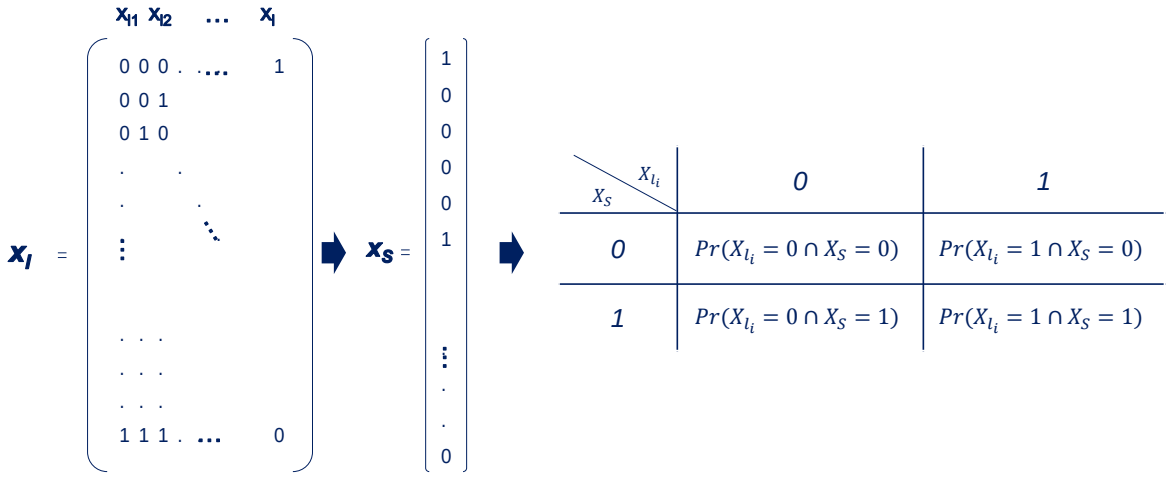

Figure 22: Illustration of the MCS approach for component state simulation, system state evaluation, and based on this, determination of the fourfold table concerning the component and system failure events.

7.3 Reliability importance measures in continuous systems

In Chapter 7.2, the IMs are defined for binary components and a system failure definition based on the binary system state variable X_S. For continuous system performance measures, we suggest a metric based on the derivative of the performance with respect to p_{F_i}, the component failure probability. We investigate the use of the continuous system performance function $\tau(\boldsymbol{x_l})$ in the definition of the IMs. This is expected to bring a couple of benefits. For the binary system state one needs to prescribe a threshold t on the performance function to define the system failure. With the continuous measure, there is no need for a threshold, i.e., the IM is not dependent on the additional variable t. Furthermore, for calculating the classical measures BM and CI, in the simulation data, there may be cases with only little or no system failure events. In this situation, the MCS estimate becomes rather inaccurate.

The derivation of the system damage metric in order to deduct component importance measures is related to the suggested differential important measure (DIM) by Borgonovo and Apostolakis (2001). DIM is defined as the derivation of a risk metric describing a

system damage to the change in a generic parameter (such as the failure rate of a component). DIM can be understood as a more generic interpretation of the IMs suggested in the following.

In the following, we suggest IMs for continuous systems, defined as the derivation of the expected value of the performance function $\tau(\boldsymbol{x_l})$ with respect to the component failure probability $\frac{\partial \mathrm{E}[\tau(\boldsymbol{x_l})]}{\partial p_{l_i}}$. The definition is applied to the case of the graph efficiency model and to the case of the power load loss model.

7.3.1 Graph efficiency sensitivity

We suggest an efficiency-based importance measure that describes the change in the expected value of the overall graph efficiency E_{norm}, see Equation (16), with a change in the component failure probability:

$$ES_i = \frac{\partial E[E_{norm}]}{\partial p_{l_i}} \tag{45}$$

By writing the expected value of the normalized efficiency as

$$\begin{aligned} E[E_{norm}] = \; & E\left[E_{norm}\middle|X_{l_i}=1\right] Pr(X_{l_i}=1) + E\left[E_{norm}\middle|X_{l_i}=0\right] Pr(X_{l_i}=0) \\ = \; & E\left[E_{norm}\middle|X_{l_i}=1\right] p_{l_i} + E\left[E_{norm}\middle|X_{l_i}=0\right](1-p_{l_i}), \end{aligned} \tag{46}$$

it is seen that the efficiency measure can be computed as

$$ES_i = E\left[E_{norm}\middle|X_{l_i}=1\right] - E\left[E_{norm}\middle|X_{l_i}=0\right]. \tag{47}$$

A deterministic version of this measure can be found in Latora and Marchiori (2004), where the importance of a component is measured in analogy to a $(n-1)$-contingency approach. They measure the decrease in network efficiency after one single component is removed from the graph.

7.3.2 Load loss sensitivity

In analogy to the graph efficiency sensitivity measure in the previous section, we additionally suggest an importance measure based on the loss of load. It describes the change in

the expected value of the overall loss of load with a change in the component failure probability:

$$LS_i = \frac{\partial E[L_{norm}]}{\partial p_{l_i}} \tag{48}$$

By writing the expected value of the normalized loss of load L_{norm}, Equation (20), as:

$$\begin{aligned} E[L_{norm}] = & \; E\left[L_{norm}\middle|X_{l_i}=1\right] Pr(X_{l_i}=1) + \; E\left[L_{norm}\middle|X_{l_i}=0\right] Pr(X_{l_i}=0) \\ = & \; E\left[L_{norm}\middle|X_{l_i}=1\right] p_i + \; E\left[L_{norm}\middle|X_{l_i}=0\right](1-p_{l_i}), \end{aligned} \tag{49}$$

it is seen that the sensitivity measure can be computed in analogy to Equation (47):

$$LS_i = E\left[L_{norm}\middle|X_{l_i}=1\right] - \; E\left[L_{norm}\middle|X_{l_i}=0\right]. \tag{50}$$

7.4 Importance measures in cascading system failure events

There are studies in literature that reflect on the problem of component importance or criticality in cascading failure systems (Zio and Sansavini, 2011) as discussed earlier; however, there are only few studies that combine the problem of component importance and cascading failures in power grid networks subject to natural hazard events (Ouyang et al., 2012), see Table 3. However, in Ouyang et al. (2012) it is not used the concept of importance in its commonly used sense but rather it is identified critical components (i.e. critical substations) based on their topological degrees without analysis of the system performance in cascading failure events dependent on the component performance.

In this thesis it is going to be applied the concept of component importance against the backdrop of cascading failure events and natural, i.e. spatially distributed hazard impacts, as discussed in the following.

The above Importance Measures (IM), Birnbaum Measure (BM), Critically Importance (CI), Efficiency Sensitivity (ES), and Load Sensitivity (LS) include a derivation with respect to the failure probability of the component. In cascading system failure events triggered by (external) natural hazard events, we suggest that it is relevant to distinguish

1) The failures of components caused directly by the hazard event and
2) The failures of components caused by the cascading effect.

We refer to the former as the *initial component failures* and the latter as the *cascading component failures.* Additionally, *final component failures* include both failure types.

All the above IMs (as well as others) can be defined with respect to any of these three component failure concepts. To distinguish these measures, we introduce the superscripts (i), (c), and (f) to denote the IMs relating to *initial*, *cascading*, and *final* component failure events. The corresponding definitions of the CI_i derivations, e.g., for a component l_i, can be defined as follows:

$$CI_i^{(t)} = \left(Pr\left(X_S = 1 \middle| X_{l_i}^{(t)} = 1\right) - Pr\left(X_S = 1 \middle| X_{l_i}^{(t)} = 0\right)\right) \frac{(1 - p_{l_i}^{(t)})}{1 - p_S} \tag{51}$$

with (t) indicating the 3 failure modes by the superscripts (i), (c), and (f) the (initial, cascading, or final) component reliability $p_{l_i}^{(t)}$, respectively, and the system reliability p_S.

The definitions for the initial, cascading, and final LS_i measures are given in the following, for a component l_i:

$$LS_i^{(t)} = E\left[L_{norm} \middle| X_{l_i}^{(t)} = 1\right] - E\left[L_{norm} \middle| X_{l_i}^{(t)} = 0\right] \tag{52}$$

The analogue definitions for the ES_i measures are in analogy based on the conditional expectation value of the efficiency $\mathrm{E}[E_{norm}]$:

$$ES_i^{(t)} = E\left[E_{norm} \middle| X_{l_i}^{(t)} = 1\right] - E\left[E_{norm} \middle| X_{l_i}^{(t)} = 0\right] \tag{53}$$

The measure of system performance employed in the IMs (either p_S, $\mathrm{E}[L_{norm}]$, or $\mathrm{E}[E_{norm}]$) always relates to the *final* performance of the system following the initial failures and the cascading effects.

Which of the suggested IMs should be used depends on the aim of the study and on the potential mitigation measures applied to an investigated network. In order to identify components to be reinforced against natural hazard events, the $CI^{(i)}$, $ES^{(i)}$, or $LS^{(i)}$ should be employed. Conversely, $CI^{(c)}$, $ES^{(c)}$, or $LS^{(c)}$ should be the basis for ranking and identifying components for increasing capacity against overloading.

In Figure 23, an example illustrates the calculation of the suggested IMs in a Monte Carlo Simulation framework for the evaluation of a grid or a network with a set of l lines subject to potential failure. In section 5.5.2.1, the calculation of the overall network reliability problem is explained for the MCS framework.

In each MC simulation step k, it is recorded if a component $l_i, i = 1, .., L$ failed initially

or during the cascading process. The union of both failure types is the final failure. Thus, the binary component state vector $\boldsymbol{x}_l^k$ is recorded for initial, cascading, and final failure events, respectively. In each simulation step k, based on the component state vector $\boldsymbol{x}_l^k$, the eventually damaged network is re-evaluated according to the network model applied, see Chapters 5.2.2, 5.2.3, and 5.3. The system structure function $\phi(\boldsymbol{x}_l^k)$ or the performance model $\tau(\boldsymbol{x}_l^k)$ is evaluated for each simulation sample k and the system state variable X_S is recorded as well. In case of a continuous performance function, the system failure event $X_S = 0$ would be defined e.g., according to the loss of load falling below a prescribed threshold t as explained in Chapter 5.2.3. The overall final network damage is recorded, in the example of Figure 23, and the final power loss is normalized with the load supplied in the undamaged network, L_{norm}.

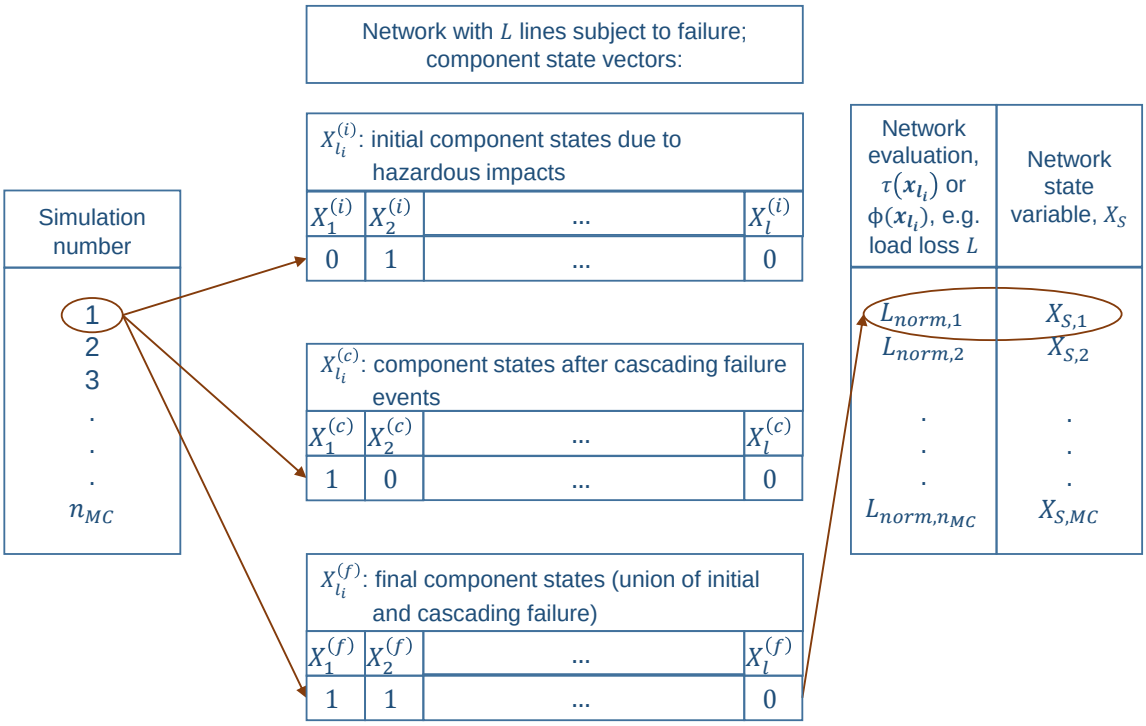

Figure 23: Visualization of the determination of the IMs differentiated with reference to initial, cascading and final failure of a component within a Monte Carlo Simulation framework.

In all n_{MC} samples, it is counted for each component l_i how often it survived/failed initially versus how often it survived/failed in the cascading process, which is recorded by the indicator function $I_{li}^{(t)} = \begin{cases} 1, & \text{for } x_{l_i}^{(t)} = 1 \text{ (functioning)} \\ 0, & \text{else (failure)} \end{cases}$.

The marginal component reliabilities can be estimated as:

$$p_{l_i}^{(t)} \approx \frac{\sum_{k=1}^{n_{MC}} I_{li}^{(t)}}{n_{MC}} \tag{54}$$

Next, the MC estimates of the conditional system reliabilities can be calculated, i.e. given the component failed (initially or in the cascading process) versus the system reliability when the component did not fail:

$$Pr\left(X_S = 1 \middle| X_{l_i}^{(t)} = 1\right) \approx \frac{1}{n_{MC}} \sum_{k=1}^{n_{MC}} I_{X_S|li}^{(t)} \left[x_S^k = 1 \middle| x_{l_i}^{k,(t)} = 1\right] \tag{55}$$

$$Pr\left(X_S = 1 \middle| X_{l_i}^{(t)} = 0\right) \approx \frac{1}{n_{MC}} \sum_{k=1}^{n_{MC}} I_{X_S|li}^{(t)} \left[x_S^k = 1 \middle| x_{l_i}^{k,(t)} = 0\right] \tag{56}$$

For the network performance, MC estimates are calculated given the component failed (initially or in the cascading process) versus the damage when the component did not fail. As a base for the measures ES and LS, the conditional mean values of the final efficiency or the final loss of load are calculated as estimates of the expected values. For the case of the cascading failure events in a network modelled by power flow equations this would be expressed as follows:

$$E\left[L_{norm} \middle| X_{l_i}^{(t)} = 1\right] \approx \frac{1}{n_{MC}} \sum_{k=1}^{n_{MC}} I_{li}^{(t)} L^k{}_{norm} \tag{57}$$

$$E\left[L_{norm} \middle| X_{l_i}^{(t)} = 0\right] \approx \frac{1}{n_{MC}} \sum_{k=1}^{n_{MC}} (1 - I_{li}^{(t)}) L^k{}_{norm} \tag{58}$$

Based on the results from Equations (54)-(58) and Equations (51)-(53) the IMs of interest can be determined.

7.5 Reliability enhancement based on IMs

Various types of mitigation measures that improve the reliability of an electrical power network are described in literature. Example measures are changes in connectivity (e.g., Rosato et al., 2007, Brummitt et al., 2012), protection of critical components (e.g., Pepyne, 2007, Johansson and Hassel, 2014), or, increasing redundancy of most critical lines by

adding (by-pass) lines (e.g, Crucitti et al., 2005, Johansson and Hassel, 2014). Holmgren (2006) assesses changes in the network vulnerability by changes in the network's $average\ vertex\ degree$, $average\ path\ length$, or $clustering\ coefficient$. One important insight by Brummitt et al. (2012) is that increasing the (inter-) connectivity of networks is not advantageous per se but can become detrimental: more interconnections can enable larger cascading events by opening up new pathways for neighboring networks or network compartments. Furthermore, new (inter-) connections increase the capacity and hence the total possible load and can thereby yield even larger cascading events than without increased connectivity. Criticality of the lines in these studies was mainly defined based on $(n-1)$-contingency analyses and centrality measures. Reliability IMs were not used to identify critical components in connection with network improvement strategies.

In this thesis, the IMs defined in the previous sections should support decision making about potential risk mitigation, i.e., reliability enhancement strategies. To this end, we investigate network improvement strategies based on the IMs differentiated according to *initial, cascading, and final* failure as proposed above. It is examined if this differentiation brings a benefit for the optimization of a decision. With this aim, the effect of strengthening selected lines, i.e. decreasing their initial failure probability versus increasing the capacity of selected lines on the network's overall reliability or performance (in terms of loss of load or network efficiency) are compared.

Two main network improvement strategies are considered:

1) Line (segment) strengthening of a prescribed ratio (e.g. 10%) of the most important lines or line segments ranked by either $CI^{(i)}$, $ES^{(i)}$, or, $LS^{(i)}$ corresponding to an increase in the resistance against the hazardous (wind) load. Line strengthening is modeled by reducing the initial line segment vulnerability to e.g., 25% or 50% of its original value.

2) Increase of the line capacity of a prescribed ratio (e.g. 10%) of the most important lines ranked by either $CI^{(c)}$, $ES^{(c)}$, or, $LS^{(c)}$ corresponding to an increase in the resistance of the lines against overloading in the cascading failure process. The capacity increase is modeled by increasing the tolerance parameter α to prescribed factors, e.g., $f_\alpha = 2$ or $f_\alpha = 4$.

The two strategies can be interpreted as two different categories of measures and activities for the infrastructure strengthening. Strategy 1) can be understood a type of measures that increase the resistance or decrease the vulnerability of components against wind loads. Examples are improved vegetation management (clearing), upgrading damaged poles and structures, strengthening poles with guy wires, or replacing overhead lines by underground cables (US Department of Energy, 2010), see Figure 24.

Increasing the capacity of complete lines (strategy 2), can be cost intensive. However, it is of interest to consider the effects on the overall system reliability if selected components could be improved in terms of their capacity to withstand power overloading.

The suggested network reliability enhancement strategies are "naturally" consequent with the character of the component, i.e. if the component is important with respect to the initiating versus the cascading event. In this thesis the strategies are supposed to give a first indication about the effectiveness and reason to distinguish the component categories as will be demonstrated in the case studies later in this thesis. In future studies the enhancement strategies could be expanded and refined to specific interests subsequently.

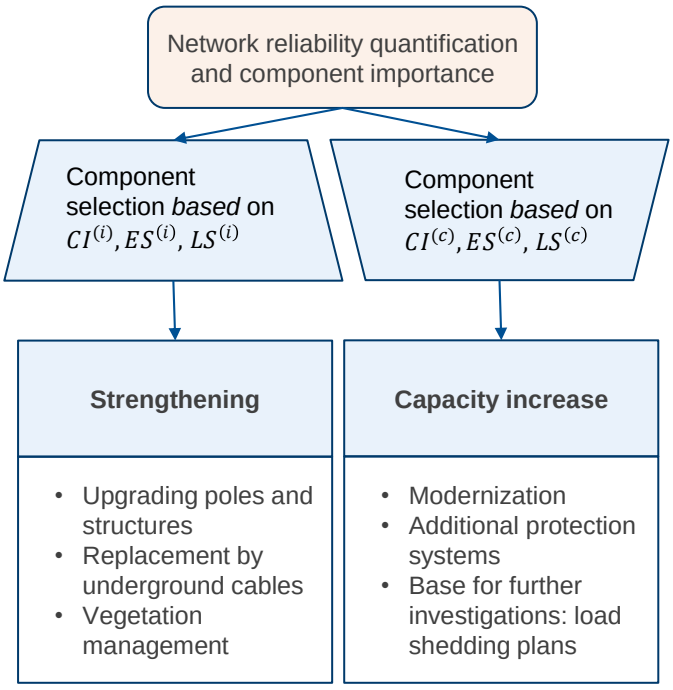

Figure 24: Improvement activities for the two alternative strategies suggested in this section based on component rankings: a) strengthening against hazard impacts, b) capacity increase for power overload prevention.

7.6 Summary

This chapter deals with the topic of component importance. Different approaches are introduced that aim at identifying the most critical components in a network, i.e. components that contribute to network reliability in one way or another. Emphasis is laid on so-called reliability importance measures for binary systems and continuous system performance definitions. It is suggested to distinguish IMs based on initial failures due to hazardous impacts from cascading failure events due to overloading after initial failure events in order to find those components, which are more important for the instant initiation of damage and those which are more responsible for the further propagation of failure events after initial triggering events. Based on these IMs, two improvement strategies are suggested that will be investigated in detail in the case studies of Part III, see Chapters 9.6, 10.4.3,

and 10.5.5.

Part III – Case studies

8 Reliability of power transmission grids subject to hurricane hazards

Parts of this Chapter are taken from Scherb et al. (2015), a peer-reviewed contribution to the International Conference on Applications of Statistics and Probability in Civil Engineering (ICASP), Vancouver, Canada, July 12-15, 2015.

8.1 Methodological framework

The overall approach used in this case study is shown in Figure 25, which is a slightly reduced version of the general framework presented in Figure 10: This case study presents a first idealized development and implementation of the probabilistic reliability analysis framework introduced in Chapter 4. Extreme winds in hurricane events are considered, which impose potential hazardous loads on components and entail potential extrinsic dependencies between network components. Additionally, the physical dependency of the network components through subsequent cascading failure processes in the network are modelled.

The hurricane hazard is modelled as a parametric function of the wind speed in 10 m height above ground. The model developed is based on the study of sample data from historical hurricane events. The advantage of the suggested wind field model is that it requires only three parameters. Assumptions are made for the hurricane eye position at landfall and the

further track above land in 1 hour time steps during 12 hours after landfall; therefore, the hurricane model developed here is a probabilistic spatial-temporal idealization.

The parameters of the component fragility curves as function of wind speed are here based on modelling assumptions from literature. The network performance is assessed based on a DC power flow model in terms of loss of load considering the power flow characteristics of the network and potential cascading failures as it is discussed following Chapter 5.4.2.

A synthetic transmission power system is investigated, the IEEE 'One Area' RTS-96 benchmark power transmission network composed of 24 nodes and 38 lines, publicly available at Christie (2000).

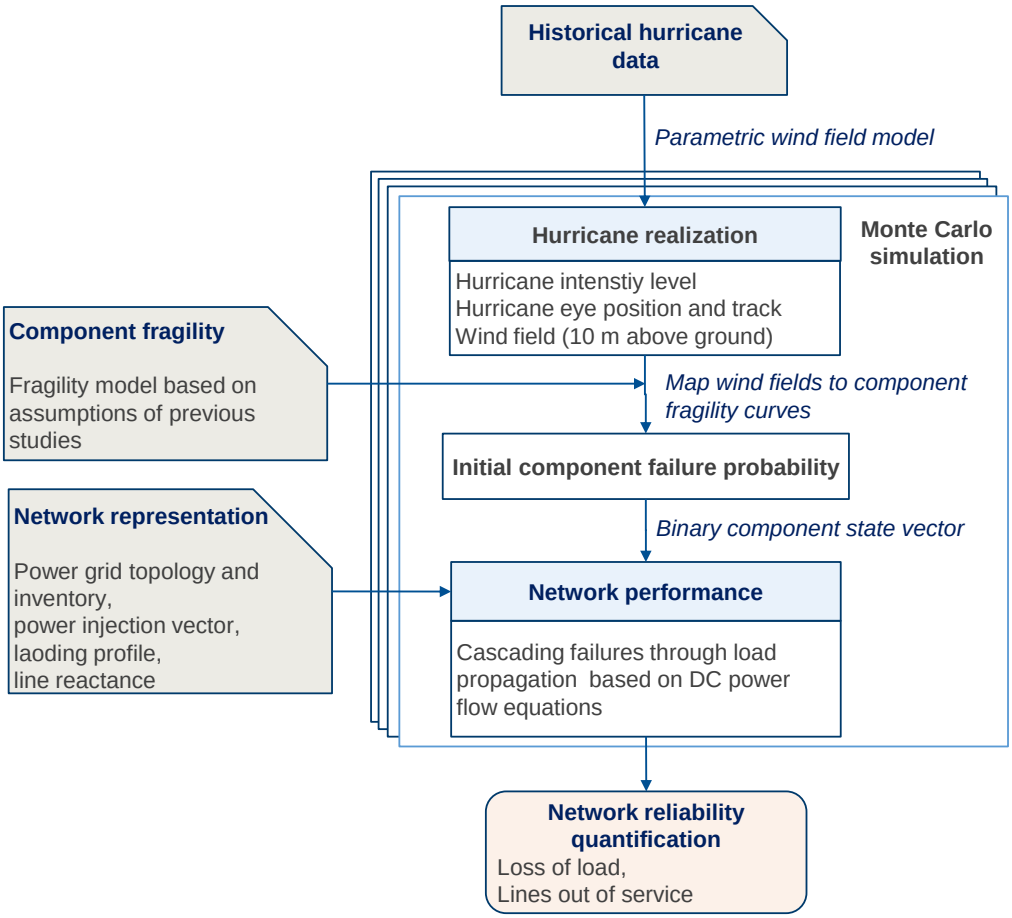

Figure 25: Methodological framework for the reliability analysis of power networks subject to hurricane hazards.

8.2 Parametric hurricane wind field model

8.2.1 Background on hurricane modelling

Hurricane modelling is a broad research field. Generally, two main focal points can be distinguished:

1) The analysis of hurricane occurrence, track, size, wind speeds, gradient wind fields, and further key parameters. The goal is to build statistical (prediction) models or physical models of the hazard.
2) Building upon 1): models for deducing design wind speeds for the use in building codes and standards; furthermore, models for estimating the risk in terms of, e.g., the expected probable maximum or the average annual (insurance) losses.

The field of probabilistic hurricane modelling and simulation builds upon pioneering studies in the 1960s to 1970s, e.g., Russell (1968) and Russell (1971) where a probabilistic simulation process is described. This was followed in the 1980s by a number of important studies by Batts (1980), Georgiou et al. (1983), and Georgiou (1985). These studies mainly share their basic approach of first obtaining some key parameters like the radius to maximum winds, the translation speed, and the coast crossing position. Given the statistical distributions of these key parameters, a Monte Carlo simulation can be conducted to sample from each distribution, and a set of simulated storms can be generated. Over the years, improvements in research were possible through the substantial increase in quantity and quality of available measured data (Powell et al. (2005), Vickery and Wadhera (2008), Vickery et al. (2009b), and Powell et al. (2010)). A detailed introduction into hurricane modelling is provided by Vickery et al. (2009a).

The development of risk assessment models is closely related to the developments of the hurricane hazard models themselves. Example studies on insurance loss models, average annual losses, and damage models for residential structures are: Huang et al. (2001b), Huang et al. (2001a), Sparks (2003), and Powell et al. (2005). They have in common that they mainly apply event-based MCS techniques for the risk assessment. Several studies have assessed specifically the vulnerability of power networks and the occurrence of outages in hurricane prone regions mainly of the US. Some more recent studies accounted for cascading failures during hurricanes in a simulation context (Winkler et al., 2010, Ouyang et al., 2012, Ouyang and Dueñas-Osorio, 2014, Javanbakht and Mohagheghi, 2014). Javanbakht and Mohagheghi (2014) suggest a hurricane model represented by static and dynamic gradient wind fields based on the analysis of hurricane Katrina. In contrast, Winkler et al. (2010), Ouyang et al. (2012), and Ouyang and Dueñas-Osorio (2014) used for their analysis the HAZUS-MH project to generate wind field simulations and to obtain site specific wind speeds in hurricane events. HAZUS is a natural hazard analysis tool

developed by the Federal Emergency Management Agency (FEMA). It is based on geographic information systems and includes an earthquake, flooding, hurricane, and storm surge model as well as corresponding damage and loss functions. Therefore, HAZUS offers a whole risk assessment framework for several assets, mainly building constructions. The methodology for the hurricane hazard type in the HAZUS package was developed by Vickery et al. (2006) and uses the hurricane model suggested in Vickery et al. (2000).

Since the focus in this study is on the behavior of the network reliability given large scale hazards and associated dependencies in component failures, we build a rather generic hazard model with limited complexity. The hurricane data analyses and model suggested is explained in the following sections.

8.2.2 Hurricane data

Example hurricane data can be accessed freely at RMS (2013)[4]. Risk Management Solutions (RMS) is hosting the HWind legacy archive. The HWind project was formerly developed and produced by the Hurricane Research Division (HRD) at the National Oceanic and Atmospheric Administration (NOAA). The HRD produced surface wind analysis of tropical cyclones from 1993 to 2013. Gridded data is available from 1998 to 2013.

HWind is a real-time Hurricane wind analysis system that is based on real-time observations of tropical cyclones that are compiled relative to the storm center. The project has the goal to improve understanding of the extent and strength of the tropical cyclones by also taking advantage of remote sensing data. Several publications describe the development of the HWind project, e.g., Powell et al. (1998) and Powell et al. (2010). These studies detail how the wind measurements are standardized and analyzed based on initial case studies on selected hurricanes including Frederic (1979), Alicia (1983), Hugo (1989), and Andrew (1992). Standardization means in this case that the data match in height (10 meter above ground), exposure (marine or open terrain over land), and averaging period (maximum sustained 1 minute wind speed), all in 3 or 6 hourly records.

Hurricanes are categorized according to their intensity, following the Saffir-Simpson hurricane wind scale (SSHWS). The SSHWS categorizes Western Hemisphere tropical cyclones by their maximum wind speeds into five categories. A storm is classified as a hurricane of category 1, if its intensity exceeds a level of 33 m/s or 119 km/h. A hurricane of category 5 has wind speeds exceeding 70 m/s or 252 km/h (NOAA, 2017). The SSHWS

[4] Data of the most severe hurricane storms every year can be downloaded at RMS: http://www.rms.com/perils/hwind/legacy-archive/storms/ [access date 2018/10/10].

is criticized for being oversimplifying because it does not take into account hurricane related events like rainfall or storm surges, but its advantage is that it is easy to understand and the classifications can provide at least some indication of the potential damage a hurricane will cause upon landfall. Generally, devastating and catastrophic damages can be expected in hurricanes starting from category 3 (NOAA, 2017).

For modelling the hurricane occurrence probability considering the different hurricane intensities, the (site-specific) probability of the hurricane falling into any one of the 5 categories needs to be known. In this case study, the distribution among hurricane categories is assumed based on Ouyang and Dueñas-Osorio (2014), as depicted in Table 7, that would reflect the conditions e.g., for Harris County, Texas, US, where an overall annual occurrence rate λ_a of hurricane hazards of about $\frac{1}{7}\ yr^{-1}$ is observed.

Table 7: Site specific probability of hurricane intensity given hurricane occurrence; probability values based on Ouyang and Dueñas-Osorio (2014) for conditions in Harris County, Texas, US, with an overall annual occurrence rate λ_a of hurricane hazards of about $\frac{1}{7}\ yr^{-1}$. Hurricane categories are based on the Saffir-Simpson hurricane wind scale (SSHWS).

Hurricane intensity [m/s]	P(Intensity | Hurricane)
1 [33-42]	0.53
2 [43-49]	0.19
3 [50-58]	0.15
4 [58-70]	0.08
5 [>70]	0.05

8.2.3 Wind field model

A hypothetical hurricane model is introduced. A hurricane event is treated as a random process in space, time, and intensity. The occurrence of hurricane events is modelled by a Poisson process with an occurrence rate λ.

A function $s(r_h)$ is fitted to observed static gradient wind fields of historical hurricane events for selected points in time, compare Figure 26 to Figure 29. A generic three-parametric function $s(r_h)$ is utilized to model the wind speed s as a function of the distance r_h from the hurricane center, Equation (59). The function yields the one minute directionless wind gust speed in 10 m height in open terrain at each site of interest within the study area.

$$s(r_h) = \frac{2r_h \cdot r_{max}(s_{max} - \omega)}{(r_h^2 + {r_{max}}^2)} + \omega \tag{59}$$

The model function $s(r_h)$ generates a circularly shaped wind field. It uses three parameters: maximum hurricane wind speed s_{max} in [m/s], the distance of the maximum wind speed from the hurricane eye r_{max} in [m], and the offset ω in [m/s], which is the asymptotic decay level of the wind field at great distances (infinity). The parameter s_{max} is defined conditionally on the hurricane intensity, by a uniform probability distribution within the wind speed intervals according to Table 8. The parameters r_{max} and ω are also modeled by independent uniform distributions.

Examples of the hurricane data together with the corresponding model fits and the corresponding wind field contour plots around the moment of land fall can be seen in Figure 26 to Figure 29.

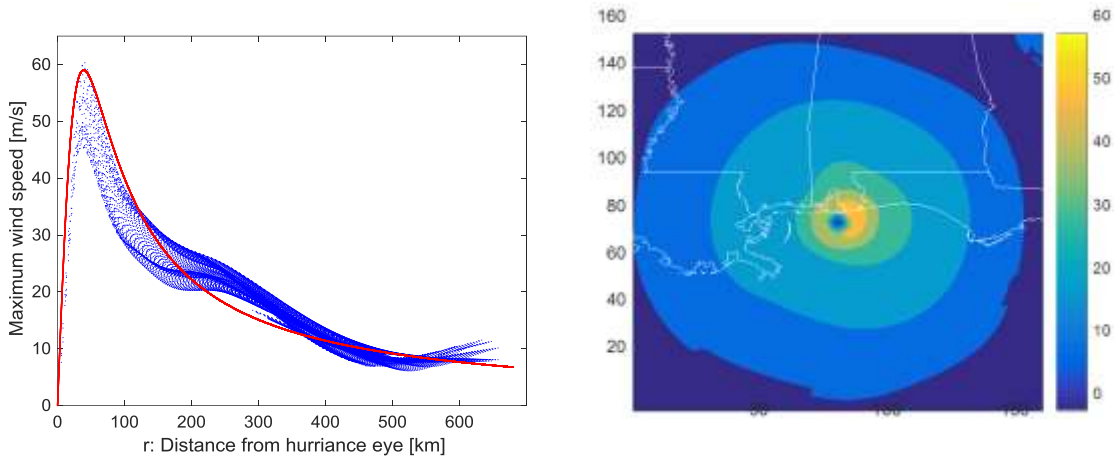

Figure 26: Hurricane Ivan. Left: Modelled maximum wind speed curve, red, Equation (59), together with data from hurricane Ivan, blue, at landfall: 2004 September 16, 06:00; Right: Wind field contour plot of the hurricane data off the coast of the US. Data refers to the maximum sustained 1 minute wind speeds in 10 m height.

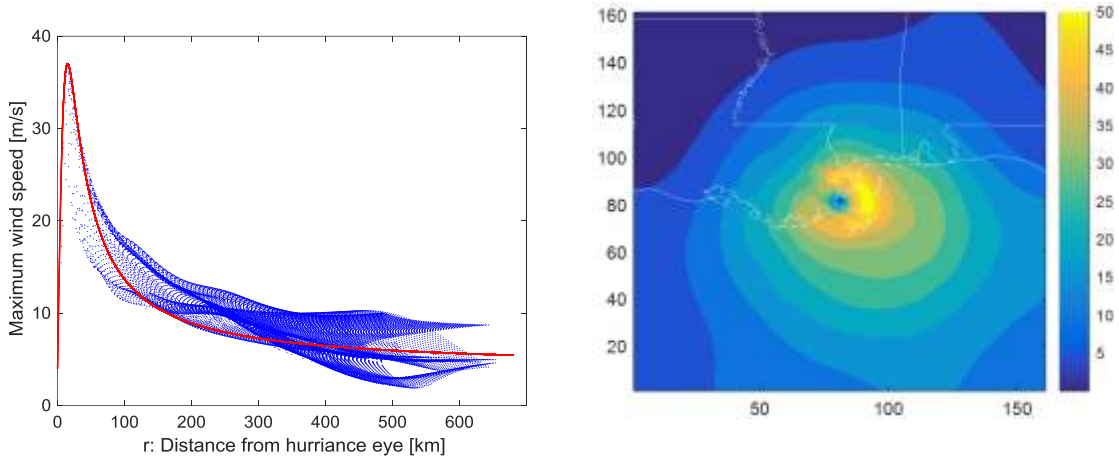

Figure 27: Hurricane Katrina. Left: Modelled maximum wind speed curve, red, Equation (59), together with data from hurricane Katrina, blue, at landfall: 2005 August 29, 12:00; Right: Wind field contour plot of the hurricane data off the coast of the US. Data refers to the maximum sustained 1 minute wind speeds in 10 m height.

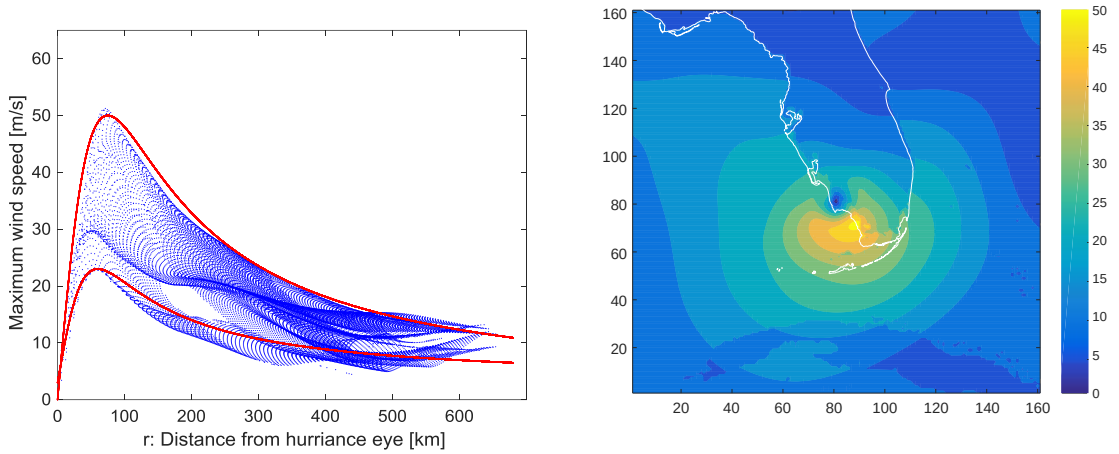

Figure 28: Hurricane Wilma. Left: Modelled maximum wind speed curves with two alternative parametrizations, red, Equation (59), together with data from hurricane Wilma, blue, at landfall: 2005 October 24, 10:30; Right: Wind field contour plot of the hurricane data off the coast of the US. Data refers to the maximum sustained 1 minute wind speeds in 10 m height.

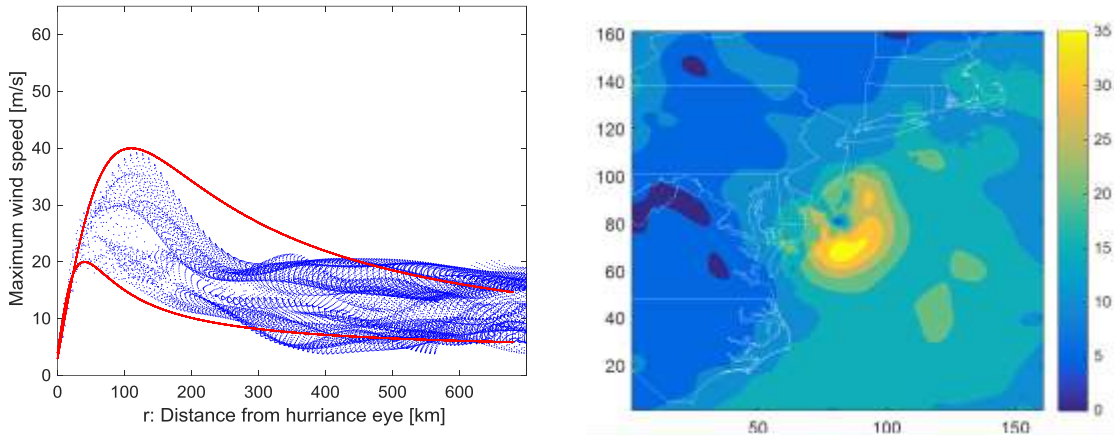

Figure 29: Hurricane Sandy. Left: Modelled maximum wind speed curves with two alternative parametrizations, red, Equation (59), together with data from hurricane Sandy, blue, before landfall: 2012 October 29, 19:30; Right: Wind field contour plot of the hurricane data off the coast of the US. Data refers to the maximum sustained 1 minute wind speeds in 10 m height.

The temporal component of the model is implemented through time steps of 1 hour after landfall (x_0, y_0, t_0), whereby the hurricane center is assumed to move 12 hours inland with a translational speed of 15 km/h according to Javanbakht and Mohagheghi (2014). The initial landfall location of the hurricane eye at the study area's lower boundary (coastline), (x_0, y_0) is chosen according to a uniform distribution. At each time step, the eye location is updated according to hurricane track direction β, which is assumed to follow a normal distribution centered on the south-to-north direction. At each time step and at each location of interest, the wind speed value is calculated according to Equation (59). An overview of all variables and assumptions is given in Table 8.

Table 8: Hurricane model variables and probability distribution assumptions.

Variable	Probability distribution and assumptions	Comments and data source
Hurricane occurrence (annual)	Poisson distribution	λ_a =1/7; (Ouyang and Dueñas-Osorio, 2014)
Landfall position	Uniform distribution	Location on lower boundary of study area (coastline, 400 km length)
Hurricane intensity (class)	Discrete distribution	(Ouyang and Dueñas-Osorio, 2014); Table 7
Maximum hurricane wind speed, s_{max} [m/s]	Uniform distribution	The hurricane intensity class determines the wind speed interval
Distance eye to s_{max}, r_{max} [km]	Uniform distribution	Range 10 to 100 km
Offset, ω [m/s]	Uniform distribution	Range 5 to 15 m/s
Track direction, β [degree]	Normal distribution	Emphasis on south-north directions; $\mu = 90°; \sigma = 15°$

8.3 Component fragility

The component fragility models describe the damage probability of the individual network components as a function of the hazard characteristics. Here, fragility models are based on the 10 m wind gust speed alone, independent of direction and duration or other hurricane parameters. As a further simplification, no distinction is made between different line types and each transmission line is seen as a single unit.

For four predefined damage levels (no, minor, moderate, and major damage), lognormal fragility curves describe the probability of the i-th component to have reached a damage state d_j as function of wind speed s:

$$Pr\big(D_i \geq d_j | S_i = s\big) = \int_0^s \frac{1}{\sigma_j \sqrt{2\pi} s} exp\left(\frac{-\big(ln(s) - \mu_j\big)^2}{2\sigma_j^2}\right) ds \tag{60}$$

The fragility functions are depicted in Figure 30. The probability of failure of a network component given wind speed $\Pr(F_i|S_i = s)$ is calculated according to:

$$Pr(F_i|S_i = s) = \sum_{d_{ij}} Pr(F_i|D_i = d_{ij})\, Pr(D_i = d_{ij}|S_i = s) \tag{61}$$

The conditional probabilities $\Pr(F_i|\mathrm{d_{ij}})$ of component failure given the damage state are summarized in Table 9.

Table 9: Fragility model variables and probability distribution assumptions.

Variable	Probability distribution and assumptions	Comments and data source
Component damage state, d_{ij}	Fragility $Pr(d_{ij}\|s)$ following Equation (60)	Parameters according to Figure 30 based on Javanbakht and Mohagheghi (2014)
Component (line segment) failure, F_i	$\Pr(F_{ij} = 1 \| d_{ij}) = [0.01, 0.1, 0.2, 0.6]$	Based on assumptions

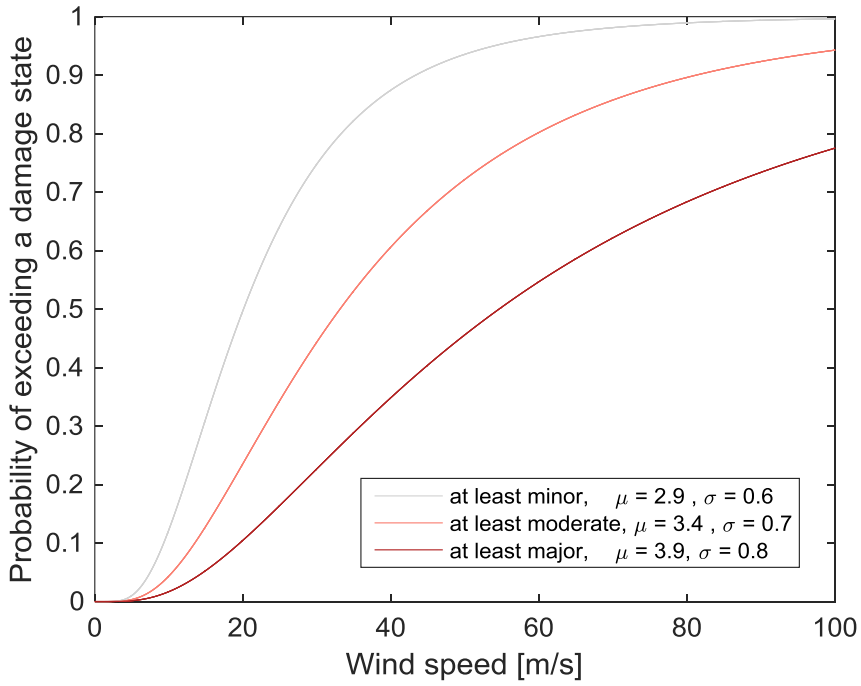

Figure 30: Fragility curves for four damage states, d_j (no, minor, moderate, and major damage). The three curves indicate at least minor damage, at least moderate, and at least major damage. The parameters are based on Javanbakht and Mohagheghi (2014).

8.4 Network response model

The network response in the course of hazardous impacts is based on the DC power flow equations following Chapter 5.4.2. The model accounts for cascading failure processes that might evolve after initial triggering events. The damage can be quantified in terms of loss of load and lines out of service.

8.5 Numerical implementation

The synthetic 24-bus system, the IEEE 96-RTS (Christie, 2000), is used in this case study. It is a reliability test system (RTS) that was derived from the RTS-79 in 1996. It is a test system often used in bulk power reliability analysis (Grigg et al., 1999) since the system represents a mid-sized benchmark system and is thus frequently utilized in a great variety of risk analyses.

The power grid is represented by a graph and is georeferenced by projecting it onto a 300 x 300 km^2 study area. Each substation and transmission line segment is assigned an x,y-coordinate. The substation capacities and the technical parameters of the transmission lines, such as reactance and capacity, are obtained from the test case file (Christie, 2000). Figure 31 depicts the test case network, together with an idealized scheme of a possible hurricane realization making landfall at the coastline.

Hurricane scenarios are simulated in a Monte Carlo simulation, with 10,000 sample realizations.

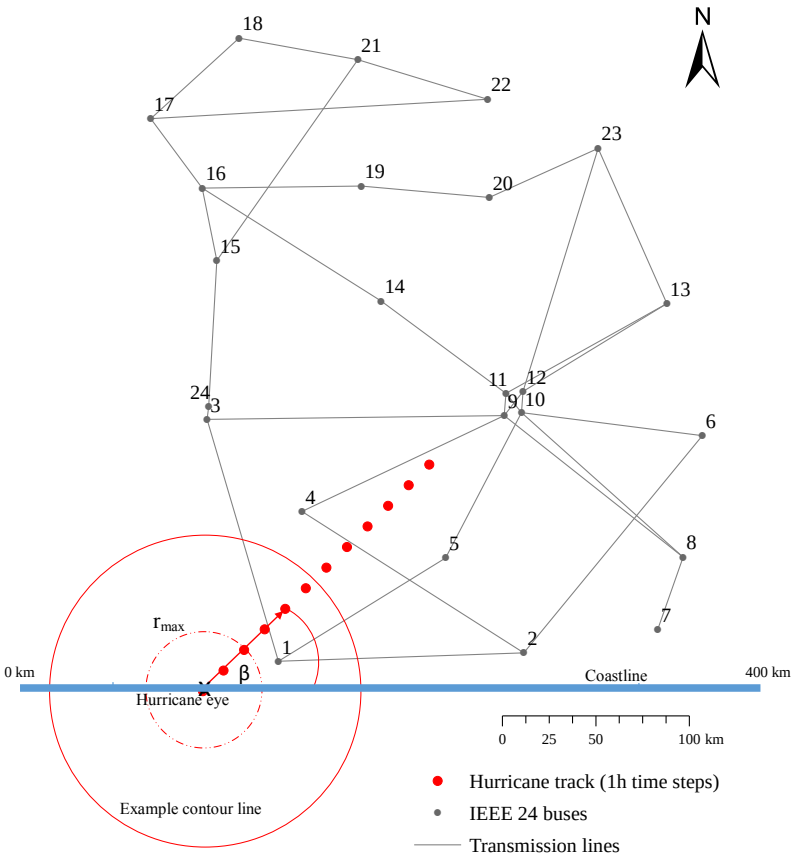

Figure 31: 2D contour lines of one realization of the wind field at landfall (x_0, y_0, t_0), indication of 1 hour time steps of hurricane eye track (red dots), and georeferenced power network in a 300 x 300 km^2 study area.

8.5.1 Simulation results

Monte Carlo simulations are conducted for varying tolerance parameter α, which determines the capacity against overloading of the power grid components. From the results of the MCS, there is only a 0.07 probability of the network remaining completely intact after a hurricane, i.e., no occurrence of initial component failures and therefore no loss of load. The probability that component failures occur but do not result in a loss of load in the grid is 0.11. This means that with a probability of 0.11 the grid is able to secure the initial failures due to the hurricane impacts. 82% of hurricanes lead to a power loss in the system of some sort. The overall average expected power loss is 69% in all MC simulations. Conditional on a loss of load occurring, the expected loss of load value is 73% of the original load supplied in the intact grid. With 0.12 probability, the overall power loss is greater than 90%. In Figure 32, a comparison is shown of the cumulative frequency diagrams of MCS based on two different tolerance parameters, $\alpha = 1.2$ versus $\alpha = 1.5$. For the higher α-value, the higher percentage of cases with no loss of load is about 20%, i.e. the system has

a higher average capacity to withstand power overloading.

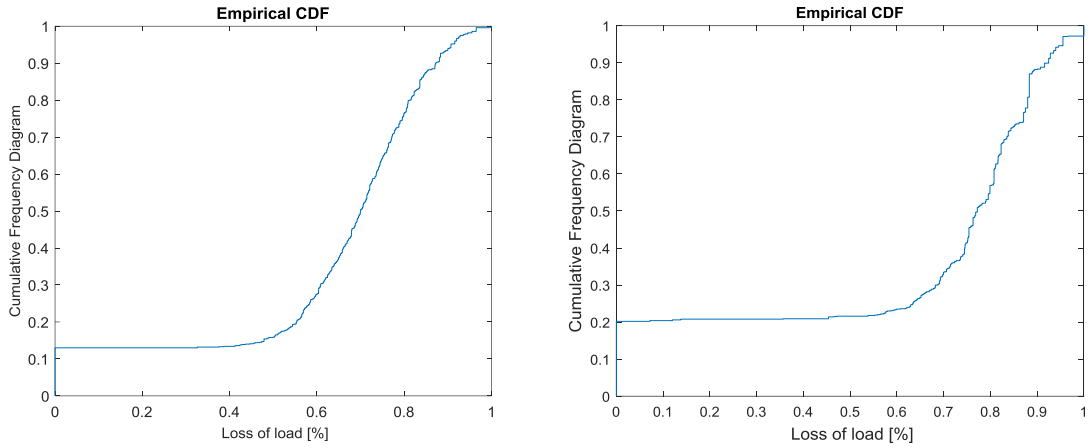

Figure 32: Cumulative frequency diagrams (CDFs) for the loss of load [%] after 1000 MCS runs without cases of no component failure events. Left: tolerance parameter $\alpha = 1.2$; Right: tolerance parameter $\alpha = 1.5$.

When comparing the number of deactivated lines after cascading failures with the number of initially triggered components, a plausible positive association can be observed. Nevertheless, already for small numbers of initially failed components, the total number of failures after cascading failures may be large. This effect has also been stated in Motter and Lai (2002), especially when the tolerance limits α for single parts of the grid or for the network as a whole are rather small. Because of this effect, the resulting load loss is not very sensitive to the number of initially failed lines especially for low α-values. However, for higher α-values the dependence becomes more visible as evident from comparing Figure 33 with Figure 34.

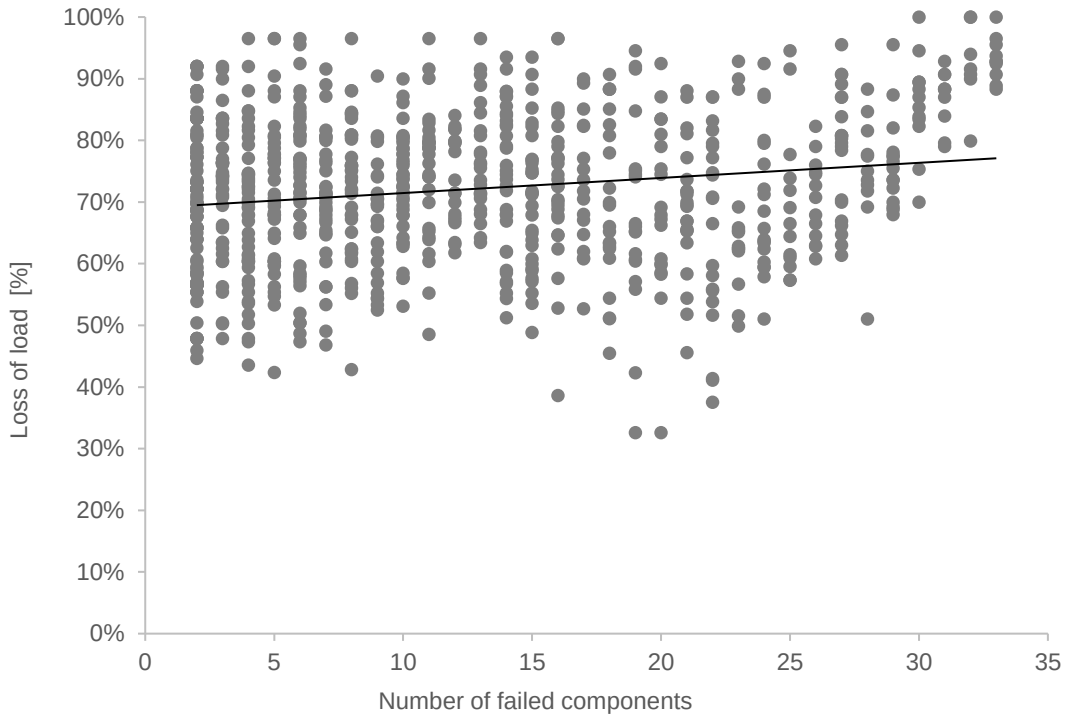

Figure 33: Dependence of power loss on number of initially failed lines based on tolerance value, $\alpha = 1.2$.

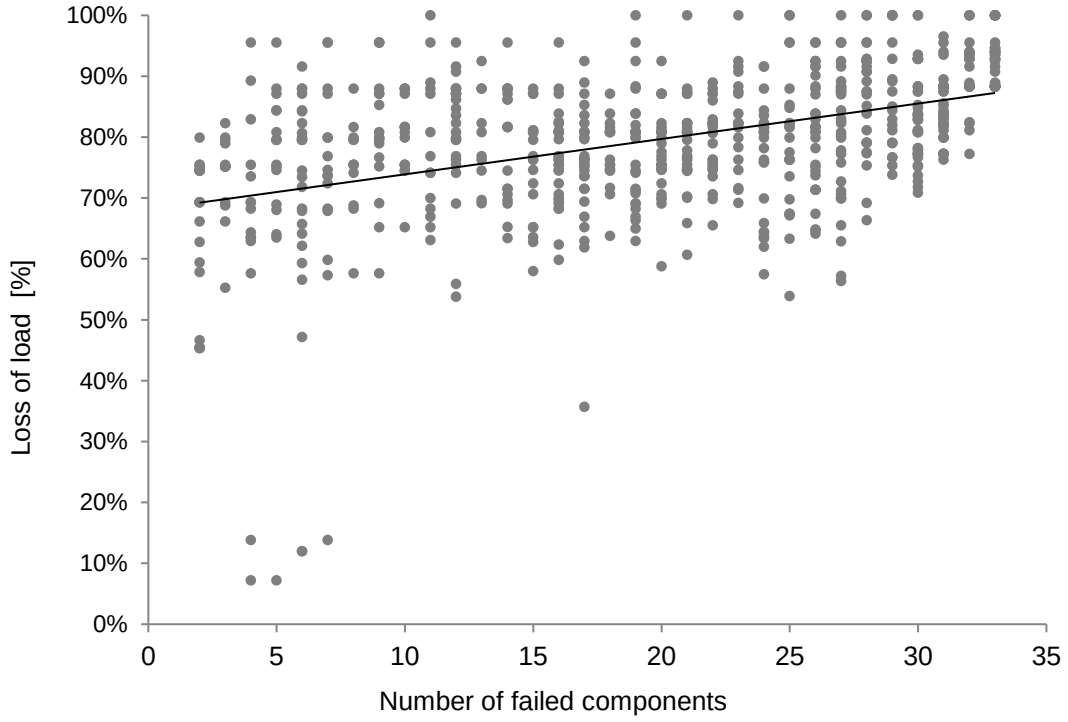

Figure 34: Dependence of power loss on number of initially failed lines based on tolerance value, $\alpha = 1.5$.

Figure 35 shows the probability of line failure and average percentage of active lines after cascading failure conditional on the different hurricane classes.

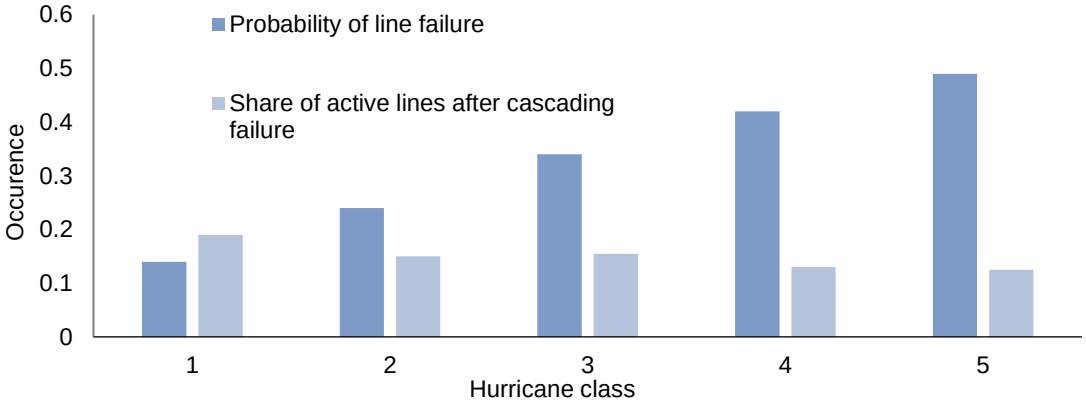

Figure 35: Hurricane intensity levels (classes 1 to 5) and occurrence ratios in the MC simulation: line failure ratio and ratio of active lines after cascading failure events.

8.5.2 Sensitivity of component and network failures

To investigate the dependence of initial components failure events on different model parameters, receiver operating characteristic (ROC) curves are evaluated and selected curves are shown in Figure 36. Generally, a ROC curve plots the model sensitivity against the complement of the model specifity. The sensitivity is defined as the probability of a model to predict correctly a failure event (true positive rate). The specifity is the probability that a model correctly predicts non-failure events (true negative rate). The greater the area underneath the ROC curve (AUC), the higher are specifity and sensitivity, and thus the better the corresponding model explains the failure event (Mason and Graham, 2002).

Here, the ROC curve is used to assess and depict the quality of the models for predicting the number of lost lines and the loss of load (%) in a hurricane event. A model can be composed of a varying selection of the model parameters to explain the target variable (loss of load or lost lines) in each simulation. The model parameters tested are: hurricane class (intensity) c, maximum wind speed s_{max}, maximum radius r_{max}, offset ω. A regression model is formulated as:

$$Model = \beta_0 + \beta_1 c + \beta_2 s_{max} + \beta_3 r_{max} + \beta_4 \omega \quad (62)$$

The resulting ROC curves enables the comparison of the performance in predicting damages. In case all β factors are non-zero (i.e. significantly different from zero) in Equation (62), all mentioned parameters are included in the model.

In Figure 36, the ROC curves characterizing the ability of the pertinent hurricane parameters in predicting component failures is shown. The highest AUC value is reached for a model combined of model variables: r_{max}, c, s_{max}. Each of these variables taken as a single independent (explaining) model variable has a distinctively differing AUC value with an increasing prognostic property: r_{max}, c, s_{max}. The maximum wind speed s_{max} alone predicts rather well the component damage caused by a hurricane in the study area, which is reflected by a relatively high AUC value of 0.8747. In other words, s_{max} differentiates well between critical hurricanes and hurricanes with lesser impact. The hurricane's offset ω alone has only a negligible predictive value concerning the component failure.

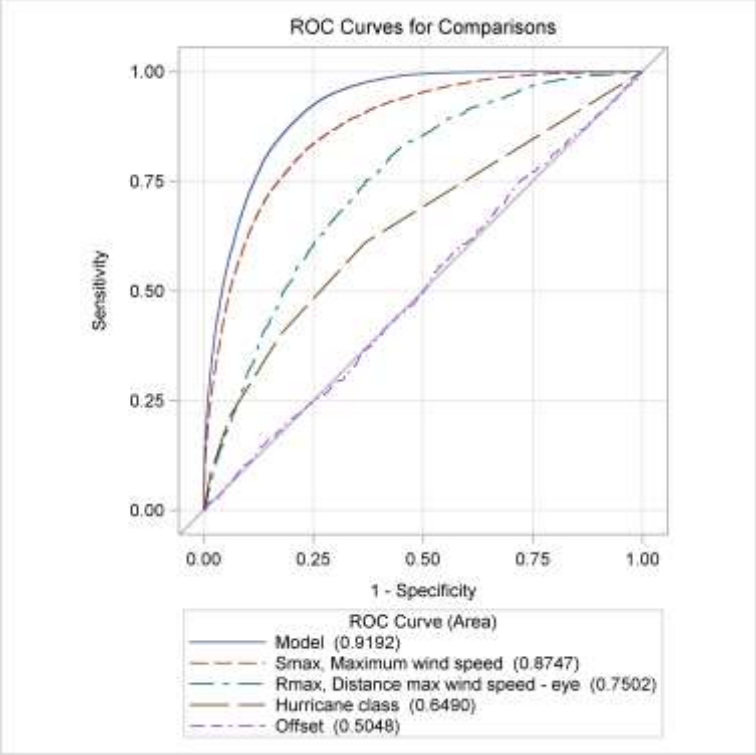

Figure 36: ROC curves: Predictive performance of the hurricane model parameters on the component failure events in a hurricane event.

The dependence of the overall system performance (loss of load), and thus, system failure after hurricane events and subsequent cascading failures on the individual parameters of the hurricane model is significantly less pronounced than for component failures, see Figure 37. The system failure event is defined as the loss of load exceeding 20% of the original load supplied in the power grid. The low impact of the hurricane parameters mainly stems

from the fact that values of power loss predicted by the applied physical network model are not very sensitive to the number of component failures, given that at least one network component failed.

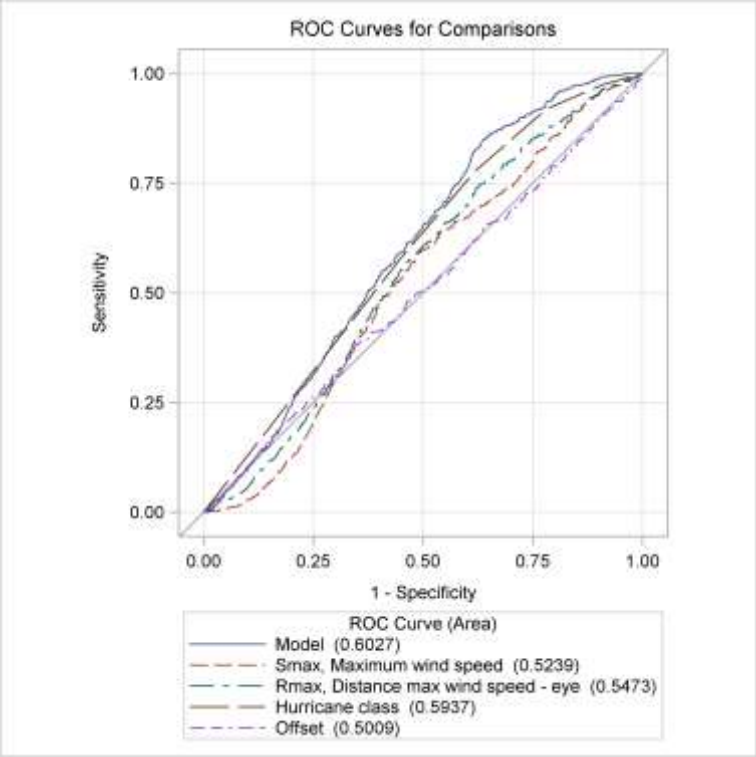

Figure 37: ROC curves: Predictive performance of the hurricane model parameters with regard to the overall network failure event, defined as exceedance of a predefined threshold for the loss of load value $t_L = 0.2$ and a tolerance parameter of $\alpha = 1.2$.

In the model setting for Figure 37, a tolerance parameter of 1.2 was selected. This is a rather low value, defining the capacity of the components against power overloading. It is found that with a higher α-value, the predictive performance of the hurricane parameters and the combined model increases, compare Figure 38. In case of $\alpha = 1.5$ the AUC value of the model increases to 0.7427 and a further increase is possible if the α-value is set to 2.0 with an AUC value of the regression model of 0.7721. The offset parameter yields an insignificant AUC value. It is observed that with a further increase of the α- value, the cascading failure processes are strongly attenuated and no large improvements in the AUC values are recorded. In both cases, r_{max} and s_{max} yield similar AUC values in the order of magnitude of 0.70, unlike in Figure 37.

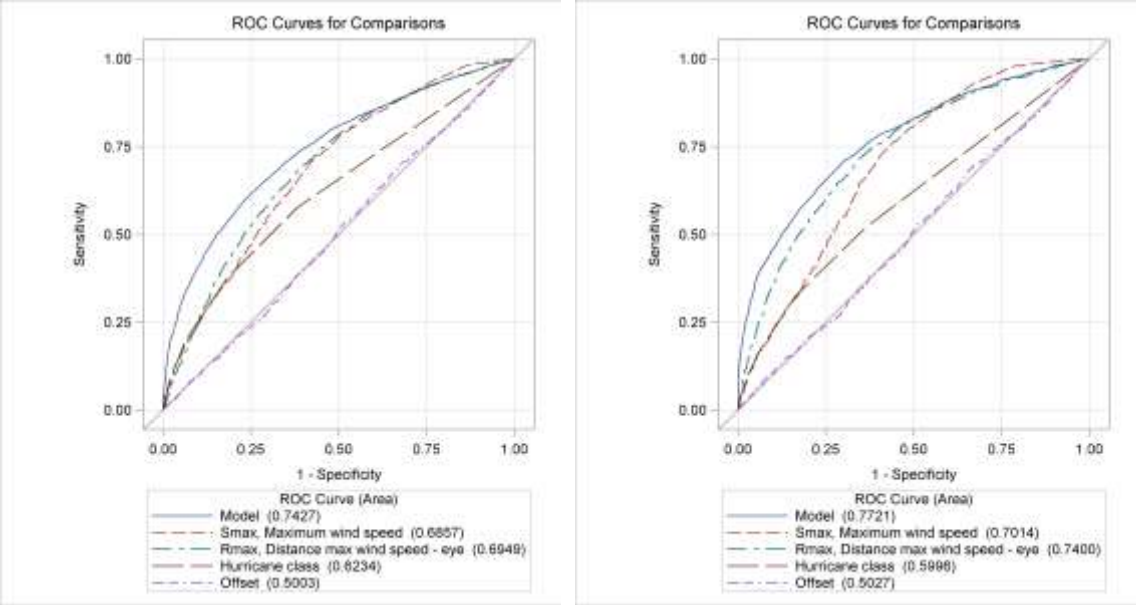

Figure 38: ROC curves: Predictive performance of the hurricane model parameters with regard to the overall network failure event, defined as exceedance of a predefined threshold for the loss of load value $t_L = 0.2$ and a tolerance parameter of $\alpha = 1.5$ (left) and $\alpha = 2.0$ (right).

8.6 Summary

The main focus of this case study is the inclusion of a physically-based system failure model within a hurricane simulation context. One achievement of this case study is the development of a generic and above all a spare hurricane wind field model. For the assumed model parameters, the network components have high probability of failure given a hurricane event. Furthermore, the physical power flow response model produces high overall system damage values in case of low α-values, i.e., it does not differentiate much between different hazard scenarios as already the failures of one or few component(s) lead to high power losses due to strong cascading effects. Thus, it is found that while the network component failure probabilities are strongly dependent on the hazard characteristics, this does not hold for the overall network damage after simulation of the cascading failures because in this case the computed average power loss level tends to be rather insensitive to the number and combination of initially triggered network components. However, real network have higher α-values. For higher α-values the predictive ability of the hurricane parameter increases significantly, which is expressed in increased AUC values of the corresponding ROC curves.

9 The Nordic grid subject to European wind storms

Parts of this Chapter are based ona paper published to Reliability Engineering and System Safety.

9.1 Methodological framework

The methodology developed in this chapter combines empirical storm data, a georeferenced power grid, a calibrated component fragility model, and a Monte Carlo simulation approach evaluating diverse aspects of potential damage to the power grid due to wind storm impacts. In Figure 39, the employed simulation-based framework for the reliability assessment of the power transmission grid subject to extreme wind loads is shown in detail. The wind load during storms is modelled by means of a spatial random field (SRF) allowing for spatial correlation, calibrated with historical data of storm events in Europe. Component fragility curves are calibrated using information about wind zone-specific construction criteria of structures (Section 9.3). Location-specific wind speed values generated with the SRF are used to evaluate component failure probabilities during a simulated event. On this basis, a binary component state vector is sampled, describing the system condition during one simulation. The resulting network during a storm event is evaluated through a directed current (DC) power flow model and quantified in terms of loss of load supply and

number of lines lost (Section 575.4.2). Finally, component rankings are calculated and component strengthening strategies are tested (Section 9.6). The overall framework suggested here is generalizable and applicable to different types of network systems exposed to loads from natural hazards.

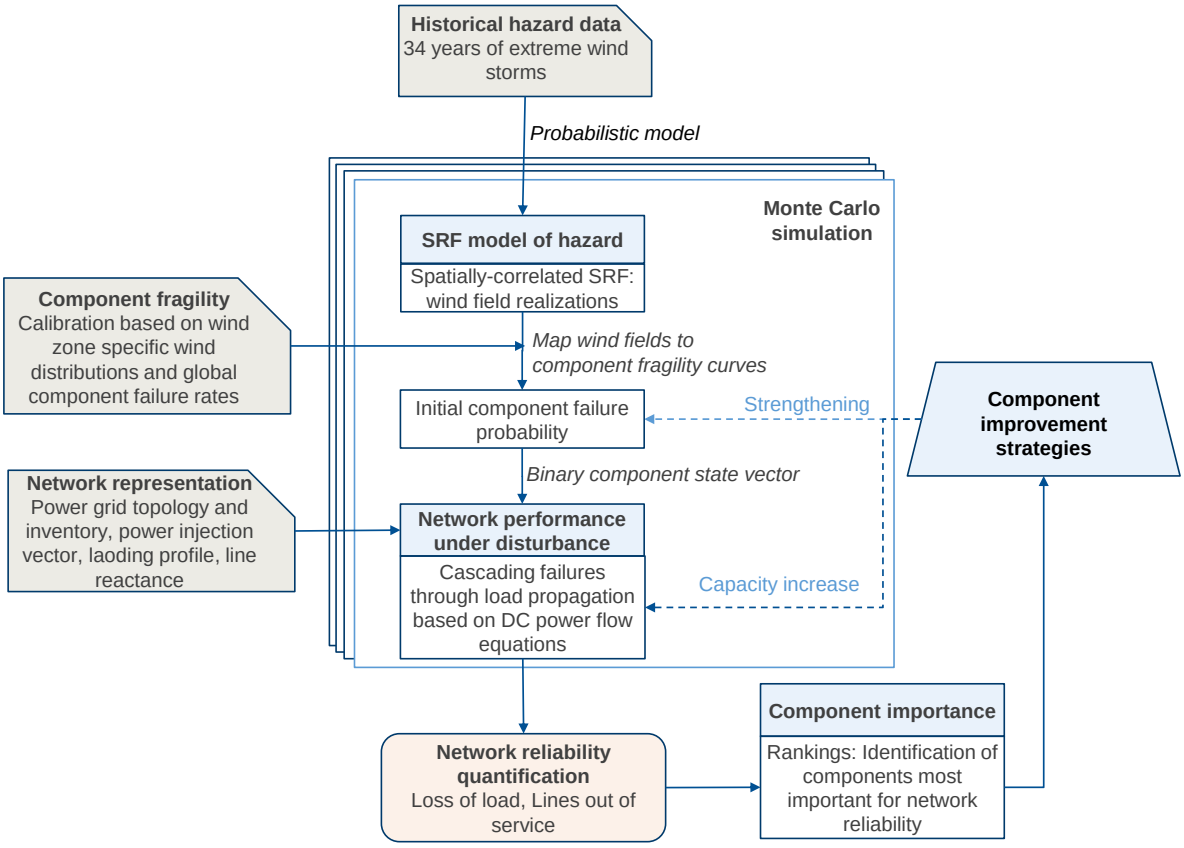

Figure 39: Illustration of the general methodological framework of this thesis as an integration of constituent models for the reliability assessment of networks subject to spatially distributed hazards.

9.2 European windstorm data and wind field simulation

9.2.1 The XWS open access catalogue of European windstorms

In Europe, extratropical storms emerge on the polar front, a frontal divide of cold, arctic air on the polar side and warmer, more humid air on the tropical side, around 60° on the northern hemisphere and mostly in the winter season between October and March. A disturbance in this generally unstable polar front leads to a cyclone, a low-pressure system,

where the warm, sub-tropical air penetrates as a warm sector into the colder air mass and slides over it. On the rear side, the colder air penetrates into the warmer air. These systems generally move following a West to East direction, with diameters ranging between 500 and 3000 km (Cigré WG B2.28, 2015, Papailiou, 2017).

Data on the most extreme windstorms in Europe in the period between 1979 and 2013/2014 is provided publicly by the "XWS (eXtreme Wind Storms) Catalogue[5]" and its generation is described by Roberts et al. (2014). In this thesis, the catalogue is used up to year 2012. The XWS catalogue covers storm events in the area of approximately 15 W - 23 E and 35 N - 70 N. It contains 52 storms, which are classified as the meteorologically most extreme among all registered storms including 23 storms that were the most severe storms in terms of insured losses in the 34 year period between 1979-2012 (Roberts et al., 2014). As a selection criterion, a specific severity index, SSI, suggested by Haylock (2011), was applied. The SSI is based on the area of the storm footprint over the mainland of Europe and the maximum storm intensity. The footprint is defined as the maximum 3 s gust at each grid point over a 72 h period during which the storm passes through the domain. The data in the catalogue is gridded with a resolution of 24 km and the wind speeds are downscaled to a 25 m height. The gust wind speeds may exceed 50 to 60 m/s over sea or exposed land areas, mostly in northern regions of Europe. The study area, which includes all the Nordic countries and beyond, amounts to 3974 geographic locations from the XWS dataset.

By using the XWS data set, the analysis is limited to wind speeds occurring during large-scale European storms. Furthermore, the present data set appears to be more representative for extreme wind speeds at the southern region of the study area, including Denmark, southern regions of Sweden and Norway. It appears to be less representative at higher latitudes due to the limited presence of the recorded storm tracks at those latitudes, see Figure 40. This approach leaves some uncertainty as to the actual local extremes of wind speed that could be observed independently of extreme large-scale circulations across Europe. However, the relevance of this approach rests on the importance of large-scale hazard events for the analysis of the general performance and reliability of regional power transmission networks.

[5] Data available at www.europeanwindstorms.org [access date 2018/12/02]

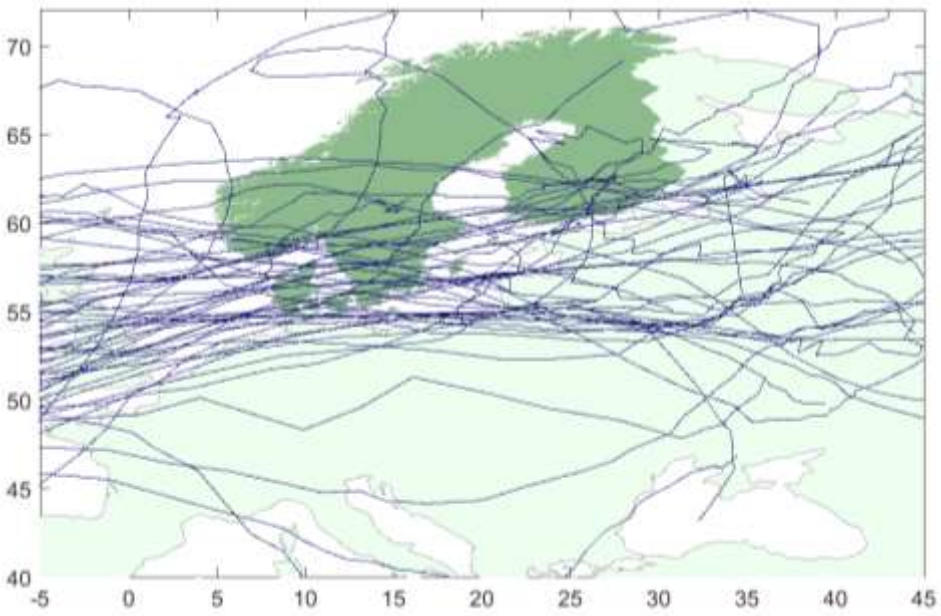

Figure 40: Windstorm tracks of the 52 storms in 1979 to 2012 in the XWS catalogue based on the corresponding maximum vorticity at 850 hPa along their pathways over Europe. Study area shown in dark green. Only slatternly tracks lay in the northern part of the Nordic countries.

9.2.2 Spatial Random Field (SRF) model

Spatial random fields are used to probabilistically model the wind speeds over the Nordic countries. The model describes the maximum 3-second gust wind speeds S [m/s] at 25 m height in the storm footprints through a spatially inhomogeneous random field. The dependence structure of the random field, which reproduces the spatial dependence due to the large-scale features of the recorded storms, is learnt from the storm data set.

First, for learning the marginal wind speed distributions at the 3974 geographic locations from the XWS dataset, we tested several probability distributions to fit the time series of storm data from the 52 storms. A comparison using the Akaike Information Criterion (AIC) and the Bayesian Information Criterion (BIC) revealed that the Weibull distribution is on average the best fit to the observed wind speeds, when compared to the Rayleigh and Gumbel distributions. Typical example distribution fits to the wind speed data at two point locations in the study area using modified versions of the Weibull, Rayleigh, and Gumbel distributions are shown in Figure 41.

The time series featured in the dataset contain instances of zero for certain combinations of storms versus locations. These instances are due to the fact that these locations were not in the footprint of the respective storm. Thus, in the fitting of the above mentioned distributions, a partition of the time series into two sets, i.e. zero versus non-zero values, is

required (zero-inflation); a distribution that allows for frequent zero-valued observations. At first, all zero instances were omitted during fitting of the Weibull marginals. This is the case for about 10% of all data. The influence of these instances was thereafter introduced in the form of the conditional probability of occurrence of a zero instance $p_0 = \Pr(S_i = 0)$, with S_i being the wind speed at location i. The resulting zero-inflated marginal CDFs are equal to the sum of p_0 and the Weibull CDF weighted with $(1 - p_0)$:

$$F_{S_i}(s_i) = p_{0i} + (1 - p_{0i})\left\{1 - exp\left[\left(-\frac{s_i}{\lambda_i}\right)^{k_i}\right]\right\}$$
$$= 1 - (p_{0i} - 1)\, exp\left[\left(-\frac{s_i}{\lambda_i}\right)^{k_i}\right] \quad (63)$$

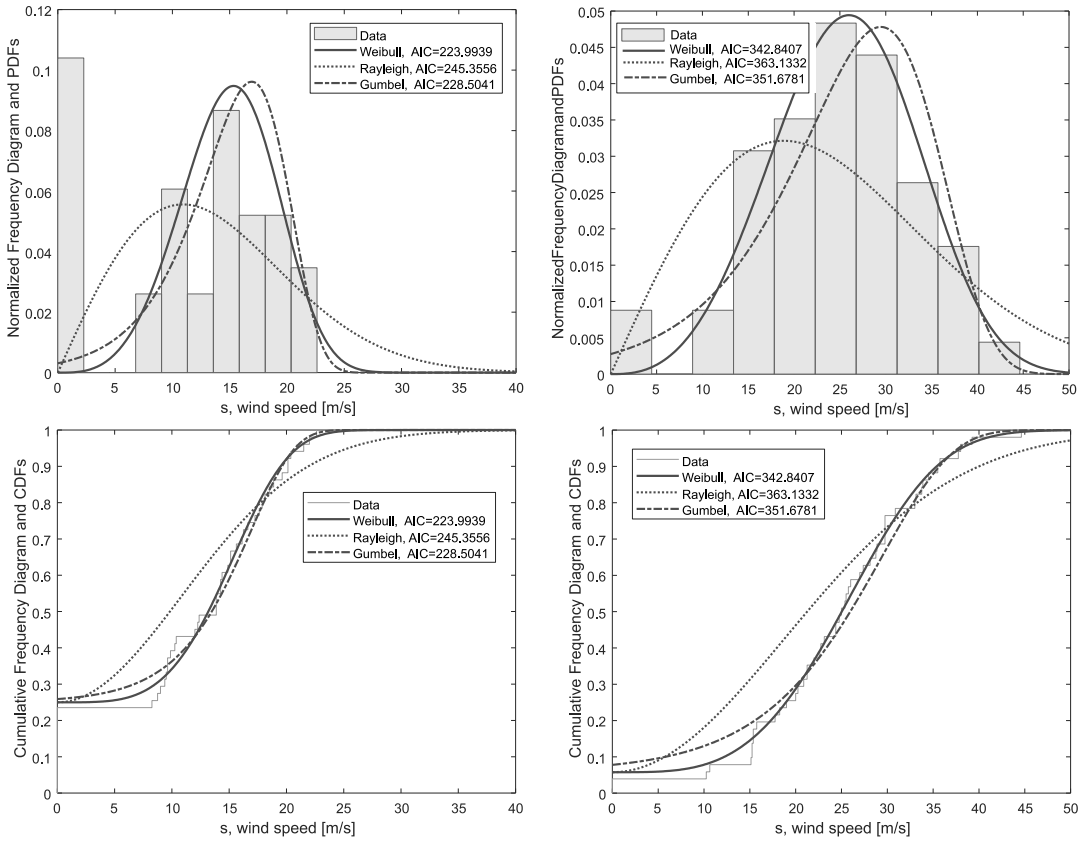

Figure 41: Distribution fits to the windstorm data set for two example locations of the 3974 data points in the Nordic countries study area. Left: Location at the eastern border of Finland; right: location at the west coast of Norway. Comparison of the Weibull, Rayleigh, and Gumbel PDFs with the empirical normalized frequency diagram and comparison of the corresponding CDFs with the empirical cumulative frequency diagram; the goodness of fit is given here in terms of the Akaike Information Criterion (AIC).

In order to simulate the random field based on the above marginals, the present study utilizes in principle the Nataf transformation (Nataf, 1962). Let $\mathbf{Z}$ denote a vector of standard normal random variables, whose elements Z_i are associated with the 3974 locations of the study area (with a resolution of app. 24 x 24 km^2). This vector is characterized by its covariance matrix, $\mathbf{\Sigma_{ZZ}}$, which is computed by first transforming each location-specific extreme wind speed data point $s_{i,j}$ into a standard normal distributed random variable:

$$z_{i,j} = \Phi^{-1}\left[F_{S_i}(s_{i,j})\right] \tag{64}$$

wherein Φ^{-1} is the inverse of the standard normal CDF and F_{S_i} is the fitted zero-inflated CDF of the wind speed at location i following Equation (63). This transformation is not uniquely defined for values $s_{i,j} = 0$. In these cases, we randomly sample the value $z_{i,j}$ from a uniform distribution between 0 and p_{0i}. The covariance matrix is then estimated by means of a maximum likelihood estimator from the data $z_{i,j}$, $j = 1, 2, \ldots, 52$, yielding $\mathbf{\Sigma_{ZZ}}$:

$$\sum\nolimits_{ZZ} = \begin{bmatrix} Var[Z_1] & Cov[Z_1, Z_2] & \cdots & Cov[Z_1, Z_n] \\ Cov[Z_1, Z_2] & \cdots & \cdots & Cov[Z_2, Z_n] \\ \vdots & \ddots & & \vdots \\ symmetric & \cdots & & Var[Z_n] \end{bmatrix} \tag{65}$$

This covariance matrix is used for generating cross-correlated, standard normal random field realizations at all point locations, Z_i, in the study area, which are transformed into the corresponding location-specific Weibull distribution by the isoprobabilistic transformation in Equation (66). This results in the cross-correlated, spatially inhomogeneous, Weibull marginally-distributed random field.

$$s_i = F_{s_i}^{-1}[\Phi(Z_i)] \tag{66}$$

Φ is the standard normal CDF and $F_{s_i}^{-1}(x)$ is the inverse of the cumulative distribution of S_i. This transformation function is surjective.

9.2.3 Relation to the annual maximum wind speed distribution

S_i is the maximum wind speed during a storm event. To obtain the distribution of the maximum wind speed at location i during a time period (e.g. the annual maxima), the distribution of S_i can be combined with a Poisson process describing (approximately) the occurrence of storm events assuming independence of the hazard occurrences. The rate of storm events is estimated as

$$\lambda_S = \frac{52}{34yr} = 1.53yr^{-1} \tag{67}$$

The empirical distribution of the annual maximum wind speed $S_{a,i}$ at location i is modeled as

$$F_{S_{a,i}}(s) = exp(-\lambda_S 1yr) \sum_{j=0}^{\infty} \frac{(\lambda_S 1yr)^j}{j!} \left[F_{S_i}(s)\right]^j \tag{68}$$

As noted previously, the statistics based on the XWS dataset should not be used to evaluate the extreme value statistics at a specific location. Nevertheless, the estimates of $F_{S_{a,i}}(s)$ allow a comparison with existing maps of extreme wind speeds as used for the design of structures, to assess the validity of the model.

Equation (69) can be transformed as shown in the following, considering the definition of $F_{S_i}(s)$ in Equation (63) with local shape parameter λ_i, scale parameter k_i, and, p_0 of the adjusted (zero-inflated) Weibull distribution, respectively.

$$F_{S_{a,i}}(s) = \begin{cases} e^{\lambda_s(-1+p_0)} & for\ s = 0 \\ e^{e^{-\left(\frac{s}{\lambda_i}\right)^{k_i}}\lambda_s(-1+p_0)} & for\ s > 0 \end{cases} \tag{69}$$

Equation (69) can be solved for a wind speed s with $s > 0$ at a specific location:

$$s(F_{S_{a,i}}) = \lambda_i \left(-ln\left(\frac{ln\, F_{S_{a,i}}}{\lambda_s(p_0 - 1)}\right)\right)^{1/k_i} \qquad for\ e^{\lambda_s(-1+p_0)} < F < 1 \tag{70}$$

Figure 42 shows the estimated 50-year return levels at each location based on $F_{S_{a,i}}(s)$ as calculated for each location in the wind data set from:

$$s(.98) = \lambda_i \left(-ln\left(\frac{ln(.98)}{\lambda_s(p_0 - 1)}\right)\right)^{1/k_i} \tag{71}$$

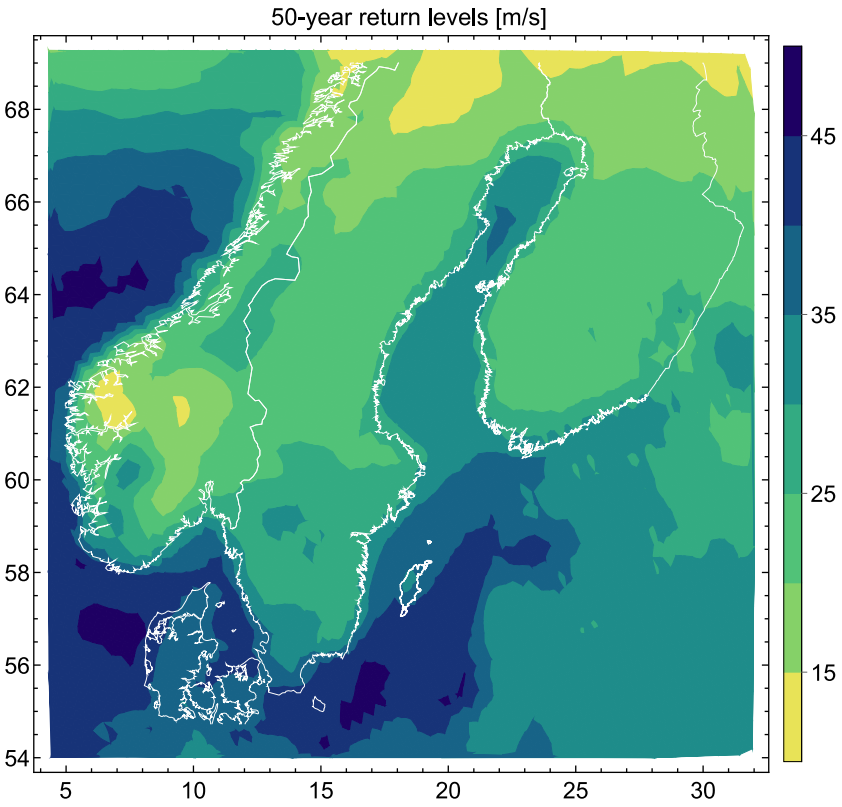

Figure 42: Estimated 50-year return levels based on the empirical distribution of the annual maximum wind speed, $F_{S_{a,i}}(s)$.

9.3 Fragility model calibration for the Nordic countries

The fragility model parameters are determined by the suggested calibration method suggested in Chapter 6.4. The wind load onto each 1 km line segment is represented by the wind speed of the location point in the spatial random field that is nearest to the line segment's midpoint.

In this case study, it is assumed that all support constructions have been planned and constructed according to Eurocode 1-4 (CEN, 1991), and the national annexes to Eurocode 1-4 provide the characteristic wind speed values v_b as a function of the geographical location for the European Nordic countries. A map with the characteristic values of the 10-minute wind speed at 10 m height, i.e. the wind zones of Norway, Sweden, Denmark and Finland, collected from the national annexes of the Eurocode 1-4, is shown in Figure 43.

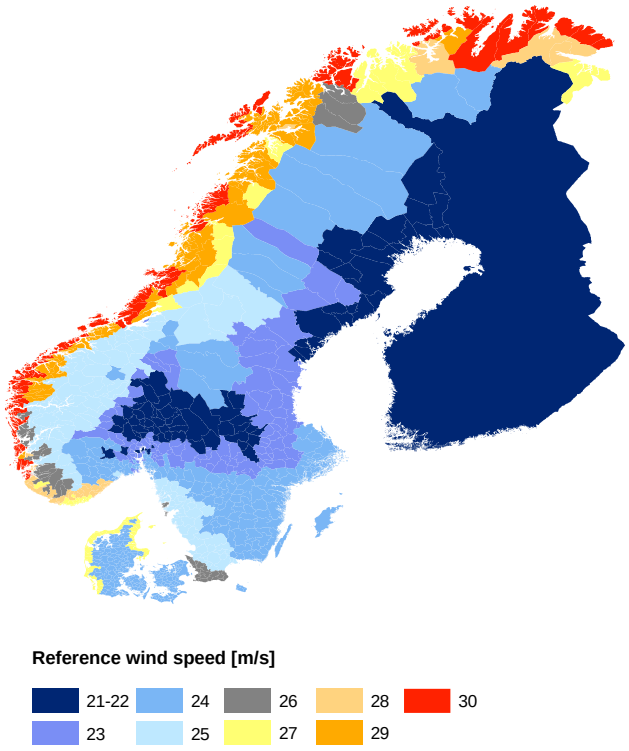

Figure 43: Characteristic wind speeds at the municipality level for Norway and Sweden and at national scales for Finland and Denmark, based on Eurocode 1-4; the wind speed values $v_{b,x}$ should reflect the 10 minutes in 10 meters height value with a return period of 50 years.

Following the procedure of Chapter 6.4, we model the capacity, and hence the fragility model, in function of the wind zones z of Figure 43. It is reminded that using the Equations (36)-(37), the calibration requires to find a single parameter; here we use $\mu_{R_{24}}$, the mean value of the capacity in the wind zone with characteristic wind speed 24 m/s, but it is irrelevant which capacity mean value is chosen.

To calibrate the fragility models, we account for the observed line failure rates over the past 16 years. Based on personal communication with contacts from the Nordic transmission system operators (Schaug-Petterson, 2017, Bratløv, 2017, Markku, 2017, Tallberg, 2017), an average failure rate r_F of about 10^{-3} failures per year and line kilometer due to wind hazards has been identified for the study area. This rate is in good accordance with failure rates found for Great Britain (Murray and Bell 2014). The estimate is an aggregate number, as it does not distinguish between different failure types, failure durations, or severity of the disturbance.

The calibration is then performed by computing the failure rate for a given value of $\mu_{R_{24}}$ with the random field wind speed representation of Section 9.2.2. and by applying Equation (38). The final value of $\mu_{R_{24}}$ is found iteratively as the value that leads to $\lambda_F \approx$

$10^{-3}\mathrm{yr}^{-1}$.

The resulting fragility functions F_{R_z} are shown in Figure 44, with parameters given in Table 10.

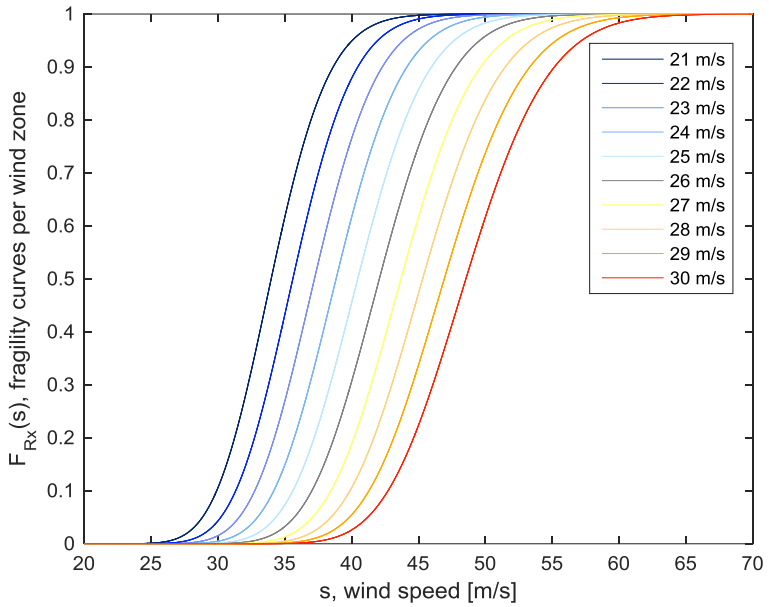

Figure 44: Calibrated fragility curves (CDFs of the lognormal distributions) for each wind zone considered. The fragility expresses the probability of failure of a 1 km line segment in function of the gust wind speed at 25 m height at a representative point (e.g. the line segment mid-point).

Table 10: Mean and standard deviation of the lognormally distributed fragility curves with constant coefficient of variation, δ of 0.1.

Fragility curve parameter	**Wind zone [m/s]**									
	21	**22**	**23**	**24**	**25**	**26**	**27**	**28**	**29**	**30**
Mean [m/s]	34.14	35.77	37.39	39.02	40.65	42.27	43.90	45.52	47.15	48.77
Standard deviation [m/s]	3.41	3.58	3.74	3.90	4.06	4.23	4.39	4.55	4.71	4.88

9.4 Numerical implementation

Maps of the Nordic countries including the Nordic power network as weighted graphs are shown in Figure 45. Estimated line reactance and line capacity values are depicted as line weights respectively. As can be seen from the figures, lines with higher reactance value

have a lower capacity and vice versa.

Andreasson et al. (2011b) introduced the model of the Nordic power system mainly based on publicly available data from Denmark, Finland, Norway, and Sweden, to demonstrate appropriate sampling techniques and concepts of system failure analysis for the Nordic region. Andreasson et al. (2011a) provided data for the model of the Nordic grid concerning network topology, transmission line parameters, power generation, and power demand derived from population density data. The model comprises 470 nodes and 646 power transmission lines. The mean line length based on the model data is 83.8 km with a minimum of 2.5 km and a maximum of 1206.5 km. The total of the line lengths amount to 53,293.4 km with a quota of 39,690 km (74%) of potentially exposed and vulnerable overhead line segments. The overall power load in the network is about 40 GW and the power generation capacity is about 82 GW.

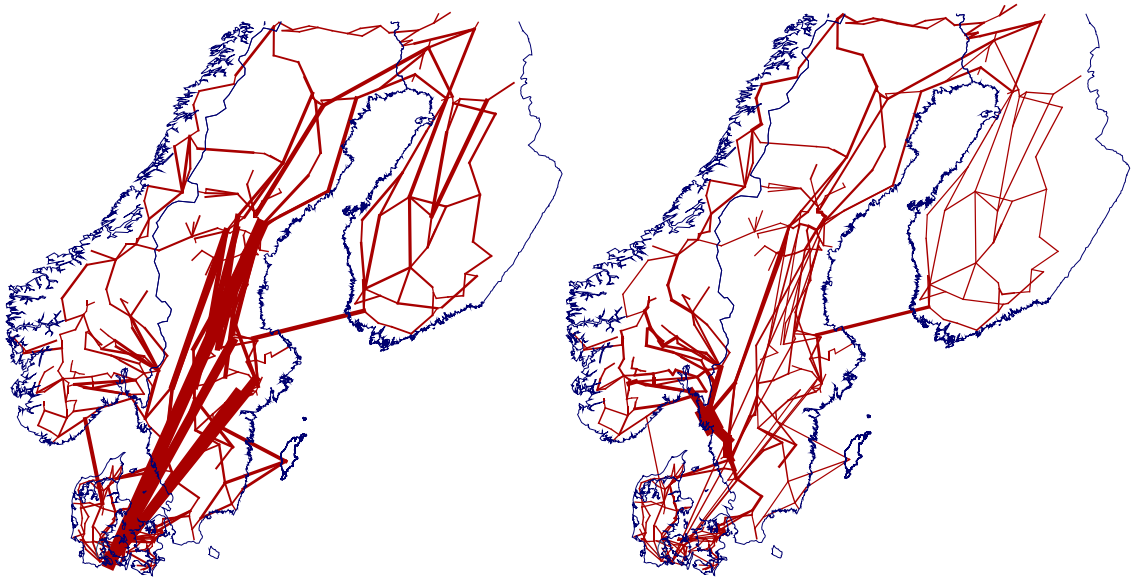

Figure 45: The Nordic grid model depicted as weighted graph. Left: Edge weights are the line reactance values. Right: Edge weights are the line capacity values, proportional to the initial load of the lines. [Mean line length 83.8 km, study area diameter about 2000 km, estimated approximate correlation length 566 km.]

The reliability analysis is performed through a Monte Carlo simulation with 10^4 samples. First, samples were drawn from the random field model of the windstorms. Thereafter, initial failures were randomly generated based on the wind speeds at each element location combined with the fragility models of Section 9.3. The resulting binary component state vectors were used as inputs to the directed current (DC) power flow model (Section 5.4.2).

9.5 Results

9.5.1 SRF realizations

Figure 46 shows the contour plot of the mean values of the local wind speeds during a storm obtained from the simulations. The southern part of the study area is more affected by the large-scale windstorms included in the study. Therefore, the local mean (and maximum) wind speed values are distinctively higher in the southern part of the study area. Consequently, this is true also for the wind load induced line failure rates.

As a plausibility check: the received mean values in Figure 46 match precisely with the mean values from the historical wind speeds data sets shown in Figure 42.

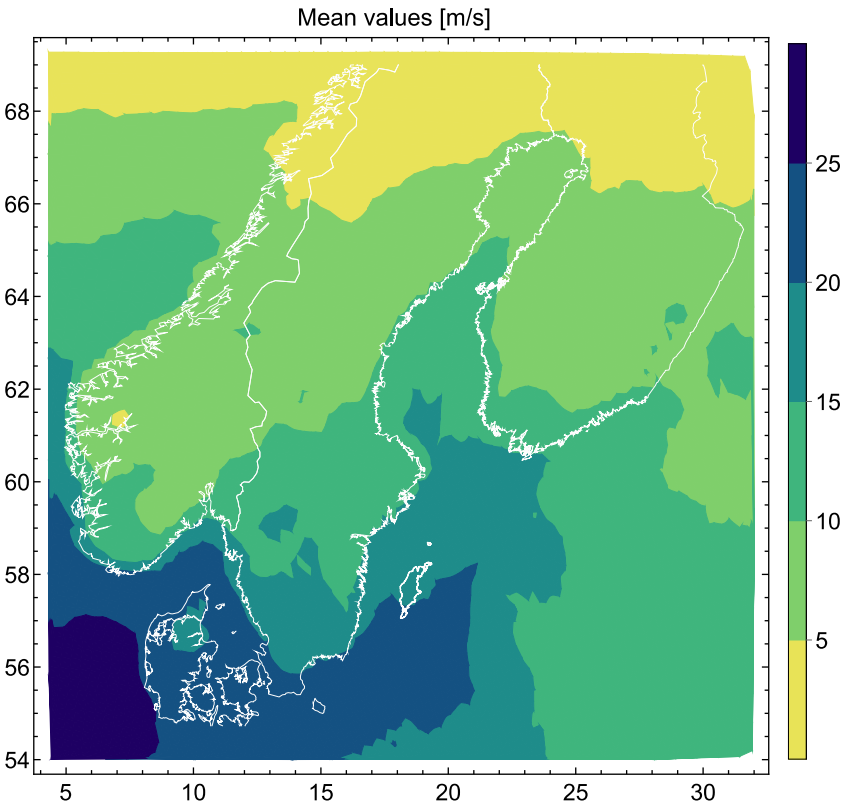

Figure 46: Wind speed contour plots in [m/s]. Local mean values of the correlated random field realizations of the European extreme storm events.

The local nature of some storms can be captured to some degree, which was tested by comparing qualitatively the storms generated with the SRF model to the real storm events. However, one could also try out an alternative model, which addressed the hybrid nature

of the data differently. In learning the statistics of the extreme wind fields representing large-scale storm events, one has to deal with events that do not cover the entire study area. As a result of this, the wind speed distribution at each point conditional on a storm event is a hybrid distribution with a finite probability of a zero value, Equation (63). An alternative approach to handling the zero values in storm records would be to describe the occurrence of a storm by means of a binary random field. One would then first learn this binary random field (with a Gaussian copula) and then describe the covariance among the wind speeds at two locations conditional on the occurrence of the same storm event at those locations. Such a model would explicitly account for the hybrid nature of the random field when describing the spatial dependence. It remains to be investigated if such a model would give improved representations of the storm footprints.

9.5.2 Initial line failure probabilities

Generally, the longer a line length is, the higher is the overall line failure probability, since a line is a series system of 1 km line segments.

The initial power load of the lines in the Nordic Grid is negatively correlated with the wind speeds, i.e. lines with a higher power demand have a lower probability of failure due to storms. An above average power load of several important central lines is observed at the south-western border of Sweden, where relatively high power loads go along with rather low line failure probabilities. This constellation leads to a negative association between the Nordic Grid initial line power load and the initial line failure probabilities, which can be seen also in comparison of Figure 46 and Figure 45.

In Figure 47 the mean failure probabilities per line segment are plotted along the line length to visualize exemplarily the potential spatial variability along the lines. The selected lines have rather high overall failure probabilities; however, at the same time, they might comprise a rather high number of segments that have a negligible failure probability. One reason for this are undersea cables. In Figure 48 the selected six lines are highlighted in the Nordic grid graph.

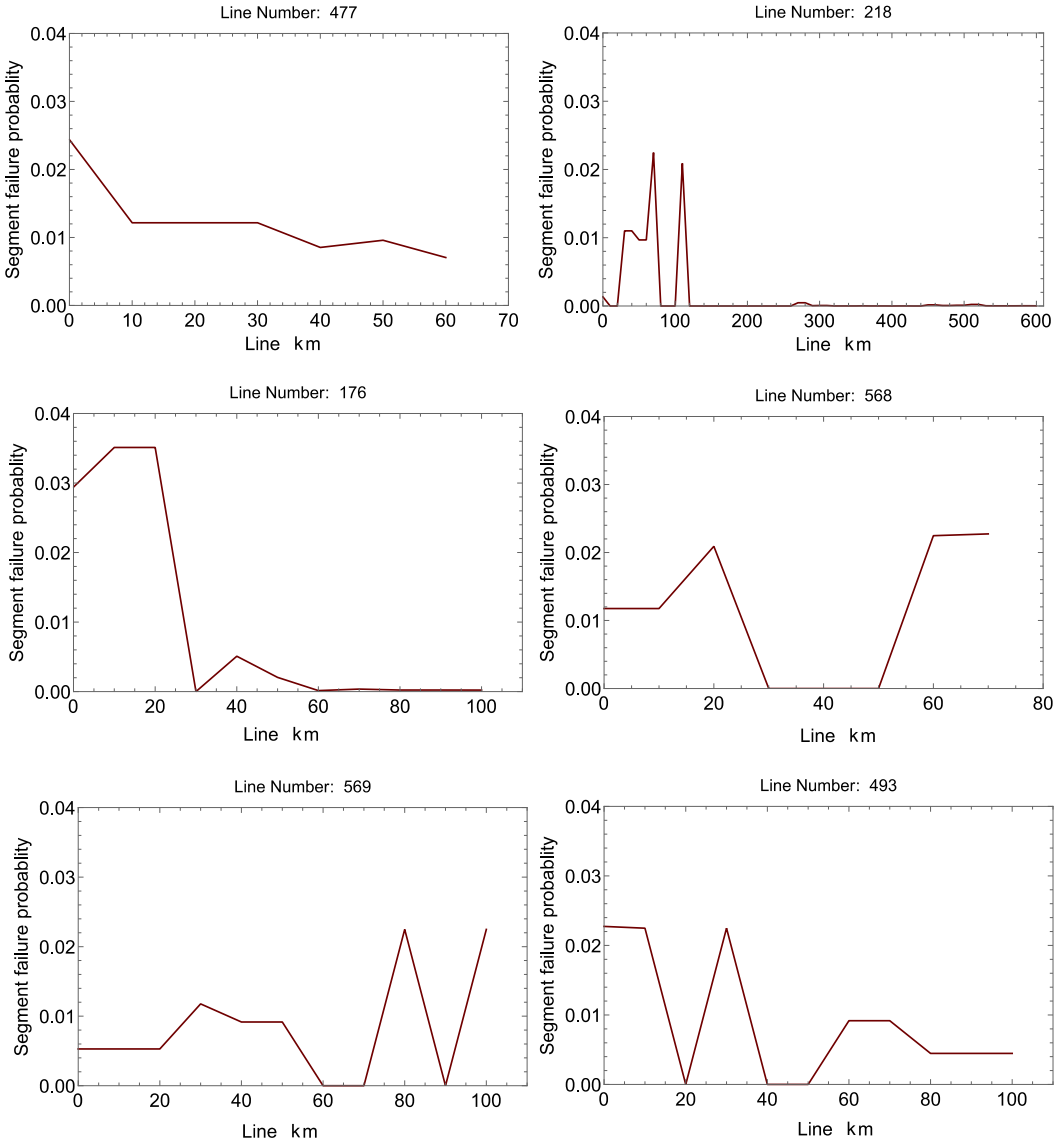

Figure 47: Mean initial segment failure probability, $p_{f,j}^{(i)}$ along the line length of 6 selected lines that are highly ranked with regard to high overall initial line failure probabilities. Near zero values are due to line segments that are not or only slightly exposed, e.g. undersea cables.

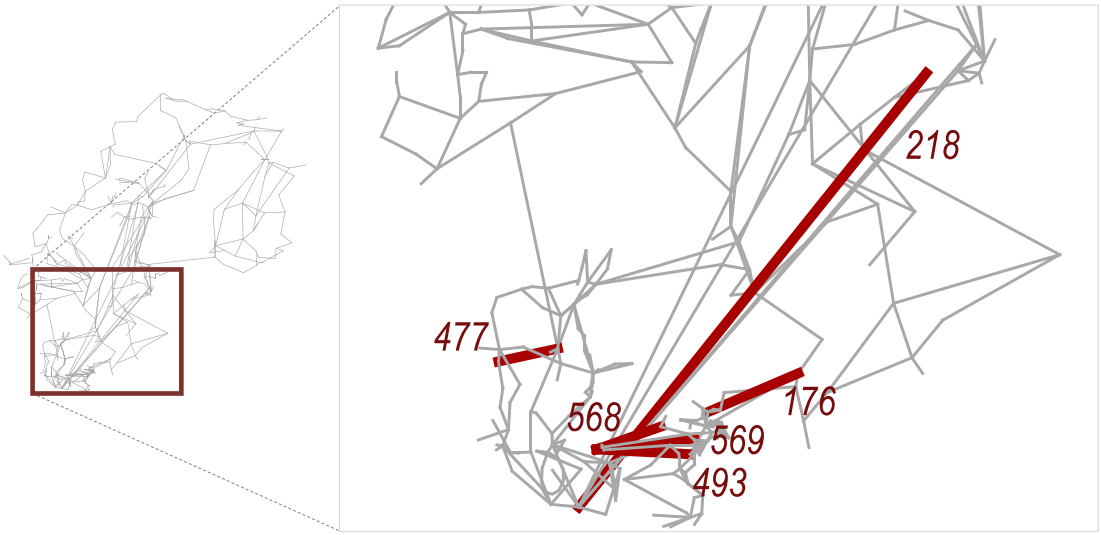

Figure 48: The Nordic Grid with highlighted lines: the red marked lines are those selected in Figure 47 they stand out with a high initial overall line failure probability.

Figure 49 shows the line connecting Sweden and Finland together with the segment failure probability levels along the line length. Note that the values range in a significant lower order of magnitude than the selected lines in Figure 48. The parts that are undersea cables have zero line segment failure probabilities in the present context, since they are not exposed to wind load.

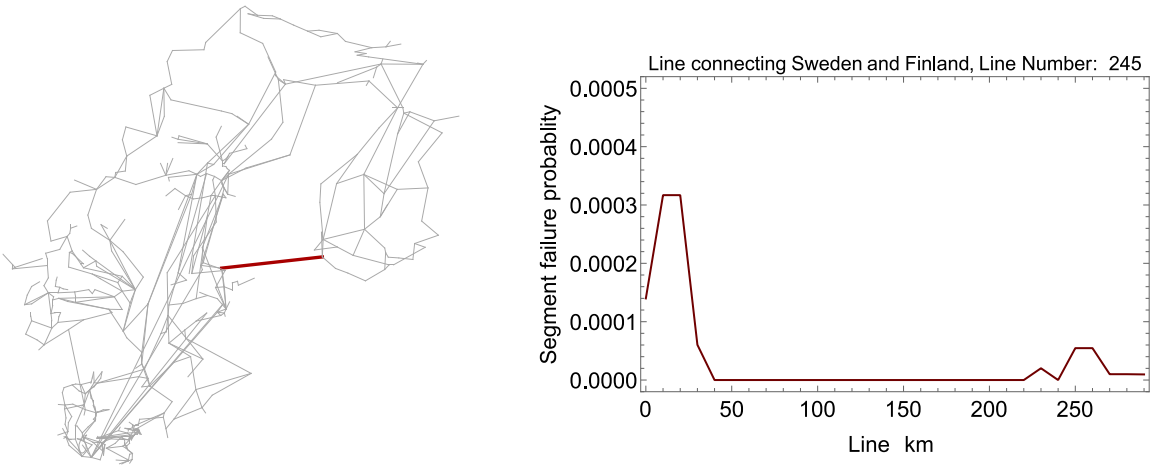

Figure 49: The transmission line connecting Sweden with Finland which lies at least partly undersea and underground is highlighted in the Nordic grid graph (left) and the corresponding mean line segment failure probability $p_{f,j}^{(i)}$ is plotted along the line length of about 290 km (right).

9.5.3 Network reliability analysis

The results on the network reliability obtained from the MC simulations are summarized in Table 11 for three selected values of the tolerance parameter α. Table 11 reports the mean and standard deviations of the overall load loss, the system failure probability and the number of failed lines. In each case, a distinction is made with regard to 'initial damage' after initial line triggering due to wind loading (before the onset of cascading failures) versus 'final damage' after the evaluation of the network considering the cascading failure processes. The system failure probabilities in Table 11 for selected α-values are calculated based on the load loss threshold t_L fixed at 0.1, defining the system failure event. A load loss that exceeds 10% of the initial load is defined as system failure. Note that the system failure probability is highly sensitive to the choice of the threshold t_L.

Table 11: Summarized statistics of the reliability analysis results for varying tolerance parameter values α. Load loss and system failure probability as well as a comparison of the number of initially and finally failed lines. Results obtained by MCS with 10^4 samples and a fixed load loss threshold t_L of 0.1.

	α = 1.1		**α = 1.5**		**α = 2.0**	
	initially	finally	initially	finally	initially	finally
Load Loss [MW]						
Mean	1804.5	38151.0	1812.6	11134.0	1823.3	3276.0
% of original load	4.5	95.4	4.5	27.8	4.6	8.2
Standard deviation	6615.6	83019.5	6657.1	37763.0	6698.0	13509.0
System failure probability						
Mean	0.015	0.177	0.015	0.082	0.016	0.036
Standard deviation	0.122	0.382	0.123	0.274	0.124	0.187
Number of failed lines						
Mean	4.7	39.2	4.7	17.8	4.7	8.6
% of original 636 lines	0.7	6.2	0.7	2.8	0.7	1.4
Standard deviation	16.7	85.6	16.7	55.1	16.7	29.6

Generally, with an increasing α-value, the network reliability strongly increases, i.e. the general vulnerability of the network with regard to cascading overloading decreases, because fewer and shorter cascading failure processes occur. For settings of the Nordic grid model with limited vulnerability (i.e. large tolerance with an α-value larger than 2.0), the dependent component failures due to the wind field have only a weak effect on the mean loss of load following the hazard, because cascading effects are minimized. As expected, the load loss, system failure, and number of lost lines recorded after the initial line triggering remain unaffected by the α-variation. These instances can be considered replicates, which show a rather high precision of the MS simulations.

The results for the load loss may not be directly transferable to real conditions, since the cascading failure model is a generic representation of the network behavior based on a

number of assumptions. However, the resulting load loss values range in a realistic order of magnitude when they are compared to the load losses of large historical blackout events. As an example, Eastern Denmark and Southern Sweden were affected by a regional power outage in September 2003 where the load not supplied amounted to 8000 MW (Elkraft System, 2003). Additionally, the order of magnitude of the load loss values compare to those reported by Andreasson et al. (2011a), where results range in between about 500 to 8000 MW.

The effect and the importance of the spatial correlation of the line failure probabilities due to the hazard impacts can be demonstrated by deleting the correlation structure of the original SRF by random permutation of the location specific failure probabilities in each single simulation step; thus, creating independently distributed but equally sized initial line failures. The failures are then still conditioned on the occurrence of a storm, but the dependence from geographical proximity is eliminated. This also leads to the disappearance of the significant negative association between the initial line power load and the initial line failure probabilities, as described in the previous section. Results from this sensitivity analysis are given in Table 12 and Figure 50: Failing lines in the Nordic Grid triggered by the empirical positively correlated wind load SRF will entail lower lost line and loss of load values compared to losses resulting from an equivalent un-correlated SRF. It shows that these considerations extend to situations where initial stochastic grid failures trigger cascading and thereby further escalate the initial load shed caused by the initially failed lines. For the Nordic Grid, load losses after cascading show to be lower in the correlated case compared to the independent case. The expected number of finally failed lines increases slightly with the un-correlated SRF as triggering cause, see Table 12.

Table 12: Mean and standard deviation of the number of initially and finally failed lines; Results based on the SRF simulations in comparison with the independence assumptions; based on varying α- values with 10,000 samples each.

		Spatially correlated SRF (naturally)		
		α = 1.1	**α = 1.5**	**α = 2.0**
Failed lines	initially	finally	finally	finally
Mean	4.7	39.2	17.8	8.6
Standard deviation	16.7	85.6	55.1	29.6
		Independence assumption		
		α = 1.1	**α = 1.5**	**α = 2.0**
Failed lines	initially	finally	finally	finally
Mean	4.7	39.9	21.7	13.6
Standard deviation	16.7	83.0	60.2	44.8

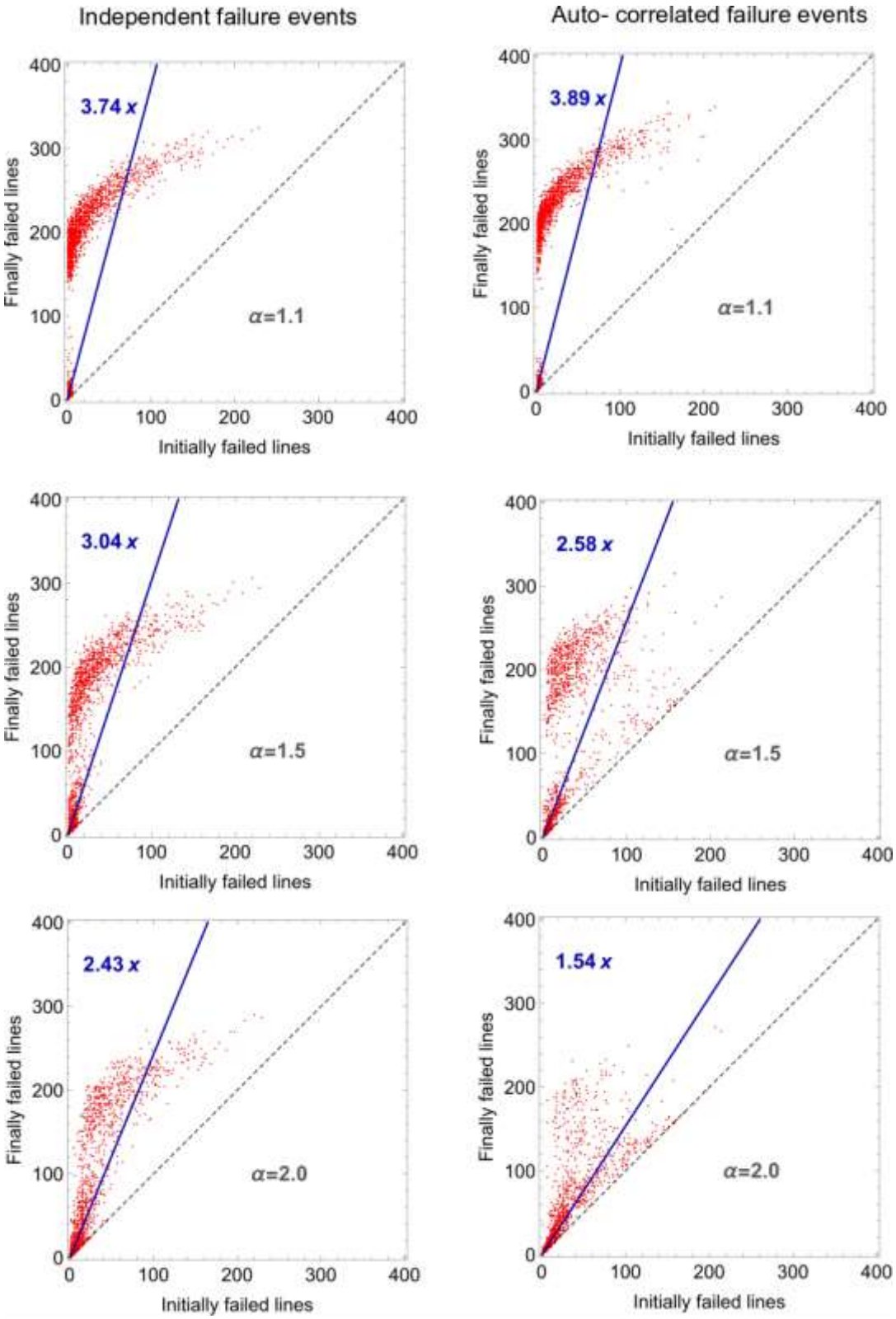

Figure 50: Finally versus initially failed lines for the case of independent failures (left) and dependent failures (right) due to SRF triggering; based on 10,000 samples under variation of the tolerance parameter α.

These findings, on a first glance, are in contradiction to the results of the study by Andreasson et al. (2011a) where it was found that with an increasing dependence in the components the network reliability decreases. An explanation for the difference in the findings could be, that in our study, it is accounted for cascading failures whereas by Andreasson et al. (2011a) no cascading processes were considered. It appears that a cascading failure process has the largest effect when just a few lines have failed initially, which is more probable with no or little (spatial) dependence. This can be explained by the observation that with increasing correlation the simulated samples with no line failure at all and those with many line failures get more and more frequent and dominant with the consequence that cascading is not triggered at all or it stops earlier since too many lines failed initially that were needed to propagate the cascading. Thus, lesser lines will fail overall, entailing reduced expected cascading depths and less expected finally failed lines with increasing correlation.

9.5.4 Component importance rankings

In this section, the IM component rankings are reported and compared for the chosen 'base case' with a fixed tolerance parameter ($\alpha = 1.5$) and load loss threshold ($t_L = 0.1$). Figure 51 visualizes the importance rankings according to CI and LS, where for each case the 50 highest ranked lines are highlighted in the graph plots. Additionally, the rankings based simply on the initial line failure probability $p_{f,i}^{(i)}$ and on the deterministic measure "load loss", LL_{n-1} are presented. The measure LL_{n-1} indicates the final loss of load after cascading failure that results from removing only one single line individually from the network. It is the $(n-1)$-contingency criterion. This analysis is conducted for each line and the resulting load loss values are determined and compared. The measure can be seen as a deterministic criterion, since it does not account for any (initial) component failure probabilities, nor does it estimate the system failure probability.

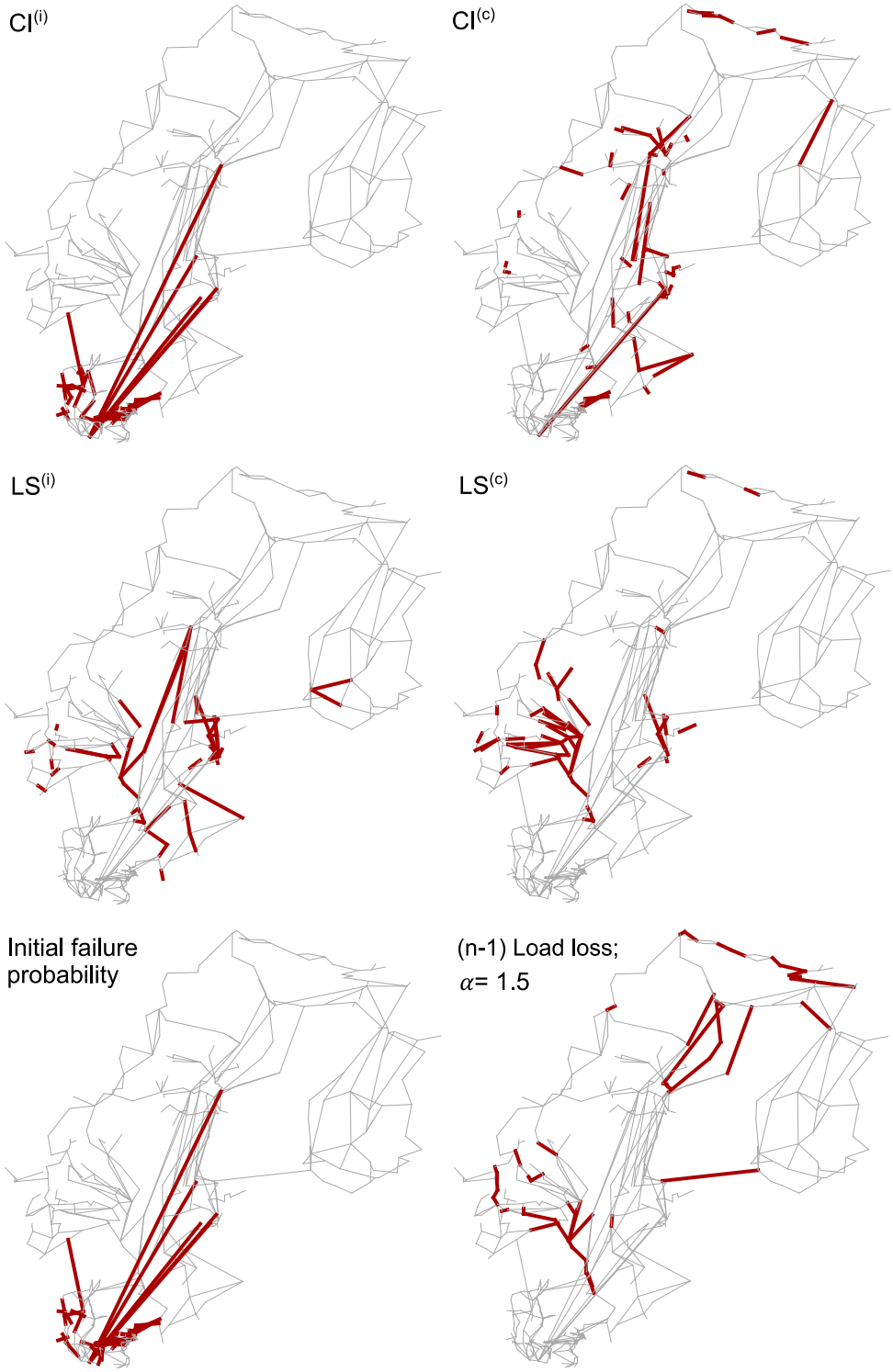

Figure 51: Nordic grid with highlighted lines: the 50 highest ranked lines are highlighted based on $\alpha = 1.5$ and $t_L = 0.1$, and based on 10,000 samples. Top-left: $CI^{(i)}$ with respect to initial failures. Top-right: $CI^{(c)}$ with respect to cascading failures. Center-left: $LS^{(i)}$ with respect to initial failures. Center-right $LS^{(c)}$ with respect to cascading failures. Down-left: 50 lines with the highest initial line failure probability $p_{f,i}^{(i)}$; Down-right: 50 lines with the highest loss of load values LL_{n-1} after $(n-1)$-contingency analysis.

The rankings based on $CI^{(i)}$ and $CI^{(c)}$ differ significantly, indicating that lines that are important for the initialization of network damage mostly do not correspond to the lines that are responsible for the further propagation of cascading overloadings. Initial line failures are most important in lines which are located in the southern part of the network and which have high initial loads. Cascading failures are most important in lines with low initial load and capacity, as these are more likely to be overloaded. Similar observations are made for the rankings of $LS^{(i)}$and $LS^{(c)}$, which also differ strongly. As expected, many of the lines that are highly ranked connect power generator nodes to the grid. Overall, the LS rankings show a similar pattern as the CI; however, the exact composition and order of the 50 highest ranked lines differs among all four IM rankings.

The rankings based on LL_{n-1} from the $(n-1)$-contingency analysis differ in comparison to the IM rankings described above. Note that the LL_{n-1}stems from an analysis that does not account for any external hazard impacts. The 50 most important lines according to LL_{n-1} are mainly lines that connect different clustered parts of the Nordic grid. E.g., the line connecting Sweden and Finland is ranked very high. Since this specific line consists of undersea cables in most parts, its failure probability due to wind hazard is zero and thus is not highly ranked with the other importance measures.

The ranking by the initial line failure probability $p_{f,i}^{(i)}$ differs from the ranking based on LL_{n-1} but it has a high overlap with the ranking following $CI^{(i)}$. The overlap between the $p_{f,i}^{(i)}$ and the $CI^{(i)}$-rankings shows that there is a high influence of the initial component failure probability in the CI importance measure.

It is observed that the similarity between all four measures is rather low for the 20 most important lines, i.e. the differences in the rankings of $CI^{(i)}$, $CI^{(c)}$, $LS^{(i)}$, $LS^{(c)}$ reflect the differences observable in Figure 51.

In addition, it is found that the rankings based on $CI^{(f)}$ are close to those based on $CI^{(c)}$ and are therefore not depicted here. Furthermore, BM and CI deliver similar results, and the five most important components even coincide. The CI is based on the BM, but additionally includes the reliability of the individual components. Here, CI is similar to BM because the component reliabilities with respect to hazardous extrinsic impacts are in the same order of magnitude. This is not the case after cascading failure processes: a lower correlation between $BM^{(c)}$ and $CI^{(c)}$ is observed in comparison to that between $BM^{(i)}$ and $CI^{(i)}$.

Additionally to the results indicated in Figure 51, the measures $CI^{(i)}$ and $LS^{(i)}$ are determined for the individual line segments. Results are not depicted here, due to the high amount of such 1 km line segments. They show that the importance of single line segments might outrange the importance of the overall line that they are contained in. Due to the long lengths of some lines, they might be composed of both, less or more exposed and

vulnerable segments, as displayed in Figure 47. The importance of the overall transmission line is thus a more generalized information.

9.6 Network reliability enhancement under extreme wind loads

The IMs are applied for hypothetical decision support on network improvement strategies. To this end, we investigate the effect of strengthening or increasing capacity of selected lines or line segments on the overall loss of load of the Nordic grid model. The following two network improvement strategies are considered, based on Chapter 7.5.

1) Line strengthening of in total 4000 km lines (i.e. 4000 line segments and approximately 10% of the overall total line length of the vulnerable part of the Nordic Grid) that are highest ranked as most important lines by either $CI^{(i)}$ or $LS^{(i)}$, corresponding to an increase in the resistance against the hazardous (wind) load. Line strengthening is modeled by reducing the initial line segment failure probability to 25% of its original value. Note that the original probability value stems from mapping the wind speed at a location into the fragility curves of Figure 44. In this set up, the received value would be lowered by 25%.
2) Increase of the line capacity of 60 out of the 636 lines (circa 10%) that are highest ranked by either $CI^{(c)}$ or $LS^{(c)}$, corresponding to an increase in the resistance of the lines against overloading in the cascading failure process. The capacity increase is modeled by increasing the tolerance parameter α by a factor of 4.

These two strategies are compared with a potential network improvement based on rankings according to the initial line failure probability $p_{f,i}^{(i)}$ of the line segments versus the deterministic measure LL_{n-1} from the $(n-1)$-contingency analysis. Additionally, they are compared to a ranking simply based on the line betweenness index, Equation (40), $B_{l,uw}$ for the unweighted graph and $B_{l,w}$ for the graph with the lines weighted by the reactance values.

In Table 13 and Table 14, the resulting mean loss of load values for two fixed values of the tolerance parameter α and based on 100,000 simulations are compared. The standard error is calculated as the standard deviation of the loss of load [MW] divided by the square root of the number of samples. Generally, both improvement strategies achieve rather high reliability improvements in terms of a decrease in the loss of load. The improvement levels are sensitive to a change in the α-value. With α-value equal to 1.5, increasing the line capacity according to $CI^{(c)}$ rankings leads to the overall best result, i.e. a decrease in the mean loss of load value by almost 50%.

Table 13: Loss of load values based on 100,000 simulations for the original grid (no improvement) compared to the improvement strategies: case of line segment strengthening versus case of line capacity increase. Results are given for α-value equal to 1.2.

α = 1.2	Line segment strengthening				Line capacity increase			
	Mean Initial Loss of load [MW]	Mean Loss of load [MW]	Standard error	Final improvement [%]	Mean Initial Loss of load [MW]	Mean Loss of load [MW]	Standard error	Final improvement [%]
Original grid	1803	25558	662	0.0	1806	25779	663	0.00
Ranking Criterion								
$CI^{(i)}$	787	16183	534	36.68	1804	26281	673	-1.95
$CI^{(c)}$	1345	22088	623	13.58	1801	16908	501	34.41
$LS^{(i)}$	893	17781	557	30.43	1813	22101	568	14.27
$LS^{(c)}$	1157	20245	589	20.79	1814	16846	505	34.65
LL_{n-1}	1659	24654	649	3.54	1806	19385	526	24.8
$p_{f,i}^{(i)}$	1143	20204	588	20.95	1813	26234	671	-1.76
$B_{l,uw}$	1451	23519	642	7.98	1808	20993	552	18.56
$B_{l,w}$	1500	24037	647	5.95	1814	20131	523	21.91

Table 14: Loss of load values based on 100,000 simulations for the original grid (no improvement) compared to the improvement strategies: case of line segment strengthening versus case of line capacity increase. Results are given for α-value equal to 1.5.

α = 1.5	Line segment strengthening				Line capacity increase			
	Mean Initial Loss of load [MW]	Mean Loss of load [MW]	Standard error	Final improvement [%]	Mean Initial Loss of load [MW]	Mean Loss of load [MW]	Standard error	Final improvement [%]
Original grid	1805	11110	380	0.0	1822	11228	385	0.00
Ranking Criterion								
$CI^{(i)}$	750	6131	287	44.81	1812	10900	376	2.92
$CI^{(c)}$	1160	7655	321	31.09	1797	5670	246	49.50
$LS^{(i)}$	961	7068	298	36.38	1802	7346	270	34.58
$LS^{(c)}$	1346	9422	350	15.19	1802	7109	231	36.68
LL_{n-1}	1346	9501	346	14.48	1821	6500	240	42.11
$p_{f,i}^{(i)}$	1156	8347	326	24.87	1801	10680	370	4.88
$B_{l,uw}$	1450	9644	364	13.20	1811	7218	266	35.71
$B_{l,w}$	1482	9750	362	12.24	1813	6700	238	40.32

Strengthening line segments according to the $CI^{(i)}$ rankings leads to a decrease in the mean load loss by about 36.7 (α equal to 1.2) and 44.8% (α equal to 1.5). Strengthening lines

according to $LS^{(i)}$ yields an improvement by about 30.4% (α equal to 1.2) and 36.4% (α equal to 1.5). If line segments are simply chosen by a ranking based on the initial failure probability ${p_{f,i}}^{(i)}$, a decrease of the overall loss of load by about 21-25% can be achieved. This indicates that the initial probability of failure associated with the hazard impacts already provides substantial information that can be used to improve the network. However, the CI and LS clearly outperform this simple measure. As expected, strengthening lines based on LL_{n-1} leads to a lower effect of 3.5% (α equal to 1.2) and 14.5% (α equal to 1.5) decrease in the loss of load value. Furthermore, improving line strength based on the Betweenness indices $B_{l,uw}$and $B_{l,w}$ also yields only limited improvements.

With regard to the strategy of capacity increase (enhanced tolerance parameter α of selected lines), the $CI^{(c)}$, $LS^{(c)}$, and deterministic indices $LL_{n-1,}B_{l.uw}$, and $B_{l,w}$ show rather high results with a decrease in the loss of load by 36% to 49.5% for α equal to 1.5. Thus, the improvement based on lines selected according to the crude deterministic measures can be substantial, although they neglect information on component and system failure probability. However, with a lower tolerance parameter, here α equal to 1.2, the performance of the $LL_{n-1,}B_{l,uw}$, and $B_{l,w}$ drops off in comparison to $CI^{(c)}$ and $LS^{(c)}$, see Table 13. As expected, the capacity enhancement based on the ranking by the initial failure probability ${p_{f,i}}^{(i)}$ does not yield high improvements for any α- value.

Using strategy 1, i.e. the improvement of the initial line failure probability, it is very important to rank the individual line segments instead of only ranking the whole lines. Identifying the specific critical line segments is much more efficient and leads to a significantly higher load loss reduction, since there are many rather long lines which are highly ranked influenced by the number of line segments, as it was demonstrated in Figure 47. The results in Table 13 (left side) are based on the assumption of the improvement of overall 4000 km line segments. To receive a reference value, the same calculation was conducted based on the improvement of the 60 highest ranked lines as a whole. Dependent on the importance measure, these 60 lines are composed of different lines and thus sum up to a different sum of length. In average this corresponds to a total km length of about 4800 km, and up to 8000 km. However, the improvement of 60 complete lines would lead to in average only half of the effect (app. 9.3% less load loss) than when specific line segments are improved (app. 17.5% less load loss). As an example, the strengthening of the 60 highest ranked lines according to $CI^{(i)}$ corresponds to an overall line length of 6010 km, would lead to a by 17.8% lower loss of load value (based on α equal to 1.2), whereas the improvement based on 4000 km of individual line segments ranked by $CI^{(i)}$ would improve the final power loss value by 31.9%.

9.7 Summary

This study assessed the performance of the power transmission grid of the European Nordic countries subject to extreme windstorm events. The hazard model is based on historical wind speed data sets of most extreme events provided in the XWS database. Correlated spatial random field realizations are generated in a Monte Carlo simulation assessment. The wind fields are mapped to component fragility curves and thus, component failure events are simulated and consequent network performance is investigated based on a DC power flow model in terms of overall loss of load. The component fragility model is calibrated for the study area so that the observed approximate historical overall line failure rate over the past 16 years is met.

It is found that the network reliability is highly sensitive to the tolerance parameter α in the cascading failure model. Generally, results for the final mean load losses compare to values found for historical large blackout events in the Nordic region. Furthermore, it is observed that the reliability of the network is higher in case of correlated initial component failures. This result stands in contradiction to the findings in Andreasson et al. (2011) who find a decreasing reliability for increasing correlated component failures in the Nordic Grid. However, our study accounts for cascading failures that are expected to be somewhat attenuated as the dependence in the initial triggering events (due to the correlation in the wind fields) is present and is of relevance.

The importance measures CI and LS are differentiated with regard to initial, cascading, and final failure events and employed in order to rank the components with regard to their influence on the overall system reliability. Finally, two component improvement strategies are suggested and it is assessed which component ranking would perform best with regard to a decrease in the overall loss of load after cascading failure triggered by initial failures during a hazard event. For both strategies, the two IM applied (CI and LS) perform similarly good with a decrease in loss of load approximately between 35% to almost 50%. The improvement potential is observed to depend strongly on the tolerance parameter α. Overall, both strategies suggested have their maximum achievements in a comparable order of magnitude. Following this analysis, the comparison of the two strategies discussed above would have to be followed by a cost benefit analyses. This means a set off of all the efforts, costs, and benefits that are equivalent to the measures of lowering the probability of failure and increasing the line capacity against power flow overload. The actual utility and expected costs could be compared, and this assessment could contribute to a potential decision support in the future. Note that increasing the capacity of lines has also other benefits as well, but will be less effective if α is higher, as expected in the real system.

10 The correlation length effect on reliability and importance

Parts of this Chapter are based on Scherb et al. (2017), published in the ASCE-ASME Journal of Risk and Uncertainty in Engineering Systems, Part B: Mechanical Engineering, and on Scherb et al. (2016), a conference contribution for the European Safety and Reliability Conference, ESREL, in Glasgow September, 2016.

10.1 Methodological framework

The methodological framework for this case study is shown in Figure 52. The specific motivation as compared to the previous studies is the investigation of the effect of spatial correlation in hazards on 1) the overall network reliability and 2) on the component importance rankings based on different importance measures (IMs). To this end, the quantification of the spatial correlation in the hazard intensity characteristic is in focus. The hazard event is idealized by a spatial random field, which is parametrized through the SRF correlation length. Therefore, a generic hazard model is formulated through a random field (SRF model) with continuously scalable spatial correlation, to study extrinsic common-cause-failure events, where extreme wind storms are one example cause. The reliability and component importance rankings are determined in function of the correlation length parameter, i.e. numerical investigations are performed for varying correlation lengths of the random field, to represent different hazard characteristics.

As in the previous case studies, the network performance assessment accounts for cascading failure processes that might occur after initial triggering events. This is done based on the models described in Chapter 5.4. Alternatively, the network reliability is assessed based on the (s-t)-connectivity problem (Section 5.2.2). This is an assessment without considering cascading failure effects which is included so that results from different performance models can be compared.

Selected importance measures are calculated to rank single components according to their influence on the overall system reliability related to initial (triggering) failures and component importance related to cascading failures. The efficiency of the proposed component importance measures is tested when they are used as a basis for planning network improvements, see Figure 52. Furthermore, a comparison with rankings based on the betweenness index and based on the assessment without cascading failures is conducted.

In the following, the implementations and results are applied to the benchmark power transmission systems IEEE 39 and IEEE 118.

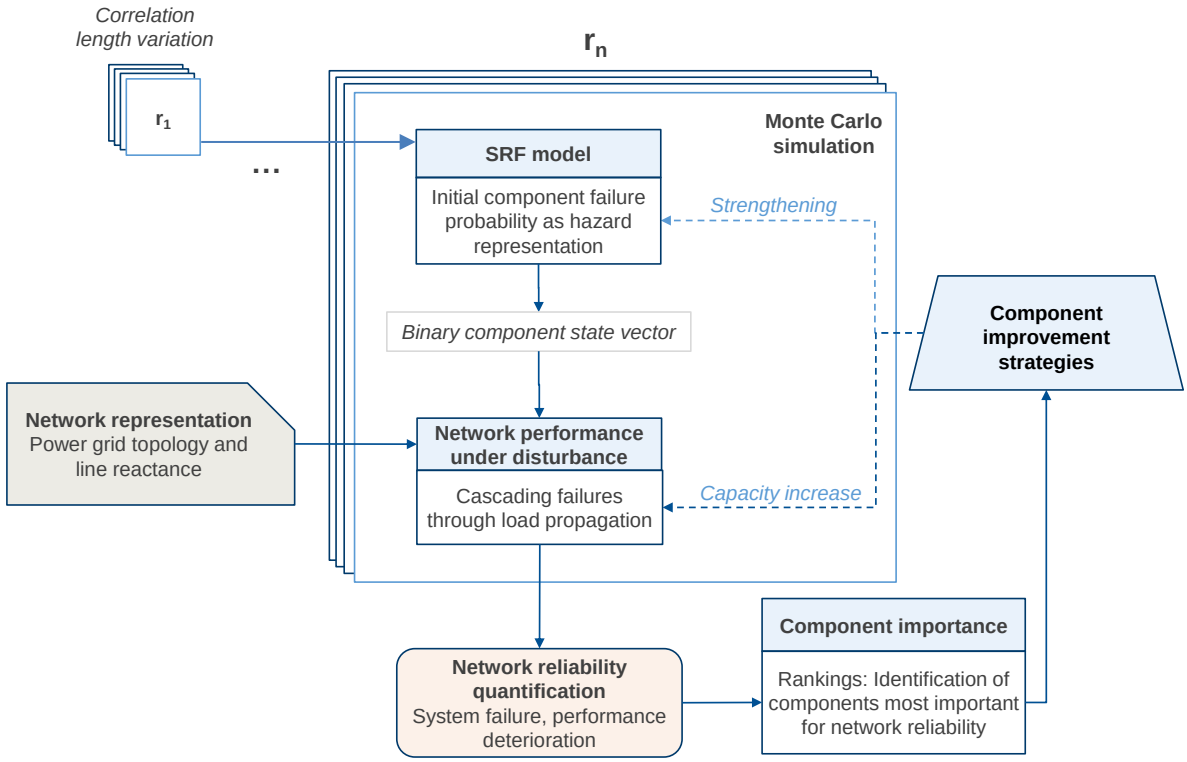

Figure 52: Overall assessment framework for the analysis with a varying correlation length r, $[r_1 \dots r_n]$ of the SRF model within a MC simulation approach.

10.2 Implementation cases

10.2.1 Benchmark IEEE 39

The network is introduced in Chapter 2.3.1. By assigning coordinates to the nodes, the network is projected onto a hypothetical study area of about 500 x 500 km^2 (Figure 53). The mean line length is 69 km, with a minimum of 25 km and a maximum of 124 km.

The performance of the IEEE 39 test case is assessed based on the graph efficiency model in Chapter 5.4.1. The graph efficiency value $E(G_{original})$ of the intact IEEE 39 network is 0.286.

The left-hand side of Figure 53 shows the lines weighted by their reactance values, and the right-hand side of Figure 53 indicates the line capacities, which are proportional to the number of shortest paths passing through the lines following Equation (15). As expected, lines with lower reactance are more likely to attract shortest paths.

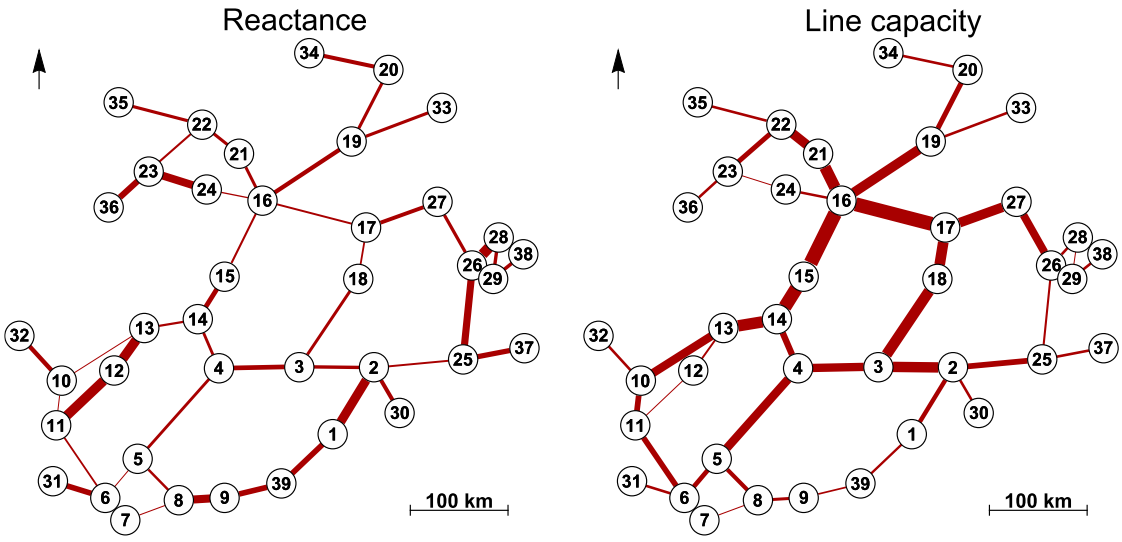

Figure 53: Plots of the IEEE 39 bus system with geo referenced nodes. Left: line thicknesses indicate the reactance values of the lines; right: thicknesses indicate the line capacities, which are proportional to the number of shortest paths passing through the lines.

10.2.2 Benchmark IEEE 118

The IEEE 118 bus benchmark system for transmission power grids is a considerably larger network than the IEEE 39. The network is introduced in Chapter 2.3.1.

The network is projected onto a hypothetical study area of about 900 x 750 km^2, by assigning coordinates to the nodes. The mean line length is 131.6 km, with a minimum of 10.8 km and a maximum of 626.6 km.

Due to its size, the IEEE 118 cannot be efficiently assessed based on the graph efficiency models where shortest paths between all node pairs need to be calculated in each cascading step. Thus, the performance of the IEEE 118 teste case is assessed based on the power flow model in Chapter 5.4.2. The overall power load in the undamaged network $L(G_{original})$ is 2605 MW.

The upper graph in Figure 54 shows the lines weighted by their reactance values, and the graph below indicates the line capacities, which are proportional to the number of shortest paths passing through the lines (the initial load) following Equation (15). As expected, lines with lower reactance are more likely to attract more power flow, and vice versa.

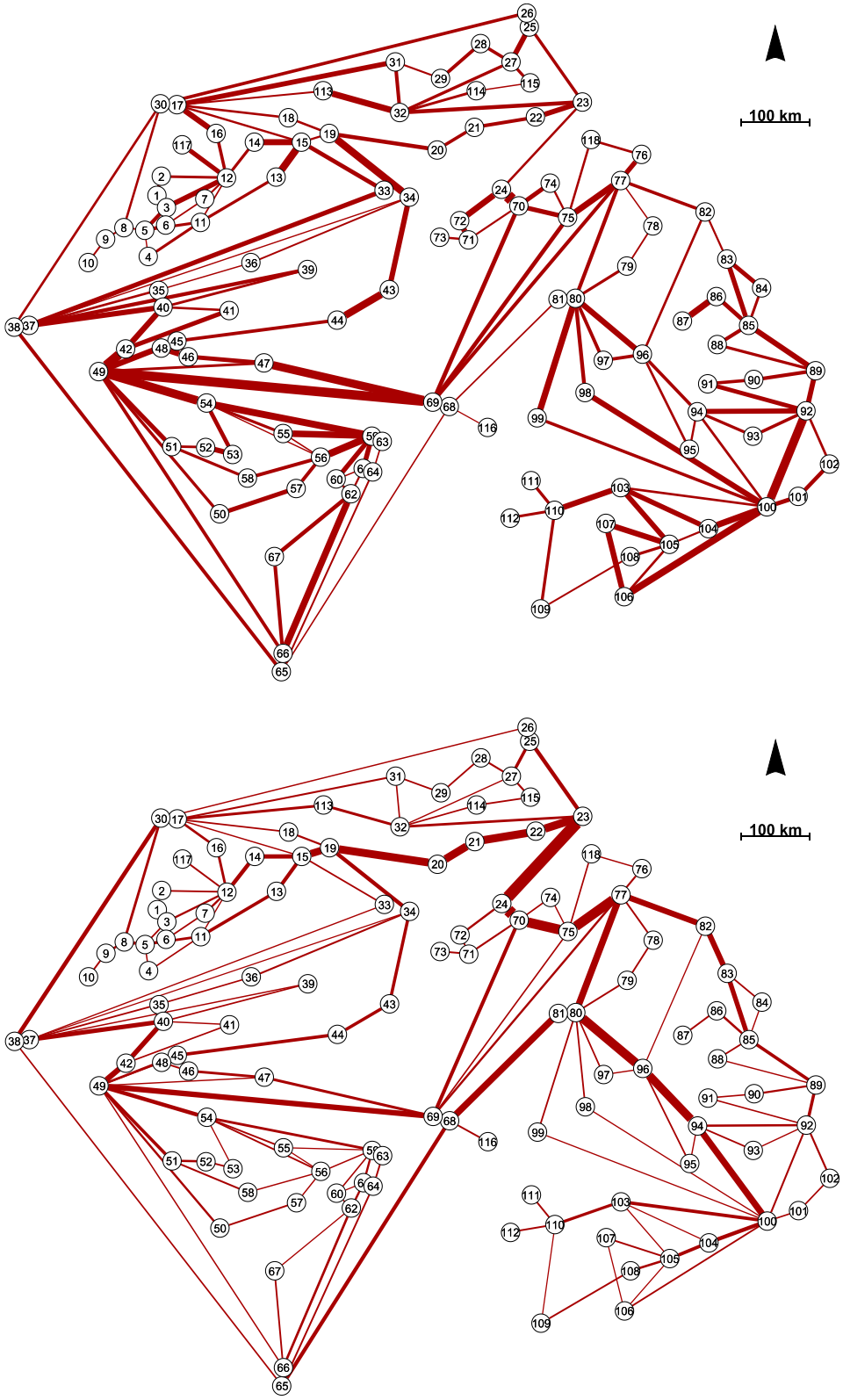

Figure 54: Plots of the IEEE 118 bus system with geo referenced nodes. At top: line thicknesses indicate the reactance values of the lines; below: thicknesses indicate the line capacities, which are proportional to the initial load, i.e. number of shortest paths passing through that line. Lines with lower reactance are more likely to attract shortest paths, and vice versa.

10.3 SRF for generic hazard representations

A strongly idealized stochastic random field model is introduced for describing line failures originating from large scale natural hazards (here wind loads). The model describes the component failure probabilities $p_{f,i}^{(i)}$ of the lines during a hazard event through a random field. Let Z denote a standard normal random field, and Z_i its value at the midpoint of line l_i. The probability of failure of line l_i during the hazard event is obtained in function of Z_i through the following isoprobabilistic transformation:

$$p_{f,i}^{(i)} = F_{P_{f,i}}^{-1}[\Phi(Z_i)] \tag{72}$$

where Φ is the standard normal CDF and $F_{P_{f,i}}^{-1}$ is the inverse CDF of the component failure probability $p_{f,i}$. It is here modelled by the beta distribution, which is a common choice for random values representing probabilities.

In the above formulation, the spatial correlation between the failure probabilities at two locations l_1 and l_2, $p_{f,1}$ and $p_{f,2}$, is represented through the underlying standard Gaussian random field Z, by means of the following covariance function:

$$C_z(h) = exp\left(-\frac{h^2}{r^2}\right) \tag{73}$$

where h [km] is the Euclidean distance between the locations of lines l_1 and l_2, and r [km] is the correlation length. The correlation structure of the resulting beta random variables is approximately described by the correlation function of Equation (73); see also Der Kiureghian and Liu (1986). The correlation length denotes the maximum distance between two points in the random field upon which their probability values are significantly correlated.

Through variations of r, a range of different scenarios of hazard events can be modelled: from random and mutually independent failure events ($r \to 0$), to large-scale fully correlated failure probabilities with spatially constant failure probabilities ($r \to \infty$). The latter case reflects a situation in which the hazard is the same throughout the entire area, but the component failure events are still independent for a given hazard event. When interpreting results for intermediate correlation lengths r, it is the relative value of r compared to the size of the infrastructure system that determines the system behavior.

The employed generic model with its one parameter (correlation length) is not able to address the specifics of a particular hazard type. Clearly, a spatial dependence model of a heat wave differs from that of a wind storm, and both are significantly more complex than

the generic model used here. If desired, for specific hazards and network locations, parametric or numerical models can be employed instead, which more accurately reflect their specific dependence structure (Winkler et al., 2010, Ouyang and Dueñas-Osorio, 2014), compare also Chapter 8. However, the use of specific hazard models impedes general conclusions about the possible principle effects of spatial correlation. In particular, any specific spatially distributed hazard is described by a non-homogenous random field, as in the Nordic grid example, and the effects of the change in the mean hazard intensity are superimposed on the effects of dependence. This motivates the use of the simple generic hazard model in this study.

10.3.1 Spatial random field realizations

In the MC simulations, the mean component failure probability during a hazard event is fixed at 0.077 and its standard deviation is fixed at 0.054. These values are motivated by the above study on hurricane impacts on component failure probabilities and network damages in electrical transmission systems (Section 8).

Realizations of the spatial random field describing the component failure probability $p_{f,i}^{(i)}$ under correlation length variation are generated for the prescribed study area of interest. Sample realizations for four selected correlation length values are visualized in Figure 55 and Figure 56 for two different hypothetical study areas: once for the IEEE 39 and once for the IEEE 118 test case system.

In the following investigations, for both case study systems, the correlation length r of the generic hazard model is varied to measure the effect of spatial correlation on system failure events, component importance, graph efficiency, and cascading depth, i.e. mean number of cascading steps before the system stabilizes, based on a Monte Carlo simulation with at least 10^4 samples. All results are calculated with an efficiency threshold of $t_E = 0.9$ and a tolerance parameter $\alpha = 1.5$, unless otherwise noted.

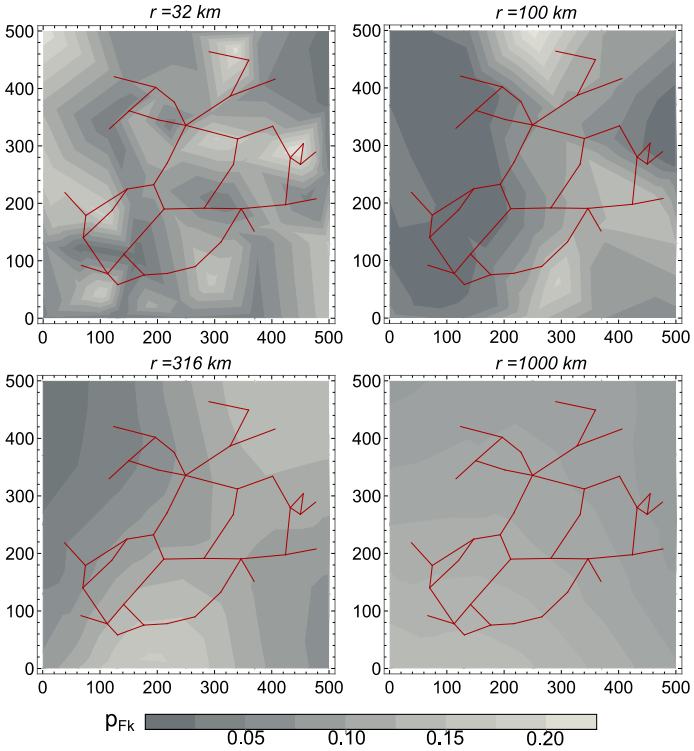

Figure 55: Contour plots of sample spatial random field realizations of component failure probabilities $p_{f,i}$ for selected values of the correlation length r, together with the IEEE 39 bus system; scale unit is km.

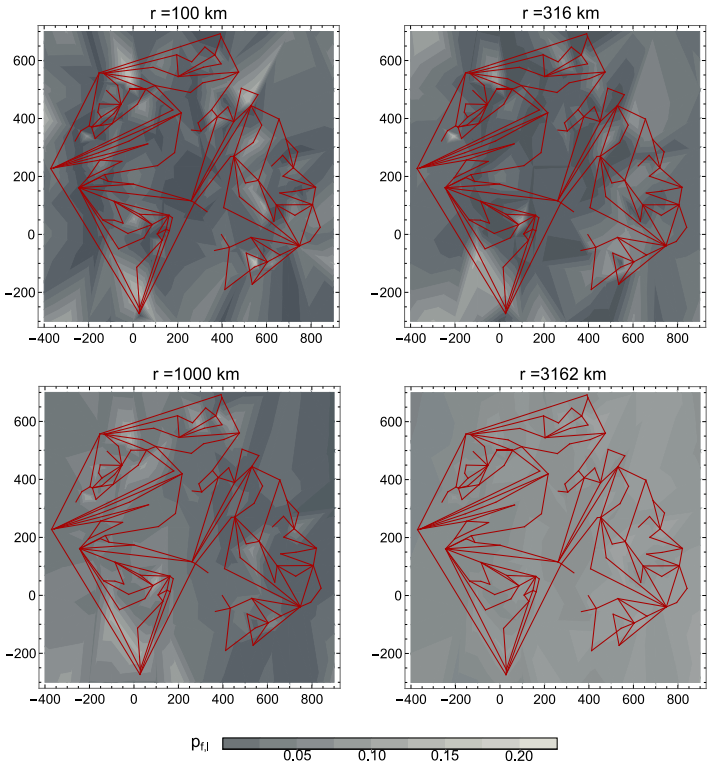

Figure 56: Contour plots of sample spatial random field realizations of component failure probabilities $p_{f,i}$ for selected values of the correlation length r, together with the IEEE 118 bus system; scale unit is km.

10.4 Results for IEEE 39

10.4.1 Network reliability as a function of the hazard correlation length

The network performance is expressed in terms of lost lines (initially and finally) and the declining graph efficiency in case of lost lines. The initially failed lines following a hazard event are compared with the number of finally failed lines after the cascading process. In Figure 57 and Table 15, this comparison is performed for the case of independent component failure probabilities ($r \to 0$) and fully dependent component failure probabilities ($r \to \infty$). It is observed that with increasing correlation length ($r \to \infty$), the variance of the number of initially failed lines increases. This effect is weaker for the finally failed lines. The mean number of initially failed lines is by definition the same for all correlation lengths as mentioned above. However, the expected number of finally failed lines increases slightly with decreasing correlation length. This effect can be explained by the fact that the cascading failure process has the largest effect when just a few lines have failed initially, which is more probable with no or little dependence.

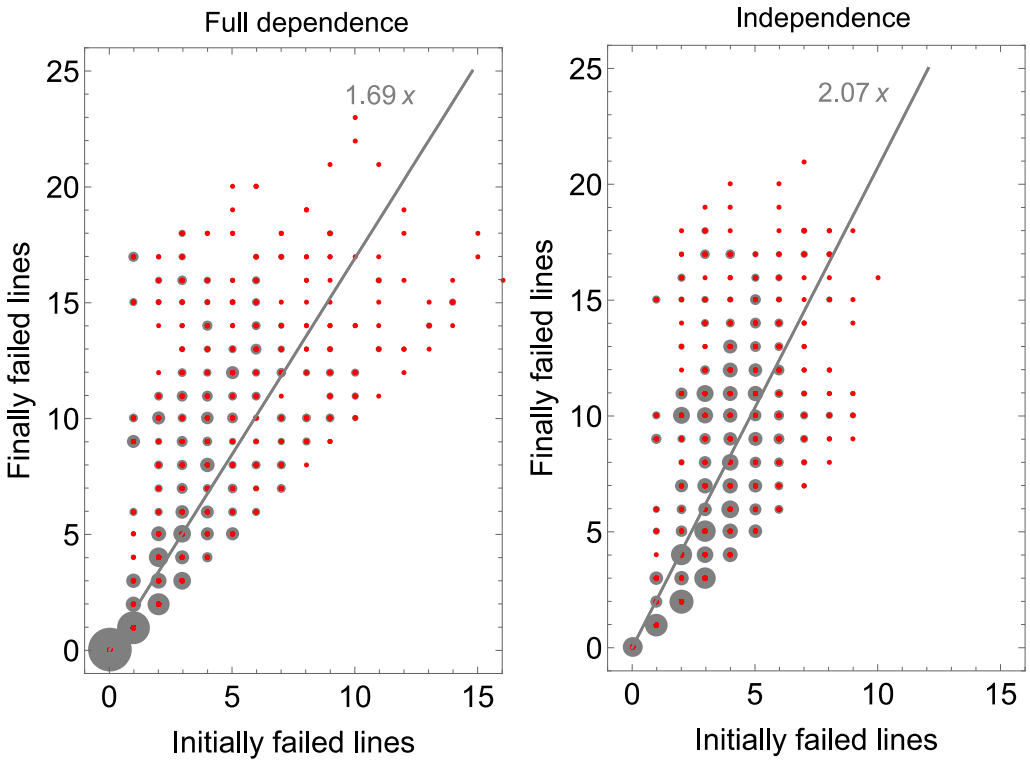

Figure 57: Finally versus initially failed lines for the case of full dependence (left) and independence (right); based on 10,000 samples with $\alpha = 1.5$; grey circles indicate the frequency of the data points in the sample space.

Table 15: Mean and standard deviation of the number of initially and finally failed lines; comparison of the independence and full dependence assumptions.

Failed lines	**Parameter**	**Independence** ($r = 0$)	**Full dependence** ($r = \infty$)
Initially	Mean	3.54	3.57
	Standard deviation	1.81	3.10
Finally	Mean	7.94	7.28
	Standard deviation	4.69	5.50

Means and standard deviations of graph efficiencies $E_{norm}(G_i)$ are shown in Figure 58, as a function of the correlation length r and the tolerance parameter α. The left-hand side of Figure 58 shows that the overall graph efficiency is increasing with the correlation length r. This result, which may at first glance appear counterintuitive, is consistent with the effect shown in Figure 57. With increasing correlation length it is more likely that no line failures or a larger number of line failures occur initially; in both cases, cascading processes will be attenuated or will not be triggered at all. The vulnerability of the system is larger for small values of α. For systems with limited vulnerability (α larger than 3.0), the correlation length has only a weak effect on the mean efficiency following the hazard, because cascading effects are limited.

The standard deviation of the efficiency increases significantly with increasing correlation length (Figure 58 right). This can be explained with the increasing variance in the component failure probability, which is observed for higher values of r (compare with Figure 57 and Table 15).

Changes in the mean and standard deviation occur mainly in the range 100 – 1000 km, which corresponds to the order of magnitude of the network size. For correlation lengths smaller than 100 km, the behavior is similar to the uncorrelated case, whereas for correlation lengths larger than 1000 km, it approaches that of the fully correlated case. The results for small correlation lengths are affected by the simplified discretization of the lines, in which the failure probability of the lines is evaluated at the line midpoints. When considering the distributed nature of the lines, the failure probabilities of the individual lines would increase with decreasing correlation.

The system failure probability depends strongly on α. The lower the α-value, the higher is the system failure probability, and the less pronounced is the dependency of the system failure probability on the initial efficiency threshold. The dependency on the correlation length is similar in all constellations considered here and may again be explained by the increasing ‘variance between samples’ caused by the increasing correlation in the stochastic vector fields.

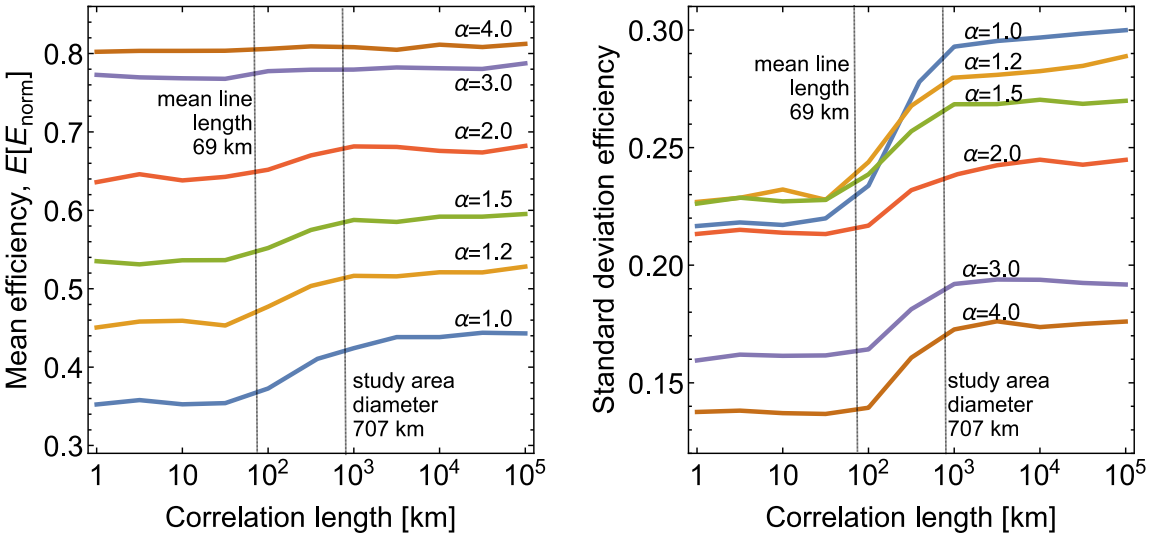

Figure 58: Network performance as function of the correlation length with varying α value. Left: mean overall graph efficiency E[E_{norm}]; right: standard deviation of overall graph efficiency; based on 10,000 samples each per correlation length value and α value combinations.

10.4.2 Component importance rankings

Figure 59 visualizes the criticality importance (CI) with respect to initial failures ($CI^{(i)}$) and cascading failures ($CI^{(c)}$) for a correlation length of 100 km. The two rankings differ significantly, indicating that lines that are important for the initialization of network damage do not correspond to the lines that are responsible for the further propagation of cascading overloads. Initial line failures are most important in lines which are centrally located in the network graph and which have high initial loads. Cascading failures are most important in lines with low initial load and capacity, as these are more likely to be overloaded (see Figure 53). As expected, leaf lines are ranked as the least important ones, for initial as well as cascading failure. The resulting $CI^{(f)}$ values are close to the $CI^{(c)}$ values in the right-hand side of Figure 59 and are therefore not depicted here. BM importance measures lead to a ranking very similar to CI, these results are also omitted here.

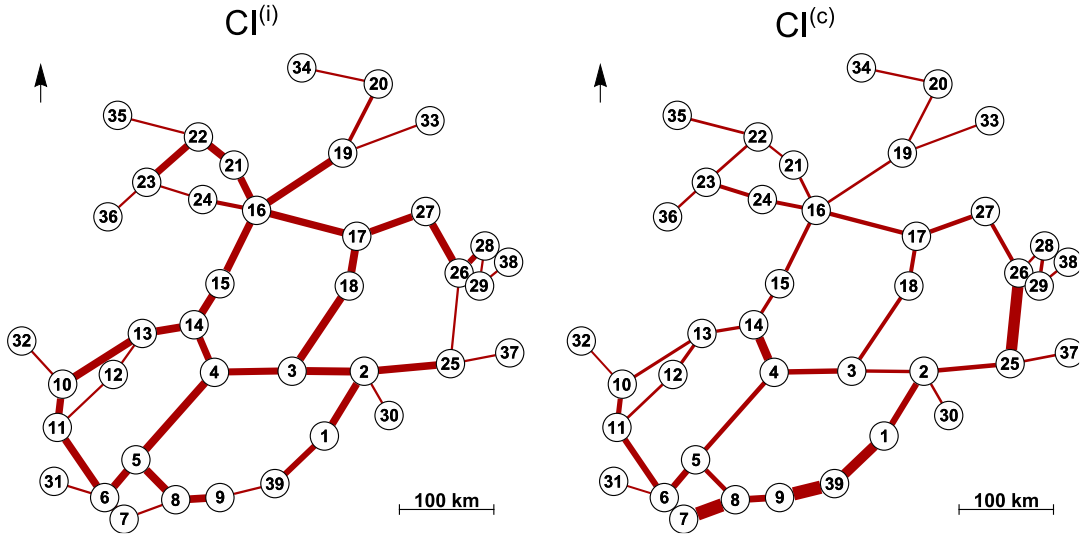

Figure 59: CI weighted graph at a correlation length of 100 km. Left: $CI^{(i)}$ with respect to initial failures; right: $CI^{(c)}$ with respect to cascading failures; with $\alpha = 1.5$ and $t_E = 0.9$; based on 10,000 samples.

In Figure 60, ES importance measures are summarized. Overall, these show a similar pattern as the CI of Figure 59. The network topology determines the $ES^{(i)}$ ranking; lines with a bypass are lower ranked, lines without bypass are in the middle range, and lines that link clusters with each other are highly ranked. The important lines with respect to cascading failures, i.e. the $ES^{(c)}$ values, are more uniformly distributed in the network.

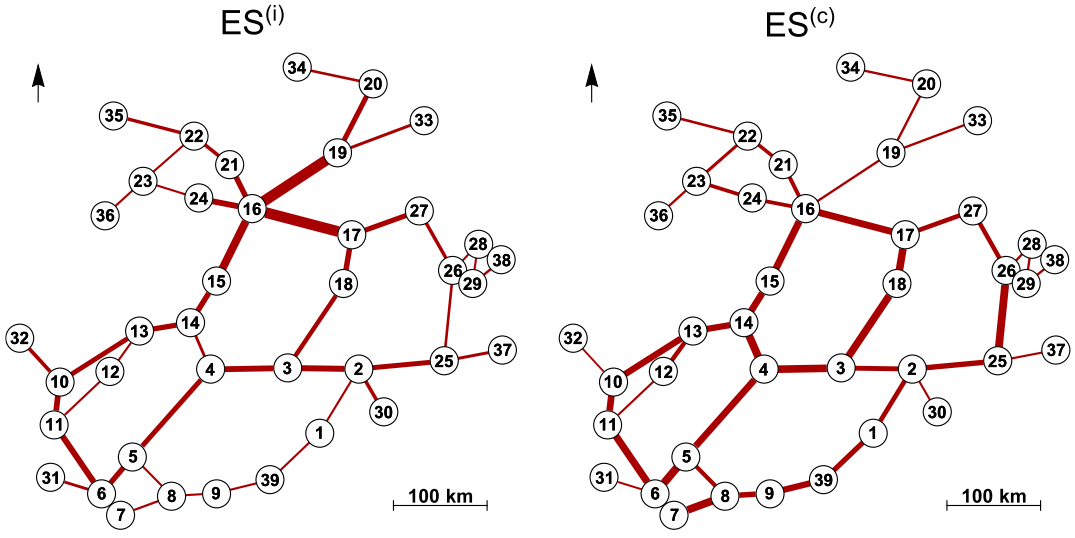

Figure 60: ES importance weighted graph at a correlation length of 100 km. Left: $ES^{(i)}$ with respect to initial failures; right: $ES^{(c)}$ with respect to cascading failures; with $\alpha = 1.5$; based on 10,000 samples.

We also compared the IM values to the betweenness index as shown in Figure 53, as an example of a topological measure. Whereas the betweenness index exhibits correlation

coefficients in the order of 0.70 with $ES^{(i)}$ and $CI^{(i)}$, its dependence with $CI^{(c)}$ and $ES^{(c)}$ is significantly less pronounced. These results indicate that the purely topological betweenness index is only partially suitable as a proxy for IMs based on the physical system performance.

Figure 61 shows the effect of the hazard correlation length on CI component importance rankings. While the values of $CI^{(i)}$ and $CI^{(c)}$ change significantly with varying correlation length, their respective rankings change only slightly. As in Figure 65, changes in CI occur mainly in the range 100 – 1000 km, corresponding to the network size. The five to ten highest ranked lines are essentially the same, independent of the variation in the correlation length. The difference in the rankings of $CI^{(i)}$ to those of $CI^{(c)}$ reflect the differences observable in Figure 59. As an example, line 9-39 is low ranked in importance with respect to failures caused by the hazard, but highly ranked in importance with respect to the cascading failure process.

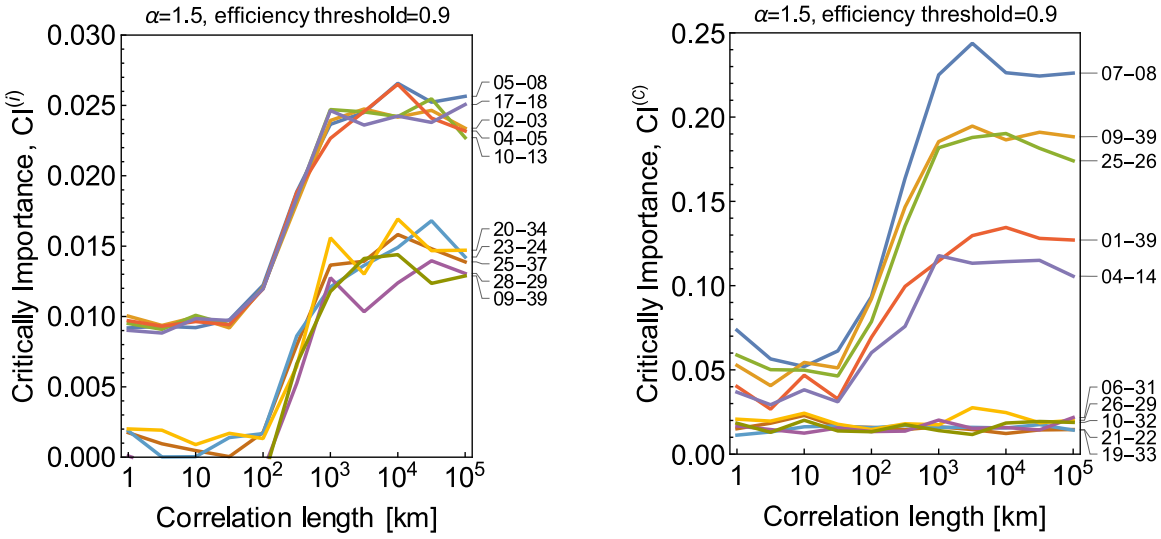

Figure 61: CI as function of correlation length. Left: $CI^{(i)}$ with respect to initial failures; right: $CI^{(c)}$ with respect to cascading failures; with $\alpha = 1.5$ and $t_E = 0.9$ each and based on 10,000 samples per correlation length value.

It is found that the rankings based on $CI^{(f)}$ are close to those based on $CI^{(c)}$ and are therefore not depicted here. Furthermore, BM and CI deliver similar results, and the five most important components coincide. The CI is based on the BM, while it additionally includes the reliability of the individual components. Here, $CI^{(i)}$ is similar to $BM^{(i)}$ because the component reliabilities with respect to hazardous extrinsic impacts are identical. This is not the case after cascading failure processes: a lower correlation between $BM^{(c)}$ and $CI^{(c)}$ is observed in comparison to that between $BM^{(i)}$ and $CI^{(i)}$.

Figure 62 depicts the rankings based on $ES^{(i)}$ and $ES^{(c)}$. The pattern is similar to the one of CI and BM, even though different lines are identified as the most important ones.

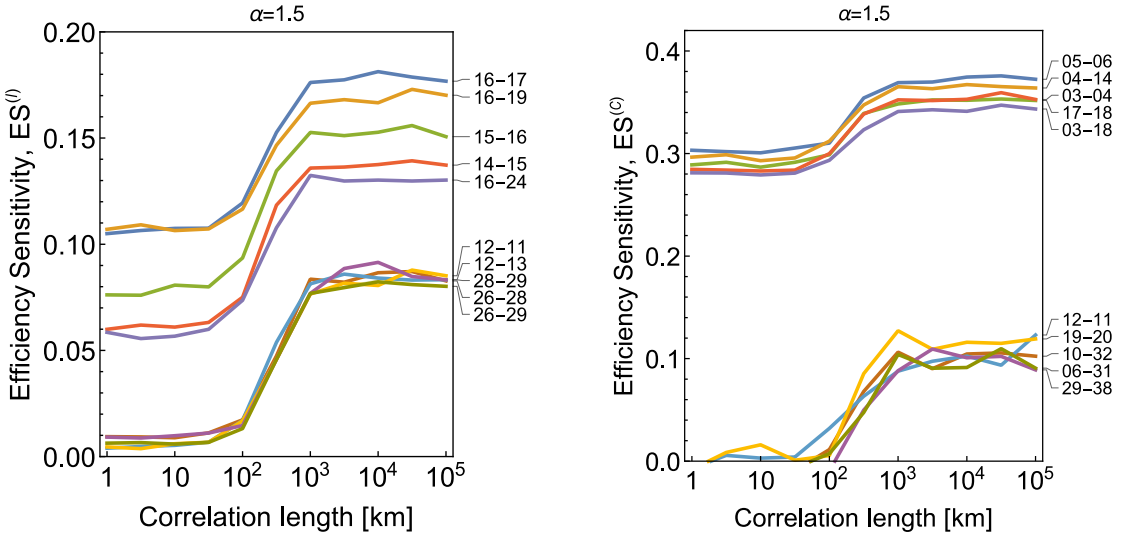

Figure 62: ES as function of correlation length. Left: $ES^{(i)}$ with respect to initial failures; right: $ES^{(c)}$ with respect to cascading failures; with $\alpha = 1.5$ each and based on 10,000 samples per correlation length value.

As Tanguy (2011) observes in his study on general CCF models and their influence on importance measures, adding CCF effects to the description of the IEEE system does not profoundly change the ranking of the lines when comparing to the independence assumption for all components. The results presented here indicate that this also holds in essence for spatial correlation effects under consideration of cascading failure processes.

In addition, we assessed the sensitivity of the results to changes in the tolerance parameter α and the efficiency threshold t_E utilized in the definition of system failure. For vulnerable systems (e.g., $\alpha < 2$ and $t_E > 0.7$), we find that the IM values are sensitive to the correlation length. In contrast, for less vulnerable systems (e.g., $\alpha > 2$ and $t_E < 0.5$), the change of the IM values with the correlation length is less pronounced. In all cases, the ranking remained essentially consistent among different correlation lengths.

10.4.3 Network reliability enhancement

Ultimately, the IMs should support decision making as it is suggested in Chapter 9.6. To this end, we investigate network improvement strategies based on the proposed IMs, by measuring the effect of strengthening or increasing capacity of selected lines on the network overall efficiency of the IEEE 39 network. Two network improvement strategies are considered:

1) Line strengthening of the five most important lines ranked by either $CI^{(i)}$ or $ES^{(i)}$, corresponding to an increase in the resistance against the hazardous (wind) load. Line strengthening is modeled by reducing the initial line failure probability to 10% of its original value.

2) Increase of the line capacity of the five most important lines ranked by either $CI^{(c)}$ or $ES^{(c)}$, corresponding to an increase in the resistance of the lines against overloading in the cascading failure process. The capacity increase is modeled by increasing the tolerance parameter α by a factor of three.

In Figure 63, the resulting mean efficiency in function of the hazard correlation length is compared. The results in Figure 63 (left) show that strengthening lines according to $ES^{(i)}$ and $CI^{(i)}$ rankings lead to similarly increased mean efficiencies, even though the rankings of the two measures do not coincide in their respective five highest ranked lines. For comparison, we also compute the resulting mean efficiency when lines are selected for strengthening following the $ES^{(c)}$ and $CI^{(c)}$ ranking. Such a strengthening of lines does not significantly affect the system performance, highlighting the suitability of $ES^{(i)}$ and $CI^{(i)}$ rankings for prioritizing network components for strengthening against initial hazard impacts.

Figure 63 (right) shows that the largest improvement of the resulting mean efficiency from increasing line capacity is obtained by selecting components according to $ES^{(c)}$. The ranking based on $CI^{(c)}$ leads to significantly lower gain in mean efficiency. As expected, $ES^{(i)}$ and $CI^{(i)}$ rankings are not suitable for identifying components for line capacity increase.

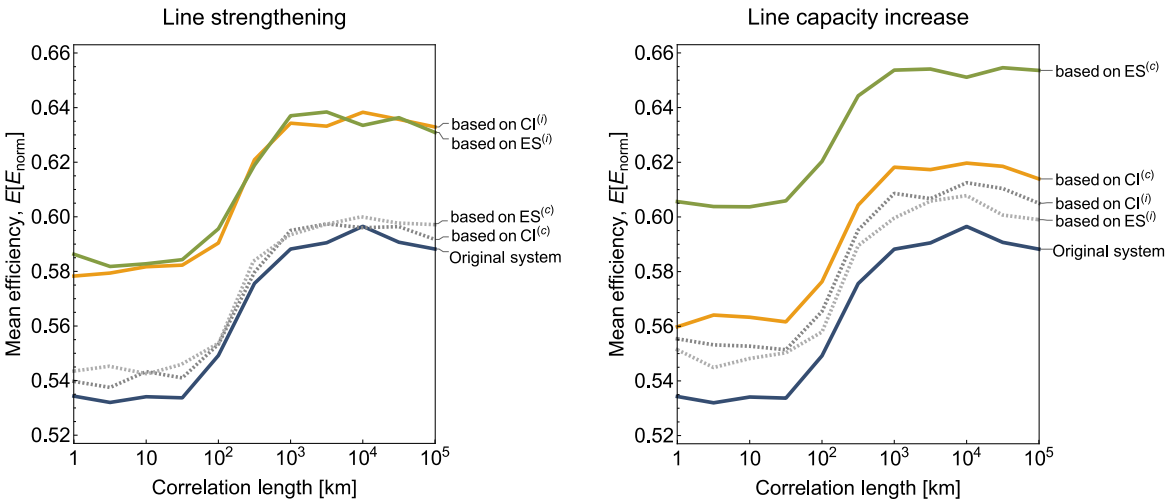

Figure 63: Mean efficiency in function of correlation length for different network improvement strategies. Left: line strengthening (decreasing the initial failure probability during the hazard event) of five selected lines; right: increasing line capacity (increasing the tolerance parameter α) of five selected lines.

10.5 Results for IEEE 118

The benchmark network IEEE 118 is investigated in the following. Due to its larger size, it is not computationally efficient to use the graph efficiency performance model, which is based on the shortest path algorithms mentioned in 5.2.2. Instead, the network reliability is based on the power flow model that was also applied in Chapter 9. However, the assessment framework and structuring of the results for IEEE 118 follow the one of the IEEE 39 case.

10.5.1 Network reliability as a function of the hazard correlation length

In Figure 57 for the IEEE 39 case, the initially failed lines following a hazard event are compared with the number of finally failed lines after the cascading process in Figure 64 and Table 16. This comparison is performed for the case of independent component failure probabilities ($r \to 0$) and fully dependent component failure probabilities ($r \to \infty$). For the IEEE 118 case we find that with increasing correlation length, the variance of the number of initially failed lines increases. This effect is weaker for the finally failed lines. It is again observed that the expected number of finally failed lines increases slightly with decreasing correlation length and that the cascading failure process has the largest effect when just a few lines have failed initially, which is more probable with no or little dependence.

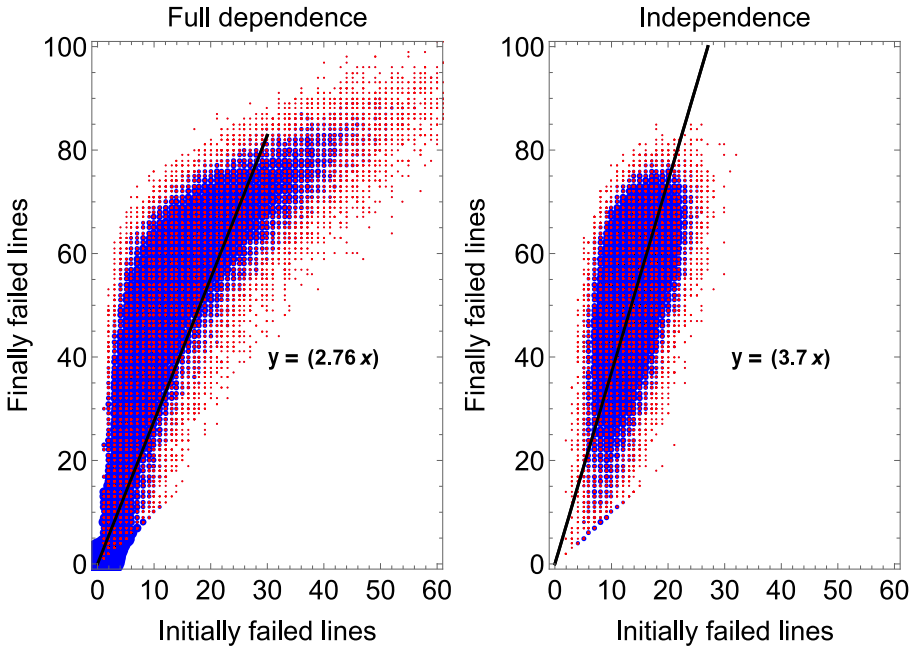

Figure 64: Finally versus initially failed lines for the case of independence (right) and full dependence (left); based on 10,000 samples with $\alpha = 1.5$; blue circles indicate the frequency of the data points in the sample space.

Table 16: Mean and standard deviation of the number of initially and finally failed lines; comparison of the independence and full dependence assumptions.

Failed lines	**Parameter**	**Independence** ($r \to 0$)	**Full dependence** ($r \to \infty$)
Initially	Mean	13.73	13.77
	Standard deviation	3.57	10.36
Finally	Mean	52.55	45.77
	Standard deviation	12.05	22.79

Means and standard deviations of the remaining load supply values $1 - L_{norm}$ are shown in Figure 65, as a function of the correlation length r and the tolerance parameter α. It is confirmed in this case study that the mean load supply values increase with the correlation length r in accordance with the effect shown in Figure 64, and in Figure 58 for the IEEE 39 test case: the cascading processes seem to be attenuated or not triggered at all, if either no line failures or by contrast, a larger number of line failures occur initially due to the influence of positive correlation. As compared to the IEEE 39 case, the effect of the correlation length on the mean values are less pronounced for medium α-values. This could be either due to a different and lower vulnerability of the IEEE 118 and also due to the different cascading failure model used in this case study. Changes in the mean and standard deviation occur mainly in the range 125 – 1200 km, which again corresponds to the order of

magnitude of the network size.

It needs to be underlined that the results are influenced by the way the lines are segmented. As mentioned before, considering the distributed nature of the lines, the failure probabilities of the individual lines would increase with decreasing correlation.

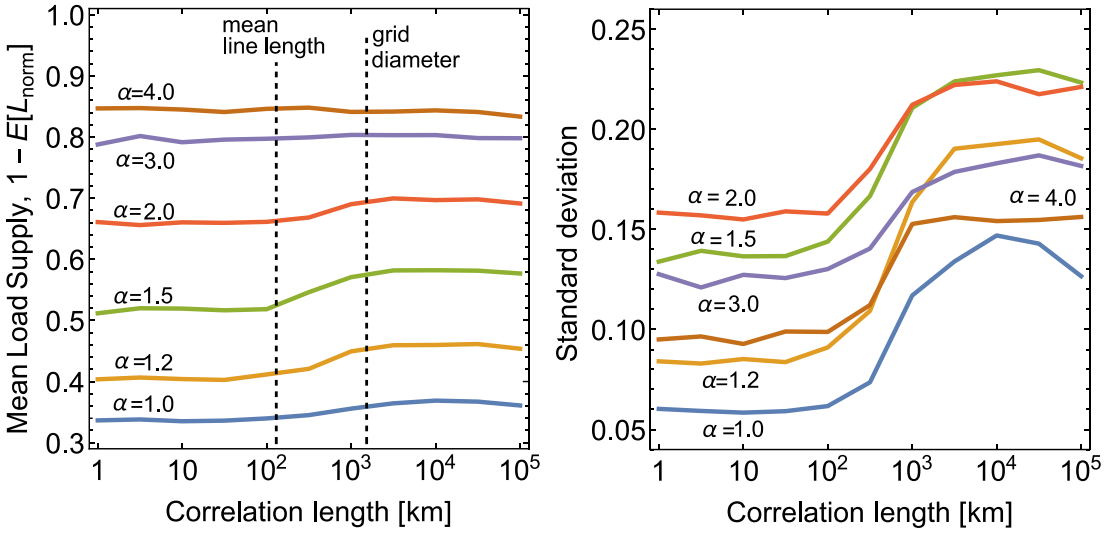

Figure 65: Network performance as function of the correlation length with varying α value. Left: mean overall power loss E[L_{norm}]; right: standard deviation of L_{norm}; based on 10,000 samples per correlation length value and α value combinations.

10.5.2 Network reliability based on (s-t)-connectivity probability

For comparative purposes, in this section the network reliability is assessed by the use of an alternative model while the overall assessment framework is taken over from the previous sections. Network reliability is evaluated based on the (s-t)-connectivity probability described in Section 5.2.2, which means that there is no consideration for cascading failure processes. Thus, we show in the following what difference it makes, if cascading failure processes are considered versus if they are neglected.

The network/system failure event is defined in the following as the disconnection of two prescribed, selected source (s) and target (t) nodes. For illustration purposes, the system failure event is defined to be the disconnection of the generator and load nodes 25 and 65 of the IEEE 118. Both nodes have relatively low *node degree* values. As above, the correlation length r of the generic hazard model is varied to investigate the effect of spatial correlation on reliability and IMs and system reliability, and IMs are evaluated with a Monte Carlo simulation with 10^4 samples.

In Figure 66 the system failure probability as a function of correlation length is shown.

The function is s-shaped, i.e. the system failure probability increases with increasing correlation length. This change of the reliability with correlation length is to be expected for a redundant system, in which correlation among components' failures leads to a reduction of effective redundancy and hence to an increase in system failure probability. For a non-redundant system, the opposite effect would be expected.

When comparing the results in Figure 66 to those in the previous section they show to be contradicting at a first glance. When the network is evaluated by applying the power flow based cascading failure model, the performance, and thus, reliability increases with spatial dependence. By contrast, the system reliability decreases, i.e. the system failure probability increases, with the spatial dependence if no cascading failure is accounted for. Thus, it has a discernible effect on the results, if one accounts for load redistribution and cascading failure events.

As above in Figure 65, the changes in the function occur within a range of the correlation length that corresponds to the lengths of individual lines up to the diameter of the study area. For smaller correlation lengths, the individual line reliabilities are approximately independent, whereas for correlation lengths significantly larger than the study area diameter, the line reliabilities are fully dependent.

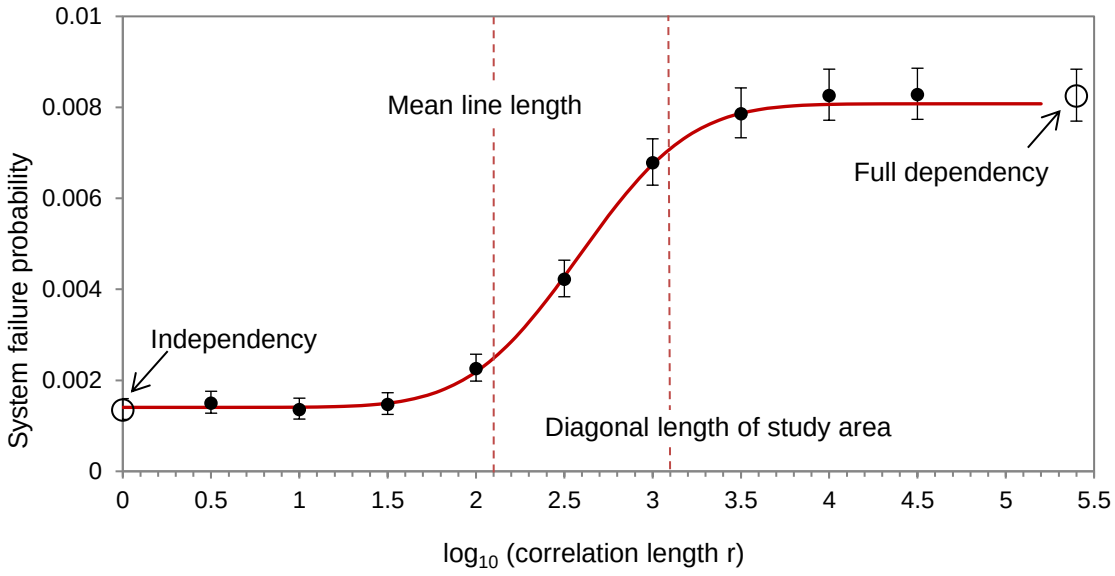

Figure 66: Dependence of the system failure probability on the correlation length of the spatial random field. Limiting cases are the failure probabilities of the system with independent components and with fully dependent components. The vertical bars show the 95% credible intervals from the MC sampling.

Note, that the results based on the (s-t)-connectivity probability are highly influenced by the choice of the source and target nodes. Their topological and spatial position in the network determines the number of possible cut set events that separate the two nodes. If, for example, a leaf node would be selected, the system failure probability would decisively

depend on the failure probability of the line connecting this leaf node.

10.5.3 Component importance rankings

First, the IMs are calculated based on the results in Section 10.5.1, i.e. similar as for the IEEE 39, the $CI^{(i)}, CI^{(c)}, LS^{(i)}$, and $LS^{(c)}$ are applied. Figure 67 visualizes the criticality importance (CI) with respect to initial failures ($CI^{(i)}$) and cascading failures ($CI^{(c)}$) for a correlation length of 3162 km. That the two rakings differ significantly shows that lines which are important for the initialization of network damage do not correspond to the lines that are responsible for the further propagation of cascading overloads in the IEEE 118.

The differentiation by the $CI^{(i)}$ ranking is comparably low compared to the differentiation by the $CI^{(c)}$ranking. Taking a closer look at Figure 67 reveals that those components outstanding in the $CI^{(c)}$ranking, are distinctively low ranked by the $CI^{(i)}$ ranking. Some of the highly ranked lines according to $CI^{(c)}$, are functioning as 'bridges' between connected larger network parts, e.g., this is the case for line connecting nodes 23 and 24 where node 24 is a rather important generator node. Generally, leaf lines are ranked as the least important ones, for initial as well as cascading failure.

In Figure 68, LS importance measures are summarized. It seems that long bypass lines that link network parts are highly ranked by the $LS^{(i)}$.

The important lines with respect to cascading failures, i.e. the $LS^{(c)}$ values, are more uniformly distributed in the network than for the $CI^{(c)}$; however, the two measures show an accordance in some of the rather highly ranked lines, e.g., lines connecting nodes 29 and 31, nodes 19 and 20, or nodes 23 and 24.

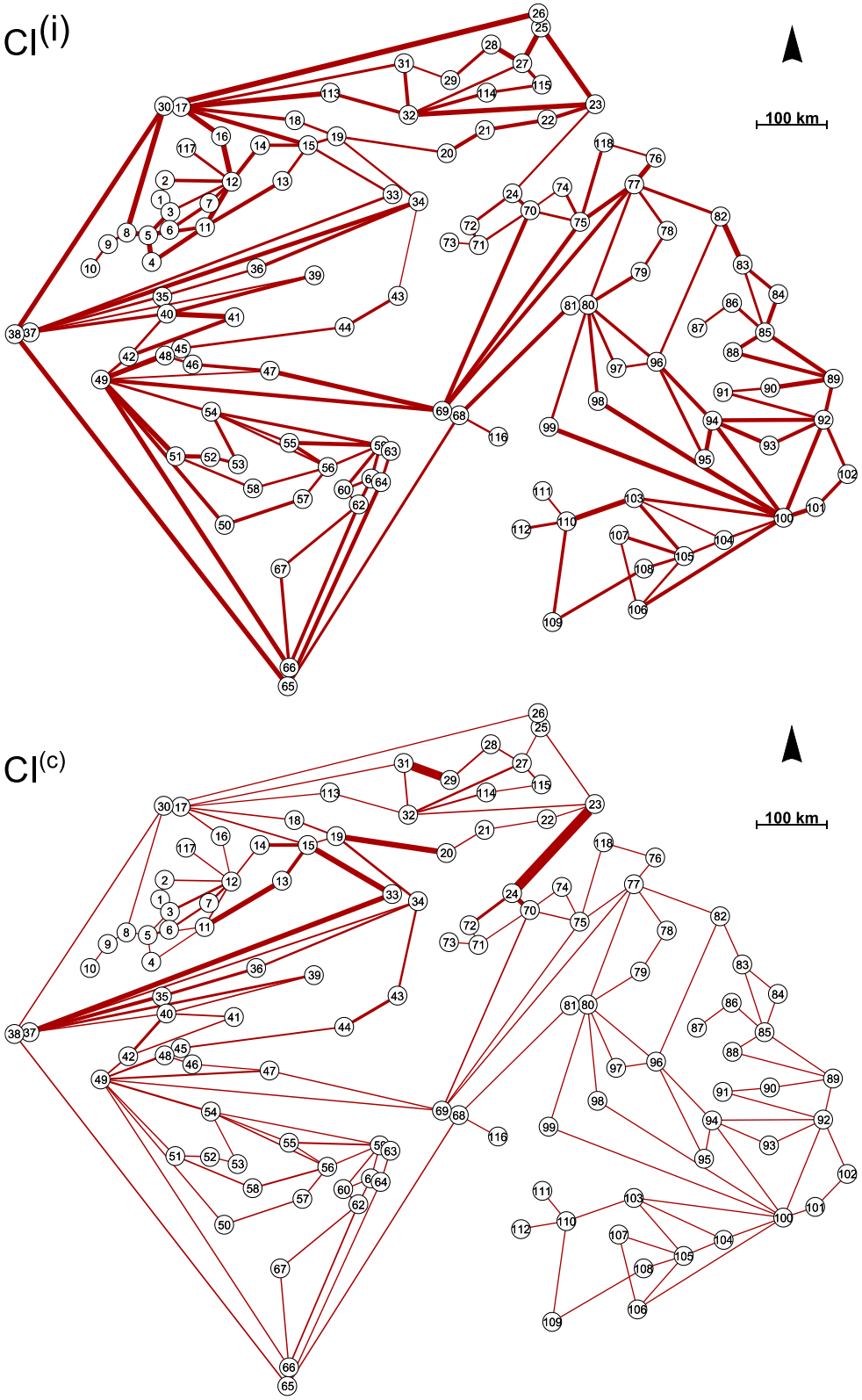

Figure 67: CI weighted graph at a correlation length of 3162 km. Up: $CI^{(i)}$ with respect to initial failures; Below: $CI^{(c)}$ with respect to cascading failures; with $\alpha = 1.5$ and $t_E = 0.9$; based on 10,000 samples.

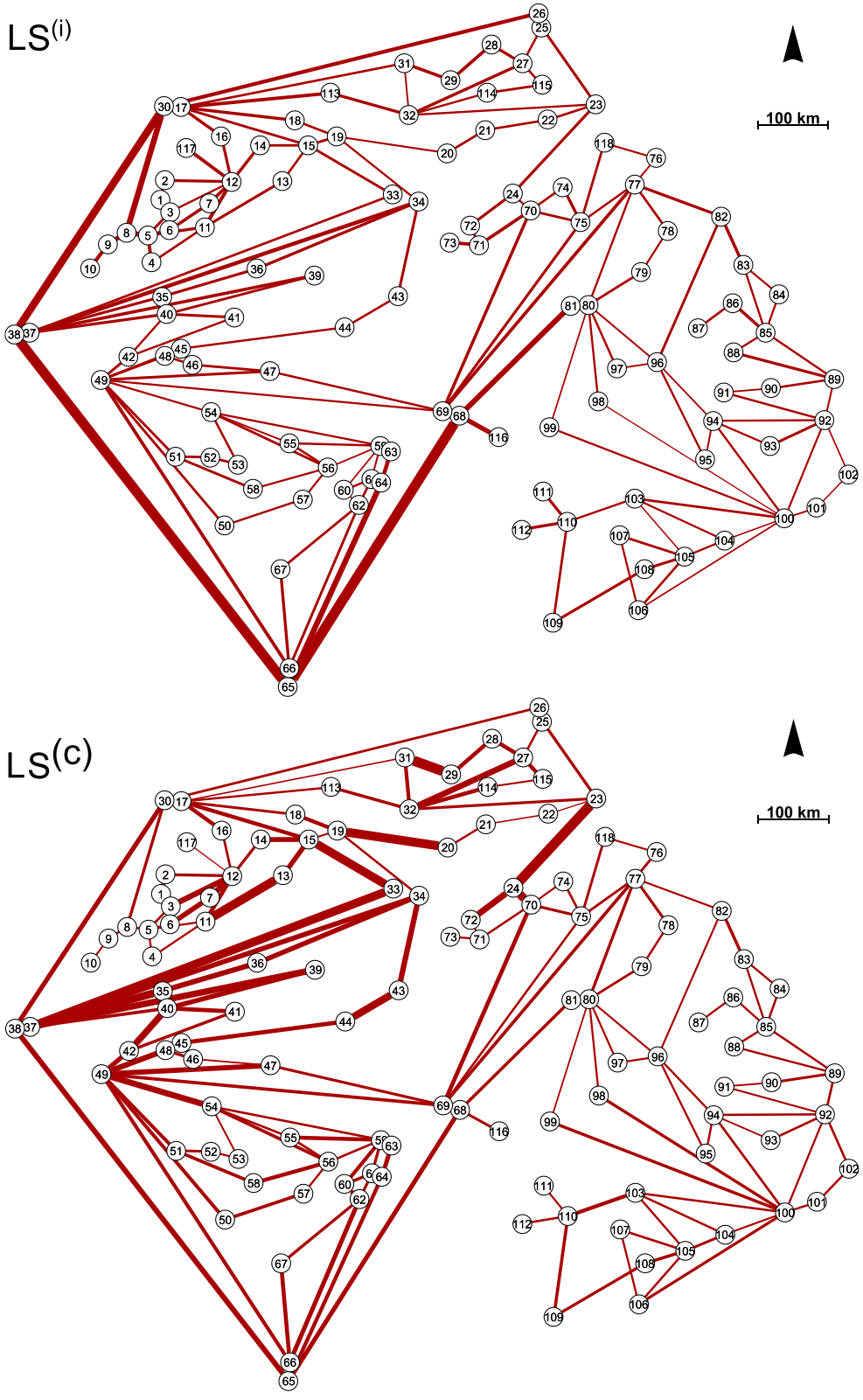

Figure 68: LS importance weighted graph at a correlation length of 3162 km. Left: $LS^{(i)}$ with respect to initial failures; right: $LS^{(c)}$ with respect to cascading failures; with $\alpha = 1.5$; based on 10,000 samples.

Figure 69 and Figure 70 show the effect of the hazard correlation length on CI and LS component importance rankings. While the absolute values of the IM change significantly with varying correlation length, the overall component rankings remain generally the same, especially in the composition of the highest and lowest ranked 10 to 20 lines. Figure 70 depicts the rankings based on $LS^{(i)}$ and $LS^{(c)}$. The pattern is similar to the one of CI, even though different lines are identified as the most important ones. The measure $LS^{(i)}$and $CI^{(i)}$ have one line in common that they rank most important, namely the line connecting node 38 and 65. The rankings of the most important components by $LS^{(c)}$ and $CI^{(c)}$ have even stronger agreement on the most important lines.

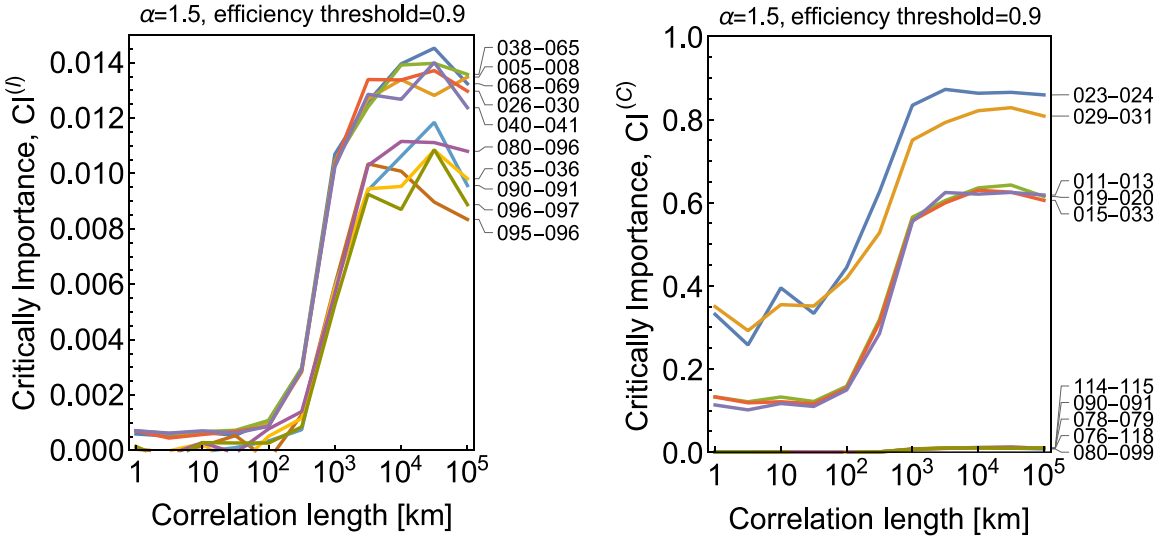

Figure 69: CI as function of correlation length. Left: $CI^{(i)}$ with respect to initial failures; right: $CI^{(c)}$ with respect to cascading failures; with $\alpha = 1.5$ and $t_L = 0.9$ each and based on 10,000 samples per correlation length value.

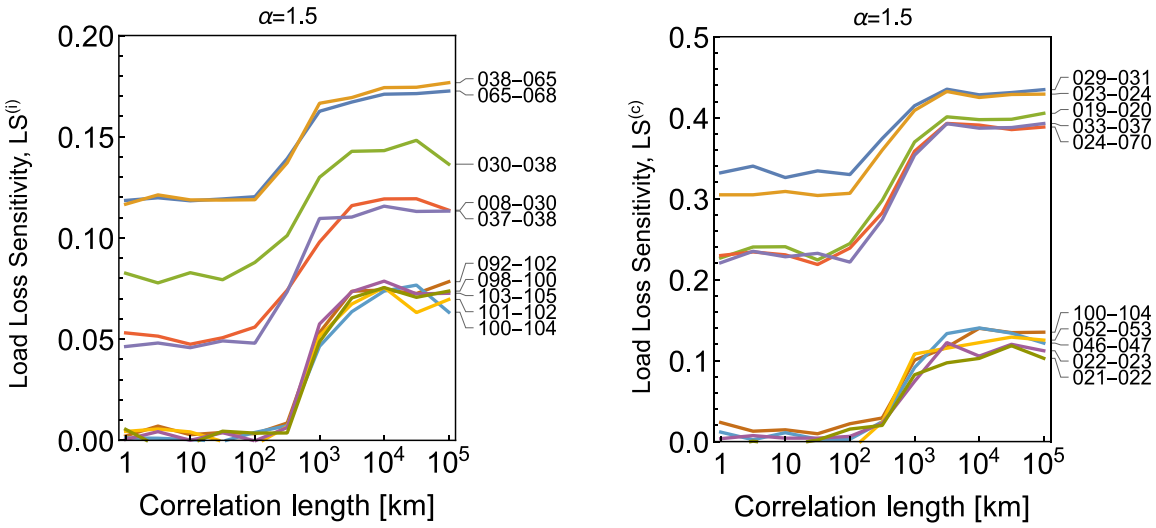

Figure 70: LS as function of correlation length. Left: $LS^{(i)}$ with respect to initial failures; right: $LS^{(c)}$ with respect to cascading failures; with $\alpha = 1.5$ each and based on 10,000 samples per correlation length value.

10.5.4 Comparison of component rankings

We compare the IM rankings obtained above to the betweenness index B_l as an example of a purely topological measure. $B_{l,w}$ is the number of shortest paths passing through a line as defined in Section 7.1.1 and as it has been calculated and used by Dwivedi et al. (2009) for the IEEE 118 system. Furthermore, the comparison is made with the CI measure obtained from the reliability assessment without cascading failure based on the (s-t)-connectivity problem in Section 10.5.2.

Table 17 gives an overview of the rankings based on CI for the 10 highest ranked lines. It can be seen that the rankings from the three different model concepts are rather different besides a few exceptions. E.g., line connecting nodes 38 and 65 occurs in several rankings while node 65 is a power generation station in the IEEE 118. The betweenness index does not take into account any deteriorations on the network, so, there is no inference concerning the actual damage that a line failure of high importance may cause. The (s-t)-connectivity concept is a purely topological approach that also delivers rather different results as when actual cascading processes are additionally taken into account.

Table 17: Comparison for the ten highest ranked lines according to $CI, CI^{(i)}, CI^{(c)}$ for the (s-t)-connectivity problem and the cascading failure model IEEE 118. Additional listing of the betweenness index as it is also given in Dwivedi et al. 2009. The results for the CI values are given for the correlation length value of 1000 km.

Deterministic measure (Dwivedi et al. 2009)	**(s-t)-connectivity**	**Cascading failure model**	
$B_{l,w}$	CI	$CI^{(i)}$	$CI^{(c)}$
65-68	23-25	38-65	19-20
38-65	25-27	5-8	15-33
30-38	26-25	68-69	11-13
68-81	26-30	26-30	33-37
80-81	23-24	12-16	24-70
8-30	38-65	40-41	14-15
17-30	42-49	92-93	43-44
65-66	30-38	64-65	35-37
5-8	34-43	45-49	24-72
49-66	19-34	49-69	40-42

It is emphasized, that each of the rankings shown here contain some uncertainties stemming from the modelling approaches. For each model individually, a rather detailed sensitivity analysis should be conducted to see how the rankings are affected by changes in model parameters (e.g., the power load threshold, the tolerance parameter α, the choice of the (s-t)-node pair). In order to measure the effect on the performance when IM rankings are used to improve components, the test of different enhancement strategies is conducted similar to Section 10.4.3 in the following.

10.5.5 Network reliability enhancement

Some network improvement strategies based on the proposed IMs are tested in the following, similar as in the case studies before, by measuring the effect of strengthening or increasing capacity of selected lines on the network performance of the IEEE 118 benchmark. Two network improvement strategies are considered:

1) Line strengthening of the 10 or 20 most important lines ranked by either $CI^{(i)}$ or $LS^{(i)}$, corresponding to an increase in the resistance against the hazardous (wind) load. Line strengthening is modeled by reducing the initial line failure probability to 10% or 1% of its original value. Results are compared to the case, when improvements would be based on the rankings from $CI^{(c)}$ or $LS^{(c)}$.

2) Increase of the line capacity of the 10 or 20 most important lines ranked by either $CI^{(c)}$ or $LS^{(c)}$, corresponding to an increase in the resistance of the lines against overloading in the cascading failure process. The capacity increase is modeled by increasing the tolerance parameter α by a factor of two. Results are compared to the case, when improvements would be based on the rankings from $CI^{(i)}$ or $LS^{(i)}$.

For the improvement strategy 1), the results are shown in Figure 71. Line strengthening according to $LS^{(i)}$ and $CI^{(i)}$ rankings lead to similarly increased mean power supply values over the variation of the correlation length even though the rankings of the two measures do not coincide in their respective highest ranked lines. Choosing the 10 most important lines and lowering their initial failure probability to 10% respectively, increases the final mean load supply percentage by about 4%. If the failure probability of 20 most important lines is set only 1%, this provides an improvement of about 6%. In all cases, the LS cuts the CI slightly out.

As it has been shown in Figure 63, choosing lines for strengthening following the $LS^{(c)}$ and $CI^{(c)}$ ranking, this does not significantly affect the system performance, highlighting the suitability of $LS^{(i)}$ and $CI^{(i)}$ rankings for prioritizing network components for strengthening against hazard impacts.

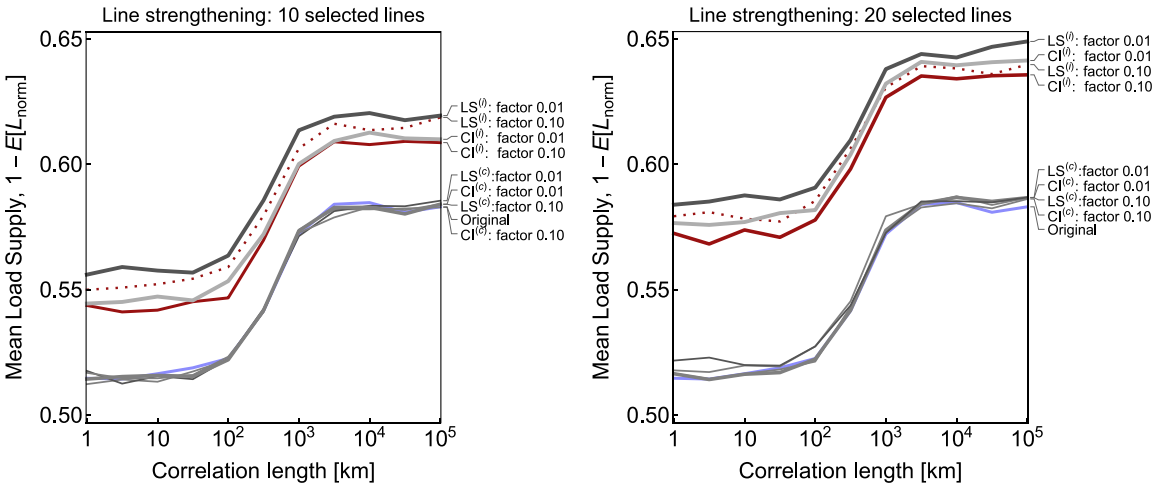

Figure 71: Mean load supply in function of correlation length for the line strengthening improvement strategy (decreasing the initial failure probability during the hazard event of 10 versus 20 selected lines; based on 10,000 samples. "Number of lines is more decisive than factor."

Figure 72 left shows the results received after the capacity values of 10 lines have been doubled. The line capacity improvement according to $LS^{(c)}$ and $CI^{(c)}$ brings overall slightly more improvements than the line capacity improvement according to $LS^{(i)}$ and $CI^{(i)}$. The difference becomes more distinct when in total 20 lines are selected for capacity increase, Figure 72 right: the effect on the network performance becomes the highest for $LS^{(c)}$ followed by $CI^{(c)}$.

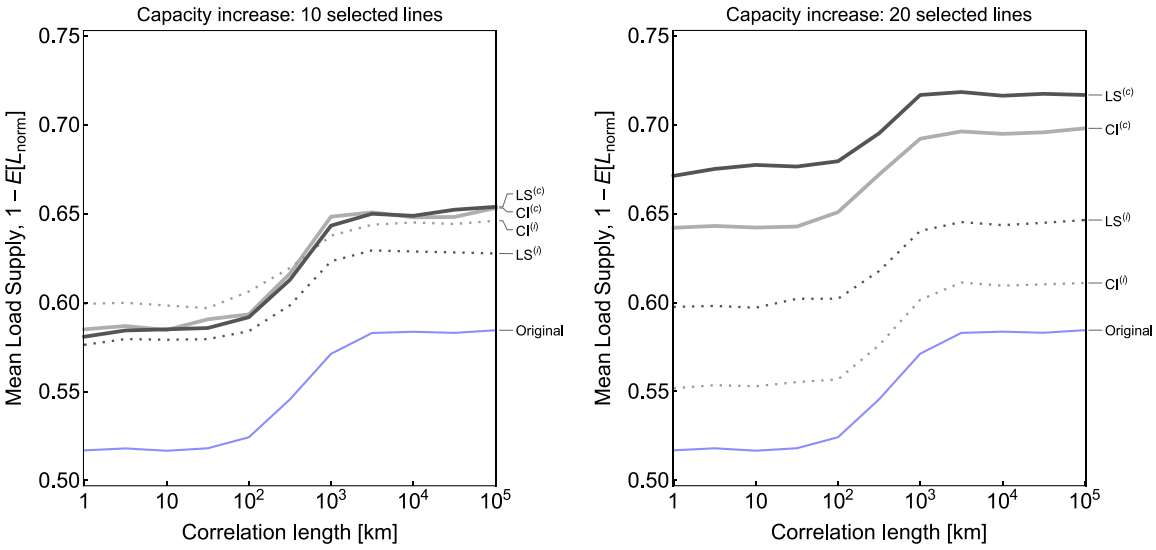

Figure 72: Mean load supply in function of correlation length for the capacity improvement strategy (increasing the line α parameter of 10 versus 20 selected lines by factor 2); based on 10,000 samples.

One interesting question for further research could be to dynamically / iteratively improve the system: i.e., improve the highest ranked line after a first analysis and component ranking and after that, reevaluate the system and identify the next most important component to improve under the changed conditions. It is still to find out, if this method could lead to a somewhat optimized improvement strategy.

10.6 Summary

The aim of this case study is an improved understanding of the importance of components in a network under large-scale spatially dependent hazards and internal cascading failure processes in the network. The two network performance models based on graph efficiency and power flow equations are applied, the former on the IEEE 39 and the letter on the IEEE 118.

The results indicate that the spatial correlation has a discernible influence on the system reliability and component importance measures. However, the component rankings are only mildly affected by the spatial correlation which indicates that component importance analysis can be performed without considering the spatial dependence explicitly. As Tanguy (2011) observes in his study on general CCF models and their influence on importance measures, adding CCF effects to the description of the IEEE system does not profoundly change the ranking of the lines when comparing to the independence assumption for all components. The results of this chapter indicate that this also holds for spatial

correlation effects under consideration of cascading failure processes. Note that in the analysis of a real system, the change in the mean failure rate with spatial location must be included, hence a detailed analysis of the hazard is nevertheless necessary and correlation cannot be omitted. The study shows that an increasing spatial dependence leads on average to smaller system failure events, if the mean failure rate in the lines is fixed and if it is accounted for cascading failure processes. In an experiment, where no cascading failure is modelled and accounted for, the system failure probability increases with spatial correlation.

The use of separate importance measures, considering on the one hand initial (triggering) component failures caused directly by the hazard event, and on the other hand cascading component failures, reflects the fact that different measures are necessary for increasing component reliability with respect to the two failure modes. Generally, the component importance rankings differ significantly between the two IM definitions. The importance of lines with respect to failures caused by the initial hazard is related to their initial capacity. The components that are of largest importance for the cascading process are lines with smaller capacity, which are located parallel to lines with the highest capacities. In both cases, the lines identified as the most important ones differ significantly from the ranking based solely on a topological measure such as the betweenness index shown in Table 17. An application of the proposed importance measures for selecting lines for strengthening or capacity increase shows that they can support defining network improvement strategies.

Part IV – Reflections

11 Discussion

The major findings are discussed in the following. Additionally, we address practical problems arising from the real world and consider to what extent solutions can be provided based on the methodology developed. Limitations of the adopted approaches and promising further research directions complement this chapter.

11.1 Interpretation of results

Dependencies in systems - is it relevant to consider the correlation observed in the spatial distributions of natural hazards and their effects?

One focus of this thesis is the implementation and the study of dependencies in system reliability analysis since it is well known ignoring correlation in statistical data and models may entail biased or misleading results. The externally triggered common cause failures (CCF) and the internal cascading failure effects are examined, as well as their impacts on the components' reliability and their influence on the overall system reliability.

The external sources for dependencies in a system repose on diverse factors. One source of dependencies are large scale natural hazards that show correlation, which means that a) components are affected simultaneously and, b) adjacent locations experience more similar hazard intensities than locations farther apart from each other. In this thesis it was attempted to learn if it is generally relevant to consider correlated natural hazard impacts in system reliability analysis, and if so, in which cases would this be of special interest and

importance? Internal sources for dependencies of failure probabilities are potential cascading failure effects of connected components in cases of load re-distributions following components' overload. Besides modeling aspects, a central question to answer is how to effectively realize the CCF concept in models for reliability analysis of networks? In this thesis, to this end, three different hazard modelling approaches are investigated in Chapters 8-10:

- a three-parametric hurricane wind field model based on information of selected hurricanes (Chapter 8),
- a spatial random field approach (SRF) based on historical European storm data (Chapter 9), and
- a generic SRF model for the hazard representation with a continuous scalability of the correlation length (Chapter 10).

The study on the Nordic electric power grid in Chapter 9 is the attempt to more realistically depict a real-world network exposed to hazards, i.e., the hazard simulation is based on real event and damage data.

In the investigations based on real-life hurricane or storm data in Chapter 8 and 9, the correlation structure in the data is fixed and its potential continuous influence as such cannot be investigated in detail. Therefore, in Chapter 10, a highly idealized but flexible hazard model is proposed and elaborated. In this way, it is possible to consistently and continuously control the correlation length parameter and thus examine the effect of a varying spatial dependence on particular component characteristics and on general network performance parameters. In this idealized context, it can be shown that the overall reliability is markedly affected by a variety of variables: In the absence of cascading effects, increasing correlation induces increased system failure probabilities, which may be explained by the interference of correlation and redundancy inherent in electrical power grids. On the other hand, when cascading is relevant, the system failure probabilities decrease with increasing spatial dependence. It is possible that overall system damage is attenuated due to increasing correlation: either too little initially failed components prevent triggering further increasing loss due to cascading faults, or, too much initial damage limits the further spread of failure due to less remaining intact components for the propagation of cascading failure.

The illustrative problems investigated in this thesis confirm that the spatial dependence should be explicitly considered if the correlation length of the hazard is in the range between the average lengths of the individual transmission lines and the diameter of the entire system. For smaller correlation lengths, the hazard can be modeled by independent failure probabilities, for larger correlation lengths, it can be modeled by fully dependent failure probabilities, which corresponds to classical common cause failure models. This insight could represent an essential benefit over current practice where network reliability is assessed without (simultaneously) accounting for correlated natural hazard impacts and cascading failure.

The reliability results are highly dependent on the choice of the network performance model and on the cascading failure model. In this regard, the appropriate degree of abstraction plays a major role. The larger the network, the more computationally expensive is the reliability assessment in general. In this thesis, different models have been implemented in order to depict the network performance in case of disturbances. Among these, the DC power flow model is the model with the lowest degree of abstraction among the selected performance models. However, some authors argue that one should generally aim at using AC power flow models for this type of analysis (e.g., Van Hertem et al., 2006, Vaiman et al., 2012, Li et al., 2017). The application of the present study framework, but alternatively with an AC power flow model as performance function, could be matter of future research. Overall it can be stated that if cascading failures are accounted for in the performance function models, they strongly influence the overall reliability results compared to the consequences of the initial component failures, especially against the backdrop of distinct spatial dependencies. In case of the DC power flow model, the overall reliability results are highly sensitive to a change in the tolerance parameter α, which determines the strength of cascading failure processes. However, for the study on the Nordic grid, the results in terms of power supply losses compare quite well to the order of magnitude of losses that have been found for historical large blackout events in those Nordic countries.

Component fragility - How to derive a valid model for the component fragility?

A novel calibration method for the fragility model is suggested based on requirements of the relevant structural codes. Design requirements derived from characteristic wind speeds in defined wind zones of the study area are calibrated with the observed line failure rate per km and per year to obtain wind zone specific component fragility curves. In Chapters 6 and 9, this fragility model is developed and implemented, respectively, in order to assess the performance of the power transmission grid of the European Nordic countries during large-scale windstorm events. It shows that the fragility model is an efficient solution, especially in case there is only little historical failure data available. Through our approach we circumvent the need to develop fragility models at the component level which is a distinctive feature of this study.

Note that future research should include additional types of component vulnerability, which is imparted by the impacts of further environmental hazards (other than windstorms) relevant in the investigated study area. Nevertheless, the fragility calibration procedure detailed and applied to wind storms in this thesis provides a generalizable framework: the modeling of the vulnerability of lines to storm events, might also be adopted in extended analyses.

Component importance and network improvement strategies

The further general aim of this thesis is an improved understanding and differential quantification of the relative importance of the components in a network under large-scale spatially dependent hazards and externally triggered failures as well as subsequent internal cascading failure processes in the network.

A main innovation of this thesis is that it addresses component reliability with respect to those two failure modes explicitly as they are specific for a system with potential cascading failure processes as a consequence of initially failed components. Thus, we introduced the use of separate importance measures, considering on the one hand initial (triggering) component failures caused immediately by the hazard event itself, and on the other hand by cascading component failures. By doing so, the framework enables to quantitatively distinguish between components that are most important for the primary initiation of a damaging cascading failure event and those that are relevant for the propagation of the subsequently induced failure events cascading into the remaining network. This differentiation can lead to efficient overall network improvement measures as discussed in the following.

A focus is laid on the importance measures CI (Critically Importance) and LS (Load loss Sensitivity) in Chapter 9 and 10. The importance of lines with respect to failures caused by the initial hazard events is related to their initial load capacity. On the other hand, there is a tendency that the components that are of largest importance for the cascading process and thus for the overall reliability, are those lines with smaller power load capacity, which are located parallel to lines with the highest capacities. In both of the cases (initial and cascading failures), the groups of lines identified as the most important ones differ significantly from each other as well as from highly ranked line groups based solely on topological measures, such as for example the betweenness index.

An application of the proposed importance measures for selecting power lines for strengthening against initial failure or capacity increase demonstrated their suitability for defining network improvement strategies. Two main network improvement strategies are considered: (a) increasing the resistance against wind storms of selected line segments and (b) increasing the line capacity of selected lines. In several case studies it is assessed which component rankings perform best with respect to an increase in the overall performance, which refers, e.g., to a decrease in the overall loss of load caused by wind storm events. For example, in the study of the Nordic grid, for both strategies, the two IMs applied (CI and LS) perform similarly well with a decrease in loss of load approximately between 35% to almost 50%. The reliability can be increased significantly by either lowering the initial failure probability of components selected based on 'initial' IMs (e.g., $CI^{(i)}$, $LS^{(i)}$) or by increasing the line capacity of components selected based on 'cascading' IMs (e.g., $CI^{(c)}$, $LS^{(c)}$). The improvement potential is observed to depend strongly on the tolerance parameter α of the cascading failure model. We also find that the commonly used $(n-1)$-contingency analysis leads to a good although no optimal ranking of components

for implementing improvement strategy (b).

Finally, we addressed the question how a varying correlation length of spatially distributed hazard intensities might affect component importance rankings. The results indicate that the spatial correlation has a discernible influence on the absolute values of the component importance measures. However, and in contrast to the network reliability, none of the investigated component importance rankings showed to be significantly affected by the dependence structure of the spatial random fields (Chapter 10). The component importance rankings were found to be similar for any fixed correlation length value, which has already been stated by Tanguy (2011) in his study on general CCF models and their influence on importance measures. Thus, it is concluded, that component importance analysis can be performed without considering the spatial dependence explicitly. Nevertheless, in the analysis of a real-world system, the change in the mean failure rate with spatial location of the components must be included. Hence, a detailed analysis of the hazard is nevertheless necessary for exposed systems in any case.

11.2 Limitations and future research

The main focus of this work is the inclusion of a system failure model within a hurricane simulation context. Our methods are a contribution to a fast, preliminary reliability assessment for large real-world infrastructure networks. The methods help to understand the importance of components in the system under large-scale spatially dependent hazards and internal cascading failure processes in the network. We suggest a number of generalized, yet efficient network improvement strategies. Generally, the results of this study can built the basis for a further in depth analysis of individual real-world systems and, therefore, be a contribution to current analysis methods in industry practise.

However, in the analysis of a real system, one would have to specify mainly a) the hazard model, and b) the system (performance) model with regard to the specific local conditions in order to draw binding assumptions and recommendations for the individual case. The analysis in this thesis with its illustrative case studies is limited by simplifying assumptions made on the network representations, the performance models, and the concerned hazard (intensity) representations. There are numerous modelling alternatives that could be addressed in more detail: Variations in the hazard modelling, uncertainties in the component fragility modelling, and a variety of possible supplementary network performance concepts. In many modelling features, additional appropriately specified and quantified uncertainties may be added to the approaches propagated in this thesis.

The power grid models of this thesis are analyzed on a system level rather than on a component level. Since the focus is on the impact of the spatially dependent failures and the

spatial variation of the correlation of the component failure probabilities, spatially correlated failure probabilities are included in the models. However, all further specific component characteristics such as type, material, and age are not investigated in detail but rather globally modeled by fragility curves and corresponding exposure dependent failure probabilities. The results can give some indication of how the network reliability behaves in the face of hazard events with spatially dependent intensity distributions. The reported findings can be seen as important preconditions for refined analyses: hazardous impacts on systems, system reliability, as well as component failure probability and importance are analyzed. These results are the base for a subsequent calculation of the expected risk, e.g., the yearly damage in monetary terms.

A potential optimization of improvement strategies for a specific real-world infrastructure should be based on a full cost-benefit analysis, which would contain the (approximate) relative costs of the different mitigation strategies compared to the relative costs due to power outages. Improvement and mitigations strategies would be compared with regard to their specific costs and benefits as well. This means that the costs and efforts, e.g., for the strengthening of components with regard to their wind load resistance should be compared to the costs for exchanging components aiming at higher line capacity values. An upgrade of an infrastructure could also consist of a combination of the proposed improvement strategies and it could be the objective of future research whether this could be even more effective than using one single mitigation strategy. Finally, this could lead to a decision support and a life-cycle analysis of potential investment strategies for practitioners, e.g., Transmission System Operators (TSO).

For the goals of this thesis, the Monte Carlo Simulation (MCS) approach showed to be a sufficient method to answer the given research questions. However, once one would increase the complexity of the applied models, one would have to consider alternatives to the direct MCS, i.e., more efficient simulation methods considered and characterized in some detail in Section 5.5.2.2 of this work.

The IMs, as they are used in this thesis, build upon point estimates of the (un-) reliabilities that go into the respective equations. Therefore, error-propagation methods might be interesting and useful that build on interval estimates rather than on point estimates. There exists a further branch of research on so-called uncertainty importance measures, e.g., Borgonovo (2007) and Aven and Nøkland (2010) that could potentially extend the methodology and add to the results of this thesis.

For future research, the following developments in addition to those already mentioned could be of interest:

- Adjustment of the network model for more detailed and specific component characteristics and fragilities for a given study area and network infrastructure, e.g., in collaboration with concerned TSOs.

- More complete risk analysis and risk assessment, e.g., by including the social-economic consequences associated with power outages/ network damages: This implies, e.g., the consideration of critical assets and industries and the population density and social vulnerability. The inclusion of percentages of households and the amount of businesses without power after a disruptive event would enable complete cost quantification dependent on outage localization and size. Eventually, this further entails the consideration of the interplay of the power infrastructure with other critical civil and communication infrastructures like traffic, water, telecommunication, and internet networks, as it has been suggested by e.g. Kim et al. (2012); see also Wang et al. (2012) and Pant et al. (2014).

- A multi-hazard analysis including the effects of additional hazard types, which often accompany extreme winds like storm surge, precipitation, icing, and debris flow.

- Model extension by including repairable systems and the recovery time of components during and after a hazard event: Likewise, selected operational counter-actions (e.g. intentional load shedding for damage mitigation) could be included in the network performance modelling.

- Further development and refinement of the network improvement scenarios by adjusting the strategies to the actual societal needs and economic conditions of an infrastructure network.

- In depth comparisons among the different and diverse component importance measures in literature: Among all options a comparison of the IMs in this thesis to the mentioned DIM by Borgonovo and Apostolakis (2001) could be of interest.

12 Conclusion

This thesis is a contribution to the field of network reliability analysis. A special focus is on the problem of dependent network component failures and their effect on the overall system reliability. In a narrower sense, this work deals with infrastructure networks subject to natural hazard impacts. The case studies are dedicated to large-scale power transmission systems exposed to extreme wind loads. Both, the spatially dependent initial component failures and the potential subsequent failures in cascading processes in the networks are modelled. Special emphasis is on an efficient software implementation based on Monte Carlo simulation.

Three different hazard modelling approaches are developed and implemented: A parametric hurricane wind field, a spatial random field based on historical European wind storms, and a generic spatial random field. The latter generic random field allows the detailed assessment of the impact of the correlation length, which characterizes the underlying random fields, on reliability and importance measures. The wind fields are mapped to fragility curves to simulate component failure. The serviceability of the potentially degraded network is investigated employing different network performance models and measures, such as graph efficiency and a physically-based DC power flow.

Concerning the dependencies in the component failures, it is observed that the spatial correlation has a discernible influence on the system reliability. This leads to the conclusion that the adequate modelling of network reliability requires the consideration of spatial dependence in the hazard: Ignoring significant correlation may entail biased parameter estimates and invalid statistical inference, e.g. wrong confidence limits for system reliability estimates. More specifically, it has been found that the spatial dependence should be considered explicitly if the correlation length of the hazard is in the range between the average lengths of the individual lines to the diameter of the entire system because in this

interval the main shifts in the reliability values occur. For smaller correlation lengths, the hazard can be modelled by independent failure events, for larger correlation lengths, it can be modelled by fully dependent failure probabilities, corresponding to classical common cause failure models.

The interplay between external common cause failures (CCF) and cascading failure decisively affects the system reliability. It shows that if the cascading effects are considered in the model, an increasing spatial correlation in the initial component failures leads to an increase in the system reliability. However, it is observed that different network performance measures (e.g. with versus without cascading models) will deliver rather different findings. Therefore, results should be interpreted with caution and with having the model assumptions in mind.

One challenge in the field is few or missing data on failure events due to wind loads for determining fragility curve models. A new parameter calibration method is suggested in order to circumvent the lack of data about component failures in extreme wind events. The consideration in this thesis is that the infrastructure equipment, here transmission lines, are constructed to meet design requirements based on the corresponding characteristic wind speeds in the respective study region. A second input concerning the hazard is overall historical statistics on line failure events in the Nordic countries received from concerned TSOs. The method allows derivation of fragility models directly for transmission line segments including many components.

The quantification of the importance of single components in a network under large-scale spatially dependent hazards and internal cascading failure processes is a further main goal of this thesis. Therefore, modified reliability importance measures (IMs) are introduced and studied in detail, also for the more general case of a non-binary system reliability/failure definition: Efficiency sensitivity (ES) and load loss sensitivity (LS). Results are compared to selected classical IMs: Criticality Importance (CI) and Birnbaum Measure (BM). Moreover, IMs are suggested that differentiate between components that failed directly by the hazard event and that are important for the initiation of cascading failure events (e.g. $ES^{(i)}$) versus components that failed in the cascading process and that are important for the further propagation of failure events in the system (e.g. $ES^{(c)}$). Our results show that the component importance rankings depend significantly on the IM definitions, e.g. rankings differ about the initial versus cascading failure events. Moreover, the lines identified as the most important ones differ significantly from the ranking based on a topological measure such as the betweenness index. It is observed that with a varying correlation length of the spatial random wind field model, the rankings of the components are only mildly affected. Although, the absolute values of the IMs are strongly affected as is the absolute value of the system reliability.

Building on the suggested IMs, it is investigated how they can serve for efficient network reliability enhancement strategies and help finding methods to lower the network damages in hazard events. Improvement strategies such as line failure probability decrease, or line

overload capacity increase are tested. In both cases, the overall loss of load or loss of graph efficiency could be strongly lowered.

In general, the developed methods and the findings of this thesis can support the design phase or the post hazard decision making of city planners, public officials, and utility owners. The results provide indications on how to rebuild and repair the network more efficiently by identifying critical components in networks exposed to correlated failures.

Abbreviations

AC	Alternating Current
ASCE	American Society of Civil Engineers
AUC	Area under Curve
BM	Birnbaum Measure
CCF	Common Cause Failure
CDF	Cumulative Density Function
CI	Criticality Importance
DC	Directed Current
DIM	Differential Importance Measure
DNV GL	Det Norske Veritas Germania Loyd
ES	Efficiency Sensitivity
EU	European Union
FEMA	Federal Emergency Management Agency (USA)
FV	Fussel-Vesely Importance Measure
GIS	Geographic Information System
HAZUS (-MH)	Geographic information system-based natural hazard analysis tool developed by FEMA; where MH stands for Multi-Hazard
HV	High Voltage
HWind	Project by NOAA about surface wind analysis of tropical cyclones
IEEE	Institute of Electrical and Electronics Engineers
IM	Importance Measure
IS	Importance Sampling
LHS	Latin Hypercube Sampling
LS	Load Loss Sensitivity
MATCASC	MATLAB tool for cascading failure modelling
MATLAB	Software for the calculation and programming on matrices and other data structures
MATPOWER	MATLAB tool for power systems modelling
MCS	Monte Carlo Simulation
NOAA	National Oceanic and Atmospheric Administration
PDF	Probability Density Function
PGA	Peak ground acceleration
PMF	Probability Mass Function
PMU	Phasor Measurement Unit
PRA	Probabilistic Risk Assessment
RAW	Risk Achievement Worth
RBD	Reliability Block Diagram

ROC	Receiver Operating Characteristic (curve)
RRW	Risk Reduction Worth
RTS	Reliability Test System
RV	Random Variable
SRF	Spatial Random Field
SSHWS	Saffir-Simpson hurricane wind scale
SuS	Subset Simulation
TSO	Transmission System Operator
US	United States
XWS	Extreme European Wind Storm Catalogue

Nomenclature

Important notations

$G(N, L)$	Graph object
$N = \{n_1, \dots, n_n\}$	Set of n nodes of a graph G
$L = \{l_1, \dots, l_l\}$	Set of l lines of a graph G
$\boldsymbol{A} = \{a_{ij}\}$	Adjacency matrix of a graph G; with a_{ij} being weights assigned to the lines
X_S	System state variable, with $x_S \in \{0,1\}$
X_{l_i}	Component state variable
$\boldsymbol{x_l} = \left[x_{l_1}, x_{l_2}, \dots, x_{l_l}\right]^T$	l-tuple component state vector, with $x_{l_i} \in \{0,1\}$
$p_S = \Pr(X_S = 1)$	System reliability
$p_F = \Pr(X_S = 0)$	System failure probability $(1 - p_S)$
$p_{l_i} = \Pr(X_{l_i} = 1)$	Component (line) reliability
$p_{f,i} = \Pr(X_{l_i} = 0)$	Component (line) failure probability
$\phi(\boldsymbol{x_l})$	System structure function
$\tau(\boldsymbol{x_l})$	System performance function
q_k	Probability of component state vector k
n_{MC}	Number of MC simulations
p_{MC}	MC estimate of the system reliability
$e_{ij} = \frac{1}{\pi_{ij}}$	Line efficiency, of line between nodes i and j with π_{ij} being the line reactance
δ_{ij}	Shortest path/ shortest electrical distance between nodes i and j
$E(G)$	Overall graph efficiency
$E_{norm} = \frac{E(G_{damaged})}{E(G)}$	Normalized graph efficiency of a damaged graph $G_{damaged}$
$C_{ij} = \alpha_{ij} L_{ij}(0)$	Line capacity, with initial line load $L_{ij}(0)$

α_{ij}	Line tolerance parameter
t_E	Threshold for the system failure definition based on the overall graph efficiency or loss of load
π_{ij}	Line reactance
b_{ij}	Line susceptance
f_{ij}	Line active flow
P	Net active power injections at nodes $1, \dots, N$, equal to the product of the susceptance matrix **B** and voltage phase angles $\boldsymbol{\theta}$.
$\mathrm{L_{norm}}$	Normalized Loss of load of a damaged power grid
D_x	Component damage state
s	Wind speed [m/s]
r_{max}	Distance between maximum wind speed and hurricane eye
s_{max}	Maximum wind speed
ω	Offset parameter in hurricane model
λ_S	Hazard occurrence rate (e.g. Poisson parameter)
$C_Z(h)$	Covariance function
h	Distance between locations (line segment mid-points)
r	Correlation length
Σ_{ZZ}	Covariance matrix
LL_{n-1}	Load Loss according to $(n-1)$-contingency analysis
$B_{l,w}$	Line betweenness index in a weighted graph
$B_{l,uw}$	Line betweenness index in an unweighted graph
$CI^{(i),(c),(f)}$	Criticality importance *(initial, cascading, final)*
$BM^{(i),(c),(f)}$	Birnbaum measure *(initial, cascading, final)*
$ES^{(i),(c),(f)}$	Efficiency sensitivity *(initial, cascading, final)*
$LS^{(i),(c),(f)}$	Load loss sensitivity *(initial, cascading, final)*

List of Figures

List of Tables

Literature

ADACHI, T. 2007. *Impact of Cascading Failures on Performance Assessment of Civil Infrastructure Systems.* PhD thesis, Georgia Institute of Technology.

AGARWAL, P. K., EFRAT, A., GANJUGUNTE, S. K., HAY, D., SANKARARAMAN, S. & ZUSSMAN, G. Network vulnerability to single, multiple, and probabilistic physical attacks. Military Communications Conference, Milcom 2010, Oct 31-Nov 3 2010. 1824-1829.

AIGNER, M. 1984. *Graphentheorie - Eine Entwicklung aus dem 4-Farben Problem*, Springer.

ALBERT, R. & BARABÁSI, A.-L. 2002. Statistical mechanics of complex networks. *Reviews of Modern Physics,* 74**,** 47-97.

ALLEN, T. M., NOWAK, A. S. & BATHURST, R. J. 2005. Calibration to Determine Load and Resistance Factors for Geotechnical and Structural Design. *Transportation Research Circular E-C079.* Washington, D.C.: Transportation Research Board.

ANDREASSON, M., AMIN, S. & JOHANSSON, K. H. 2011a. Correlated Failures of Power Systems: Analysis of the Nordic Grid. *Workshop on Foundations of Dependable and Secure Cyber-Physical Systems (FDSCPS).* Chicago, Illinois.

ANDREASSON, M., AMINY, S., SCHWARTZ, G., JOHANSSON, K. H., SANDBERG, H. & SASTRY, S. S. 2011b. Correlated Failures of Power Systems: Analysis of the Nordic Grid; http://people.kth.se/~mandreas/publication/pdf/masterthesis.pdf.

ARIANOS, S., BOMPARD, E., CARBONE, A. & XUE, F. 2009. Power grid vulnerability: A complex network approach. *Chaos,* 19**,** 013119.

ATHAY, T., PODMORE, R. & VIRMANI, S. 1979. A Practical Method for the Direct Analysis of Transient Stability. *IEEE Transactions on Power Apparatus and Systems,* PAS-98**,** 573-584.

AU, S.-K. & BECK, J. L. 2001. Estimation of small failure probabilities in high dimensions by subset simulation. *Probabilistic Engineering Mechanics,* 16**,** 263-277.

AVEN, T. & NØKLAND, T. E. 2010. On the use of uncertainty importance measures in reliability and risk analysis. *Reliability Engineering & System Safety,* 95**,** 127-133.

BALL, M., O. & COLBOURN, C., J. 1992. Network Reliability. *Technical Research Report.* Systems Research Center.

BALL, W. W. R. & COXETER, H. S. M. 2010. *Mathematical Recreations and Essays*, Dover Publications.

BATTS, M. E., CORDES, M.R., RUSSELL, L.R., SHAVER, J.R., SIMIU, E., 1980. Hurricane wind speeds in the United States. US Department of Commerce

National Bureau of Standards.

BEDFORD, T. & COOKE, R. 2001. *Probabilistic Risk Analysis: Foundations and Methods.*, Cambrige University Press.

BÉRENGUER, C., DIEULLE, L., GRALL, A. & VASSEUR, D. 2006. Études de sensibilité, facteurs d'importance et défaillances de cause commune *Journal Européen des Systèmes Automatisés,* 40**,** 763-785.

BERNSTEIN, A., BIENSTOCK, D., HAY, D., UZUNOGLU, M. & ZUSSMAN, G. Power grid vulnerability to geographically correlated failures - Analysis and control implications. IEEE Conference on Computer Communications, April 27 - May 2 2014. 2634-2642.

BILLINTON, R. & JONNAVITHULA 1997. Composite system adequacy assessment using sequential Monte Carlo simulation with variance reduction techniques. *IEE Proceedings - Generation, Transmission and Distribution,* 144**,** 1-6.

BIROLINI, A. 2007. *Reliability Engineering : Theory and Practice* Berlin Springer.

BOMPARD, E., NAPOLI, R. & XUE, F. 2009. Analysis of structural vulnerabilities in power transmission grids. *International Journal of Critical Infrastructure Protection,* 2**,** 5-12.

BORGONOVO, E. 2007. A new uncertainty importance measure. *Reliability Engineering & System Safety,* 92**,** 771-784.

BORGONOVO, E. & APOSTOLAKIS, G. E. 2001. A new importance measure for risk-informed decision making. *Reliability Engineering & System Safety,* 72**,** 193-212.

BÖTTCHER, C. 2016. *The cost of blackouts in Europe* [Online]. RAIN Project. Available: http://rain-project.eu/cost-blackouts-europe/ [Accessed June 01 2016].

BRATLØV, A. May 15 2017. *RE: Personal communication with 'Energinet'.*

BRUCH, M., MÜNCH, V., AICHINGER, M., KUHN, M., WEYMANN, M. & GERHARD, S. 2011. Power Blackout Risks - Risk Management Options. *Emerging Risk Initiative - Position Paper* CRO Forum.

BRUMMITT, C. D., D'SOUZA, R. M. & LEICHT, E. A. 2012. Suppressing cascades of load in interdependent networks. *Proceedings of the National Academy of Sciences,* 109**,** E680-E689.

CADINI, F., ZIO, E. & PETRESCU, C.-A. Using Centrality Measures to Rank the Importance of the Components of a Complex Network Infrastructure. *In:* SETOLA, R. & GERETSHUBER, S., eds. Critical Information Infrastructure Security: Third International Workshop, CRITIS 2008, Rome, Italy, October13-15, 2008. Revised Papers, 2009// 2009 Berlin, Heidelberg. Springer 155-167.

CASCIATI, F. & FARAVELLI, L. 1991. *Fragility analysis of complex structural systems,* New York, N.Y., Taunton, Angleterre : J. Wiley and Sons, Research Studies Press.

CAVALIERI, F., FRANCHIN, P., BURITICÁ CORTÉS, J. A. M. & TESFAMARIAM, S.

2014. Models for Seismic Vulnerability Analysis of Power Networks: Comparative Assessment. *Computer-Aided Civil and Infrastructure Engineering,* 29**,** 590-607.

CEN 1991. EN 1991-1-4: Wind actions. Brussels.

CHEN, G., DONG, Z. Y., HILL, D. J., ZHANG, G. H. & HUA, K. Q. 2010. Attack structural vulnerability of power grids: A hybrid approach based on complex networks. *Physica A: Statistical Mechanics and its Applications,* 389**,** 595-603.

CHEOK, M. C., PARRY, G. W. & SHERRY, R. R. 1998. Use of importance measures in risk-informed regulatory applications. *Reliability Engineering & System Safety,* 60**,** 213-226.

CHRISTIE, R. 2000. Power Systems Test Case Archive. Washington: Electrical Engineering Department, University of Washington.

CIGRÉ WG B2.28 2015. TB 645: Meteorological Data and Analyses for Assessing Climatic Loads on OHLs.

COLBOURN, C. J. 1987. *The Combinatorics of Network Reliability,* New York, Oxford University Press.

CRUCITTI, P., LATORA, V. & MARCHIORI, M. 2004a. Model for cascading failures in complex networks. *Physical Review E,* 69**,** 045104.

CRUCITTI, P., LATORA, V. & MARCHIORI, M. 2004b. A topological analysis of the Italian electric power grid. *Physica A: Statistical Mechanics and its Applications,* 338**,** 92-97.

CRUCITTI, P., LATORA, V. & MARCHIORI, M. 2005. Locating Critical Lines in High-Voltage Electrical Power Grids. *Fluctuation and Noise Letters,* 05**,** L201-L208.

CRUCITTI, P., LATORA, V., MARCHIORI, M. & RAPISARDA, A. 2003. Efficiency of scale-free networks: error and attack tolerance. *Physica A: Statistical Mechanics and its Applications,* 320**,** 622-642.

CRUSE, T. A. 1997. *Reliability-based mechanical Design*, CRC Press.

DAEMI, T. & EBRAHIMI, A. 2012. Evaluation of Components Reliability Importance Measures of Electric Transmission Systems Using the Bayesian Network. *Electric Power Components and Systems,* 40**,** 1377-1389.

DAEMI, T., EBRAHIMI, A. & FOTUHI-FIRUZABAD, M. 2012. Constructing the Bayesian Network for components reliability importance ranking in composite power systems. *International Journal of Electrical Power & Energy Systems,* 43**,** 474-480.

DAQING, L., YINAN, J., RUI, K. & HAVLIN, S. 2014. Spatial correlation analysis of cascading failures: Congestions and Blackouts. *Scientific Reports,* 4.

DELGADILLO, A., ARROYO, J. M. & ALGUACIL, N. 2010. Analysis of Electric Grid Interdiction With Line Switching. *IEEE Transactions on Power Systems,* 25**,** 633-641.

DER KIUREGHIAN, A. & SONG, J. 2008. Multi-scale reliability analysis and updating of complex systems by use of linear programming. *Reliability Engineering and System Safety,* 93**,** 288-297.

DIJKSTRA, E. W. 1959. A note on two problems in connexion with graphs. *Numerische Mathematik,* 1**,** 269-271

DOBSON, I., CARRERAS, B. A. & NEWMAN, D. E. 2001. An Initial Model for Complex Dynamics in Electric Power System Blackouts. *Hawaii International Conference on System Sciences.* Maui, Hawaii: IEEE.

DONGWEI, W., DA HUO, GUIQING, L. & YIANYIAN, C. 1996. Reliability Analysis of Lifline Networks with Vertex and Correlation Failures. *Eleventh World Conference on Earthquake Engineering.* Acapulco, Mexico: International Association for Earthquake Engineering.

DUEÑAS-OSORIO, L. 2005. *Interdependent Response of Networked Systems to Natural Hazards and Intentional Disruptions.* PhD thesis, Georgia Institute of Technology.

DUEÑAS-OSORIO, L. & VEMURU, S. M. 2009. Cascading Failures in Complex Infrastructure Systems. *Structural Safety,* 31**,** 157-167.

DUNN, S., GALASSO, C., WILKINSON, S., MANNING, L. & ALDERSON, D. Development of Empirical Fragility Curves for Electrical Supply Systems Subjected to Wind Hazard. 12th Intern. Conf. on Applications of Statistics and Probability in Civil Engineering, 2015 Vancouver.

DWIVEDI, A., YU, X. & SOKOLOWSKI, P. Identifying vulnerable lines in a power network using complex network theory. IEEE International Symposium on Industrial Electronics, 5-8 July 2009. 18-23.

ELKRAFT SYSTEM 2003. Strømafbrydelsen i Østdanmark og Sydsverige 23. September 2003. Ballerup.

ELLINGWOOD B., R., ROSOWSKY D., V., LI, Y. & KIM JUN, H. 2004. Fragility Assessment of Light-Frame Wood Construction Subjected to Wind and Earthquake Hazards. *Journal of Structural Engineering,* 130**,** 1921-1930.

ELLINGWOOD, B. R. & TEKIE, P. B. 1999. Wind Load Statistics for Probability-Based Structural Design. *Journal of Structural Engineering,* 125**,** 453-463.

ELLINGWOOD, B. R. & TEKIE, P. B. 2001. Fragility Analysis of Concrete Gravity Dams. *Journal of Infrastructure Systems,* 7**,** 41-48.

ENERDATA. 2017. *Global Energy Statistical Yearbook 2017* [Online]. Available: https://yearbook.enerdata.net/electricity/ [Accessed June 06 2018].

ENERGISTYRELSEN 2015. Energistatistik 2014. København: Danmarks Statistik.

ENTSOE. May 15 2018. *RE: Personal communication with 'Entsoe', Nov 18, 2018.*

ESPIRITU, J. F., COIT, D. W. & PRAKASH, U. 2007. Component criticality importance measures for the power industry. *Electric Power Systems Research,* 77**,** 407-420.

FIKKE, S. 2017. Overhead Lines and Weather. *In:* PAPAILIOU, K. O. (ed.) *Overhead Lines.* Springer International Publishing Switzerland.

FISHMAN, G. S. 1986. A Comparison of Four Monte Carlo Methods for Esitmating the Probability of s-t Connectedness. *IEEE Transactions on Reliability,* R-35**,** 145-156.

FLEMING, K. N. 1975. *Reliability model for common mode failures in redundant safety systems,* United States, Instrument Society of America.

FLOYD, R. W. 1962. Algorithm 97: Shortest path. *Commun. ACM,* 5**,** 345.

FORD, L. R. & FULKERSON, D. R. 1956. Maximal flow through a network. *Canadian Journal of Mathematics,* 8**,** 399-404.

FREEMAN, L. C. 1977. A Set of Measures of Centrality Based on Betweenness. *Sociometry,* 40**,** 35-41.

GANDINI, A. 1990. Importance and sensitivity analysis in assessing system reliability. *IEEE Transactions on Reliability,* 39**,** 61-70.

GEORGIOU, N. P. 1985. *Design wind speeds in tropical cyclone-prone regions.* Ph.D. Thesis, University of Western Ontario.

GEORGIOU, P., DAVENPORT, A. G. & VICKERY, B. J. 1983. Design wind speeds in regions dominated by tropical cyclones. *Journal of Wind Engineering & Industrial Aerodynamics,* 13**,** 139-152.

GHANNOUM, E. 2017. Structural and Mechanical Design. *In:* PAPAILIOU, K. O. (ed.) *Overhead Lines.* Springer International Publishing Switzerland.

GIRVAN, M. & NEWMAN, M. E. J. 2002. Community structure in social and biological networks. *Proceedings of the National Academy of Sciences,* 99**,** 7821-7826.

GÖNEN, T. 2015. *Electrical Power Transmission System Engineering: Analysis and Design, Thrid Edition*, CRC Press.

GRAINGER, J. & STEVENSON, W. J. 1994. *Power System Analysis*, McGraw-Hill.

GRIGG, C., WONG, P., ALBRECHT, P., ALLAN, R., BHAVARAJU, M., BILLINTON, R., CHEN, Q., FONG, C., HADDAD, S., KURUGANTY, S., LI, W., MUKERJI, R., PATTON, D., RAU, N., REPPEN, D., SCHNEIDER, A., SHAHIDEHPOUR, M. & SINGH, C. 1999. The IEEE Reliability Test System-1996. A report prepared by the Reliability Test System Task Force of the Application of Probability Methods Subcommittee. *IEEE Transactions on Power Systems,* 14**,** 1010-1020.

GUIKEMA, S. D. 2009. Natural disaster risk analysis for critical infrastructure systems: An approach based on statistical learning theory. *Reliability Engineering & System Safety,* 94**,** 855-860.

GUIKEMA, S. D., NATEGHI, R., QUIRING, S. M., STAID, A., REILLY, A. C. & GAO, M. 2014. Predicting Hurricane Power Outages to Support Storm Response Planning. *Access, IEEE,* 2**,** 1364-1373.

HAN, S.-R., GUIKEMA, S. D. & QUIRING, S. M. 2009a. Improving the Predictive Accuracy of Hurricane Power Outage Forecasts Using Generalized Additive Models. *Risk Analysis,* 29**,** 1443-1453.

HAN, S.-R., GUIKEMA, S. D., QUIRING, S. M., LEE, K.-H., ROSOWSKY, D. & DAVIDSON, R. A. 2009b. Estimating the spatial distribution of power outages during hurricanes in the Gulf coast region. *Reliability Engineering & System Safety,* 94**,** 199-210.

HASTINGS, W. K. 1970. Monte Carlo sampling methods using Markov chains and their applications. *Biometrika,* 57**,** 97-109.

HAYLOCK, M. R. 2011. European extra-tropical storm damage risk from a multi-model ensemble of dynamically-downscaled global climate models. *Natural Hazards and Earth System Sciences,* 11**,** 2847-2857.

HENNEAUX, P., LABEAU, P.-E. & MAUN, J.-C. 2012. A level-1 probabilistic risk assessment to blackout hazard in transmission power systems. *Reliability Engineering & System Safety,* 102**,** 41-52.

HILBER, P. & BERTLING, L. 2007. Component reliability importance indices for electrical networks. *International Conference on Power Engineering, IPEC* Singapore.

HINES, P., COTILLA-SANCHEZ, E. & BLUMSACK, S. 2010. Do topological models provide good information about electricity infrastructure vulnerability? *Chaos,* 20**,** 033122.

HODGE, N. 2012. Emerging risks on the horizon - Energy Risk. *Global Risk Dialogue.* Munich: Allianz Global Corporate & Specialty AG.

HOLME, P., KIM, B. J., YOON, C. N. & HAN, S. K. 2002. Attack vulnerability of complex networks. *Physical Review E,* 65**,** 056109.

HOLMGREN, Å. J. 2006. Using Graph Models to Analyze the Vulnerability of Electric Power Networks. *Risk Analysis,* 26**,** 955-969.

HUANG, Z., ROSOWSKY, D. V. & SPARKS, P. R. 2001a. Hurricane simulation techniques for the evaluation of wind-speeds and expected insurance losses. *Journal of Wind Engineering and Industrial Aerodynamics,* 89**,** 605-617.

HUANG, Z., ROSOWSKY, D. V. & SPARKS, P. R. 2001b. Long-term hurricane risk assessment and expected damage to residential structures. *Reliability Engineering & System Safety,* 74**,** 239-249.

IEEE 1973. Common Format For Exchange of Solved Load Flow Data. *IEEE Transactions on Power Apparatus and Systems,* PAS-92**,** 1916-1925.

JAVANBAKHT, P. & MOHAGHEGHI, S. 2014. A risk-averse security-constrained optimal power flow for a power grid subject to hurricanes. *Electric Power Systems Research,* 116**,** 408-418.

JAVANBARG, M., SCAWTHORN, C., KIYONO, J. & ONO, Y. 2009. Multi-Hazard Reliability Analysis of Lifeline Networks. *TCLEE 2009.* American Society of Civil

Engineers.

JIRUTITIJAROEN, P. & SINGH, C. 2008. Comparison of Simulation Methods for Power System Reliability Indexes and Their Distributions. *IEEE Transactions on Power Systems,* 23**,** 486-494.

JOHANSSON, J. & HASSEL, H. 2014. Impact of Functional Models in a Decision Context of Critical Infrastructure Vulnerability Reduction. *Vulnerability, Uncertainty, and Risk.* American Society of Civil Engineers.

JONCZY, J. & HAENNI, R. A new approach to network reliability. 5th International Conference on Mathematical Methods in Reliability,MMR'07, 2007.

KANG, W.-H. 2011. *Development and application of new system reliability analysis methods for complex infrastructure systems.* PhD thesis, University of Illinois at Urbana-Champaign.

KATAFYGIOTIS, L. S. & ZUEV, K. M. 2008. Geometric insight into the challenges of solving high-dimensional reliability problems. *Probabilistic Engineering Mechanics,* 23**,** 208-218.

KELLER, W. & MODARRES, M. 2005. A historical overview of probabilistic risk assessment development and its use in the nuclear power industry: a tribute to the late Professor Norman Carl Rasmussen. *Reliability Engineering & System Safety,* 89**,** 271-285.

KIM, Y., KANG, W.-H. & SONG, J. 2012. Assessment of Seismic Risk and Importance Measures of Interdependent Networks using a Non Simulation-Based Method. *Journal of Earthquake Engineering,* 16**,** 777-794.

KOÇ, Y. 2015. *Measuring the Robustness of Power Grids: A Complex Networks Theory Approach.* PhD thesis, Delft University of Technology.

KOÇ, Y., VERMA, T., ARAUJO, N. A. M. & WARNIER, M. 2013. Matcasc: A tool to analyse cascading line outages in power grids. *IEEE International Workshop on Intelligent Energy Systems (IWIES)***,** 143-148.

KOÇ, Y., WARNIER, M., MIEGHEM, P. V., KOOIJ, R. E. & BRAZIER, F. M. T. 2014. The impact of the topology on cascading failures in a power grid model. *Physica A: Statistical Mechanics and its Applications,* 402**,** 169-179.

KUO, W. & ZHU, X. 2012. *Importance measures in reliability, risk, and optimization : principles and applications,* Chichester, West Sussex, U.K., Wiley.

LAROCCA, S., JOHANSSON, J., HASSEL, H. & GUIKEMA, S. 2015. Topological Performance Measures as Surrogates for Physical Flow Models for Risk and Vulnerability Analysis for Electric Power Systems. *Risk Analysis,* 35**,** 608-623.

LATORA, V. & MARCHIORI, M. 2001. Efficient Behavior of Small-World Networks. *Physical Review Letters,* 87**,** 198701.

LATORA, V. & MARCHIORI, M. 2004. How the science of complex networks can help developing strategies against terrorism. *Chaos, Solitons & Fractals,* 20**,** 69-75.

LAW, A. M. & KELTON, W. D. 1991. *Simulation Modeling & Analysis*, McGraw-Hill International Editions.

LÊ, M. 2014. *Quantitative evaluation of network reliability.* PhD thesis, Technische Universität München.

LI, J., DUEÑAS-OSORIO, L., CHEN, C. & SHI, C. 2017. AC power flow importance measures considering multi-element failures. *Reliability Engineering & System Safety,* 160**,** 89-97.

LI, J. & HE, J. 2002. A recursive decomposition algorithm for network seismic reliability evaluation. *Earthquake Engineering & Structural Dynamics,* 31**,** 1525-1539.

LI, W. 2011. *Probabilistic Transmission System Planning,* Hoboken, New Jersey, John Wiley & Sons, Inc. .

LIM, H.-W. & SONG, J. 2012. Efficient risk assessment of lifeline networks under spatially correlated ground motions using selective recursive decomposition algorithm. *Earthquake Engineering & Structural Dynamics,* 41**,** 1861-1882.

LIM, H.-W., SONG, J. & KURTZ, N. 2015. Seismic reliability assessment of lifeline networks using clustering-based multi-scale approach. *Earthquake Engineering & Structural Dynamics,* 44**,** 355-369.

LISNIANSKI, A., FRENKEL, I. & DING, Y. 2010. *Multi-state System Reliability Analysis and Optimization for Engineers and Industrial Managers,* London, Springer-Verlag

LIU, H., DAVIDSON, R., ROSOWSKY, D. & STEDINGER, J. 2005. Negative Binomial Regression of Electric Power Outages in Hurricanes. *Journal of Infrastructure Systems,* 11**,** 258-267.

LIU, H., DAVIDSON, R. A. & APANASOVICH, T. V. 2008. Spatial generalized linear mixed models of electric power outages due to hurricanes and ice storms. *Reliability Engineering & System Safety,* 93**,** 897-912.

LOH, W. W. 1994. *On the Method of Control Variates.* PhD thesis, Stanford University.

MARKKU, P. May 11 2017. *RE: Personal communication with 'Fingrid', May 11, 2017.*

MASON, S. J. & GRAHAM, N. E. 2002. Areas beneath the relative operating characteristics (ROC) and relative operating levels (ROL) curves: Statistical significance and interpretation. *Quarterly Journal of the Royal Meteorological Society,* 128**,** 2145-2166.

MCKAY, M. D., BECKMAN, R. J. & CONOVER, W. J. 1979. A Comparison of Three Methods for Selecting Values of Input Variables in the Analysis of Output from a Computer Code. *Technometrics,* 21**,** 239-245.

MELCHERS, R. E. 1999. *Structural Reliability Analysis and Prediction, 2nd Edition*, John Wiley & Sons Ltd.

MENG, F. C. 1996. Comparing the importance of system components by some structural characteristics. *IEEE Transactions on Reliability,* 45**,** 59-65.

MENSAH, A. F. & DUENAS-OSORIO, L. Outage predictions of electric power systems under Hurricane winds by Bayesian networks. Probabilistic Methods Applied to Power Systems (PMAPS), 2014 International Conference on, 7-10 July 2014. 1-6.

MOSLEH, A. 1991. Common cause failures: An analysis methodology and examples. *Reliability Engineering & System Safety,* 34**,** 249-292.

MOSLEH, A., FLEMING, K. N., PARRY, G. W., PAULA, H. M., WORLEDGE, D. H. & RASMUSON, D. M. 1988. Procedures for treating common cause failures in safety and reliability studies: procedural framework and examples. *NUREG/CR-4780.* Newport Beach, CA: U.S. Nuclear Regulatory Commission.

MOTTER, A. E. & LAI, Y.-C. 2002. Cascade-based attacks on complex networks. *Physical Review E,* 66**,** 065102.

MOTTER, A. E., NISHIKAWA, T. & LAI, Y.-C. 2002. Range-based attack on links in scale-free networks: Are long-range links responsible for the small-world phenomenon? *Physical Review E,* 66**,** 065103.

MURRAY, A. T. & GRUBESIC, T. H. 2007. *Critical Infrastructure*, Springer.

NATAF, A. 1962. Détermination des distributions de probabilités dont les marges sont données. *Comptes rendus de l'Académie des sciences,* 225**,** 42-43.

NATEGHI, R., GUIKEMA, S. & QUIRING, S. M. 2014. Power Outage Estimation for Tropical Cyclones: Improved Accuracy with Simpler Models. *Risk Analysis,* 34**,** 1069-1078.

NEUMAYER, S. & MODIANO, E. Network Reliability with Geographically Correlated Failures. INFOCOM, Proceedings IEEE, 14-19 March 2010. 1-9.

NEUMAYER, S., ZUSSMAN, G., COHEN, R. & MODIANO, E. Assessing the impact of geographically correlated network failures. MILCOM 2008 - IEEE Military Communications Conference, 16-19 Nov 2008. 1-6.

NEWMAN, M. E. J. 2003. The Structure and Function of Complex Networks. SIAM Review.

NEWMAN, M. E. J. 2008. The mathematics of networks. *The New Palgrave Dictionary of Economics.* Basingstoke: Palgrave Macmillan.

NOAA 2017. Tropical cyclones names and definitions. *In:* CENTER, N. H. (ed.) *National weather service instruction 10-604.* Department of Commerce Operations and Services

NORTH AMERICAN ROCKWELL, C., EDISON ELECTRIC, I. & ELECTRIC POWER RESEARCH, I. 1970. *On-line stability analysis study RP90-1, October 12, 1970,* Palo Alto, Calif., Electric Power Research Institute.

NVE. 2017. *Norges vassdrags- og energidirektorat* [Online]. Available: https://www.nve.no/ [Accessed 2017-09-10].

OSCE 2016. Protecting Electricity Networks from Natural Hazards. Vienna: Organization for Security and Co-operation in Europe (OSCE).

OUYANG, M. & DUEÑAS-OSORIO, L. 2012. Time-dependent resilience assessment and improvement of urban infrastructure systems. *Chaos: An Interdisciplinary Journal of Nonlinear Science,* 22**,** 033122.

OUYANG, M. & DUEÑAS-OSORIO, L. 2014. Multi-dimensional hurricane resilience assessment of electric power systems. *Structural Safety,* 48**,** 15-24.

OUYANG, M., DUEÑAS-OSORIO, L. & MIN, X. 2012. A three-stage resilience analysis framework for urban infrastructure systems. *Structural Safety,* 36–37**,** 23-31.

OUYANG, M., PAN, Z., HONG, L. & ZHAO, L. 2014. Correlation analysis of different vulnerability metrics on power grids. *Physica A: Statistical Mechanics and its Applications,* 396**,** 204-211.

PANIGRAHI, P. 2013. *Topological Analysis of Power Grid to Identify Vulnerable Transmission Lines and Nodes.* Master of Technology in Control and Automation, National Institute of Technology, Rourkela.

PANT, R., HALL, J., BARR, S. & ALDERSON, D. 2014. Spatial Risk Analysis of Interdependent Infrastructures Subjected to Extreme Hazards. *Vulnerability, Uncertainty, and Risk.* American Society of Civil Engineers.

PANTELI, M., PICKERING, C., WILKINSON, S., DAWSON, R. & MANCARELLA, P. 2017. Power System Resilience to Extreme Weather: Fragility Modelling, Probabilistic Impact Assessment, and Adaptation Measures. *IEEE Transactions on Power Systems,* PP**,** 1-1.

PAPAILIOU, K. O. 2017. *Overhead Lines,* Cham Springer International Publishing.

PAPAIOANNOU, I. 2012. *Non-intrusive finite element reliability analysis.* PhD thesis, Technische Universität München.

PEPYNE, D. 2007. Topology and cascading line outages in power grids. *Journal of Systems Science and Systems Engineering,* 16**,** 202-221.

POWELL, M., H. HOUSTON, S., R. AMAT, L. & MORISSEAU-LEROY, N. 1998. *The HRD real-time hurricane wind analysis system*.

POWELL, M., MURILLO, S., DODGE, P., UHLHORN, E., GAMACHE, J., CARDONE, V., COX, A., OTERO, S., CARRASCO, N., ANNANE, B. & ST. FLEUR, R. 2010. *Reconstruction of Hurricane Katrina's wind fields for storm surge and wave hindcasting*.

POWELL, M., SOUKUP, G., COCKE, S., GULATI, S., MORISSEAU-LEROY, N., HAMID, S., DORST, N. & AXE, L. 2005. State of Florida hurricane loss projection model: Atmospheric science component. *Journal of Wind Engineering and Industrial Aerodynamics,* 93**,** 651-674.

RAHNAMAY-NAEINI, M., PEZOA, J. E., AZAR, G., GHANI, N. & HAYAT, M. M. Modeling Stochastic Correlated Failures and their Effects on Network Reliability. Computer

Communications and Networks (ICCCN), Proceedings of 20th International Conference on, July 31 - Aug 4 2011. 1-6.

RAIFFA, H. & SCHLAIFER, R. 1961. *Applied statistical decision theory,* Harvard University, Boston, Division of Research, Graduate School of Business Adminitration.

RAUSAND, M. & HØYLAND, A. 2004. *System Reliability Theory Models, Statistical Methods, and Applications,* New Jersey, John Wiley & Sons. Inc.

RENAUD, F. G. 2006. Environmental components of vulnerability. *In:* BIRKMANN, J. (ed.) *Measuring Vulnerability to Natural Hazards: Towards Disaster Resilient Societies.* Tokio, New York, Paris: United Nations University Press.

RMS. 2013. *RMS HWIND legacy archive* [Online]. Risk Management Solutions, Inc. Available: http://www.rms.com/perils/hwind/legacy-archive/storms/ [Accessed 2017/11/21].

ROBERTS, J. F., CHAMPION, A. J., DAWKINS, L. C., HODGES, K. I., SHAFFREY, L. C., STEPHENSON, D. B., STRINGER, M. A., THORNTON, H. E. & YOUNGMAN, B. D. 2014. The XWS open access catalogue of extreme European windstorms from 1979 to 2012. *Natural Hazards and Earth System Sciences,* 14**,** 2487-2501.

ROKNEDDIN, K. 2013. *Reliability and risk assessment of networked urban infrastructure systems under natural hazards.* PhD thesis PhD thesis, Rice University.

ROSAS-CASALS, M. & COROMINAS, B. 2009. Assessing European power grid reliability by means of toplogical measures. *WIT transactions on ecology and the environment,* 121**,** 257-537.

ROSAS-CASALS, M., VALVERDE, S. & SOLÉ, R. V. 2007. Topological Vulnerability of the European Power Grid under Errors and Attacks. *International Journal of Bifurcation and Chaos,* 17**,** 2465-2475.

ROSATO, V., BOLOGNA, S. & TIRITICCO, F. 2007. Topological properties of high-voltage electrical transmission networks. *Electric Power Systems Research,* 77**,** 99-105.

RUSSELL, L. R. 1968. *Probability distribution for Texas Gulf coast hurricane effects of engineering interest.* Ph.D. Thesis, Stanford University.

RUSSELL, L. R. 1971. Probability distributions for hurricane effects. *Journal of the Waterways, Harbors and Coastal Engineering Division,* 97**,** 139-154.

SACCOMANNO, F. 2003. *Electric power systems,* Piscataway, NJ, IEEE Press.

SALEH, J. & MARAIS, K. 2006. *Highlights from the early (and Pre-) history of reliability engineering. Reliability Engineering and System Safety, 91, 249-256*.

SALMAN, A. 2016. *Risk-based assessment and strengthening of electric power systems subjected to natural hazards.* PhD thesis, Michigan Technological University.

SALMAN, A. M. & LI, Y. 2018. A probabilistic framework for multi-hazard risk mitigation

for electric power transmission systems subjected to seismic and hurricane hazards. *Structure and Infrastructure Engineering***,** 1-21.

SCHAUG-PETTERSON, J. May 16 2017. *RE: Personal communication with 'Statnett', May 16, 2017.*

SCHERB, A., GARRÈ, L. & STRAUB, D. Probabilistic Risk Assessment of Infrastructure Networks Subjected to Hurricanes. 12th International Conference on Applications of Statistics and Probability in Civil Engineering, ICASP 12, July 12-15 2015 Vancouver. Canada.

SCHERB, A., GARRÈ, L. & STRAUB, D. 2017. Reliability and Component Importance in Networks Subject to Spatially Distributed Hazards Followed by Cascading Failures. *ASCE-ASME Journal of Risk and Uncertainty in Engineering Systems, Part B: Mechanical Engineering,* 3**,** 0210071-0210079.

SCHERB, A., GARRÈ, L., YANG, Y. & STRAUB, D. Component importance in infrastructure networks subject to spatially distributed hazards. European Safety and Reliability, ESREL, September 25-29 2016 Glasgow.

SCHULTZ, M. T., SIMM, J. D., GOULDBY, B. P. & WIBOWO, J. L. 2010. Beyond the factor of Safety: Developing Fragility Curves to Characterize System Reliability *Water Resources Infrastructure Program.* Washington: US Army Corps of Engineers - Engineer Research and Development Center.

SCHWAB, A. J. 2009. *Elektroenergiesysteme - Erzeugung, Transport, Übertragung und Verteilung elektrischer Energie. 3. Auflage,* Karlsruhe, Springer-Verlag Berlin Heidelberg.

SEDLACEK, J. 1968. *Einführung in die Graphentheorie*, B.G. Teubner Verlagsgesellschaft.

SHAFIEEZADEH, A., ONYEWUCHI, U. P., BEGOVIC, M. M. & DESROCHES, R. 2014. Age-Dependent Fragility Models of Utility Wood Poles in Power Distribution Networks Against Extreme Wind Hazards. *IEEE Transactions on Power Delivery,* 29**,** 131-139.

SHINOZUKA, M., FENG, M., LEE, J. & NAGANUMA, T. 2000. Statistical Analysis of Fragility Curves. *Journal of Engineering Mechanics,* 126**,** 1224-1231.

SHPUNGIN, Y. & GERTSBAKH, I. B. 2009. *Models of Network Reliability: Analysis, Combinatorics, and Monte Carlo*, Taylor & Francis Group.

SIMM, J., B. GOULDBY, P. SAYERS, J. FILKWEERT, S. WERSCHING, AND M. BRAMLEY. Representing fragility of flood and coastal defences: Getting into the detail. *In:* P. SAMUELS, S. H., W. ALLSOP, AND J. HARROP, ed. European Conference on Flood Risk Management (FLOODrisk 2008), 30 Sep– 2 Oct 2009 Oxford, UK. 621–631.

SIVANAGARAJU, S. & SREENIVASAN, G. 2009. *Power System Operation and Control*, Pearson.

SONG, J. & DER KIUREGHIAN, A. 2003. Bounds on System Reliability by Linear

Programming. *Journal of Engineering Mechanics,* 129**,** 627-636.

SONG, J. & KANG, W.-H. 2009. System reliability and sensitivity under statistical dependence by matrix-based system reliability method. *Structural Safety,* 31**,** 148-156.

SPARKS, P. R. 2003. Wind speeds in tropical cyclones and associated insurance losses. *Journal of Wind Engineering and Industrial Aerodynamics,* 91**,** 1731-1751.

STAID, A., GUIKEMA, S., NATEGHI, R., QUIRING, S. & GAO, M. 2014. Simulation of tropical cyclone impacts to the U.S. power system under climate change scenarios. *Climatic Change,* 127**,** 535-546.

STATTNET, FINGRID, LANDSNET, KRAFTNÄT, S. & ENERGINET.DK 2014. Nordic Grid Development Plan 2014.

STEWART, M. & MELCHERS, R. E. 1998. *Probabilistic Risk Assessment Of Engineering Systems*, Springer.

STRAUB, D. 2017. Lecture notes in engineering risk analysis. Technische Universität München.

STRAUB, D. & DER KIUREGHIAN, A. 2008. Improved seismic fragility modeling from empirical data. *Structural Safety,* 30**,** 320-336.

STROGATZ, S. H. 2001. Exploring complex networks. *Nature,* 410**,** 268-276.

SULLIVAN, M. J., MERCURIO, M. & SCHELLENBERG, J. 2009. Estimated Value of Service Reliability for Electric Utility Customers in the United States. *Ernest Orlando Lawrence Berkley National Laboratory.* U.S. Energy Analysis Department.

TALLBERG, T. July 04 2017. *RE: Personal communication with 'SVK', Jul 04, 2017.*

TANGUY, C. Importance measures and common-cause failure in network reliability. *In:* BÉRENGUER, C., GRALL, A., SOARES G. , ed. European Safety and Reliability Conference, ESREL, 18-22 September 2011 Troyes, France. CRC Presss Tayler & Francis Group, 1052-1060.

UCTE 2004. Final Report of the Investigation Committee on the 28 September 2003 Blackout in Italy.

US DEPARTMENT OF ENERGY 2010. Hardening and Resiliency: U.S. Energy Industry Response to Recent Hurricane Seasons.

US DEPARTMENT OF ENERGY 2017. Electric Disturbance Events (OE-417) Annual Summaries Washington, DC

VAIMAN, M., BELL, K., CHEN, Y., CHOWDHURY, B., DOBSON, I., HINES, P., PAPIC, M., MILLER, S. & ZHANG, P. 2012. Risk Assessment of Cascading Outages: Methodologies and Challenges. *IEEE Transactions on Power Systems,* 27**,** 631-641.

VAN DER BORST, M. & SCHOONAKKER, H. 2001. An overview of PSA importance measures. *Reliability Engineering & System Safety,* 72**,** 241-245.

VAN HERTEM, D., VERBOOMEN, J., PURCHALA, K., BELMANS, R. & KLING, W. L. Usefulness of DC power flow for active power flow analysis with flow controlling devices. The 8th IEE International Conference on AC and DC Power Transmission, ACDC 2006. , 28-31 March 2006. 58-62.

VAURIO, J. K. 1998. An implicit method for incorporating common-cause failures in system analysis. *Reliability, IEEE Transactions on,* 47**,** 173-180.

VERMA, T. 2012. *Vulnerability of Power Grids to Cascading Failures.* Master thesis, TU Delft.

VESELY, W. E. 1977. Estimating common cause failure probabilities in reliability and risk analyses: Marshall--Olkin specializations. *In:* J. B. FUSSELL & BURDICK, G. R. (eds.) *Nuclear Systems Reliability Engineering and Risk Assessment.* Philadelphia.

VESELY, W. E., DAVIS, T. C., DENNING, R. S. & SALTOS, N. 1983. Measures of risk importance and their applications.: US Nuclear Regulatory Commission.

VICKERY, P. J., LIN, J., SKERLJ PETER, F., TWISDALE LAWRENCE, A. & HUANG, K. 2006. HAZUS-MH Hurricane Model Methodology. I: Hurricane Hazard, Terrain, and Wind Load Modeling. *Natural Hazards Review,* 7**,** 82-93.

VICKERY, P. J., MASTERS, F. J., POWELL, M. D. & WADHERA, D. 2009a. Hurricane hazard modeling: The past, present, and future. *Journal of Wind Engineering and Industrial Aerodynamics,* 97**,** 392-405.

VICKERY, P. J., SKERLJ, P. F. & TWISDALE, L. A. 2000. Simulation of Hurricane Risk in the U.S. Using Empirical Track Model. *Journal of Structural Engineering,* 126**,** 1222-1237.

VICKERY, P. J. & WADHERA, D. 2008. Statistical Models of Holland Pressure Profile Parameter and Radius to Maximum Winds of Hurricanes from Flight-Level Pressure and H*Wind Data. *Journal of Applied Meteorology and Climatology,* 47**,** 2497-2517.

VICKERY, P. J., WADHERA, D., A. TWISDALE, L. & LAVELLE, F. 2009b. U.S. Hurricane Wind Speed Risk and Uncertainty. *Journal of Structural Engineering,* 135**,** 301-320.

WANG, S., HONG, L. & CHEN, X. 2012. Vulnerability analysis of interdependent infrastructure systems: A methodological framework. *Physica A: Statistical Mechanics and its Applications,* 391**,** 3323-3335.

WANG, W., LOMAN, J. & VASSILIOU, P. 2004. Reliability importance of components in a complex system. *Proceedings of the Reliability and Maintainability Annual Symposium, RAMS 2004.*

WANG, Y., CHEN, C., WANG, J. & BALDICK, R. 2016. Research on Resilience of Power Systems Under Natural Disasters - A Review. *IEEE Transactions on Power*

Systems, 31**,** 1604-1613.

WANG, Z., SCAGLIONE, A. & THOMAS, R. J. Electrical centrality measures for electric power grid vulnerability analysis. 49th IEEE Conference on Decision and Control (CDC), 15-17 Dec 2010. 5792-5797.

WATTS, D. J. & STROGATZ, S. H. 1998. Collective dynamics of small-world networks. *Nature,* 393**,** 440-442.

WETZEL, C. 2009. *Zur probabilistischen Betrachtung von Schienen- und Kraftfahrzeugsystemen unter zufälliger Windanregung.* Dissertation, Universität Karlsruhe (TH).

WHITEHOUSE 2013. Economic Benefits of Increasing electric grid resilience to weather outages. Washington Executive Office of the President.

WIERMAN, T. E., RASMUSON, D. M. & MOSLEH, A. 2007. Common-Cause Failure Database and Analysis System: Event Data Collection, Classification, and Coding. *In:* LABORATORY, I. N. (ed.) *NUREG/CR-6268.* Washington, DC: Idaho National Laboratory.

WINKLER, J., DUEÑAS-OSORIO, L., STEIN, R. & SUBRAMANIAN, D. 2010. Performance assessment of topologically diverse power systems subjected to hurricane events. *Reliability Engineering & System Safety,* 95**,** 323-336.

WOOD, A. J. & WOLLENBERG, B. F. 1996. *Power generation, operation, and control,* New York Wiley.

XINGBIN, Y. & CHANAN, S. Expected power loss calculation including protection failures using importance sampling and SOM. IEEE Power Engineering Society General Meeting, 6-10 June 2004. 206-211 Vol.1.

ZHU, D., CHENG, D., BROADWATER, R. P. & SCIRBONA, C. 2007. Storm modeling for prediction of power distribution system outages. *Electric Power Systems Research,* 77**,** 973-979.

ZIO, E. 2009. Reliability engineering: Old problems and new challenges. *Reliability Engineering & System Safety,* 94**,** 125-141.

ZIO, E. 2014. Vulnerability and Risk Analysis of Critical Infrastructures. *Vulnerability, Uncertainty, and Risk.* American Society of Civil Engineers.

ZIO, E. & PICCINELLI, R. 2010. Randomized flow model and centrality measure for electrical power transmission network analysis. *Reliability Engineering & System Safety,* 95**,** 379-385.

ZIO, E. & SANSAVINI, G. 2011. Component Criticality in Failure Cascade Processes of Network Systems. *Risk Analysis,* 31**,** 1196-1210.

ZUEV, K. 2014. *Subset Simulation Method for Rare Event Estimation: An Introduction*, Springer-Verlag Berlin Heidelberg

ZUEV, K. M., WU, S. & BECK, J. L. 2015. General network reliability problem and its

efficient solution by Subset Simulation. *Probabilistic Engineering Mechanics,* 40**,** 25-35.